# INFLUENCE OF MIXTURE COMPOSITION ON PERFORMANCE OF COLD-BONDED FLY ASH AGGREGATE CONCRETE

*A THESIS*

*submitted by*

**GLORY JOSEPH**

*for the award of the degree of*

**DOCTOR OF PHILOSOPHY**

**BUILDING TECHNOLOGY AND CONSTRUCTION MANAGEMENT DIVISION**
**DEPARTMENT OF CIVIL ENGINEERING**
**INDIAN INSTITUTE OF TECHNOLOGY MADRAS**
**CHENNAI 600 036**

**DECEMBER 2008**

# THESIS CERTIFICATE

This is to certify that the thesis entitled "**INFLUENCE OF MIXTURE COMPOSITION ON PERFORMANCE OF COLD-BONDED FLY ASH AGGREGATE CONCRETE"** submitted by **Ms. Glory Joseph** to the Indian Institute of Technology; Madras for the award of the degree of **Doctor of Philosophy** is a bonafide record of research work carried out by her under my supervision. The contents of this thesis, in full or in parts, have not been submitted to any other Institute or University for the award of any degree or diploma.

Chennai 600 036
Date:

**Prof. K.Ramamurthy**
(Research Guide)

Professor
B.T.&C.M. Division
Department of Civil Engineering
I.I.T. Madras

# ACKNOWLEDGEMENTS

Countless people are behind what I am today. First of all, I thank God, the Almighty for putting all these wonderful personals on my path.

I am very happy to have worked as a doctoral research scholar at I.I.T Madras. I have great pleasure to warmly thank my research guide Prof. K. Ramamurthy for all his guidance and support, which have enabled me in the completion of this research work. His enthusiasm, integral view, analytical skills and passion for research have made a deep impression on me. I owe him for his dedication, generosity, patience in correcting and directing me in the path of research.

I would like to place on record, my sincere appreciation to Prof. K. Rajagopal, head of the Department of Civil Engineering for all the administrative support and encouraging words. Also I extend my sincere thanks to Prof. S. Mohan, former head of the department for all his valuable supports.

I also wish to place on record my sincere gratitude to Prof. A. Ramachandraiah, Prof. S. Swarnamani and Prof. R. Velmurugan who apart being members of my doctoral committee, have been most helpful in offering very useful and encouraging comments at various stages of my research work. I really appreciate the discussions with Dr. Manu Santhanam and thank him.

All the faculty members of the BT&CM Division – Prof. Ravindra Gettu, Prof. M.S. Mathews, Prof. K. N. Satyanarayana, Prof. Koshy Varghese, Dr. K. Ananthanarayanan and Dr. Ashwin Mahalingam have been very co-operative and displayed keen interest in my progress. I express my sincere thanks to all of them.

I wish to express my special thanks to Dr. E.K.K Nambiar and Dr. R. Manikandan for their advice, encouragement, and discussions throughout the course of this work.

I am pleased to record my gratitude to Cochin University of Science and Technology, for sponsoring me for the Ph.D programme under the Q.I.P. scheme and the support extended by the Division of Civil Engineering.

The staff of concrete lab will always have a special place in my heart for all the efforts they have put in towards the successful completion of my experimental work. Messers M. Soundarapandiyan, Murthy, Krishnan, Dhanasekaran, Ms. A. Malarvizhi, all have contributed their might. I am also thankful to all the staff members of the Civil Engineering Department Office, Stores section and DCF for their excellent cooperation.

I wish to thank Premkumar, Premraj, Palani, Durga Prasad, Krishna and Vijay who admirably and unstintingly helped me physically through all the laboratory work.

I am also thankful to all my fellow research scholars, Indu Sivaranjani, Prakash, Dr. P.P. Anilkumar, Venkatesan, Shajathnan, Paul, Dr. Uma, Dr. Ramesh Babu, Dr. Kanagasabhapathi, Senthilkumar, Rajasekar, Ganesh, Rakesh, Rajesh, Cinderala and many others- for all their valuable support. The encouragement, moral support and timely help from Jayasree and Geetha are greatly acknowledged.

Finally, I wish to express my indebtedness to my family members who have supported me in all possible ways. In particular, I wish to record my deepest appreciation to my mother, my husband Dr. Baby Joseph and my daughters for their boundless support, patience and understanding during the course of this research work.

**GLORY JOSEPH**

# ABSTRACT

**KEYWORDS:** Cold-bonded fly ash aggregate, Workability, Compressive strength Response Surface Methodology, Mixture proportioning, Permeation, Porosity, Sorptivity, Chloride ion penetrability, BSEI, Autogenous curing, Moisture migration, Degree of hydration.

Artificial aggregates from fly ash facilitate high volume utilization of fly ash in concrete and conservation of natural resources in addition to the reduction in density of concrete and total cost of construction. While sintered fly ash aggregate requires a heat treatment in the range of 1000-1200 ºC, cold bonding renders aggregate production less expensive with minimum energy consumption. The strengthening of pelletized fly ash in cold bonding (temperature: 5-100 °C) is due to the formation of C-S-H gel during the hydration from the chemical reaction between CaO and water and the pozzolanic character of the fly ash.

Review indicates only limited studies on concrete using cold-bonded fly ash aggregate though several studies have been reported on the characteristics and mechanical properties of lightweight concrete using sintered/expanded aggregates. Since cold-bonded aggregate has lower crushing value and higher water absorption, the characteristics of concrete that are specific to the sintered aggregate properties cannot be applied directly to cold-bonded aggregate concrete. Most of the studies on cold-bonded aggregate concrete have been confined to the mechanical properties of concrete and that too with relatively higher cement content (> 400 kg/m$^3$) thereby introducing a strong matrix phase in the concrete. This investigation aims at an in-depth study on the influence of mixture composition on workability, strength and permeation behaviour of cold-bonded aggregate concrete through statistically designed experiments. The objectives also include studying the influence of Class-F

fly ash on the behaviour of cold-bonded aggregate concrete and autogenous curing of concrete under different curing conditions.

Cold-bonded aggregate produced in the laboratory by pelletizing of Class-C fly ash, utilizing parameters of pelletization for maximizing the efficiency and adopting normal water curing was used as coarse aggregate (conforming to grading requirement of ASTM C 330, 2005) in this study after characterizing its properties. Preliminary studies on workability and mechanical properties of cold-bonded aggregate concrete were carried out through single factor experiments. Statistically designed experiments based on Response Surface Methodology (RSM) were then planned with the objective of developing prediction models in terms of mix proportioning variables viz., cement content, water content and volume fraction of cold-bonded aggregate, for understanding the influence of mixture variables and their interaction effect on workability, strength and permeation behaviour of concrete. For a given water content, the workability is highly improved with an increase in volume fraction of cold-bonded aggregate in the mix. Relation between concrete strength and constituent mortar strength together with the observations on failure surface indicate that strength of concrete is mainly governed by the initiation of failure in matrix or matrix-aggregate bond in concretes below a cement content of 300 kg/m$^3$, whereas at higher cement content the predominant failure mode changes to aggregate fracture and concrete strength decreases with an increase in volume fraction of cold-bonded aggregate. Model equations for workability and compressive strength are used to derive relationships to serve as typical mix proportioning methodology for cold-bonded fly ash aggregate concrete. Bonding qualities of concrete with plain and deformed bars has been assessed through pull out test.

The influence of mixture composition on the permeation behaviour of concrete has been studied through permeable porosity, water absorption, sorptivity and Rapid Chloride Penetrability Test. Though cold-bonded aggregate is highly porous, permeation of concrete appears to be more dependent on the porosity of the mortar phase than on the porosity of aggregate. Back Scattered Electron Image (BSEI) has been used to demonstrate the influence of mix composition on the microstructure of both matrix and matrix-aggregate interface of cold-bonded aggregate concrete.

The effect of Class-F fly ash on strength and permeation of cold-bonded fly ash aggregate concrete due to partial replacement of cement and also as replacement material for sand has been investigated. While the cement replacement must be restricted based on the compressive strength requirement at desired age, replacement of sand with fly ash appears to be advantageous from early days onwards with higher enhancement in strength and higher utilization of fly ash (around 0.6 $m^3$ of fly ash in unit volume of concrete) in mixes of lower cement content. Replacement of sand with fly ash is effective in reducing sorption and chloride ion penetrability attributable to the densification of both matrix and matrix-aggregate interfacial bond observed through BSEI.

Autogenous curing of cold-bonded aggregate concrete has been studied by subjecting it to three curing regimes viz. mist curing, sealed condition and air curing. Moisture movement from aggregate to concrete at various ages is estimated and correlated to paste-aggregate proximity. Degree of hydration and strength of concrete are observed to be almost insensitive to curing condition. The autogeneous curing of cold-bonded aggregate concrete can be effectively utilized with no variation in strength or porosity as compared to mist-curing, if it is properly covered to minimize the evaporation loss.

# TABLE OF CONTENTS

**Title** **Page No.**

**Table of Contents (Contd.,)** **Page No.**

**Table of Contents (Contd.,)** **Page No.**

**Table of Contents (Contd.,)** **Page No.**

**Table of Contents (Contd.,)** **Page No.**

**Table of Contents (Contd.,)** **Page No.**

# LIST OF TABLES

**List of Tables (Contd.,)** **Page No.**

# LIST OF FIGURES

**List of Figures (Contd.,)** **Page No.**

**List of Figures (Contd.,)** **Page No.**

**List of Figures (Contd.,)** **Page No.**

**List of Figures (Contd.,)** **Page No.**

# NOTATIONS

| | |
|---|---|
| $f_c$ | cube compressive strength of concrete |
| $W_{sat}$ | weight of vacuum saturated sample in air |
| $W_{wat}$ | weight of vacuum saturated sample in water |
| $W_{dry}$ | weight of oven-dried sample |
| c | cement content |
| w | water content |
| w/c | water cement ratio |
| CA/TA | ratio of coarse aggregate volume to total aggregate volume |
| $C_A$ | % volume of coarse aggregate in total aggregate volume |
| $n_f$ | number of points on the factorial portion of the design |
| a | distance to the axial points |
| $\tau$ | bond stress |
| $d$ | nominal diameter of bar |
| $l$ | embedment length of the bar |
| $i$ | cumulative volume absorbed per unit area of inflow surface |
| $S$ | sorptivity |
| t | elapsed time |
| $V_e$ | water consumed during hydration due to chemical shrinkage |
| CS | chemical shrinkage |
| $\rho_w$ | density of water |
| $\alpha_{max}$ | maximum degree of achievable hydration |
| $w_n$ | non-evaporable water content |

# CHAPTER 1

# INTRODUCTION

## 1.1 GENERAL

Concrete is the most widely used construction material. Its manufacturing process consumes large amount of natural materials/resources and therefore construction can have substantial negative impact on the environment. As aggregate comprises between 60 to 70% by volume of concrete, the extraction of natural aggregate causes serious threat to the landscape and produces erosion problems and deterioration of natural areas (CIB, 1999), and hence the production of concrete using artificial aggregate appears as a promising alternative to mitigate these problems. These artificial aggregates, most of which are lightweight also offer extra benefits in concrete owing to the reduction in density of concrete. Lightweight aggregate manufactured using waste material like fly ash, sludge ash, bottom ash and blast furnace slag, not only conserves natural resources but also reduces the total cost of construction. It also reduces the environmental problems caused by large-scale dumping of these waste materials.

## 1.2 LIGHTWEIGHT AGGREGATE CONCRETE (LWAC)

Lightweight aggregates, which are known for their high porosity, reduce the density of concrete from which emerges almost all other advantages. The reduced density of lightweight concrete offers saving in material and thus the cost, reduction in dead load of the structure facilitating economical design of supporting structures and substructures, better earthquake resistance, faster building rates and lower haulage and handling costs. Floor slab where high strength is not a major consideration, large amount of lightweight aggregate concrete can be used to reduce the dead weight of

floors of high rise buildings (Clarke, 1993). Lightweight concrete in general, is produced either for structural or thermal insulation purposes. Lightweight aggregate concrete is widely used in structural application as compared to other type of lightweight concretes (aerated concrete, no fines concrete etc.) as the strength of concrete can be controlled to the required level by varying the volume and/or type of the aggregate. Reduced density has a direct bearing on thermal conductivity. The porous system provides better thermal insulation and improves comfort condition in building. Lightweight aggregate concrete uses either natural or artificial lightweight aggregate (LWA) with bulk density ranging from 400 to 880 kg/m$^3$ for coarse aggregate and up to 1120 kg/m$^3$ for fine lightweight aggregate (ASTM C330, 2005). The characteristics of the aggregate depend on the raw material and the process of manufacture. Since the physical and mechanical properties of these aggregates differ greatly from each other, significant variations in concrete properties are observed with the variation in the type of aggregate. The influence of aggregate characteristics on the quality of concrete has been highlighted by many researchers (Aitcin and Mehta, 1990; Zhang and Gjorv, 1990a; Nilson et al., 1995). The important properties of concrete influenced by the aggregates are workability, strength, modulus of elasticity, density, durability, thermal conductivity, shrinkage and creep. Hence the properties of concrete are to be investigated and established independently for each type of aggregate.

### 1.2.1 Classification of Lightweight Aggregate Concrete

Based on application, the lightweight aggregate concrete has been classified by Holm (1994) into insulating concrete, moderate strength concrete and structural concrete. The range of density, compressive strength and thermal conductivity associated with each class of concrete are summarised in Table 1.1.

Table 1.1 Properties of different class of LWAC (Holm, 1994)

| Concrete Grade | Insulating concrete | Insulating/Moderate strength concrete | Structural concrete (ASTM C330, 2005) |
|---|---|---|---|
| Density (kg/m$^3$) | 240-800 | 800-1440 | 1600-1840 |
| Strength (MPa) | 0.7-3.4 | 3.4-17 | > 17 MPa |
| Thermal conductivity(W/m ºK) | 0.065-0.22 | 0.22-0.43 | - |

Lightweight aggregate concrete is also classified as no-fines lightweight aggregate concrete and continuously graded lightweight aggregate concrete based on the mixture composition. In no-fines concrete, the fine aggregate is omitted; creating voids between the coarse aggregate particles. In continuously graded LWAC, the particles are surrounded by mortar and the volume of voids between the aggregate particles is reduced (Rudnai, 1963).

### 1.2.2 A brief History of Lightweight Aggregate Concrete

Although lightweight aggregate concrete has become much more familiar in recent years, it is not a new class of building material. Lightweight concrete made up of natural porous aggregates of volcanic origin such as pumice, scoria etc. was in use from ancient age itself. Sumerians used this in building The Babylon in the 3$^{rd}$ millennium B.C. (Chandra and Berntsson, 2004). Lightweight aggregate concrete was frequently used by the Romans; the 44 m diameter dome of Pantheon built in the second century A.D is composed of cast in-situ concrete using pumice aggregate. In the United States, during World War II, ships ranging in capacity from 3000 to 140000 tonnes were built with LWAC and their successful performance led to an extended use of structural LWAC in buildings and bridges. The development of lightweight aggregate concrete has been very much depended on the locally available raw materials for the production of lightweight aggregate. In USA, Germany and Norway a broad variety of LWA types have been developed since 1920 based on

expanded shale (Liapor) and expanded clay (Leca), ranging from very low density to high strength products. In the U.K in 1960, later 1973 in Germany and in 1985 in the Netherlands on the other hand, technology have been developed for producing LWA using fly ash (Lytag and Aardelite). These materials are commercially produced in large quantity in different gradation and weights. Offshore gravity base tank, Scotland (1990), Westminster Bridge strengthening (1996), and Canada Square, London (1998-2001) are examples of some modern structures where sintered fly ash aggregate (Lytag, 2007) has been used to reduce the dead weight of the structure. Though structures were erected world-wide using commercially available sintered or autoclaved fly ash aggregates since 1960's, cold-bonded fly ash aggregate produced with water curing process is still in research stage.

## 1.3 LIGHTWEIGHT AGGREGATE

Lightweight aggregates develop low particle specific gravity because of the cellular pore system. Most of the natural lightweight aggregates such as pumice, diatomite, scoria, and cinder are of volcanic origin and their properties mainly depend on their origin. Natural lightweight aggregates have limited application, due to their non-availability at most locations. The natural materials used for producing artificial LWA are perlite, vermiculite, clay, shale and slate while the industrial byproducts are pulverized fuel ash, blast furnace slag, industrial waste, sludge etc. The production technique of artificial aggregate relies either on expansion or agglomeration. Expansion develops when either steam is generated, as in the case of molten slag, or a suitable mineral is heated to fusion temperature, at which pyroplasticity occurs simultaneously with the formation of gas which bloats the aggregate (Chandra and Berntsson, 2004). Agglomeration takes place when some of the materials melt at temperatures above 1100 ºC and the particles that make up the finished aggregate are

bonded together by fusion (Clarke, 1993). Aggregates produced through expansion or sintering process becomes costlier because of heavy investment in terms of plant and equipment and high temperature treatment.

### 1.3.1 Lightweight Aggregate from Fly Ash

With the increase in construction activities, the demand for lightweight aggregate has become quite high. Due to the non-availability of suitable natural material for its use as lightweight aggregate, the research focus is now towards the production of artificial aggregate from industrial by-products and/or wastes. Also, the environmental considerations are receiving increased attention with regard to the use of industrial by-products/wastes. The most widely available industrial waste is coal fly ash from thermal power station. Conversion of fly ash into aggregate, allows its large scale utilization by the construction industry. This aggregate can be produced by adopting established techniques like pelletization or compaction and hardening process such as sintering, autoclaving or cold-bonding. Sintering is the method widely used in commercial production of fly ash aggregate. Depending on the fineness and chemical composition of raw materials, aggregate production through cold agglomeration of fly ash has been initiated recently to reduce the energy consumption and cost. The research on concrete with cold-bonded fly ash aggregate has also started gaining importance in the last few years (Chang and Shieh, 1996; Baykal and Doven, 2000; Chi et al. 2003; Gesoglu et al. 2004, 2006).

## 1.4 MOTIVATION FOR THE PRESENT STUDY

Due to the tremendous environmental problems caused by large scale dumping of fly ash, the research focus is now towards the high volume utilization of fly ash. Effective utilization of fly ash in India is only about 38% out of 112 million tonnes produced

per year (Fly ash mission India, 2006). Fly ash generation is expected to increase in the coming years and therefore fly ash management is an important area of national concern. Sustained research and development work on the utilization of fly ash for various productive uses have been carried out. Major attention of the construction industry has been devoted to the use of fly ash in the cement manufacture and in concrete as cement replacement. Fly ash is being used in the manufacturing of bricks, blocks as well as in the construction of roads. The production of fly ash aggregate and fly ash aggregate concrete has not gained confidence in the Indian construction industry due to lack of data on material properties and design guidelines for fly ash aggregate concrete. In this context, an in depth study on properties of cold-bonded fly ash aggregate concrete from ash generated in India is deemed necessary.

## 1.5 ORGANIZATION OF THE THESIS

A general introduction of lightweight aggregate concrete, its classification, and advantages along with the motivation for the present study have been presented in the preceding sections of this chapter. A critical review of literature pertaining to investigation on lightweight aggregate and lightweight aggregate concrete with special emphasis on their physical, chemical, mechanical and functional properties is presented in Chapter 2. Chapter 3 outlines the objectives and scope of the present work.

Chapter 4 describes the properties of cold-bonded fly ash aggregates and its effect on workability and mechanical properties of concrete. Experimental investigation covering a wide range of mixture composition parameters including the moisture condition of the aggregate have been undertaken with an objective of developing predictive relations for workability and compressive strength, using statistically

designed experiments. Studies on bond strength of cold-bonded aggregate concrete have also been discussed in this chapter.

The influence of mixture composition on permeation characteristics of concrete is the subject of Chapter 5. The results have been correlated using micro-structural studies on cold-bonded aggregate concrete to understand the permeation behaviour. Chapter 6 discusses the strength and permeation behaviour of cold-bonded aggregate concrete for the influence of use of Class-F fly ash, as replacement of cement or sand. Chapter 7 deals with the behaviour of cold-bonded aggregate on autogenous curing of concrete through an assessment of moisture migration from the aggregate, degree of hydration, compressive strength and permeation characteristics by subjecting concrete to different curing regimes. The salient conclusions drawn from the present research work and scope for further studies are summarised in Chapter 8.

# CHAPTER 2

# REVIEW OF LITERATURE

## 2.1 GENERAL

Lightweight aggregate concrete exhibits considerable difference from normal weight concrete in their fresh and hardened state properties in addition to relatively lower density (ACI 211.2, 1990; Clarke, 1993; Chandra and Berntsson, 2004). The difference starts from mixing stage onwards owing to relatively higher water absorption of aggregate and is extended to the hardened concrete exhibited through the degree of homogeneity, extended curing, failure mode and durability of concrete which are related to the physical and micro-structural properties of the aggregate. Hence a systematic review has been made in this chapter for understanding the general properties of lightweight aggregate concrete and identifying the need for the present study. A review on the manufacture and properties of fly ash aggregate is presented first, followed by earlier investigations on lightweight aggregate concrete.

## 2.2 REVIEW OF MANUFACTURE OF FLY ASH AGGREGATE

The manufacturing process of lightweight aggregate from fly ash has been elaborated by Bijen (1986). Production of pellets and hardening of green pellets are the two main steps in the manufacture of artificial aggregates from fly ash. The pellets are formed by either pelletization (disc granulation, drum granulation, cone granulation and mixer granulation) or compaction techniques (uni-directional piston type compaction, roll pressing, extrusion and pellet mills). A typical flow chart for the production of aggregate using fly ash is depicted in Fig. 2.1.

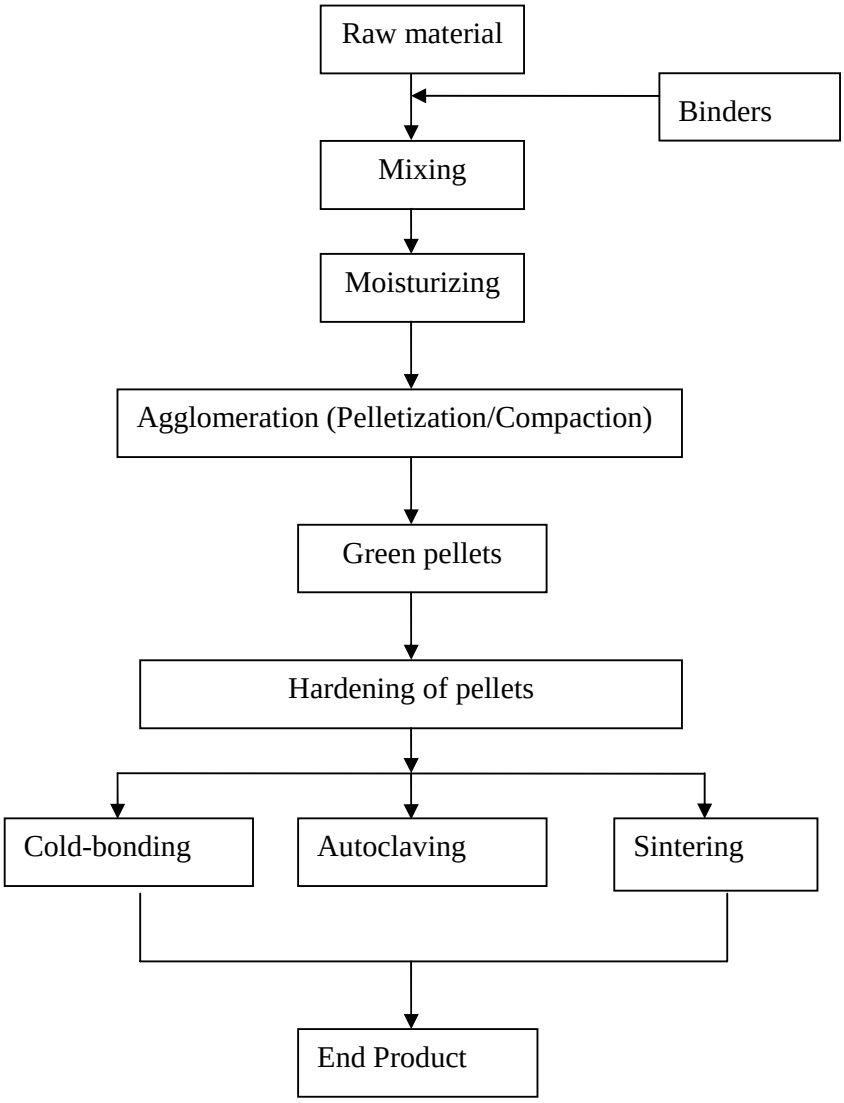


Fig. 2.1 Flow chart for the production of fly ash aggregate

### 2.2.1 Agglomeration Process

In the agglomeration through pelletization process, the pellets are formed without external compaction forces. The moisturized fly ash particles adhere together as a result of mechanical and capillary forces produced by the material moving inside a rotary device. When a fine-grained material is moisturized, a thin liquid film develops on the surface of each grain. As the moisturized particles contact each other, bridges are formed at the points of contact and bonding forces develop gradually as these particles are rotated into balls. The capillary force plays a significant role in the

magnitude of coherence of particles and is a function of particle diameter and meniscus angle between the particle and liquid binder. The pellets attain strength by mechanical forces which are produced when the balls bump against each other and against the walls of the pelletizer (Jaroslav and Ruzickova, 1998; Baykal and Doven, 2000). Disc type pelletizer is most commonly used as it is easier to control the size distribution of pellets. The green pellets are too weak to be used as aggregate. Therefore, the particles have to be bonded more firmly by subjecting the pellets to a suitable hardening technique.

In compaction technique an external compaction force is applied for making the aggregate. Aggregate produced by extrusion method are to be broken after the hardening process to get the required size fraction. The aggregate produced through compaction/extrusion process is reported to be denser and stronger as compared to the pelletized aggregate (Bijen, 1986).

### 2.2.2 Hardening Process

Irrespective of the method of agglomeration, the different hardening processes adopted are (i) cold-bonding (≤100°C), (ii) autoclaving (100-250°C) and (iii) sintering (>1000°C). Hardening of fly ash aggregate occurs due to two types of bonding (i) matrix bonding, formed by reaction of a bonding material with part of fly ash particle and (ii) material bridge bonding. Fig 2.2 shows a schematic of these two types of bonding. While the matrix bonding occurs in cold-bonded and autoclaved aggregates, a material bridge bonding happens during sintering.

#### 2.2.2.1 Cold-bonding

In cold-bonding, under normal water curing or steam curing, the fly ash reacts with calcium hydroxide to form a water-resistant bonding material, which accounts for the

pozzolanic reactivity of fly ash. Strengthening of pellets is the result of formation of C-S-H gel during the reaction (Bijen, 1986). Cold-bonded aggregate have been produced both with Class-F fly ash (Chi et al., 2003) and Class-C fly ash (Gesoglu et al., 2004; Manikandan and Ramamurthy, 2007). Depending on the material composition and fineness of fly ash, binders like cement and lime, being source of calcium hydroxide, have been used as admixture to improve the pelletization efficiency and aggregate properties through pozzolanic activity of fly ash (Yang and Huang, 1998; Baykal and Doven, 2000; Gesoglu, 2004).

Matrix bonding

Material bridge bonding

Fig.2.2 Types of bonding in the hardening process (Bijen, 1986)

**2.2.2.2 Autoclaving**

During autoclaving (high pressure steam curing) the lime (added/CaO available in fly ash) reacts with fly ash in the presence of water to form calcium silicate hydrate, a strength-giving compound. In contrast to the calcium silicate hydrate phase formed at room temperature, the compound formed through autoclaving of fly ash is crystalline in nature and the degree of crystallinity depends on the temperature and period of autoclaving. Bonding between the particles is of matrix type. The advantages of autoclaving over cold-bonding are reduction in period of curing, stronger matrix type bond between the fly ash particles resulting in lower drying shrinkage and creep of the aggregate (Bijen, 1986).

#### 2.2.2.3 Sintering

Sintering is widely used for the production of high strength artificial aggregate. The purpose of sintering is to fuse the fly ash particles together at the points of mutual contact. Bonding by material bridge occurs in the sintering process. Fly ash aggregate becomes chemically inert to most of the materials encountered in building construction and in particular, are immune to alkali-aggregate reaction (Chandra and Berntsson, 2004). Sintering temperature which usually ranges between 1000 and $1200^0$C depends on physical and chemical properties of fly ash (Rudnai, 1963; Short and Kinniburgh, 1963). Sintering strand is used in commercial production of aggregate. Sintered aggregate possess higher crushing strength, lower apparent density and water absorption than autoclaved and cold-bonded aggregates (Wegen and Bijen, 1985).

Table 2.1 summarizes the types of fly ash aggregate used by researchers in their studies. While most of the earlier studies were carried out using commercially available sintered fly ash aggregate, laboratory made cold-bonded aggregate has been used in a few investigations.

Table 2.1 Review on type of fly ash aggregate used by researchers

| Author (Year) | Type of fly ash aggregate used |
|---|---|
| Swamy and Lambert (1981) | Lytag |
| Arnaouti and Sangakkara (1984) | Lytag |
| Wegan and Bijen (1985) | Lytag |
| Zhang and Gjorv (1990a) | Sintered fly ash |
| Wasserman and Bentur (1997) | Lytag |
| Verma et al. (1998) | Laboratory made sintered aggregate |
| Al-Khaiat and Haque (1998) | Lytag |
| Yang and Huang (1998) | Laboratory made cold-bonded aggregate |
| Kayali et al. (1999) | Lytag |
| Baykal and Doven (2000) | Laboratory made cold-bonded aggregate |
| Balendran et al. (2002) | Lytag |
| Chi et al. (2003) | Laboratory made cold-bonded aggregate |
| Gesoglu et al. (2004, 2006) | Laboratory made cold-bonded aggregate |

## 2.3 PROPERTIES OF LIGHTWEIGHT AGGREGATE

The wide diversity in the source of fly ash and the manufacturing process of aggregate would result in the distinct behaviour of concrete. As a first step, it is useful to understand physical properties (surface characteristics, microstructure, density and water absorption) and the strength of aggregate as they directly influence the properties of concrete.

### 2.3.1 Surface Characteristics

Depending on the source of raw material and method of production, lightweight aggregates exhibit considerable differences in particle shape and texture. The shape may be cubical, rounded, angular, or irregular. Texture range from relatively smooth skin to highly irregular surface with large exposed pores (Swamy and Lambert, 1981; Zhang and Gjorv, 1990a). The particle shape and surface texture directly influence workability, coarse-to-fine aggregate ratio, cement requirement and water demand in concrete mixes, as well as other physical properties (Holm, 1994). Smooth and rounded particles require less cement paste to produce workable mixes compared to rough-textured and angular particles (Metha and Monteiro, 2005). Porous surface permits the penetration of cement paste, resulting in the formation of a better paste-aggregate bond.

### 2.3.2 Microstructure

The type of raw material and the hardening process has significant effect on the microstructure and thus the properties of aggregate. Properties such as density, water absorption and strength of porous materials and their relative influence on concrete properties are all dependent on its microstructure. Swamy and Lambert (1983) have reported that the porosity of aggregate varies between 25 and 75%. Based on the

microstructure examination of aggregate it is reported that the pores of various size (4 nm to 1 mm) and shape are uniformly distributed throughout its cross section with most of the pores irregular in shape and are of open and closed nature (Swamy and Lambert, 1983; Zhang and Gjorv, 1990b). Interconnected pores, which are responsible for the higher water absorption has also been observed in some types of lightweight aggregate. Owing to the higher porosity of lightweight aggregate, the interfacial transition zone (ITZ) in concrete is reported to have improved, resulting in an increased bond between aggregate and paste, and reduction in deposition of hydration products such as calcium hydroxide (CH) and ettringite (Zhang and Gjorv, 1990b). In aggregates produced by heat treatment, researchers have observed a denser outer layer, which varied with the types of aggregate (Swamy and Lambert, 1981; Zhang and Gjorv 1990b; Wassermen and Bethur, 1996). Gesoglu et al. (2007) reported that there was no clear distinction between the outer shell and the interior of cold-bonded aggregate; but observed a denser outer shell with reduced porosity and smaller pores when the same aggregate was surface treated with water glass ($Na_2O$ + $Si_2O$).

### 2.3.3 Density

The density of LWA is related to specific gravity of raw materials used, pore size and its distribution and the manufacturing technique (Harikrishnan and Ramamurthy, 2004; Gesoglu et al., 2004). Due to the presence of inter-particle pores in the aggregate and lower specific gravity of raw materials, the particle density of LWA has been observed to be lower than that of normal weight aggregate (Zhang and Gjorv, 1990a; Tay et al., 2002; Kimura et al., 2004; Gesoglu et al, 2006), while the cold-bonded aggregate to be relatively denser than sintered aggregate (Bijen, 1986). During heat treatment (i) more pores are formed in the aggregate by the trapping of

escaping gases on material expansion and (ii) un burnt coal content in fly ash converted into ash, leading to a lower particle density. Addition of binders like cement and lime to improve the characteristics of cold-bonded aggregate have also increased the particle density (Yang and Huang, 1998; Baykal and Doven, 2000). Table 2.2 summarises the bulk density of LWA reported in the literature (Zhang and Gjorv, 1990a; Neville, 2004; Baykal and Doven, 2000; Wainwright and Cresswell, 2001; Chi et al., 2003).

Table 2.2 Bulk density of lightweight aggregates

| Type of aggregate | Bulk density, kg/m$^3$ |
|---|---|
| Expanded slag | 650 |
| Rotary kiln Expanded Clay | 400 |
| Sinter-strand expanded clay | 650 |
| Expanded slate | 700 |
| Sintered fly ash aggregate | 875 |
| Pumice | 500-800 |
| Vermiculite | 60-200 |
| Bottom ash | 920 - 985 |
| Incinerator sewage sludge ash | 630 - 830 |
| Cold-bonded fly ash aggregate | 857 – 1400 |

### 2.3.4 Water Absorption Characteristics

Swamy and Lambert (1983), Wegen and Bijen (1985), Zhang and Gjorv (1990a), Yang and Huang (1998) and Gesoglu et al. (2004) reported that the water absorption of LWA was considerably higher (12 % to 45%) than normal weight aggregate due to the presence of interconnected pores and cracks. Most of the researchers observed that nearly 50 to 90% of the aggregate's 24 hour water absorption took place within 30 minutes (Swamy and Lambert, 1983; Wegen and Bijen, 1985; Zhang and Gjorv, 1990a; Chang and Shieh 1996; Lo et al., 1999). Zhang and Gjorv, (1990a) have

reported that the water absorption of whole sample of sintered aggregate was 30% less than that of half cut sample because of the denser outer shell structure. Hence an assessment of the water absorption characteristics of LWA before concrete production is critical to the process because the water absorption plays an important role in the way the concrete behaves in the fresh state. Though the higher absorbing tendency of LWA causes problem in the fresh state (i.e., workability), it is reported to result in several benefits in hardened concrete such as (i) reduced autogenous shrinkage (Kohno et al., 1999; Bentur et al., 2001; Lura et al., 2001), (ii) autogeneous curing (Weber and Reinhardt, 1997), (iii) extended cement hydration by the supply of water from the saturated LWA (Al-Khaiat and Haque, 1998; Lo et al., 1999) and (iv) improved interfacial transition zone (Zhang and Gjorv, 1990b). Holm (1994) concluded that higher water absorption capacity of aggregate also reduced the permeability of concrete by the formation of additional hydration products in the pores and capillaries.

### 2.3.5 Strength of Aggregate

It has been widely reported that the strength of LWA mainly depended on the pore structure of LWA owing to the physical and chemical compositions of raw materials and hardening method adopted (Bijen, 1986; Zhang and Gjorv, 1990a; Tay et al., 2002; Wasserman and Bentur, 1997). Formation of material bridge bond due to the fusion of fly ash particles at high temperature causes the sintered aggregate to be stronger than cold-bonded aggregate. Chi et al. (2003) and Harikrishnan and Ramamurthy (2006) report that the strength of aggregate was also influenced by the addition of binders during pelletiztaion. Addition of lime or cement to the fly ash has been reported to improve the strength of cold-bonded aggregate due to the enhanced pozzolanic reactivity of fly ash (Yang and Huang, 1998; Baykal and Doven, 2000;

Tangtermsirikul and Wijeyewickrema, 2000). Increase in strength of aggregate with an increase in fineness of raw materials has been observed by Cheeseman et al. (2005), Harikrishnan and Ramamurthy (2006) and Gesoglu et al. (2007). Surface treatment with water glass ($Na_2O + Si_2O$) is stated to result in marked increase in the strength of aggregate, being an activator and its reaction with $Ca(OH)_2$ to produce additional C-S-H (Gesoglu et al., 2007). Naturally available LWA such as volcanic cinder, pumice and scoria possess very low strength due to the higher porosity.

As lightweight aggregate possesses relatively higher water absorption and porosity and lower strength, their influence on the fresh and hardened properties of concrete and thus on the mixture design are different from that of normal weight aggregate concrete. Hence, as a next step, a review on the characteristics of lightweight aggregate concrete has been presented.

## 2.4 PROPERTIES LIGHTWEIGHT AGGREGATE CONCRETE

Table 2.3 presents an overview of research on lightweight aggregate concrete with different types of aggregate. The review on properties is classified into fresh state (workability) and the hardened properties. The hardened properties are further classified into physical (microstructure and density), mechanical (compressive and tensile strengths, modulus of elasticity, drying shrinkage, creep and bond and anchorage) and functional characteristics (permeation characteristics, carbonation, freeze-thaw behaviour, abrasion resistance, thermal conductivity and fire resistance).

### 2.4.1 Fresh Properties

A reasonable amount of work has been reported on hardened properties, while limited fresh state characteristics have been reported. Compared to concrete with normal weight aggregate, mixing procedure and workability of LWAC requires special

attention as it is influenced by the moisture condition and water absorption rate of the aggregate. It is preferable to use pre-soaked aggregate to realize the effective water-cement (w/c) ratio in the mix and to minimize the possibility of loss of slump as the concrete is being mixed, transported and placed and to maintain uniform quality of concrete (ACI 211.2, 1990). In the case of concrete using dry aggregate, the rate of water absorption of aggregate will be helpful in deciding the additional mixing water for compensating the absorption during mixing and transportation. Swamy and Lambert (1983) recommend the following mixing sequence for achieving good homogeneity and high performance; (i) lightweight aggregate is mixed for about one minute with approximately one-third of the mixing water, (ii) mixing continues with the addition of cement and sand and (iii) addition of remaining water followed by 3 minutes of final mixing. However, a two-stage mixing, with initial stage of mortar mixing and then aggregate and remaining water is also in practice (Chandra and Berntsson, 2004).

Workability tests, although carried out in normal manner, researchers suggest that they need to be interpreted differently. The slump test tends to underestimate the workability because of the lower aggregate density and less force for deformation (Chandra and Berntsson, 2004). A low-density mixture with a slump of 50-75 mm can be placed under condition that would require a slump of 75-125 mm for normal density concrete (Hossain, 2004). It has also been reported that smooth textured lightweight aggregate increases the workability, i.e. replacement of normal weight aggregate with lightweight aggregate of spherical shape and smooth texture has been observed to reduce the water demand for attaining same workability (Bai et al., 2004). Lightweight aggregate concrete for pumping needs high workability, i.e., a value of flow higher than 600 mm as determined by the flow table test.

Table 2.3 Review on lightweight aggregate concrete

| Author ( year) | Materials used | | | Properties/Parameters | | | | | | | |
|---|---|---|---|---|---|---|---|---|---|---|---|
| | | Admixture | | | | | | | | | |
| | Type of Aggregate | Mineral | Chemical | Fresh property | Density | Strength and elastic modulus | Effect of curing | Shrinkage | Durability | Functional properties | Micro-structure |
| Swamy and Lambert (1983) | SF | | | | ✓ | ✓ | ✓ | | | | |
| Dhir et al. (1984) | EC,ES | Fly ash | WR | | ✓ | ✓ | | ✓ | | | |
| Wegen and Bijen (1985) | SF | | | | ✓ | ✓ | | ✓ | ✓ | | |
| Slate et.al. (1986) | ES | | WR | | ✓ | ✓ | | | | | |
| Wilson and Malhotra (1988) | ES | Silica fume, fly ash | SP | | ✓ | ✓ | | ✓ | ✓ | | |
| Zhang and Gjorv (1991a,1991b,1992) | EC, SF | Silica fume | Dispers-ing agent | | ✓ | ✓ | | | ✓ | | ✓ |
| Sarkar et al. (1992) | EC | Silica fume | WR | | | ✓ | | | | | |
| Nilson et al. (1995) | ES | Silica fume | SP | | | ✓ | | | | | ✓ |
| Chang and Shieh (1996) | CBF, SF | | SP | | ✓ | ✓ | | | | | |
| Topcu (1997) | NL | | | ✓ | ✓ | ✓ | | | | | |
| Weber and Reinhardt (1997) | EC | Silica fume | SP | | ✓ | ✓ | ✓ | | | | ✓ |
| Yang and Huang (1998) | CBF | | SP | | | ✓ | | | | | |
| Al-Khaiat and Haque (1998) | SF | Silica fume | SP | | ✓ | ✓ | ✓ | ✓ | ✓ | | |
| Verma et al.(1998) | SF | | | | | ✓ | | | | | |
| Kayali et al.(1999) | SF | Silica fume | SP | | ✓ | ✓ | | ✓ | | | |
| Kohno et al. (1999) | ES | | SP | | | | | ✓ | | | |
| Jamal et al. (1999) | EC | | | | ✓ | ✓ | | ✓ | ✓ | | |
| Lo et al. (1999,2004,2006) | EC | | WR | | ✓ | ✓ | | ✓ | ✓ | | ✓ |
| Videla and Lopez (2000) | EC,NL | | | ✓ | ✓ | ✓ | | | | | |
| Baykal and Doven (2000) | CBF | | | | ✓ | ✓ | | | | | |
| Chia and Zhang (2002) | EC | Silica fume | SP | | | | | | ✓ | | |
| Gao et al. (2002) | AL | Fly ash, Silica fume | WR | | | ✓ | | | ✓ | | ✓ |
| Lura et al. (2001) | ES | | | | | ✓ | | ✓ | | | |
| Mannan and Ganapathy (2002) | OPS | | SP | | ✓ | ✓ | | ✓ | | | |
| Chi et al.(2003) | CBF | | SP | | | ✓ | | | | | |
| Sahin et al. (2003) | NL | | | ✓ | | ✓ | | | | | |
| Gesoglu et al. (2004, 2006,2007) | CBF | Silica fume | SP | | ✓ | ✓ | | ✓ | | | |
| Hossain K.M.A(2004) | NL | | | ✓ | ✓ | ✓ | | ✓ | | | |
| Sari et al. ( 2005) | NL | | SP, AEA | | ✓ | ✓ | | | | | |
| Chia et al., 2005 | EC | Silica fume | SP | ✓ | | | | | | | |
| Gunduz and Ugur (2005) | NL | | | | ✓ | ✓ | | | ✓ | | |
| Teo et al. (2007) | OPS | | SP | | ✓ | ✓ | | ✓ | | | |
| Chen and Liu (2008) | EC | Fly ash, Silica fume, BS | SP | ✓ | ✓ | ✓ | | | | | |

SF-Sintered Fly ash, EC-Expanded Clay, ES-Expanded Shale, CBF-Cold-bonded Fly ash, AL-All-in Lightweight aggregate, OPS-Oil Palm Shell, NL-Natural LWA
BS- Blast furnace Slag, WR-Water Reducer, SP-Superplasticizer, AEA- Air Entraining Agent

### 2.4.2 Physical Properties

#### 2.4.2.1 Microstructure

The type of aggregate and its pore-structure determines the nature of microstructure of LWAC and its properties. Investigations into the microstructure of LWAC have revealed that the interaction of LWA and the mortar is quite different from that in concrete with conventional crushed granite aggregate; cement paste can penetrate into the pores of the surface layer of aggregate, the interface is characterized by a mechanical interlocking in combination with a chemical interaction in the form of pozzolanic reaction (Zhang and Gjorv, 1990b, c). The 'wall effect' that appears at the surface of the aggregate of normal weight concrete does not occur on the interfacial transition zone of LWAC (Lo and Cui, 2004). Zhang and Gjorv (1990b) have pointed out that the aggregate with a dense outer layer has an ITZ similar to that in concrete with normal weight concrete, whereas aggregate having porous outer layer results in dense and homogenous ITZ. Wasserman and Bentur (1996) have investigated the nature of ITZ of LWAC with polymer treated and normal sintered fly ash aggregate and the difference observed in ITZ and strength of concrete is attributed to the porosity and absorption capacity of aggregate. In addition to the micro-structural characteristics of LWA, the nature of ITZ in LWAC is also reported to depend on the particle size distribution and viscosity of the paste (Zhang and Gjorv, 1992). Generally, the micro cracks significantly weaken the interfacial region of normal concrete because of the induced stresses by differential movements, such as drying shrinkage or temperature changes and elastic mismatch between aggregate and cement matrix. As the elastic modulus of lightweight aggregate is closer to that of the matrix, the stress concentrations are significantly lower at the aggregate-matrix interface of LWAC and thereby lesser micro cracking (Bremner and Holm, 1986).

#### 2.4.2.2 Density

Many physical and mechanical properties of LWAC depend on its density. A reduction in the density results in improved functional properties viz., fire resistance, thermal insulation and acoustical properties, while causing a reduction in mechanical properties like compressive strength, modulus of elasticity and tensile/compressive strength ratio. The density of concrete depends on factors such as proportion of ingredients, physical characteristics of LWA, type and volume fraction of aggregate, w/c ratio, cement content and proportion of mineral admixtures. An increase in the percentage of LWA is reported to reduce the density of concrete, proportional to the amount of LWA (Demirboga et al., 2001; Sahin, et al., 2003; Hossain, 2004). According to Short and Kinniburgh (1963), the density of concrete can be further reduced by the use of lightweight fines (instead of sand). Incorporation of mineral admixtures (fly ash, silica fume etc.) can also reduce the density of concrete due to lower specific gravity of these mineral admixtures compared to cement (Demirboga et al., 2001).

### 2.4.3 Mechanical Properties

#### 2.4.3.1 Compressive strength

The strength of lightweight aggregate concrete is generally determined by the individual strengths of the aggregate and mortar as well as the type of stress distribution, which is further affected by the relative values of elastic modulus of the aggregate and mortar (Grubl, 1979; Chi et al. 2003). The failure in lightweight aggregate concrete most often has been observed through the aggregate than around it (Clarke, 1993). The type of LWA, its physical characteristics and particle strength are stated to be the limiting factors in controlling the achievable concrete strength (Grubl, 1979; Wilson and Malhotra, 1988; Clarke, 1993). However the strength of LWAC is

also reported to be highly influenced by other factors like degree of saturation of aggregate, cement content, inclusion of mineral admixtures, method and period of curing, water-binder ratio, specimen shape and size. Table 2.4 presents a review on the strengths and modulus of elasticity of lightweight aggregate concrete reported for various types of lightweight aggregate. Though the compressive strength of concrete in general increases with an increase in its density, the strength of concrete is also affected by the type of aggregate (Clarke, 1993). Cold-bonded aggregate concrete resulted in a relatively lower strength than sintered aggregate concrete in spite the former is relatively denser (Table 2.4). Wasserman and Bentur (1996) reported that pore structure of LWA and its effect on the aggregate-matrix interfacial bond have marked influence on the compressive strength of concrete.

The compressive strength of concrete (with cement content more than 400 kg/m$^3$) has been reported to decrease with volume fraction of LWA as it is weaker than the matrix (Chi et al., 2003; Gesoglu, 2004; Hossain, 2004). It has also been concluded that the influence of LWA content on the compressive strength diminishes at low strength level of concrete (Swamy and Lambert, 1983). Addition/replacement of mineral admixtures such as fly ash, silica fume and slag has been stated to enhance the compressive strength. Due to higher pozzolanicity, silica fume significantly increases the early strength (Wilson and Malhotra, 1988; Gesoglu, 2004). Degree of saturation of aggregate also has significant effect in controlling the strength of concrete (Lura, 2003) and the strength is reported to increase with an increase in pre-wetting time of aggregate (Lo et al., 2004). Saturated LWA supplies water to the surrounding matrix and accelerates the cement hydration resulting in dense matrix and increased compressive strength (Wasserman and Bentur, 1996). This effect is beneficial in low w/c ratio, where considerable amount of unhydrated cement is

present. In concrete with a low water-cementitious ratio, Kohno et al. (1999) report that the early age self-desiccation was reduced due to supply of water from the porous aggregate. Vaysbaurd (1996) concludes that such reduction in self desiccation in turn reduces the micro-cracks and voids in the system and increases the durability.

Table 2.4 Review on strength and elastic modulus of LWAC

| Author (year) | Type of aggregate | SSD sp. gravity / Dry bulk density($kg/m^3$) | Water Absorption (%) | Cement /Binder content ($kg/m^3$) | Fresh density of concrete ($kg/m^3$) | Compressive strength, $f_c$ ( MPa) | Split tensile strength (MPa) (Regression Equation) | Modulus of Rupture (MPa) (Regression Equation) | Static elastic modulus (GPa) (Regression Equation) |
|---|---|---|---|---|---|---|---|---|---|
| Gesoglu et al. (2004) | Cold-bonded fly ash | 1.78 | 24 | 436-600 | 1950-2170 | 20.8-47.3 | 1.86-3.94 ($0.27\ f_c^{0.67}$) | - | 14.2-24.4 |
| Lo et. al. (2004) | Expanded clay | 405 | 8.7 | 420-450 | 1757-1920 | 29.2-42.9 | - | 3.46-4.56 ($0.69\ f_c^{0.5}$) | 15-20.3 |
| Hossain (2004) | Volcanic pumice | 763 | 37 | 430-490 | 1733-1880 | 24-28 | 2.2-2.6 | | 10-10.5 |
| Chi et al. (2003) | Cold-bonded fly ash | 1.65-1.76 | 20.8-30.4 | 453-602 | 1939-2175 | 21.3-48.2 | - | - | 13.3-23.9 |
| Curico et al. (1998) | Expanded clay | 785 | 8 | 501 | 1904 | 80.5 | 5.2 | 7.8 | 24 |
| Al-Khaiat and Haque (1998) | Sintered fly ash | 1.76 | 13.1 | 550 | 1820 | 51 | 3.3 | 4.4 | 26.1 |
| Chang and Shieh (1996) | Cold-bonded fly ash | 1.64 | 23.8 | 522 | 2084 | 33.9 | 2.92 | 2.37 | 22.3 |
| Zhang and Gjorv (1991a) | Expanded clay, Sintered fly ash | 1.07-1.44[8] | 8-13 | 440-660 | 1595-1865 | 57 – 102 | 3.5- 5.6 ($0.23\ f_c^{0.67}$) | 5.4-7.3 ($0.73\ f_c^{0.67}$) | 17.8-25.9 |
| Dhir et al.(1984) | Expanded clay/shale | 1.64 | 13.5 | 300-600 | 1693-1786 | 20-60 | 2.6-4.2 ($0.12\ f_c$-$0.001\ f_c^2$) | - | 12-18 ($2.7 f_c^{0..49}$) |
| Swamy and Lambert(1983) | Sintered fly ash | 1.76 | 13.1 | 250-485 | 1980-2035 | 20-60 | 2.13-4.58 ($0.3\ f_c^{0.64}$) | 3.12-5.08 ($0.9\ f_c^{0.43}$) | 15.5-22 ($5.82 f_c^{-32}$) |

$f_c$: cube compressive strength, *dry particle density

Weber and Reinhardt (1997) have reported that the saturated lightweight aggregate can act as water reservoirs supporting continuous internal curing and maintain internal humidity at a higher level for a longer period of time and LWAC is relatively insensitive to curing conditions. However, many researchers have concluded that the compressive strength of LWAC is also influenced by the curing conditions though the aggregate facilitates the internal curing (Swamy and Lambert, 1983; Dhir et al, 1984;

Slate et al. 1986; Smadi and Migdady, 1991; Al- Khait and Haque, 1998). Swamy and Lambert (1983) observed no significant variation in 28-day compressive strength between water cured and air cured sintered fly ash aggregate concrete. But the improvement in strength after 1-year was observed to be higher in water cured concrete than the air cured specimen.

#### 2.4.3.2 Tensile strength

The tensile strength (both split tensile and flexural tensile strengths) of LWAC reported by various researchers and the relationship between compressive and tensile strength of concrete for different lightweight aggregates are summarized in Table 2.4. It can be observed that the relationship between strength characteristics of concrete is also influenced by the type of aggregate. Review indicated that the tensile strength of concrete is more sensitive to the curing condition. As the water content in lightweight aggregate concrete is higher, in drying situations (without any curing), a greater moisture gradient is developed in concrete, which is reported to cause a reduction in the tensile strength (Clarke, 1993). Swamy and Lambert (1983) have reported that the tensile to compressive strength ratio ranges from 8 to 11% and 5 to 11% respectively for water cured and air cured specimen. Dhir et al. (1984) also have reported similar behaviour. Pfeifer (1967) conclude that the split tensile strength of LWAC tends to increase with an increase in sand content. Lydon and Balendran (1980) have observed 20 to 30% lower uniaxial tensile strength in high strength lightweight concrete with sintered fly ash and clinker aggregate than that of normal weight concrete of similar w/c ratio and volume of coarse aggregate. Inclusion of fiber reinforcement causes 50 to 100% increase in the tensile strength of LWAC (Gao et al., 1997; Balendran et al., 2002; Kayali et al., 2003). It has been concluded that the addition of silica fume in

cold-bonded aggregate concrete mixes with low w/c ratio improved the split tensile strength compared to mixes with high w/c ratio (Gesoglu et al., 2004).

#### 2.4.3.3 Modulus of elasticity

The elastic modulus and stiffness of concrete is influenced by the modulus and volume fraction of both mortar and aggregate. According to FIP (1983), the modulus of elasticity of lightweight aggregate mainly depends on the particle density, the shape and the volume of pores in the aggregate and it corresponds to a parabolic function of the particle density of aggregate. In the case of artificial aggregate, it is not easy to obtain the information about the elastic properties as in rock-based aggregate. Nilsen et al. (1995) and Yang (1997) have adopted a composite theory based on Mori-Tanka model to determine the aggregate modulus. Elastic modulus of LWAC and the prediction relationships proposed by various researchers summarised in Table 2.4 demonstrate the influence of aggregate type in determining elastic properties of concrete. Zhang and Gjorv (1991a) state that in addition to the stiffness and volume of aggregate, the paste-aggregate bond is also a decisive factor in the modulus of elasticity of concrete. Chi et al. (2003) and Gesoglu et al. (2004) have observed that the modulus of elasticity of concrete with cold-bonded aggregate has gradually decreased with an increase in aggregate content. In concrete with low volume fraction of lightweight aggregate, the elastic modulus of concrete is reported to be independent of aggregate type and mainly controlled by the w/c ratio of the paste (Chi et al., 2003).

#### 2.4.3.4 Drying shrinkage

Loss of moisture from the concrete causes drying shrinkage and is considered to be an important parameter in lightweight aggregate concrete used for structural purpose.

The drying shrinkage is also attributed to the porosity and absorption capacity of different aggregates, i.e., higher the porosity of aggregate, the higher its drying shrinkage (Hossain, 2004). The drying shrinkage of LWAC also depends on factors such as (i) amount of shrinkage medium like cement and pozzolanic materials viz., fly ash and silica fume, (ii) volume fraction of aggregate, (iii) resistance of aggregate and (iv) ambient temperature and humidity. The shrinkage characteristic of LWAC is not clear because of the difference in opinion regarding the rate and total shrinkage reported by researchers. A reduction of 3 to 35 % in drying shrinkage is reported for concrete which replaced lightweight fines with sand (Pfeifer, 1968). Wegen and Bijen (1985) observed higher drying shrinkage in concrete with autoclaved aggregate as compared to those with sintered aggregate even though there was not much difference in their absorption capacities. Higher drying shrinkage of autoclaved aggregate concrete has been attributed to the smaller restraining effect due to lower modulus and the shrinkage of the aggregate itself. Nilsen and Aitcin (1992) concluded that LWAC with expanded shale had 30 to 50% lower shrinkage as compared to concrete with normal weight aggregate which was attributed to the presence of higher moisture in the lightweight aggregate. Shrinkage of LWAC containing dense fine aggregate has been observed to be similar to that of normal weight concrete, attributing it to the relief of restraint by creep and the continuous supply of moisture from saturated aggregate (Clarke, 1993). Sarkar et al. (1992) have reported that a good bond between the aggregate and the surrounding matrix provides resistance against the change in length induced by moisture or thermal effects. In addition to this positive effect, LWA prevents self-desiccation at early age and delays the occurrence of shrinkage cracking (Gesoglu et al., 2004). However, Neville (2004) indicates that LWAC possess higher shrinkage than normal weight concrete due to lower elastic modulus of the resisting medium (lightweight aggregate).

Al-Khaiat and Haque (1998) have reported moderately high shrinkage strain (640 micro strain) in concrete with sintered aggregate subjected to 6 days of curing and thereafter exposed to drying. Kayali et al. (1999) observed that the drying shrinkage in concrete with sintered fly ash aggregate and cementitious content of 785 kg/m$^3$ was twice as that of normal weight concrete with a cementitious content of 485 kg/m$^3$. A longer period is required in LWAC to slow down the rate of shrinkage as compared to normal weight concrete. Use of steel fibers has been reported to reduce the shrinkage (Kayali et al., 1999). Concrete with higher volume fractions of cold-bonded aggregate has exhibited higher weight loss and shrinkage strain due to excess water released by saturated aggregate (Gesoglu et al., 2004). Addition of silica fume has been observed to reduce the drying shrinkage due to densification of hydrated cement paste (Haque, 1996; Gesoglu, 2004).

#### 2.4.3.5 Creep

Creep of LWAC has been observed to be influenced by factors such as age of concrete and loading, modulus of elasticity of aggregate, rate of moisture loss, stress to strength ratio and both water and cement content of the mix composition (Arnaouti and Sangakkara, 1984; Wegen and Bijen, 1985; Tasdemir et al., 1988; Wilson and Malhotra, 1988). Higher creep strains are produced in LWAC as compared to normal weight concrete due to lower modulus of elasticity of aggregate and greater rate of moisture loss (Wilson and Malhotra, 1988). But the influence of paste content on the creep of lightweight aggregate concrete is the same as in the case of concrete with normal weight aggregate (Rutledge and Neville, 1966). Arnaouti and Sangakkara (1984) observed in sintered fly ash aggregate concrete that (i) basic creep was independent of specimen size and (ii) even though drying creep was higher for smaller specimen at the initial stage, the influence of specimen size was negligible as

period increases. The creep, in most cases, decreases with an increase in strength of concrete. It also reduces with an increase in sand content (Pfeifer, 1968). The creep of concrete with sintered aggregate reported to be lower than that in concrete with autoclaved aggregate, since the creep of sintered material is much smaller than autoclaved material (Wegen and Bijen, 1985). LWAC incorporating mineral admixtures such as silica fume and fly ash exhibited a reduction in creep which is attributed to the improvement in strength of concrete resulted from the pozzolanic action and filler effect (Wilson and Malhotra, 1988; Gesoglu et al., 2004).

#### 2.4.3.6 Bond and anchorage

Reinforcement bond in LWAC is influenced by the proportion of concrete, casting and compacting methods, concrete strength and type of reinforcing bar (Rudnai, 1963). In comparison to normal concrete of similar compressive strength, the bond strength of lightweight concrete with sintered aggregate has been observed to be around 75% of normal concrete (Orangun, 1967). Campione et al. (2005) have reported that the maximum value of bond strength was highly influenced by the brittle nature of lightweight aggregate. Anchorage in lightweight aggregate concrete was reported to be lower than that of normal weight concrete due to lower bearing strength caused by relative weakness of lightweight aggregate (Clarke, 1993). Mor (1992) observed that bond slip properties of concrete was influenced by the type of aggregate in high strength mix. In lightweight aggregate concrete, the compatibility between the aggregate and matrix minimises cracking due to differential strains under stress and allows the concrete to utilize fully the adhesion developed between the concrete and the steel reinforcing bar. The bond strength of lightweight aggregate concrete was observed to vary between 20 and 42% of its compressive strength depending on the type of aggregate and curing method adopted (Teo et al., 2007).

### 2.4.4 Functional Properties

#### 2.4.4.1 Permeation characteristics

While the lightweight aggregate is rather porous in nature, several researchers have reported that the permeation characteristics of LWAC was equal to or lower than that of concrete with normal weight aggregate (Zhang and Gjorv 1991b; Vaysburd, 1996; Chia and Zhang, 2002). Such beneficial behaviour have been attributed to (i) denser interfacial zone, (ii) a more unified and homogeneous structure and (iii) reduction in internal stresses due to volume changes in the initial unloaded state (Zhang and Gjorv, 1991b). Furthermore, the frequency of micro-cracks caused by shrinkage in the interfacial zone is low due to the deformability of aggregate. Hence, the permeability of concrete is mostly controlled by quality of mortar matrix rather than the type of coarse aggregate used. An increase in cement content reduces the permeability, but beyond a certain level, the permeability is reported to increase with cement content. At higher cement content, occurrence of micro-cracks (due to increased heat of hydration) increases permeability considerably. Zhang and Gjorv (1991b) have reported that replacement of fine LWA with natural sand reduces the permeability. AL-Khaiat and Haque (1998) attribute the permeability to curing condition; water curing improves the permeability than air curing. Lydon (1995) has reported that the permeability of adequately cured LWAC was comparable to normal weight concrete of similar 28-day strength, but the severity due to early drying was higher in air dried LWAC as accessible pores become available fairly quickly during drying.

The factors influencing chloride ion penetration in LWAC are observed to be the same as those stated for water permeability. Chandra and Berntsson (2004) have reported that chloride penetration depends on the amount of CH and calcium aluminate ($C_3A$) in the mortar matrix. CH reacts with penetrated chloride ion, forms

leachable compound, causing porosity to the mortar matrix whereas $C_3A$ reacts with the chloride ion forms inert products like 'friedals salt' ($3CaO.Al_2O_3.CaCl_2.10H_2O$). Therefore, addition of mineral admixtures like silica fume and fly ash having more silica and alumina content is advantageous in reducing the chloride ion penetration. A review on the studies of chloride ion penetration in lightweight aggregate concrete is presented in Table 2.5.

Table 2.5 Review on chloride ion penetration in lightweight aggregate concrete

| Author (s) | Test Method | Type of aggregate | Type of concrete and salient observation |
|---|---|---|---|
| Lo et al. ( 2006) | ASTM C 1202 | Expanded clay | Studies on concrete with air entraining agents. Resistance decreases with air content |
| Babu and Babu (2003) | ASTM C 1202 and corrosion studies | Expanded polystyrene | Increased resistance in mixtures with silica fume. Total charge passed less than 1000 Coulombs. |
| Chia and Zhang (2002) | ASTM C 1202 and Immersion test. | Expanded clay | Increased resistance with reduction in w/c ratio and incorporation of silica fume. Resistance of LWAC is in the same order as through corresponding normal weight concrete. |
| Carlsson (2000) | Diffusion method | Expanded clay | Warm and cold curing on diffusion coefficient and chloride concentration is compared. Depth of concrete for a fixed concentration of chloride is not much affected by curing condition |
| Bilodeau et al., (1995) | ASTM C 1202 | Aggregate with water absorption 5.2 to 22.6% | Chloride penetration depends on water absorption property of aggregate. Low resistance in concrete with aggregate of high absorption. Resistance increases with compressive strength. |
| Gjorv et al. (1994) | Modified AASHTO T 277 | Expanded clay | Permeability and diffusivity increases with increase in curing temperature. More in concrete with wet lightweight aggregates. |
| Zhang and Gjorv (1991b) | Modified AASHTO T 277 | Expanded clay and sintered fly ash | Chloride penetration 'very low' in mixtures with high cementitious content. Higher resistance with silica fume. |

### 2.4.4.2 Carbonation

Carbonation of LWAC mainly depends on the duration of exposure, w/c ratio, type of cement, curing and environmental conditions (Mays and Barnes, 1991; Batis et al., 1996). Lydon (1987) has pointed out that in concrete with cement content of 350

kg/m$^3$ and above, the type of aggregate is having only marginal influence on carbonation whereas the cement content and exposure conditions are the main influencing factors. Mixtures with higher cement content perform better; showing lower depths of carbonation (Gunduz and Ugur, 2005). Measurement of carbonation depth on LWAC samples after 20 years exposure by Mays and Barnes (1991) showed values ranging from 6 to 25 mm, indicating that the carbonation depth in most cases were lower than the concrete cover. Haque et al. (2004) concluded that the effect of initial curing on the depth of carbonation was marginal in LWAC with sand as fine aggregate compared to total lightweight aggregate concrete in hot marine environment.

#### 2.4.4.3 Freeze-thaw behaviour

The freeze-thaw resistance of LWAC is governed by the degree of saturation of voids in the aggregate (Wegen and Bijen, 1985; Johnston and Malhotra, 1987; Wilson and Malhotra, 1988; Holm, 1994). Relatively higher amount of absorbed water in the aggregate is reported to result in severe freeze-thaw conditions (Wegen and Bijen, 1985). But from the field studies, Lydon (1987) stated that freeze-thaw resistance of LWAC was better than non air-entrained normal weight concrete. The difference in laboratory and field observation is attributed to the conditioning of laboratory samples prior to freeze-thaw test. Lightweight aggregate concrete with a high degree of saturation, when used in structures exposed to air, drying has strong effect on improving their durability against freezing and thawing, except some initial frost damage immediately after placing (Fujiki et al., 1998). Wilson and Malhotra (1988) reported that high strength lightweight aggregate concrete exhibited satisfactory resistance to freezing and thawing cycle. Khayat (1991) observed that relatively dry high strength lightweight concrete was not susceptible to the type of frost action

encountered in cryogenic environments, while the compressive and tensile strengths of saturated concrete were reduced by 11 and 20 % respectively after 5 gradual frost cycles. Gao et al. (2002) have reported that the addition of fly ash prevented the formation of micro-cracks and suppressed its propagation thereby increased the durability of LWAC with respect to frost action.

#### 2.4.4.4 Abrasion resistance

Abrasion resistance of lightweight aggregate concrete improves with increase in compressive strength. Clarke (1993) reports that the resistance can be improved by (i) combining relatively soft coarse aggregate with a hard fine aggregate, (ii) improving the quality of the matrix and (iii) use of surface treatments. The use of natural sand in lightweight aggregate concrete improves resistance to abrasion since the coarse aggregate is depressed slightly below the surface during the floating and troweling operation. The type of bond developed in LWAC is also reported to be helpful in enhancing the resistance to abrasion and observed to be comparable to that of normal concrete (Chandra and Berntsson, 2004).

#### 2.4.4.5 Thermal conductivity

Thermal conductivity depends on pore structure and pore size distribution of lightweight aggregates and the cement paste matrix. As the thermal conductivity is a function of density, light porous aggregate will produce concrete of relatively lower thermal conductivity. While the thermal conductivity of normal concrete is reported to be in the range of 1 to 1.5 W/mK, the thermal conductivity of lightweight aggregate concrete varies from 0.15 to 0.7 W/mK (Demirboga and Gul, 2003; Wang and Tsai, 2006). Thermal conductivity is also stated to be influenced by the moisture content of the concrete. Since wet concrete transmits heat better than dry concrete, increase in

moisture content of aggregate increases the thermal conductivity of concrete (Loudon, 1979). Demirdag and Gunduz (2008) have stated that higher cement content causes an increase in thermal conductivity because of the increased density. Reduction in thermal conductivity (maximum of 43.5 %) is reported with an increase in replacement level of cement with mineral admixtures such as silica fume and fly ash in expanded perlite aggregate concrete (Demirboga and Gul, 2003). Fly ash has higher potential in decreasing thermal conductivity because of its amorphous texture than silica fume.

#### 2.4.4.6 Fire resistance

The pore structure and moisture content concrete are the most deciding factors for the fire resistance of concrete (Chandra et al., 1980). The residual strength of LWAC after fire exposure is reported to be higher than normal weight concrete because of low thermal conductivity and thermal expansion of LWAC (Chandra et al, 1980; Jau and Wu, 1995). Low thermal expansion of LWAC is attributed to the significantly lower coefficient of thermal expansion of the lightweight aggregate than the granite aggregate (FIP, 1983). LWAC of higher strength made with rich matrix has a deleterious effect on the fire resistance owing to the lower permeability and building up of higher vapour pressure (Chandra and Berntsson, 2004). However, this can be reduced significantly by polymer addition and incorporation of polypropylene fiber, which creates a channel for releasing vapour at higher temperature (Chandra et al., 1980). Bilodeau et al. (2004) have concluded that the LWAC with high absorption capacity aggregate in saturated condition was more susceptible to spalling than concrete with low absorption aggregate. In the case of low absorption capacity aggregate, there was no significant difference between concrete using saturated

aggregate and dry aggregate in the volume of spalling when concrete was exposed to hydrocarbon fire.

## 2.5 NEED FOR THE PRESENT STUDY

Overall review highlights that limited studies have been reported on concrete using cold-bonded fly ash aggregate. Since cold-bonded aggregate exhibit lower crushing value and higher water absorption, the characteristics of concrete which are specific to sintered aggregate properties cannot be applied directly to cold-bonded aggregate concrete. Most of the studies on cold-bonded aggregate concrete have been confined to the mechanical properties of concrete and that too with relatively higher cement content (> 400 kg/m$^3$) thereby introducing a strong matrix phase in the concrete. Hence a systematic study on the fresh and hardened properties of cold-bonded aggregate concrete covering a wide range of parameters is felt necessary to understand the concrete behaviour with variation in mixture proportions**.**

# CHAPTER 3

# OBJECTIVES AND SCOPE OF THE PRESENT STUDY

## 3.1 GENERAL

From the critical review of earlier research on lightweight aggregate concrete the need for an in depth study on the properties of cold-bonded fly ash aggregate concrete has been brought out in the previous chapter. The objectives and scope for the present study have been defined in the following sections.

## 3.2 OBJECTIVES

The objectives of present study are:

i. To investigate the influence of mixture composition on workability, strength and permeation behaviour of cold-bonded aggregate concrete through statistically designed experiments.

ii. To study the influence of fly ash as cement/fine aggregate replacement in cold-bonded aggregate concrete on its compressive strength and permeation behaviour.

iii. To investigate the influence of cold-bonded fly ash aggregate on the autogenous curing characteristics of concrete under different curing conditions.

## 3.3 SCOPE

The scope of the study is limited to the following with respect to raw materials used and methodology adopted:

i. The study is restricted to concrete with cold-bonded fly ash aggregate produced in the laboratory using a typical Class-C fly ash.

**ii.** Study on permeation behaviour of concrete is limited to porosity, sorption and rapid chloride ion penetrability.

iii. For studies on partial replacement of cement and fine aggregate with fly ash, a typical Class-F fly ash has been used.

# CHAPTER 4

# WORKABILITY AND STRENGTH BEHAVIOUR OF COLD-BONDED FLY ASH AGGREGATE CONCRETE

## 4.1 GENERAL

A critical review of literature presented in Chapter 2 indicates that aggregate, which constitutes a major volume in concrete, has significant influence on the properties of concrete. The characteristics of aggregate that are significant to the concrete properties include water absorption, porosity, particle size distribution, shape and surface texture, crushing strength and elastic modulus. This chapter discusses (i) the influence of mixture composition on workability and mechanical properties of concrete through single factor experiments, (ii) regression models and response surface developed for the workability and strength of cold-bonded aggregate concrete in terms of mix proportioning variables through statistically designed experiments based on Response Surface Methodology and (iv) a typical mixture design guidelines for cold-bonded aggregate concrete.

## 4.2 COLD-BONDED FLY ASH AGGREGATE

### 4.2.1 Materials Used

Fly ash conforming to Class-C as per ASTM C 618 (2005) was used through out the study for the production of cold-bonded aggregate in the laboratory. The Physical and chemical characteristics of fly ash used is summarised in Table 4.1.

### 4.2.2 Production of Cold-bonded Fly Ash Aggregate

Cold-bonded aggregate produced from normal water curing of pelletized fly ash has been adopted for the entire experimental study of this investigation as it consumes

very less energy against accelerated curing methods such as autoclaving or steam curing. Pelletization was carried out in the laboratory using a disc pelletizer (Fig. 4.1). The parameters of the pelletization viz., angle and speed of revolution of pelletizer, duration of pelletization, admixture/binder content and the moisture content for maximizing the pelletization efficiency were fixed from an earlier study on the influence of pellitization on production of fly ash aggregate (Manikandan, 2006). The speed and angle of pelletizer were maintained at 55 rpm and 55º respectively for obtaining maximum pelletization efficiency (the ratio of the mass of aggregate of size greater than 4.75 mm produced to the fly ash used), maximum strength and minimum water absorption of the aggregate. The fly ash was moistened by spraying water (30% by weight of fly ash) during the first 3 minutes of agglomeration process and the duration of pelletization was limited to 13 minutes. The green pellets were kept under shade (at room temperature) for 24-hours for sufficient hardening and then subjected to normal water curing (at a temperature range of 27 $\pm$ 2 ºC) for 28 days. The aggregate size fraction passing 12.5 mm and retained in 4.75 mm sieve was used in the present study (Fig. 4.2).

Table 4.1 Physical and chemical properties of fly ash used for aggregate production

| **Physical properties** | | |
|---|---|---|
| Specific gravity | 2.64 | |
| Fineness ($m^2$/kg) | 414 | |
| **Chemical properties** | | |
| | (% by mass) | ASTM C618 (Class-C) |
| Silicon dioxide ($SiO_2$), % | 31.62 | - |
| Calcium Oxide (CaO), % | 17.17 | >10 |
| Alumina ($Al_2O_3$) % | 30.11 | - |
| Ferric Oxide ($Fe_2O_3$),% | 8.94 | - |
| Magnesia (MgO), % | 3.71 | 5 (max) |
| Sodium Oxide ($Na_2O$),% | 0.74 | - |
| Potassium Oxide ($K_2O$), % | 0.10 | - |
| Sulphuric anhydride ($SO_3$), % | 5.72 | - |
| Manganese Oxide (MnO), % | 0.02 | - |
| Loss on Ignition, % | 3.18 | - |
| $SiO_2 + Al_2O_3 + Fe_2O_3$ | 70.67 | 50 (min) |

Fig.4.1 View of disc pelletizer

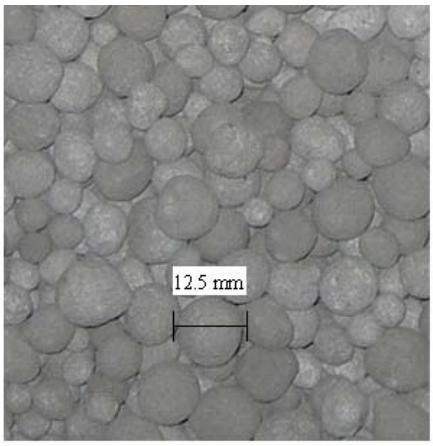


Fig. 4.2 Cold-bonded aggregate

### 4.2.3 Properties of Cold-bonded Fly Ash Aggregate

#### 4.2.3.1 Water absorption and porosity

The water absorption of aggregate is significant in concrete production as it determines the amount of water available during mixing and the effective w/c ratio of the mix. Only the open pores which are interconnected take part in permeation. Water absorption and open porosity (volume of permeable pores) of aggregate was determined at different periods of curing after drying the aggregates in an oven at a temperature range of 100 $\pm$ 5 °C to a constant mass. 500 g of oven dried aggregate was used for both the tests. For estimating water absorption, oven dried aggregates were immersed in water for 24 hrs and then the mass of saturated surface dry aggregate was measured. The water absorption is the increase in mass expressed as a percentage of oven-dried mass. Open porosity in the aggregate was calculated from

samples saturated under vacuum (following the procedure in ASTM C 1202 (2005) using the equation $\frac{(W_{sat} - W_{dry})}{(W_{sat} - W_{wat})} \times 100$ where, $W_{sat}$ and $W_{wat}$ are the weight of the vacuum saturated sample in air and water respectively and $W_{dry}$ represents the weight of oven dried sample.

Fig. 4.3 shows the influence of curing on the 24 hr water absorption and open porosity of aggregate. As the period of curing increased from 3 to 28 days the water absorption and porosity of aggregate was observed to reduce respectively from 25.5 to 20.5% and 44.6 to 38 %. The reduction in water absorption and porosity with period of curing is due to the refinement of pores and formation of dense structure in the aggregate, owing to the hydration and pozzolanic reaction of ashes. However the water absorption of this aggregate is relatively higher compared to the absorption of sintered fly ash aggregate (13.1% (Table 2.4)).

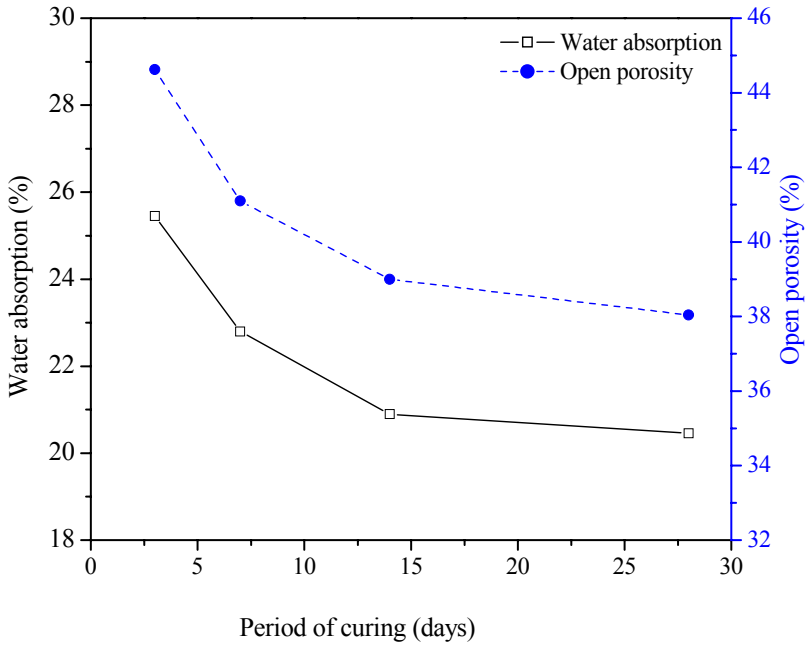


Fig. 4.3 Water absorption and porosity of cold-bonded aggregate with curing period

Apart from water absorption, the rate of absorption of aggregate is important to arrive at the optimal period of pre-soaking of aggregate. Fig. 4.4 presents the rate of water absorption of 28–day cured samples represented as a percentage of its 24 hour water absorption. It can be observed that more than 85% of the 24 hour water absorption occurred within the first 10 minutes of soaking and about 93% within 30 minutes.

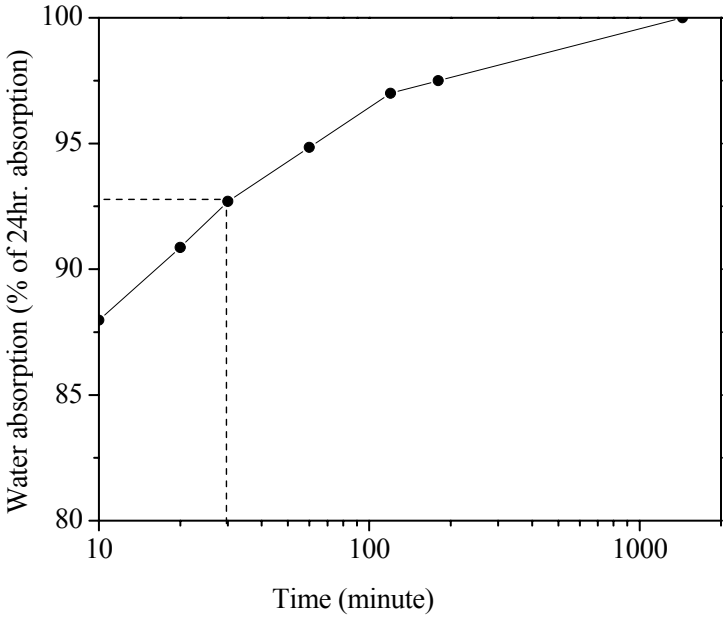


Fig. 4.4 Rate of water absorption of cold-bonded aggregate

#### 4.2.3.2 Strength of aggregate

In the case of porous artificial aggregate, the direct determination of strength cannot be done as in natural aggregate where the evaluation through specimens of parent rock is possible. Hence the strength of artificial aggregate is generally assumed to be related to the resulting 'ceiling strength' of concrete (FIP, 1983). However, the aggregate can be evaluated through standard tests such as abrasion resistance, impact and aggregate crushing value/ten percent fines value. Since the crushing value test is insensitive to the variation in strength of aggregates whose crushing value exceeds 25% (Neville, 2004), the strength of cold-bonded aggregate has been evaluated

through ten percent fines value (IS 2386: part IV, 2002) and crushing strength (BS 812: part 110, 1990). For the determination of 10% fines value, aggregates with grain size 10-12.5 mm were used while for the crushing strength evaluation, aggregates of 12.5 mm nominal size were used.

In crushing strength test, individual pellets were placed between two parallel plates and loaded with constantly increasing force, till the failure occurs. Statistically representative number of aggregates was determined according to ASTM E 122 (2000). The sample size, $n = \left( \frac{u \times V_o}{e} \right)^2$; Where $V_o$ is the coefficient of variation, 'e' is the allowable sampling error and 'u' (1.96) is the factor corresponding to an approximate probability of 0.05 that the sampling error will not exceed the maximum allowable error 'e'. The sample size "n" was determined as 4 (for maximum coefficient of variation of 0.098 and maximum allowable error as 0.1 times the expected value of crushing strength) and used for the test.

Fig. 4.5 shows the gain in strength of aggregate with period of curing. Development of strength in aggregate with curing in both test methods follows almost the same pattern. The strength of 3-day cured aggregate is observed to be more than 70% of its 28-day strength. This may be due to the high alumina content present in the fly ash (Table 4.1) causing faster rate of hydration (Mehta and Monteiro, 2005). XRD pattern of raw fly ash and cold-bonded aggregate presented in Fig. 4.6 indicates that phases like anhydrite and di-calcium silicate present in the fly ash are converted into hydration products like ettringite, gypsum and calcium silicate hydrate resulting in refinement of pores and improvement in the strength of aggregate.

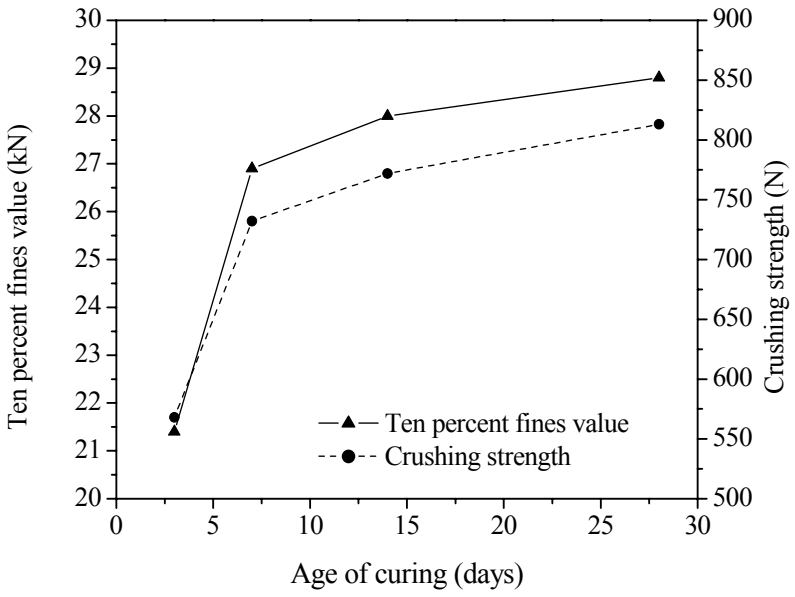


Fig 4.5 Variation in strength of aggregate with period of curing

The 10% fines value of 28-day cured cold-bonded aggregate (28.8 kN) is lower than those reported for sintered fly ash aggregate (60 to 80 kN) (Manikandan, 2006) and expanded clay aggregate (60 kN) (Videla and Lopez, 2000). The lower 10% fines value of cold-bonded aggregate may be due to the absence of hard shell and rigid bonding in cold-bonded aggregate. However, the crushing strength of aggregate used in the present study is higher than that reported for cold-bonded aggregate by Gesoglu, et al., 2007.

Table 4.2 summarises the physical and mechanical characteristics of 28-day cured cold-bonded aggregate. The density of aggregate (995 kg/m$^3$) is marginally higher than the upper limit (880 kg/m$^3$) defined for lightweight aggregate (ASTM C 330, 2005). However, the bulk density and specific gravity of cold-bonded aggregate is observed to be only 60 to 70% of that of normal weight crushed granite aggregate.

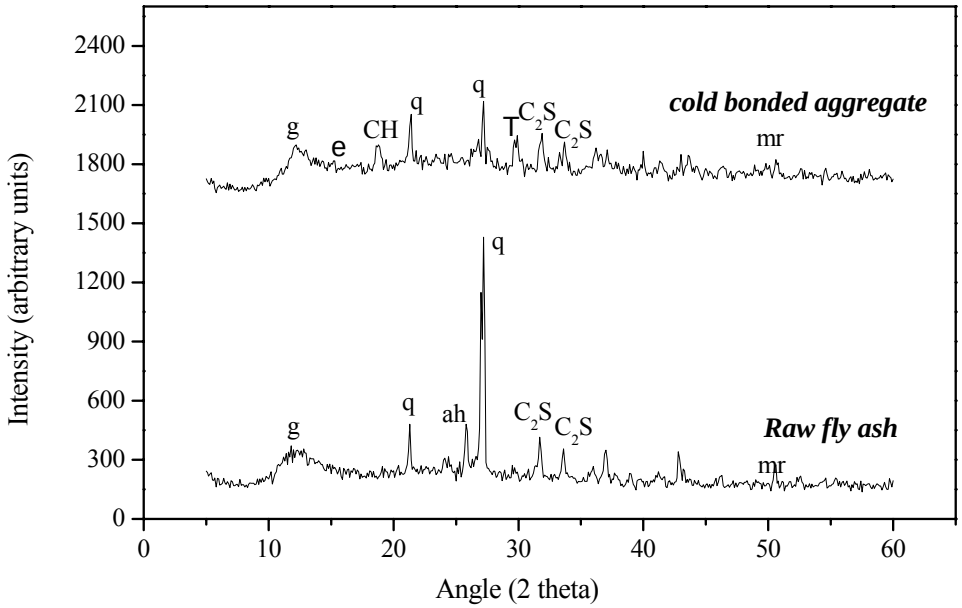


| | |
|---|---|
| ah - anhydrite ($CaSO_4$), | q - quartz ($SiO_2$) |
| $C_2S$ - di calcium silicate ($Ca_2SiO_4$) | CH - calcium hydroxide ($Ca(OH)_2$) |
| $C_3S$ - tri calcium silicate ($Ca_3SiO_5$) | e - ettringite ($Ca_6Al_2(SO_4)_3(OH)_{12}\ 26H_2O$ |
| g - gypsum ($CaSO_4\ 2H_2O$) | T - Tobermorite: C-S-H-Calcium Silicate Hydrate |
| mr - merwinite ($Ca_3\ mg(SiO_4)_2$) | |

Fig. 4.6 XRD pattern of raw fly ash and cold-bonded aggregate

Table 4.2 Physical and mechanical properties of 28-day cured aggregate

| Property | Cold-bonded Aggregate | Test Method |
|---|---|---|
| Dry loose bulk density ($kg/m^3$) | 995 | ASTM C 29 (2005) |
| Saturated surface dry sp. gravity | 1.98 | ASTM C127 (2004) |
| Open porosity (%) | 38.03 | Vacuum saturation |
| 30-min water absorption (%) | 19.04 | - |
| 24–h water absorption (%) | 20.46 | ASTM C127 (2004) |
| 10 % fines (kN) | 28.8 | IS 2386: Part IV (2002) |
| Crushing strength (N) | 813 | BS 812 : Part 110 (1990) |

#### 4.2.3.3 Moisture loss from aggregate due to drying

In order to understand the moisture transport from cold-bonded aggregate during drying, 28-day cured saturated surface dried aggregate was exposed to different

drying conditions and loss in weight and moisture content in the aggregate were measured. For this purpose, three different aggregate samples of 500 g each (retaining in 4.75 mm sieve and passing 12.5 mm sieve) was exposed to varied relative humidity (RH) levels (90%, 70% and 50%) in humidity chamber at 20±1 ºC for 28 days. After weighing, the aggregate was dried in an oven at 105 ºC for 24 hours to determine the dry weight. Fig. 4.7 presents the influence of RH on the loss of absorbed water from the aggregate. At 90% RH itself a significant quantity of moisture loss (about 9 % by its weight) from the aggregate was observed; i.e. about 45% of the total water absorption of aggregate. This amount of absorbed water is thus readily available for transport to the cement paste while it self desiccates, since it is weakly bound by capillary forces to the pores of aggregates (Lura, 2003) causing favourable condition for autogenous curing in concrete which is discussed in detail in Chapter 7. A further reduction in RH below 90% has resulted in about 3 to 4% reduction in the moisture content in the aggregate. The moisture content in the aggregate is reduced to 7.8% at a relative humidity of 50%.

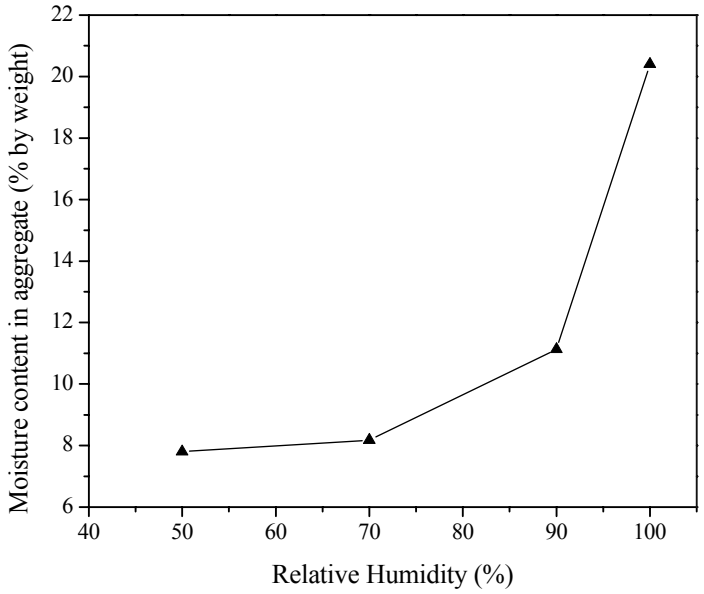


Fig. 4.7 Influence of RH on moisture content in aggregate (after 28 days)

## 4.3 COLD-BONDED FLY ASH AGGREGATE CONCRETE

To start with single factor experiments have been undertaken in concrete of different mixture proportions by varying the proportioning variables viz. cement content, volume fraction of cold-bonded aggregate and w/c ratio to identify the factors and factor levels for the second stage of experiments based on statistical tool of Response Surface Methodology. The influence of cold-bonded aggregate on the fresh and hardened mechanical properties of concrete such as compressive strength, split tensile strength, flexural strength and elastic modulus of concrete with variation in mix composition are discussed in this section.

### 4.3.1 Materials

The properties of constituent materials used for the production of cold-bonded aggregate concrete viz., cement, sand and cold-bonded aggregate have been presented in this section.

Cement: Ordinary Portland Cement of 53 grade conforming to IS 12269 (2004) was used. The chemical and physical properties of the cement are summarised in Table 4.3.

Fine Aggregate: Fine aggregate was of locally available natural river sand with saturated surface dry specific gravity of 2.62 and water absorption of 1 %. Fineness modulus of aggregate was 2.4 and conforming to Zone II as per IS 383 (2002). The particle size distribution of aggregate is presented in Fig. 4.8.

Coarse Aggregate: In all the mixtures, 28 day cured cold-bonded aggregate with physical and mechanical properties as mentioned in Table 4.2 was used as coarse aggregate. Particle size distribution of cold-bonded aggregate with the grading requirement of coarse lightweight aggregate (ASTM C 330, 2005) is also presented in

Fig. 4.8. Normal concrete cast for comparison of properties used crushed granite aggregate of specific gravity 2.71 and water absorption of 1%.

Table 4.3 Physical and chemical properties of cement used

| **Chemical properties** | | |
|---|---|---|
| | Cement | |
| | % by mass | IS 12269 (2004) |
| $SiO_2$ | 19.3 | - |
| CaO | 61 | - |
| $Al_2O_3$ | 5.687 | - |
| $Fe_2O_3$ | 6.036 | - |
| MgO | 1.875 | 6 |
| $Na_2O$ | - | - |
| $K_2O$ | - | - |
| $SO_3$ | 1.67 | 2.5 |
| MnO | - | - |
| Loss on Ignition | 0.2693 | 4 |
| Soluble residue | 1.489 | 2 |
| $Al_2O_3$/ $Fe_2O_3$ | 0.94 | 0.66 |
| $SiO_2 + Al_2O_3 + Fe_2O_3$ | - | - |
| **Physical properties** | | |
| Fineness ($m^2$/kg) | 391 | |
| Specific gravity | 3.13 | |
| 28-day comp.strength (MPa) | 54.3 | |

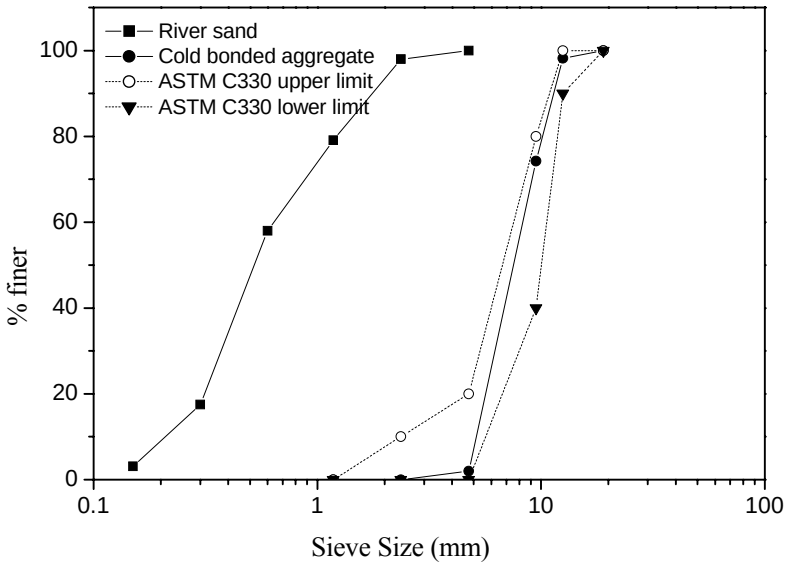


Fig.4.8 Particle size distribution of aggregate

### 4.3.2 Mix Proportions

The mix proportioning was done on absolute volume basis by considering 2.5% (ACI 211.2, 1990) as the entrapped air in the concrete. The cement content, w/c ratio, and CA/TA (coarse aggregate volume to total aggregate volume) ratio used in the first stage of study are presented in Table 4.4.

Table 4.4 Parameters of mixture composition

| Cement content ($kg/m^3$) | Water content($kg/m^3$) | w/c ratio | CA/TA (Vol.%) |
|---|---|---|---|
| 250 | 150,175 | 0.6, 0.7 | 35 , 50, 65 |
| 350 | 175,210 | 0.5. 0.6 | 35, 50, 65 |
| 450 | 175,225 | 0.39,0.5 | 35, 50, 65 |

While using aggregates having higher water absorption characteristics the literature suggests two methods to overcome early slump loss; (i) addition of excess water to compensate water absorption or (ii) pre-soaking of aggregates. In the present study, aggregate was soaked for a period of 30 minutes (which account for 93% of 24 hr water absorption). The water required for the effective w/c ratio in the mix as indicated in Table 4.4 was added during mixing. Chandra and Berntsson (2004) suggest that lightweight concrete when mixed in two stages, i.e. mortar and then with aggregate is characterized by good homogeneity and high performance. Hence first the cement, water and fine aggregate were mixed for 2 minutes and after adding cold-bonded aggregate, the mixing was continued for a further period of 3 minutes.

### 4.3.3 Properties of Fresh Concrete

#### 4.3.3.1 Fresh density

Fresh density of concrete measured for the above mixes are given in Table 4.5. The fresh density ranges between 1988 and 2192 $kg/m^3$ which is marginally higher to

qualify as lightweight aggregate concrete (ACI 211.2, 1990). Relatively higher specific gravity of cold-bonded aggregate and use of natural sand as fine aggregate caused the concrete to exceed the limit for density. Fig. 4.9 presents the influence of cold-bonded aggregate content on the density of concrete. For a given cement content, linear reduction in density is observed with an increase in volume fraction of cold-bonded aggregate in concrete. In general, 10 to 17% reduction in density is observed as compared to normal weight concrete (having a fresh density of 2400 kg/m$^3$).

Table 4.5 Density of fresh concrete

| Cement content (kg/m$^3$) | Water content (kg/m$^3$) | Fresh Density (kg/m$^3$) | | |
|---|---|---|---|---|
| | | CA/TA (35%) | CA/TA (50%) | CA/TA (65%) |
| 250 | 150,175 | 2179, 2144 | 2104, 2072 | 2029, 1999 |
| 350 | 175,210 | 2168, 2120 | 2099, 2054 | 2030, 1988 |
| 450 | 175,225 | 2192,2123 | 2126,2062 | 2060,2001 |

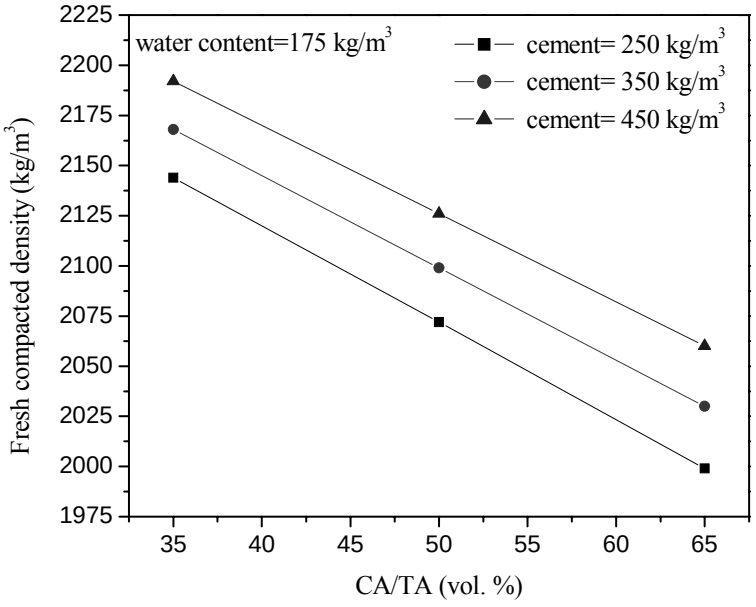


Fig. 4.9 Variation in density with cold-bonded aggregate content (water content = 175kg/m$^3$)

#### 4.3.3.2 Workability of concrete

Workability of concrete has been measured through slump and compacting factor (CF) tests (IS 1199, 2004). The variation in slump with water content for different mixes is presented in Fig. 4.10. For constant water content the slump of concrete increases appreciably with an increase in volume fraction of cold-bonded aggregate. This increase in workability can be attributed to (i) the reduction in specific surface caused by the increase in coarse aggregate and consequent reduction in fine aggregate content in the mixture, (ii) the spherical shape and smooth surface texture of cold-bonded aggregate and (iii) the reduction in voids due to the increase in spherical aggregate content. The spherical shape of the aggregate reduces the friction at the aggregate-paste interface producing a 'ball-bearing effect' compared to angular particles of sand at the point of contact and allowing the concrete to move more freely (Demirboga et al., 2001). It is also observed that the increase in water requirement with increase in cement content for achieving concrete of constant slump is quite marginal. This may be attributed to the reduction in aggregate content caused by increase in cement content, which makes the mix relatively more cohesive.

For achieving a constant workability, the water demand reduces with an increase in aggregate content. This reduction in water demand may have beneficial effect in producing concrete of same strength with relatively lower cement content. Bai et al. (2004) observed substantial reduction in water demand when natural sand and basalt aggregate were replaced with furnace bottom ash and sintered aggregate which were of spherical in shape. In general, the results of the present study corroborate well with the observations of Videla and Lopez (2000) that the lightweight aggregate content is the main parameter controlling the water content-slump relationship.

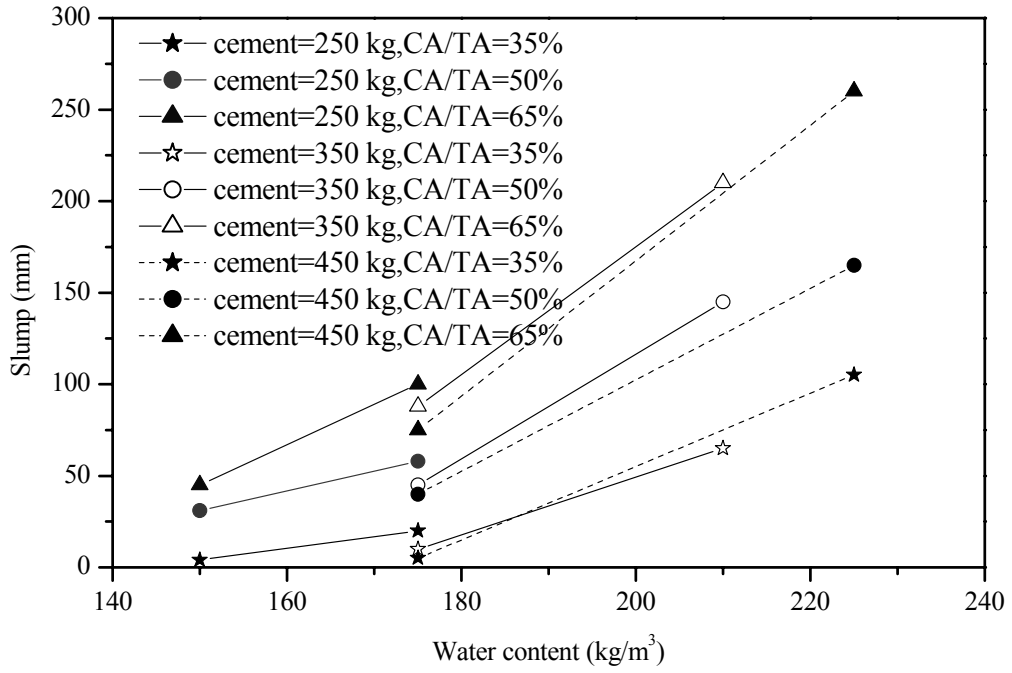


Fig. 4.10 Variation in slump of concrete with water content

The effect of cold-bonded aggregate content on the compacting factor is presented in Fig. 4.11. Similar to the slump, the compacting factor is also significantly influenced by the CA/TA ratio apart from water content. The effect due to cement content is negligible while comparing mixes with same water content. A relatively higher compacting factor in mixtures with lower water content may be due to the homogeneous nature of the mixture owing to the less density difference between mortar and saturated density of cold-bonded aggregate which reduces segregation.

Slump Loss: Loss of slump with time has been studied on concrete with 450 kg/m$^3$ cement and water content of 225 kg/m$^3$. The variation in slump with time as percentage of the initial slump, presented in Fig. 4.12 shows that the slump loss can be prolonged with an increase in the volume fraction of cold-bonded aggregate. As compared to concrete with a CA/TA of 65%, about 15 to 20% slump reduction with time has been observed in concrete with a CA/TA of 35%. The probable reasons

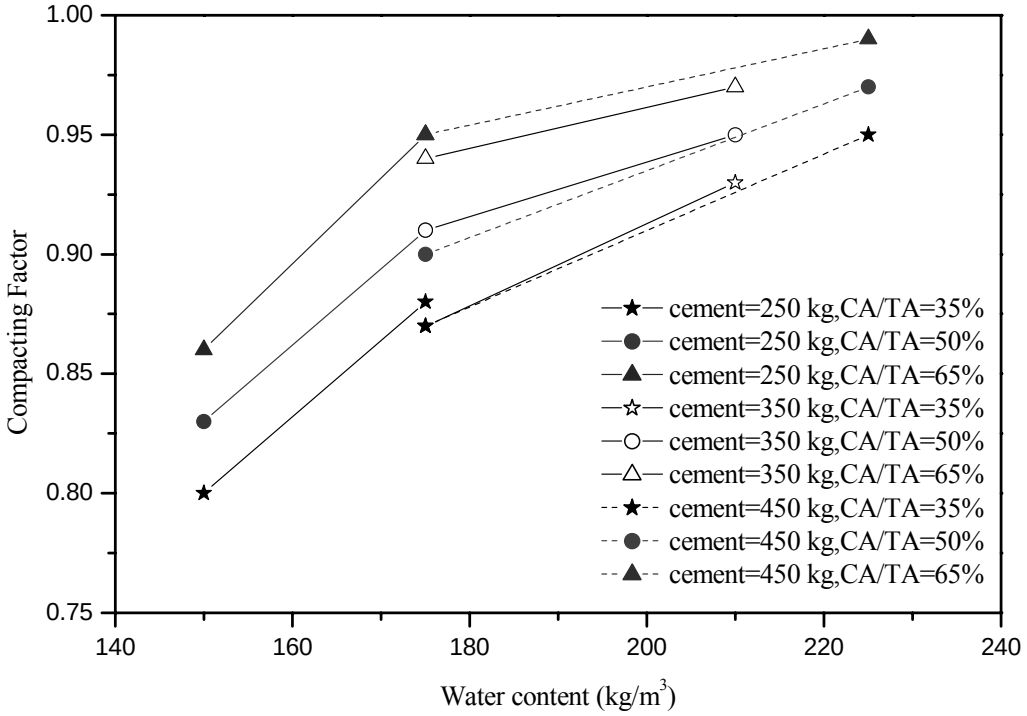


Fig. 4.11 Variation in compacting factor with water content

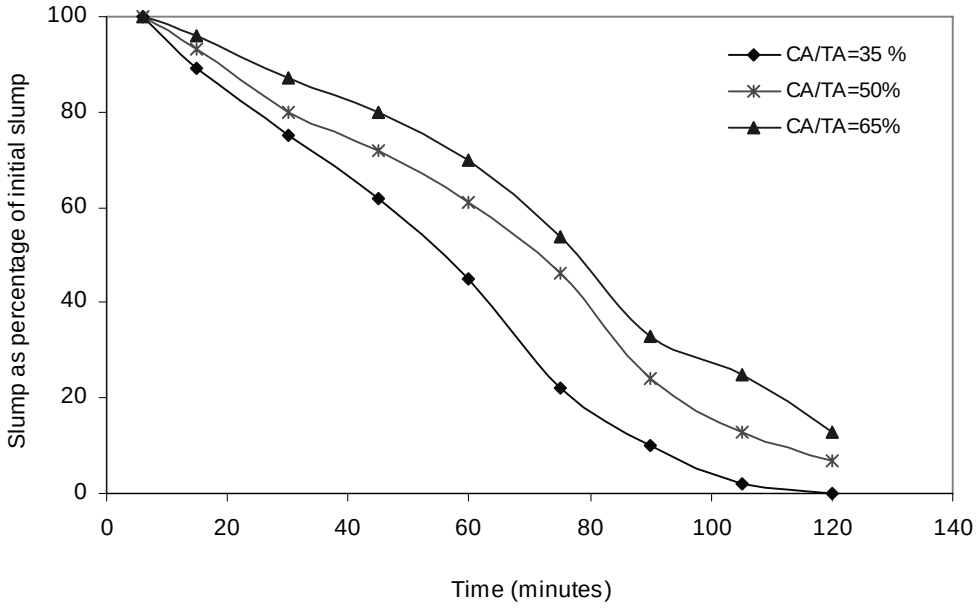


Fig. 4.12 Variation of slump with time

attributed are (i) the reduction in frictional force associated with the aggregate bulk and (ii) the moisture transfer occuring between the saturated aggregate and the hydrating cement paste when there is a reduction in the humidity of the hydrating paste. Poon et al. (2004) have observed similar slower progress of slump loss when crushed granite aggregate was replaced by saturated recycled aggregate with a 24 hr. water absorption of 6.92%.

### 4.3.4 Properties of Hardened Concrete

Specimens were cast from each mix composition for the 28-day evaluation of compressive strength, split tensile strength, flexural strength and modulus of elasticity. Dimensions and number of specimens (statistically represented sample size according to ASTM E 122-2000 (section 4.2.3.2)) used in each test is given in Table.4.6. Specimens with mixture proportions of constituent mortar which formed the part of concrete in the respective mixes (with same w/c and fine aggregate/cement ratio) were mixed separately in a mortar mixer and cast to study the influence of cold-bonded aggregate on the strength and failure of concrete.

Table 4.6 Specimen dimensions and sample size.

| Properties tested | Dimension (mm) | No. of specimen | Test method |
|---|---|---|---|
| Compressive strength | 100 x100 x 100 | 6 | IS 516 (2004) |
| Split tensile strength | 100 x 200 cylinder | 4 | ASTM C 496 (2004) |
| Flexural strength | 100 x 100 x 500 | 4 | ASTM C 78 (2002) |
| Modulus of elasticity | 150 x 300 cylinder | 4 | ASTM C 469 (2002) |
| Mortar, Comp. strength | 50 x 50 x 50 | 6 | ASTM C 109 (2002) |

All the specimens were demoulded after 24 hours of casting and kept in a mist room maintained at a temperature of 23$\pm$2 ºC and 98$\pm$2% relative humidity up to 28 days. Equilibrium density of hardened concrete calculated from oven-dry density of

samples (ASTM C 567, 2005) is presented in Table 4.7. The equilibrium density is varied from 1931 to 2170 kg/m$^3$ due to the variation in mixture composition, similar to those observed in the case of fresh density.

Table 4.7 Equilibrium density of concrete

| Cement content (kg/m$^3$) | Water content(kg/m$^3$) | w/c ratio | Equilibrium Density (kg/m$^3$) | | |
|---|---|---|---|---|---|
| | | | CA/TA (35%) | CA/TA (50%) | CA/TA (65%) |
| 250 | 150,175 | 0.6, 0.7 | 2121,2079 | 2038,2009 | 1967, 1931 |
| 350 | 175,210 | 0.5. 0.6 | 2126,2055 | 2055,1992 | 1978,1921 |
| 450 | 175,225 | 0.39,0.5 | 2170,2073 | 2102,2013 | 2025,1946 |

#### 4.3.4.1 Compressive strength

Fig. 4.13 presents the variation in 28-day compressive strength of concrete with cement content, w/c and CA/TA ratios. As the w/c ratio increases distinct variation in compressive strength is observed with change in cement content. At a given w/c ratio, the strength of concrete decreases with an increase in volume fraction of cold-bonded aggregate for mixes with cement content of 450 kg/m$^3$ and 350 kg/m$^3$ whereas the strength increases with an increase in cold-bonded aggregate content in concrete with 250 kg/m$^3$ cement content. The difference in behaviour is due to the change in predominant failure mode with variation in cement content which is discussed in detail in the next section. In mixes with higher cement content the reduction in strength with volume fraction of aggregate is more pronounced at low w/c ratio. The variation in strength of concrete with aggregate is observed to be minimal at w/c of 0.6 and cement content of 350 kg/m$^3$ (i.e., at a strength level of around 35 MPa). Hence it appears beneficial to use relatively higher aggregate content in mixes with lower cement content and vice versa.

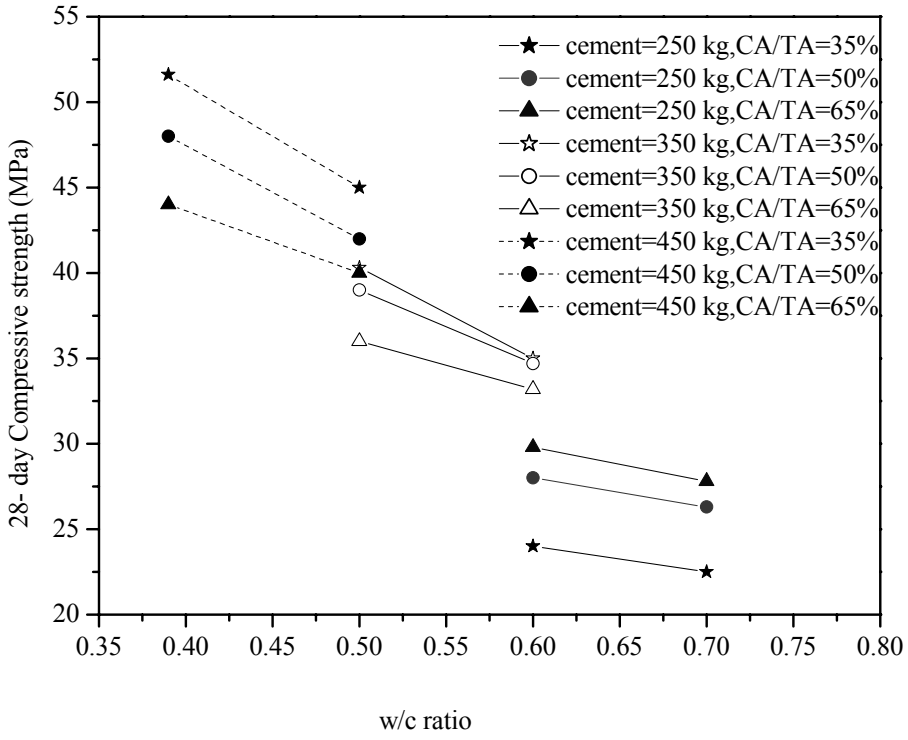


Fig. 4.13 Variation in 28-day compressive strength with w/c ratio

#### 4.3.4.2 Relation between strength of concrete and constituent mortar

To explain the above difference in behaviour of cold-bonded aggregate concrete with cement content, concrete is considered as a two-phase composite system in which coarse aggregates are embedded in a matrix of hardened mortar (Nilsen et al., 1995; Yang 1996). For this purpose, the 28-day compressive strength of concrete and constituent mortar of the concrete are compared in Fig. 4.14 for different volume fractions of aggregate. Up to around 30 MPa, the strength of concrete is marginally higher than that of constituent mortar in the mix, which is attributed to failure initiated in the matrix or aggregate-matrix bond, i.e. behaviour is controlled by the strength of the mortar as in normal weight concrete (Slate et al., 1986).

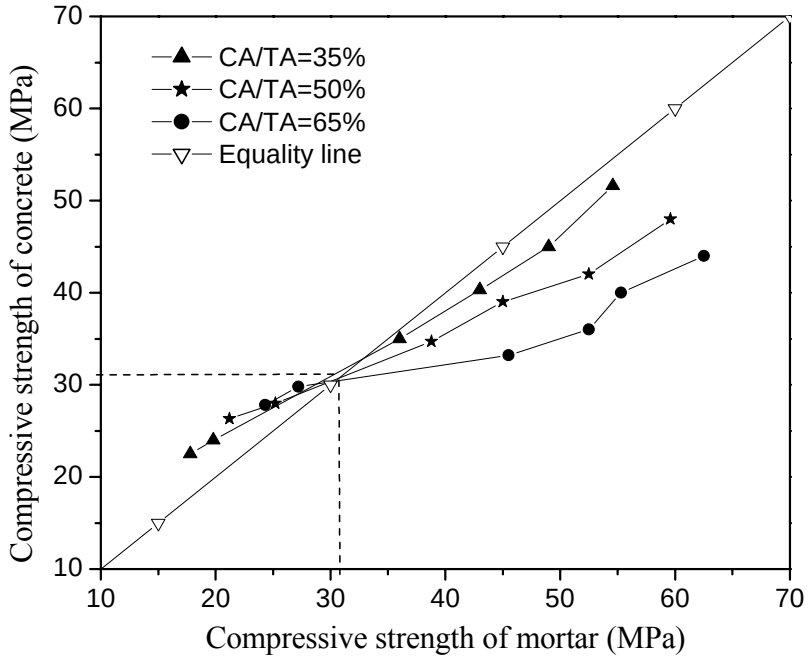


Fig. 4.14 Relation between strength of mortar and concrete

The failure surface of concrete in Fig. 4.15 (a) exhibits no or very little aggregate fracture, indicating that the failure occurred in mortar, i.e., around the aggregate. Beyond 32 MPa, the strength of cold-bonded aggregate concrete is lower than that of corresponding mortar. This difference increases with increase in cement content as well as cold-bonded aggregate content in the mix, wherein the strength of concrete is controlled by the aggregate fracture (Fig. 4.15 (b)). Chi et al., 2003 and Gesoglu et al., 2004 have reported a similar reduction in strength of cold-bonded aggregate concrete with an increase in volume fraction of aggregate with cement content from 400 kg/m$^3$.

Maximum achievable strength of concrete: As aggregate governs the failure of concrete in concretes of higher cement content, in order to understand the maximum strength which can be achieved by cold-bonded aggregate concrete, tests have been carried out on specimens cast with cement content of 550 kg/m$^3$ and 450 kg/m$^3$ with w/c ratio of 0.3 and 0.35 respectively, i.e., with high cement content and low w/c ratio. Commercially available superplasticizer has been added during mixing to

maintain workability to slump of 50 $\pm$ 10 mm. The 28-day strength of concrete presented in Table 4.8 shows that improvement in strength due to increase in cement content from 450 to 550 kg/m$^3$ is less and becomes marginal at CA/TA of 65% even though aggregate can supply any additional water required for hydration in the case of self-desiccation as would be discussed in Chapter 7. The reason for the very less improvement in strength with increase in cement content can be attributed to the effect of aggregate on the "limit compressive strength" (highest possible strength) of concrete (FIP, 1983). It is stated that at this limiting compressive strength, strength of lightweight aggregate concrete in which tensile strength of constituent mortar is very high, is governed by the tensile strength of aggregate.

(a) Failure around the aggregate (strength of concrete <30 MPa)

(b) Failure through the aggregate (strength of concrete >35 MPa)

Fig. 4.15 Typical failure pattern of cubes tested at 28 days (CA/TA = 50%)

Table 4.8 28-day compressive strength of concrete with high cement content

| Cement content (kg/m$^3$) | w/c ratio | 28-day Compressive Strength (MPa) | | |
|---|---|---|---|---|
| | | CA/TA (35 %) | CA/TA (50 %) | CA/TA (65 %) |
| 450 | 0.35 | 53.5 | 50.5 | 48.0 |
| 550 | 0.3 | 56.0 | 52.5 | 49.0 |

#### 4.3.4.3 Split tensile strength, Flexural strength and Modulus of elasticity

Variation in split tensile and flexural strengths of cold-bonded aggregate concrete with w/c ratio for different cement content and CA/TA ratio is presented in Figs. 4.16 and 4.17 respectively. Split tensile and flexural strengths exhibit almost similar variation as that of compressive strength. Tensile strength of concrete increases with an increase in CA/TA ratio where mortar controls the failure of concrete and it reduces with an increase in CA/TA ratio where the aggregate fracture is predominated.

The relationship of split tensile strength and flexural strength with cube compressive strength ($f_c$) obtained through regression analysis of the results for each volume fraction of aggregate is presented in Table 4.9. This indicates that these relationships are influenced by the volume fraction of cold-bonded aggregate in the mix composition. It is observed that the flexural strength associated with higher volume fraction of aggregate is marginally less compared to low volume fraction at the same strength level. Tensile properties of cold-bonded aggregate concrete are observed to be lower than those reported for sintered or expanded aggregate concrete (Table 2.4) of the similar strengths where the aggregate is harder than cold-bonded aggregate.

Table 4.9 Relationship between compressive strength and other mechanical properties

| CA/TA (Vol. %) Property | Regression Equation ($R^2$ value) | | |
|---|---|---|---|
| | 35% | 50% | 65% |
| Split tensile strength (MPa) | $0.278\ f_c^{0.635}$ (0.997) | $0.279\ f_c^{0.632}$ (0.969) | $0.310\ f_c^{0.599}$ (0.961) |
| Flexural strength (MPa) | $0.615\ f_c^{0.499}$ (0.997) | $0.645\ f_c^{0.488}$ (0.984) | $0.710 f_c^{0.423}$ (0.994) |
| Static elastic modulus(GPa) | $5.53\ f_c^{0.423}$ (0.992) | $5.25\ f_c^{0.435}$ (0.968) | $5.94\ f_c^{0.401}$ (0.951) |

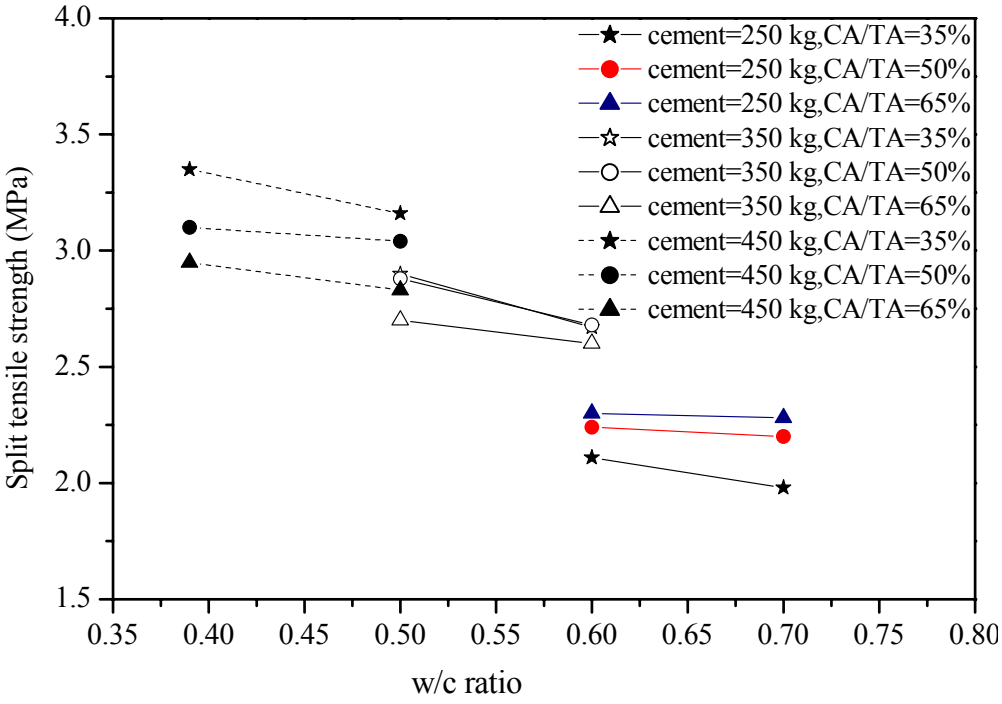


Fig. 4.16 Variation of split tensile strength with w/c ratio

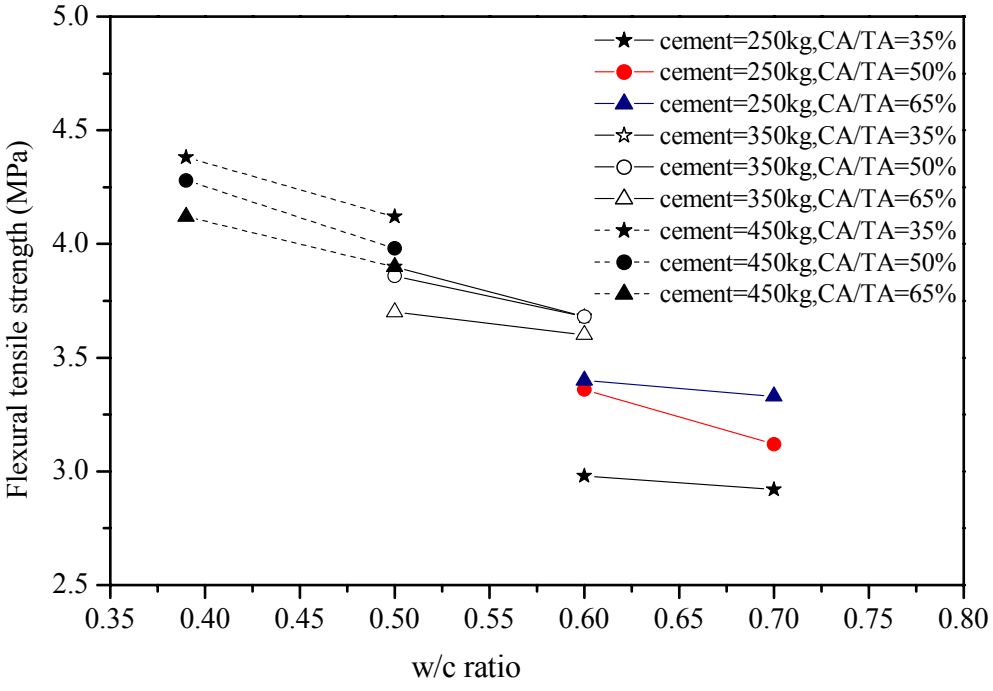


Fig. 4.17 Variation of flexural tensile strength with w/c ratio

Fig. 4.18 presents the variation of static elastic modulus with ratio of coarse aggregate to total aggregate in the mix for a range of cement content and water-cement ratio. The modulus of elasticity increases with an increase in CA/TA ratio at 250 kg/m$^3$ cement content, while it is fairly a constant at a cement content of 350 kg/m$^3$ and reduces with an increase in CA/TA ratio at 450 kg/m$^3$ cement content. The variation in modulus of elasticity is relatively predominant at lower CA/TA ratio, which also emphasizes the influence of cold-bonded aggregate content in concrete. Table 4.8 shows the difference in relation between modulus of elasticity and compressive strength of concrete with volume fraction of cold-bonded aggregate. The elastic modulus is observed to be marginally higher compared to those reported (Table 2.4) for concrete with sintered or expanded aggregate. The higher value of elastic modulus may be attributed to the higher density of cold-bonded aggregate than that of sintered/expanded aggregate.

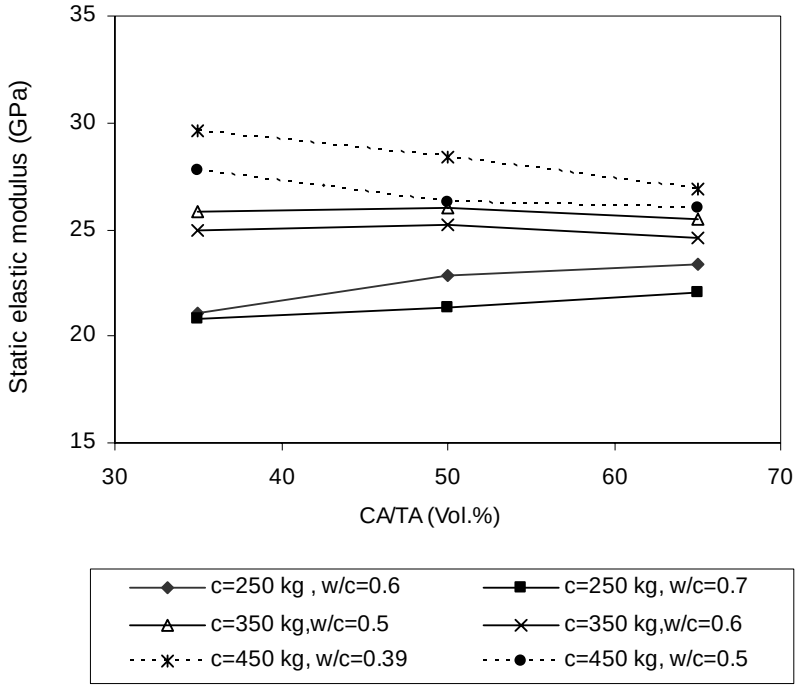


Fig. 4.18.Variation of elastic modulus with volume % of cold-bonded aggregate

## 4.4 MODELS FOR WORKABILITY AND STRENGTH

Single factor experiments discussed in the previous section indicated that all the three proportioning variables of the mix viz. cement content, water content and CA/TA ratio have profound influence on the fresh and hardened properties of cold-bonded aggregate concrete. Hence as a next step, a statistically designed experiment has been planned to (i) understand the influence of parameters of mixture composition and their possible interaction effects on the workability and compressive strength of concrete over a wide range of values for the parameters, (ii) develop models for workability and compressive strength and (iii) propose typical mixture design guidelines for cold-bonded fly ash aggregate concrete, based on the range of parameters investigated.

### 4.4.1 Statistical Model Based on Response Surface Methodology (RSM)

Cement content, water content, CA/TA ratio and moisture condition of the aggregate at the time of mixing were taken as factors in the experimental design based on response surface methodology to develop detailed relationship between these factors and responses (workability and strength). For providing equal precision of estimates in all direction, a central composite design (Montgomery, 2001) with rotatability or equal precision was selected. Central composite design takes central points and axial points along with factorial points in the analysis. The parameter, distance to the axial points (a) from the design centre depends on the factorial points and can be calculated as $(n_f)^{1/4}$ for rotatable design where $n_f$ is the number of points used in the factorial portion of the design. The components of the central composite design with equal precision are given in Table 4.10

The relationship between the response and the variables of mix composition was fitted using quadratic regression model of the following form.

$$y = b_o + \sum_{i=1}^{k} b_i x_i + \sum_{i=1}^{k} b_{ii} x_i^2 + \sum_{i<j} \sum b_{ij} x_i x_j$$

where $x_i$ (i= 1,2..... k) are quantitative variables and $b_0$ , $b_i$ are the least square estimates of the regression coefficients.

Models were chosen at a significant level of 0.01 % and also it was ensured that model terms are statistically significant (ie. Prob>F is less than 0.05).

Table 4.10 Components of central composite rotatable second order design

| No. of variables | Number of design points | | | Total run | Distance to the axial point (a) |
|---|---|---|---|---|---|
| | Factorial | Axial | Central | | |
| 2 | 4 | 4 | 5 | 13 | 1.414 |
| 3 | 8 | 6 | 6 | 20 | 1.682 |

### 4.4.2 Details of Experimental Study

Table 4.11 summarises the details of low and high level values of factors of mixture composition considered in the study. The lower and upper limit of water content was arrived as 160 and 220 kg/m$^3$ for producing workable mixes. Since cold-bonded aggregate was observed to govern the failure in mixes of higher cement content, the upper level of cement content and volume of cold-bonded aggregate were fixed as 450 kg/m$^3$ and 65% respectively. Moisture condition of cold-bonded aggregate has been considered as a category factor viz., air-dried aggregate and pre-soaked aggregate. In mixes using pre-soaked aggregate, the aggregate was soaked for 30 minutes and allowed another 10 minutes to drain out the excess water from the aggregate. The use of air-dried aggregate requires the determination of actual water content in the aggregate for arriving at additional water requirement for compensating the absorption of aggregate. For mixes with air-dried aggregate, the additional water content corresponding to 30 minutes of absorption of aggregate was added along with

the mix water. The experimental design resulted in 40 experimental runs with 20 runs in each category as shown in Table 4.12.

Table 4.11 Factors and factor levels

| Factor | Low level | High level | Type of factor | Notation |
|---|---|---|---|---|
| Cement content ($kg/m^3$) | 250 | 450 | Numeric | c |
| Water content ($kg/m^3$) | 160 | 220 | Numeric | w |
| (CA/TA), (vol.%) | 35 | 65 | Numeric | $C_A$ |
| Moisture condition of aggregate | Air-dried (Level-1) | Pre-soaked (Level-2) | Categoric | |

Table 4.12 Mix compositions for statistically designed experiment

| Run / Factors | Cement ($kg/m^3$) | Water ($kg/m^3$) | CA/TA (vol. %) | Moisture condition | Run / Factors | Cement ($kg/m^3$) | Water ($kg/m^3$) | CA/TA (vol. %) | Moisture condition |
|---|---|---|---|---|---|---|---|---|---|
| 1 | 350 | 190 | 50 | Level 2 | 21 | 350 | 190 | 75.2 | Level 1 |
| 2 | 250 | 160 | 35 | Level 1 | 22 | 350 | 139.6 | 50 | Level 2 |
| 3 | 350 | 190 | 50 | Level 1 | 23 | 350 | 190 | 24.8 | Level 1 |
| 4 | 450 | 220 | 65 | Level 2 | 24 | 350 | 190 | 50 | Level 2 |
| 5 | 518.2 | 190 | 50 | Level 1 | 25 | 350 | 190 | 75.2 | Level 2 |
| 6 | 250 | 220 | 35 | Level 2 | 26 | 250 | 220 | 65 | Level 1 |
| 7 | 450 | 160 | 65 | Level 1 | 27 | 350 | 190 | 50 | Level 2 |
| 8 | 350 | 139.6 | 50 | Level 1 | 28 | 350 | 240.5 | 50 | Level 1 |
| 9 | 350 | 190 | 50 | Level 1 | 29 | 450 | 160 | 35 | Level 1 |
| 10 | 350 | 190 | 50 | Level 2 | 30 | 350 | 190 | 50 | Level 2 |
| 11 | 181.8 | 190 | 50 | Level 2 | 31 | 350 | 190 | 24.8 | Level 2 |
| 12 | 450 | 160 | 35 | Level 2 | 32 | 250 | 160 | 35 | Level 2 |
| 13 | 250 | 160 | 65 | Level 2 | 33 | 450 | 220 | 35 | Level 1 |
| 14 | 181.8 | 190 | 50 | Level 1 | 34 | 350 | 240.5 | 50 | Level 2 |
| 15 | 350 | 190 | 50 | Level 1 | 35 | 250 | 220 | 35 | Level 1 |
| 16 | 350 | 190 | 50 | Level 2 | 36 | 350 | 190 | 50 | Level 1 |
| 17 | 450 | 220 | 65 | Level 1 | 37 | 250 | 220 | 65 | Level 2 |
| 18 | 450 | 160 | 65 | Level 2 | 38 | 518.2 | 190 | 50 | Level 2 |
| 19 | 450 | 220 | 35 | Level 2 | 39 | 350 | 190 | 50 | Level 1 |
| 20 | 350 | 190 | 50 | Level 1 | 40 | 250 | 160 | 65 | Level 1 |

### 4.4.3 Statistical Model for Workability

The regression models developed from the experimental results for quadratic response surface for workability through slump (mm) and compacting factor are presented in Table 4.13 for both air-dried and pre-soaked aggregates. The adequacy checks on models satisfy statistical requirements (R-squared value and F-value). The behaviour of concrete is discussed through response surface and contours plotted using these model equations.

Table 4.13 Model equations and statistics for workability

| Response | Response Model | $R^2$ | F- value | Prob>F |
|---|---|---|---|---|
| | *Air dried aggregate* | | | |
| Slump (mm) | 1338.09 - 1.743* c -10.468 * w-10.659* $C_A$ + 0.00371*c*w+0.07452*w*$C_A$+0.001257*$c^2$ + 0.02145*$w^2$ | 0.97 | 152.5 | < 0.0001 |
| Compacting Factor | -0.2633-6.527E-05*c+0.0092*w+0.00745*$C_A$ -3.158E-05*w* $C_A$ -1.639E-05* $w^2$ | 0.956 | 43.8 | < 0.0001 |
| | *Pre-soaked aggregate* | | | |
| Slump (mm) | 895.18-0.661 *c-9.325*w-4.643* $C_A$ + 0.06195*w*$C_A$+0.00079*$c^2$+0.0232*$w^2$- 0.0387* $C_A^2$ | 0.995 | 319.2 | < 0.0001 |
| Compacting Factor | -0.7323-8.967E-05*c+0.01302*w+ 0.010231*$C_A$-4.431E-05*w*$C_A$-2.371E-05*$w^2$ | 0.967 | 54.5 | < 0.0001 |
| c=cement content (kg/$m^3$); water content (kg/$m^3$); $C_A$= CA/TA (Vol.%) | | | | |

#### 4.4.3.1 Response surface for slump

Figs. 4.19 and 4.20 present respectively the response surface and contour plot for slump of cold-bonded aggregate concrete with air-dried and pre-soaked aggregates for a cement content of 350 kg/$m^3$, which is the center point of the factor level for cement

content. In addition to the main and quadratic effects of water content and volume fraction of cold-bonded aggregate in the mix, there exists an interaction effect of these factors on slump in both the cases.

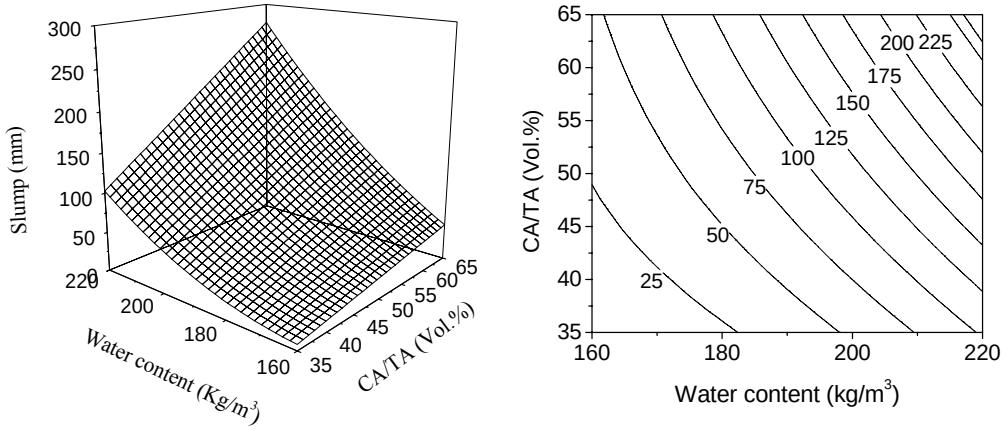


(a) Response Surface (b) Contour Plot

Fig. 4.19 Slump of concrete with air-dried aggregate (cement content =350 kg/m$^3$)

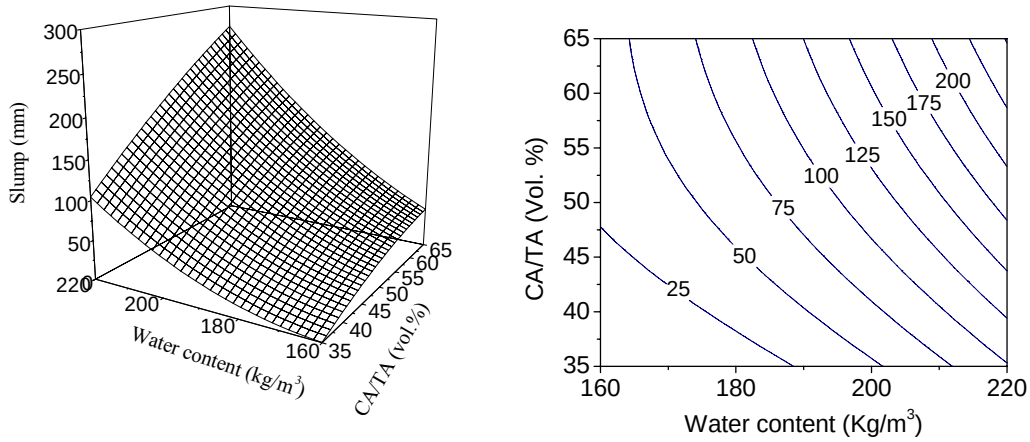


(a) Response Surface (b) Contour Plot

Fig. 4.20 Slump of concrete with pre-soaked aggregate (cement content =350 kg/m$^3$)

In general, the effect of aggregate content on slump value is more pronounced at higher water contents than at lower water content. At lower water contents (< 190 kg/m$^3$), increase in aggregate content from 35 to 65% causes an increase of slump value from 55 to 100 mm whereas at higher water content an increase of more than 125mm is observed. The primary reason for the enhancement in workability of the concrete with aggregate volume has already been discussed in section 4.3.3.2. At higher water content, the rapid increase in slump with volume fraction of aggregate may be attributed to the combined effect of improved packing and reduced surface area.

A comparison of Figs. 4.19 and 4.20 shows that even though the slump is affected by the moisture condition of aggregate, the difference is not significant, being only in the range of 15 to 30 mm. Concrete with air-dried aggregate always results in marginally higher slump than concrete with pre-soaked aggregate indicating that there is no considerable difference between the effective water available in both cases.

The variation of slump with water and cement content for constant CA/TA ratio (50%) is presented in Fig. 4.21. It can be observed that the variation in workability with cement content is less pronounced (as in normal concrete (Neville, 2004)) compared to the other two factors of the mix viz., cold-bonded aggregate and water content. An interaction effect of water and cement content is observed in concrete with air-dried aggregate which may be due to the marginal variation in the amount of paste available in the mix than that in concrete with pre-soaked aggregate.

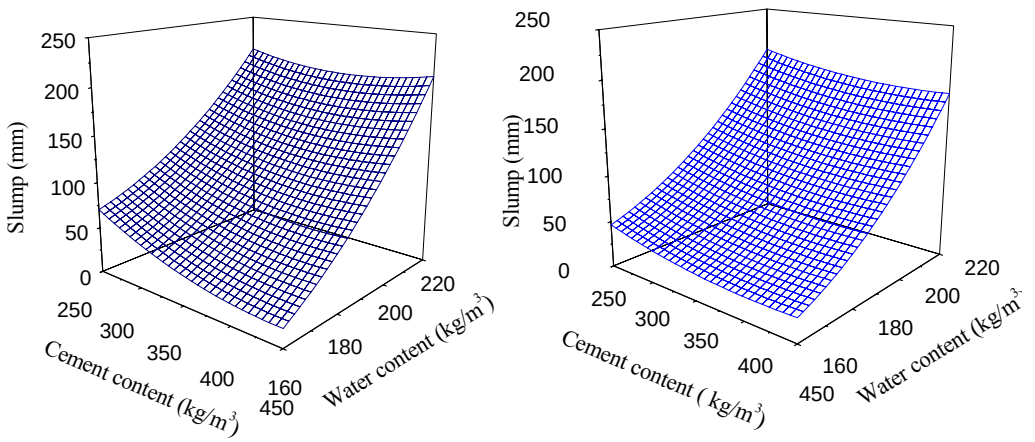


(a) Air-dried aggregate (b) Pre-soaked aggregate

Fig. 4.21 Slump of concrete with constant aggregate content (CA/TA = 50%)

#### 4.4.3.2 Response surface for compacting factor

Response of fresh concrete to the compacting factor (CF) test with variation in water content and CA/TA ratio is presented in Figs. 4.22 and 4.23. Similar to the slump behaviour the effect of both the factors and their interaction effect are significant on compacting factor. Variation of CF with aggregate is observed to be steeper at low water contents. At higher water contents (>190 kg/m$^3$), for all CA/TA ratios, the compacting factor is high (> 0.95). The CF increases from 0.86 to 0.93 with increase in CA/TA from 35 to 65% at water content of 160 kg/m$^3$ while the variation is from 0.965 to 0.99 at water content of 220 kg/m$^3$. Comparison of Figs. 4.22 and 4.23 shows that even though moisture condition of aggregate in the mix influenced the value of CF at low water contents and low volume fraction of aggregate, the influence is marginal at higher water contents, as observed in slump test.

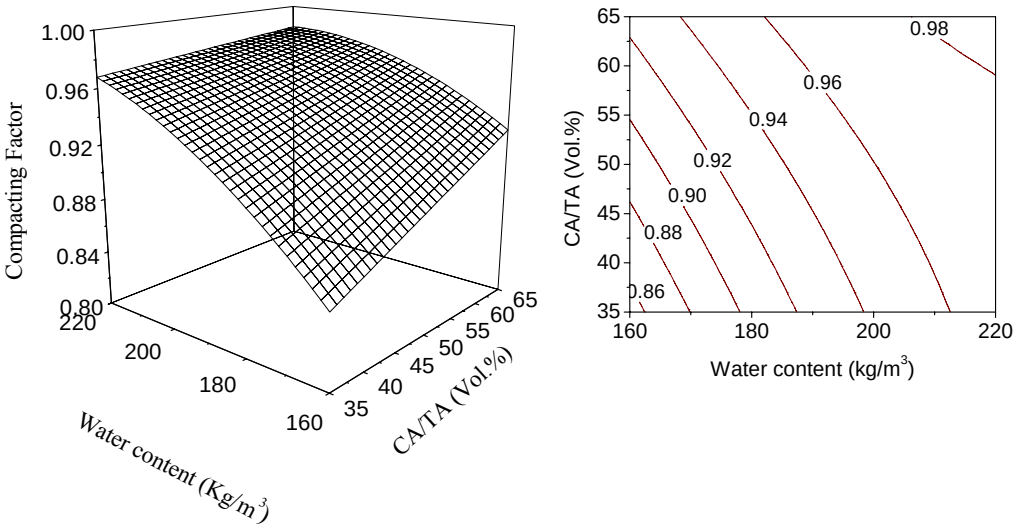


(a) Response surface (b) Contour plot

Fig. 4.22 Compacting factor of concrete with air-dried aggregate (cement content =350 kg/m$^3$)

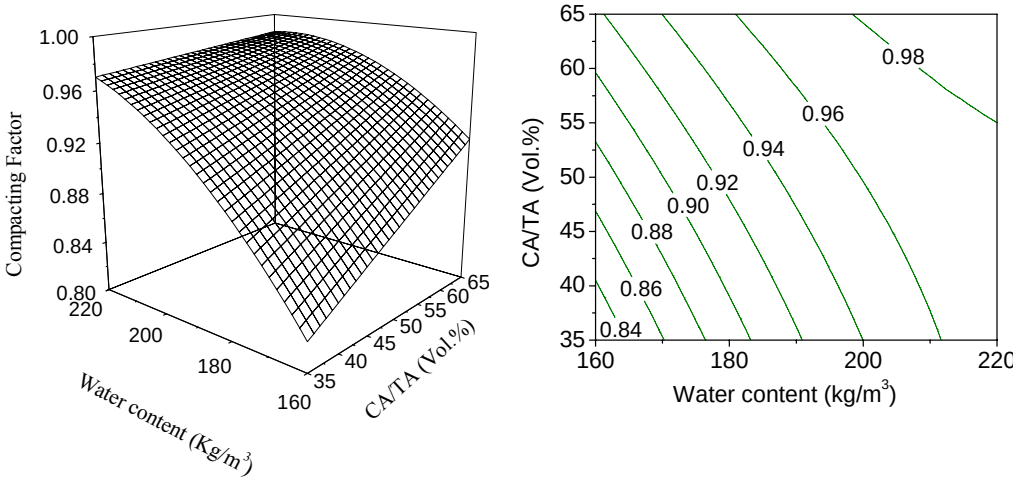


(a) Response surface (b) Contour plot

Fig.4.23 Compacting factor of concrete with pre-soaked aggregate (cement content=350 kg/m$^3$)

#### 4.4.3.3 Slump vs. compacting factor

A general pattern indicating the relation between slump values and compacting factor of cold-bonded aggregate concrete with pre-soaked aggregate is presented in Fig.

4.24. For low workability mixes, compacting factor is more appropriate while slump sensitively differentiates mixes with higher workability. This indicates that it may be practical to use compacting factor test to judge the workability of cold-bonded aggregate concrete at low workability end of scale than slump test as slump test may underestimate the workability which is typical in lightweight aggregate concrete (Clarke, 1993; Chandra and Berntsson, 2004). Both the tests are observed to be sensitive for slump value from 50 to 200 mm. Even though the relationship between slump and CF varies with volume fraction of aggregate, the variation is marginal in mixes with higher volume fraction of aggregate.

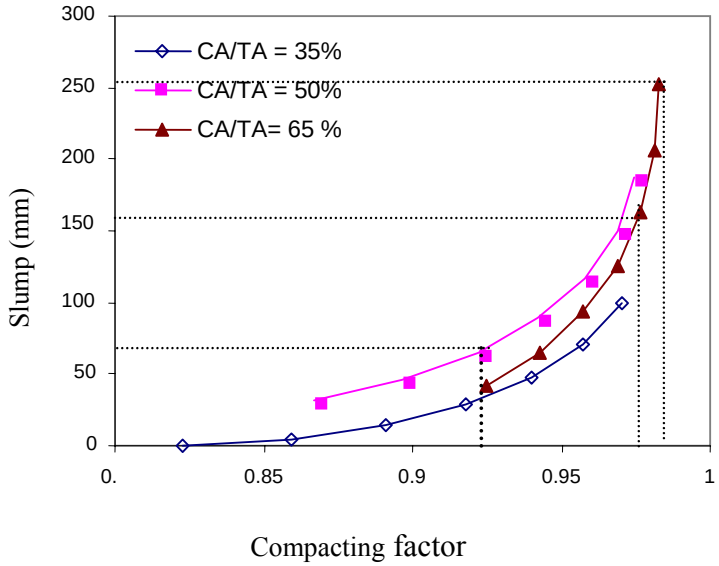


Fig. 4.24 Comparison of slump and compacting factor

### 4.4.4 Statistical Model for Compressive Strength

Model equations developed from the experimental results and quadratic response surfaces derived for compressive strength at various ages of curing are presented in this section. Table 4.14 presents the quadratic models for 7-day, 28-day and 90-day compressive strengths of concrete with air-dried aggregate and pre-soaked aggregate. In addition to the main effect and quadratic effect of all the three factors, the models

exhibit an interaction effect of cement and cold-bonded aggregate content on the compressive strength of concrete at all ages. The interaction effect of factors is further illustrated through response surface discussed in the following sections.

Table 4.14 Model equations and statistics for compressive strength

| Age | Regression model | $R^2$ | F-Value | Prob> F |
|---|---|---|---|---|
| | *Compressive Strength(MPa): Air-dried aggregate* | | | |
| 7–day | $-115.58+0.313*c+0.667*w+0.973*C_A-0.00132*c*C_A-2.065E-04*c^2-0.002098*w^2-0.005799*C_A^2$ | 0.98 | 79.47 | <0.0001 |
| 28-day | $-102.23+0.305*c+0.671*w+0.659*C_A-0.00108*c*C_A-1.761E-04*c^2-0.00215*w^2-0.00311*C_A^2$ | 0.994 | 303.2 | <0.0001 |
| 90-day | $-101.67+0.384*c+0.522*w+0.895*C_A-0.00128*c*C_A-2.732E-04*c^2-0.00176*w^2-0.00491*C_A^2$ | 0.989 | 238.2 | <0.0001 |
| | *Compressive strength (MPa):Pre-soaked aggregate* | | | |
| 7–day | $-80.328+0.317*c+0.337*w+0.857*C_A-0.0014*c*C_A-2.146E-04*c^2-0.00126*w^2-0.00427*C_A^2$ | 0.978 | 76.45 | <0.0001 |
| 28-day | $-74.169+0.297*c+0.367*w+0.794*C_A-0.0016*c*C_A-1.46E-04*c^2-0.00131*w^2-0.0029*C_A^2$ | 0.994 | 312.8 | <0.0001 |
| 90-day | $-87.32+0.369*c+0.402*w+0.945*C_A-0.00148*c*C_A-2.556E-04*c^2-0.00143*w^2-0.00491*C_A^2$ | 0.988 | 207.3 | <0.0001 |
| c=cement content (kg/m$^3$); water content (kg/m$^3$); $C_A$= CA/TA (Vol.%) | | | | |

#### 4.4.4.1 Response surface for compressive strength

Figs. 4.25 and 4.26 provide the response surfaces and contour plots for 28-day compressive strength of concrete with air-dried and pre-soaked aggregates respectively at 190 kg/m$^3$ water content (centre point of the factor water content). At this water content, an increase in cement content from 250 to 450 kg/m$^3$ reduces the w/c ratio from 0.76 to 0.42. At low CA/TA ratio, the improvement in strength of concrete with cement content is observed to be higher than that in concrete with higher volume fraction of aggregate, i.e. when cement content is increased from 250

to 450 kg/m$^3$, the compressive strength increases by 28 MPa in concrete with a CA/TA ratio of 35%, while this increase is only around 19 MPa in concrete with a CA/TA ratio of 65%. At lower cement content, (up to around 300 kg/m$^3$) there is a marginal increase in compressive strength of concrete with cold-bonded aggregate content whereas at higher values of cement content, a reduction in strength of concrete is observed with an increase in volume fraction of aggregate. This ascertains the influence of cold-bonded aggregate content on compressive strength of concrete with variation in cement content and indicates that it would be advantageous to use higher aggregate content for specified workability at low strength level. A transition region is also observed for a narrow range of cement content (approximately from 300 to 350 kg/m$^3$ and compressive strength from 30 to 35 MPa) at which no significant variation in strength of concrete with CA/TA ratio. The reason for such behaviour may be attributed to the strength of aggregate being almost the same as that of matrix or aggregate-matrix bond strength.

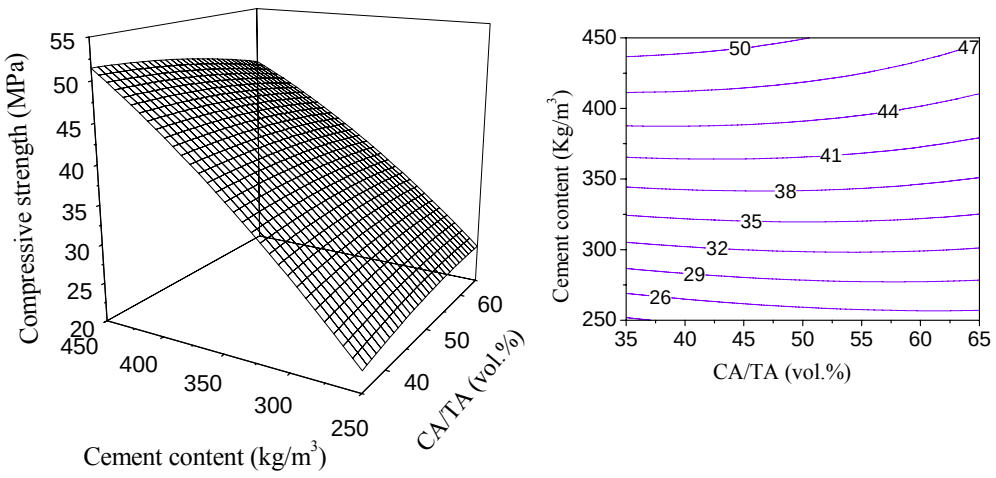


(a) Response surface (b) Contour plot

Fig. 4.25 28-day compressive strength of concrete with air-dried aggreagte (water content = 190 kg/m$^3$)

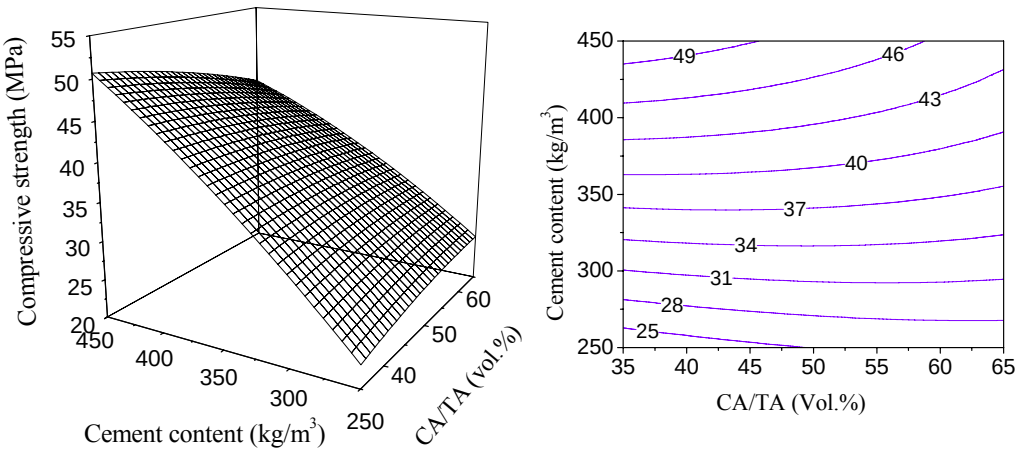


(a) Response surface (b) Contour plot

Fig. 4.26 28-day compressive strength of concrete with pre-soaked aggreagte (water content = 190 kg/m$^3$)

Table 4.15 shows the comparison between the compressive strength of cold-bonded aggregate concrete and concrete with crushed granite aggregate, which has been cast with similar mix composition. At low cement content, the strengths of concrete with crushed granite aggregate and concrete with cold-bonded aggregate are almost the same. This is attributable to the relatively lower strength of matrix and matrix phase initiating the failure in both concretes. But as the cement content increases, the strength of cold-bonded aggregate concrete deviates from normal concrete because of the existence of a stronger aggregate phase in concrete with crushed granite aggregate.

Comparison of Figs. 4.25 and 4.26 shows no marked difference in the compressive strength between concrete with air-dried and pre-soaked aggregates. Since the variation between concrete with air-dried aggregate compensated for water absorption and pre-soaked aggregate are quite marginal both with respect to workability and

compressive strength, further studies and discussions will be confined to pre-soaked aggregate.

Table 4.15 Comparison of compressive strength of cold-bonded aggregate concrete with normal weight aggregate concrete

| Cement content ($kg/m^3$) | Compressive strength (MPa) of concrete with a water content of 190 $kg/m^3$ | | | |
|---|---|---|---|---|
| | Cold-bonded aggregate CA/TA (%) | | Crushed granite aggregate CA/TA (%) | |
| | 50 | 65 | 50 | 65 |
| 250 | 25.0 | 25.8 | 23.0 | 25.0 |
| 350 | 38.1 | 36.5 | 42.5 | 41.0 |
| 450 | 48.0 | 44.0 | 52.5 | 52.0 |

#### 4.4.4.2 Variation of compressive strength with w/c ratio

The 28-day compressive strength of concrete for the range of w/c ratio i.e., 0.36 to 0.88, investigated is presented in Fig. 4.27 for three CA/TA ratios. Regression equation relating w/c ratio and compressive strength ($f_c$) according to Abram's rule, $f_c = k_1/k_2^{w/c}$ (Mehta and Monteiro, 2005) is also marked in figure. The difference in empirical constants of the equation may be attributed to the influence of cold-bonded aggregate on total porosity of concrete, variation in interaction between paste and aggregate content and matrix-aggregate bond strength in determining the concrete strength.

#### 4.4.4.3 Development of strength with period of curing

Fig. 4.28 presents the development of strength with duration of curing, wherein the 7-day and 90-day strengths are respectively around 70 to 80% and 110 to 120% of the 28-day strength. Higher percentage enhancement at 90-day strength is observed in concrete with lower cement content.

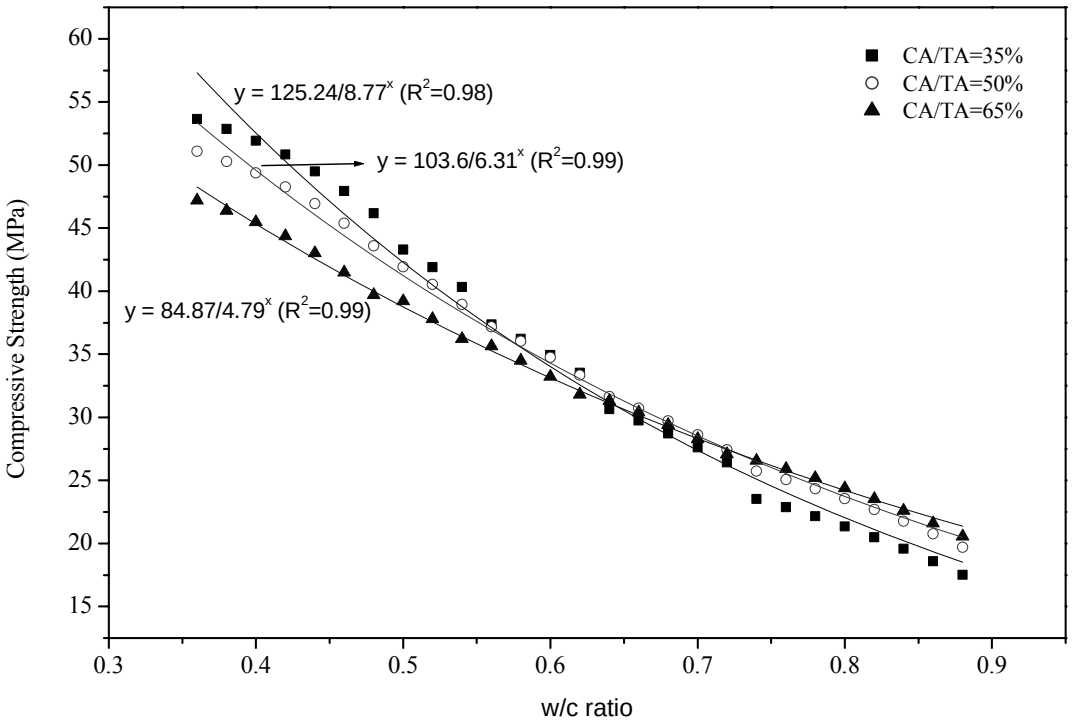


Fig. 4.27 Relationship between w/c ratio and compressive strength

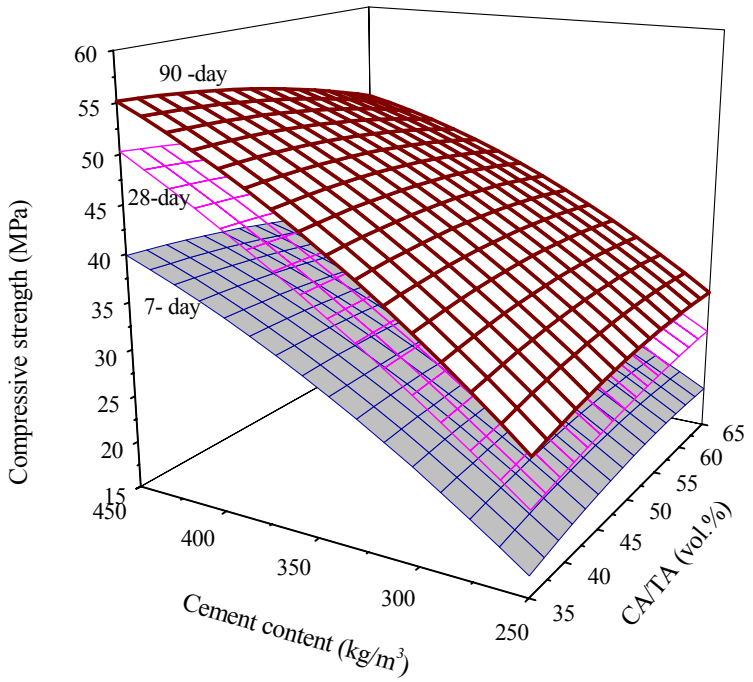


Fig. 4.28 Development of compressive strength with period of curing (water content =190 kg/m$^3$)

Even though aggregate controls the failure of concrete at higher strengths, such gain in strength with period of curing is attributed by the (i) improvement in strength of the aggregate matrix interface resulting from its mechanical interlocking with the cement paste and the chemical interaction in the form of pozzolanic reaction between the aggregate and cement paste (Zhang and Gjorv, 1992) and (ii) the improvement in aggregate strength due to refinement of pores caused by the penetration of cement paste. Similar observation has been made by Dhir et al. (1984) on lightweight aggregate concrete with 25 to 50 MPa strength range.

From the investigations on cold-bonded aggregate concrete discussed, the major points regarding mixture composition are summarised as; (i) Workability of concrete is not only a function of the water content but also greatly influenced by aggregate content; (ii) Compressive strength of concrete is also a function of volume fraction of cold-bonded aggregate in addition to the w/c ratio and cement content; (iii) Apart from the main effects, compressive strength of concrete is highly influenced by the interaction effect of cement content and volume fraction of aggregate; (iv) There is no marked difference in the workability and strength between concrete using air dried aggregates compensated for water absorption and pre-soaked aggregates; (v) The statistical equations developed for workability and strength can be effectively used for predicting the responses.

## 4.5 MIXTURE DESIGN GUIDELINES

Many of the available mixture proportioning methods are observed to be applicable to specific lightweight aggregate characteristics, for example, i) mix design charts of Swamy and Lambert (1983) and Dhir et al. (1984) respectively for sintered fly ash and expanded shale aggregates, ii) prediction relations, based on two-phase composite material approach, for slump and strength of concrete derived with pumice aggregate

and expanded clay (Videla and Lopez, 2000), and iii) proportioning method based on strength of aggregate in concrete and mortar strength double than that of aggregate strength (Chandra and Berntsson, 2004). ACI 211.2 (1990) provides a general method for selecting and adjusting mix proportions for concrete with lightweight aggregate conforming to ASTM C 330. Since concrete properties are highly influenced by aggregate characteristics and cold-bonded aggregate used in the present study does not conform to the classification of lightweight aggregate as per ASTM C 330 (2005) typical mix design relationships have been presented based on the results of the investigation discussed in the previous section.

### 4.5.1 Mix Proportioning Relationships

Using the models for workability and compressive strength typical relationships have been established to demonstrate a method of mixture proportioning for cold-bonded aggregate concrete. Fig.4.29 presents the relationship between water demand and volume fraction of cold-bonded aggregate for different slump values (Since the variation in workability is minimal with cement content, the calculation was based on a cement content value of 350 kg/m$^3$). Fig. 4.30 shows the cement content required to produce concrete of specified workability and strength. The quantity of cement for a given workability and strength is getting reduced with an increase in volume fraction of cold-bonded aggregate up to strength level of 35 MPa (Fig.4.30 a-c). But compressive strength from 35 MPa onwards (Fig. 4.30 d-f) an optimum level of cement content is noticed between 45 to 55% of volume fraction of aggregate.

Based on this, a design procedure is outlined below for cold-bonded aggregate concrete (without any admixture) with the charts developed in the study though the charts are particular to the characteristics of materials used and range of parameters investigated.

Step 1: The mean target strength is to be calculated from the specified characteristic strength and the degree of quality control (IS 456, 2000).

Step 2: If the workability is expressed as compacting factor convert the same to equivalent slump value (Fig. 4.24).

Step 3: From Fig. 4.30, the cement content and CA/TA ratio are chosen to produce concrete of specified strength and workability, maintaining lower cement content for economical mixture proportion and the requirement of minimum cement content for the exposure condition.

Step 4: The water demand corresponding to CA/TA determined in step 3 for the required workability is chosen from Fig. 4.29. The w/c ratio is to be calculated from the cement content and water content.

Step 5: The mix is proportioned on absolute volume basis, after obtaining the specific gravity of cement, sand and saturated surface dry specific gravity (30-min. absorption) of cold-bonded aggregate.

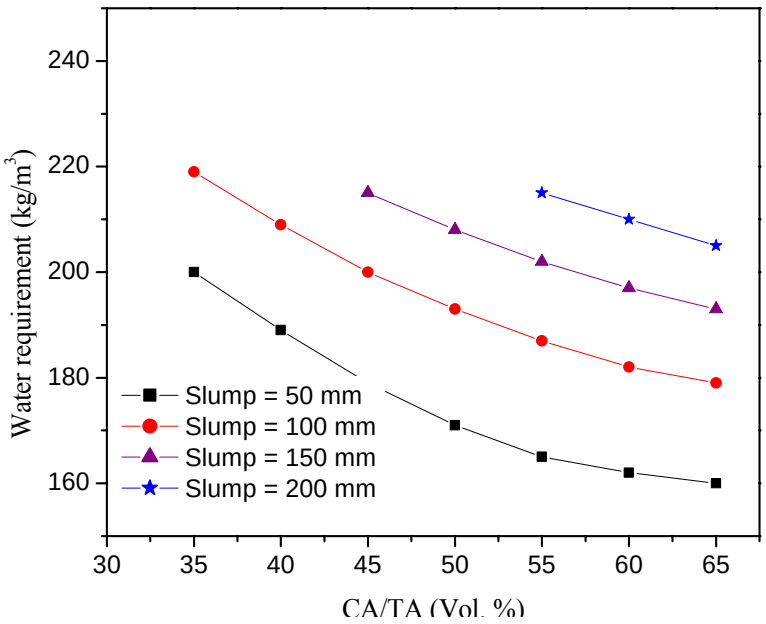


Fig. 4.29 Variation in water demand for constant slump

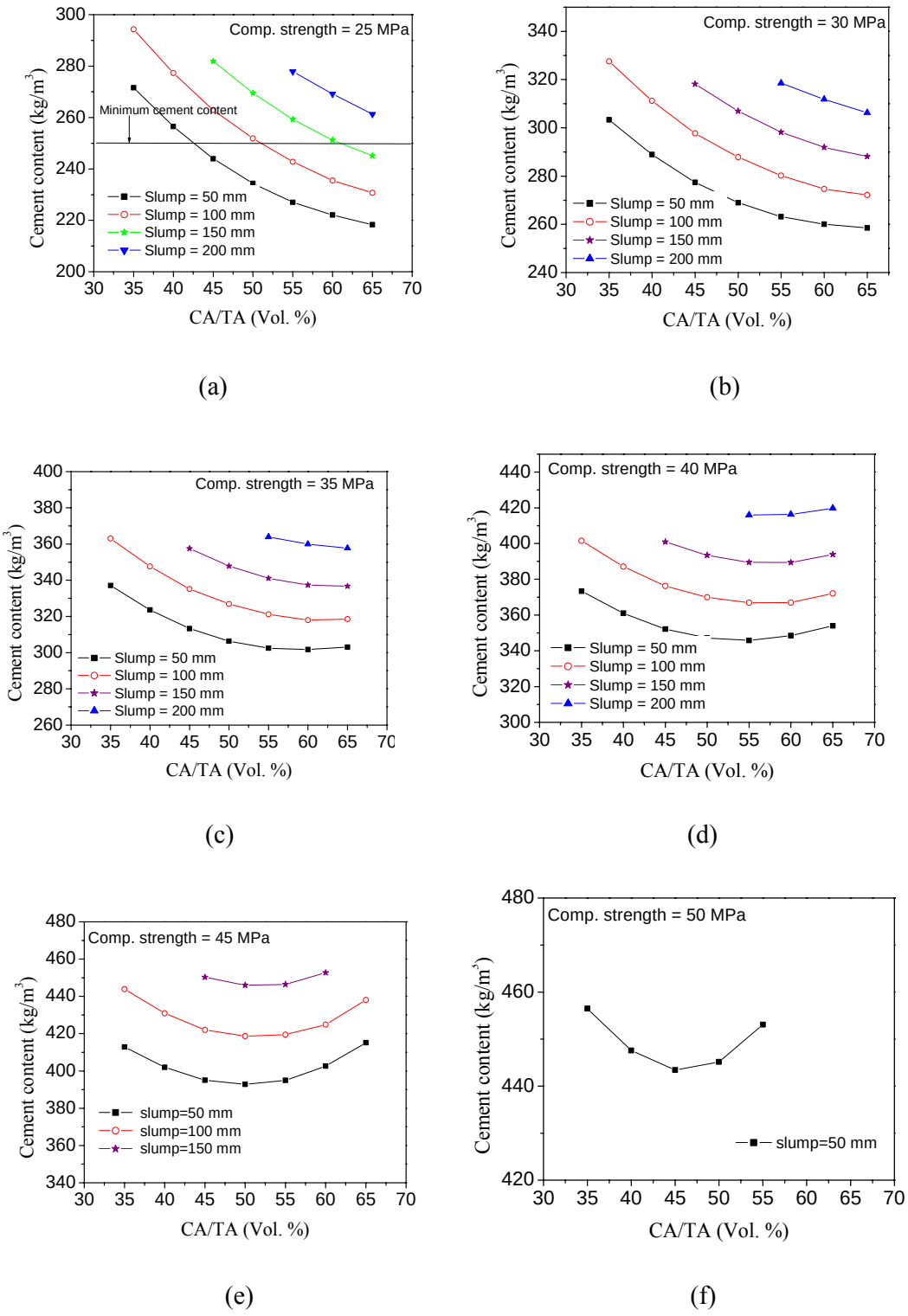


Fig.4.30 Requirement of cement content for constant strength (28-day)

## 4.6 BOND STRENGTH: PULL OUT TEST

The bond between concrete and reinforcement is of considerable importance in designing reinforced concrete structure as it ensures transfer of load to the embedded steel. The bond between steel and concrete determines anchorage and influences the distance between cracks and their width. The bond is considered as a combination of adhesion, friction and mechanical interaction between concrete and steel. From the numerous investigations on normal weight concrete it has been made clear that the aspects influencing bond behaviour are (i) concrete type, (ii) rebar geometry and (iii) loading condition and construction details (Xiao and Falkner, 2007). In this study the effectiveness of bond between cold-bonded aggregate concrete and reinforcement is determined in accordance with IS 2770 (2002) through pull out test for a comparative study of bonding qualities of concrete.

### 4.6.1 Materials and Methodology

150 mm cubes were used for bond strength test with a single reinforcing bar embedded vertically along the central axis with a helix of 6 mm diameter plain mild steel reinforcing bar at 25 mm pitch for confining the reinforcement. Table 4.16 lists the bar parameters and its yield and ultimate strength. The mix compositions used for the statistically designed experiments based on RSM with cement content and volume fraction of aggregate as factors are presented in Table 4.17. Water content was kept constant at 190 kg/m$^3$ as the variation in cement content itself would cater mixtures with wide range of compressive strength. All the specimens were cured for 28 days and three specimens were tested for bond strength in each mix.

In pull out test on plain bars, the maximum load generally represents the bond strength that can be developed between the concrete and steel and it is not different

from the load at first visible slip. But where deformed bars are used, the maximum load may correspond to a large slip which may not in fact be obtained in practice before other types of failure occur. Hence a maximum slip level of 0.25 mm at the free end of the bar is used to define maximum acceptable bond slip as per IS 2770 (2002) after which the expected damage to the structure is too large for service conditions (Mor, 1992). The ultimate bond strength has been calculated from the load corresponding to the least of the following three criteria :(i) yield point of steel has been reached, (ii) the enclosing concrete has failed, (iii) a minimum slippage of 2.5 mm occurring at the loaded end.

Table 4.16 Mechanical properties of reinforcing bar

| Bar diameter (mm) | Bar type | Yield stress ($N/mm^2$) | Ultimate strength ($N/mm^2$) |
|---|---|---|---|
| 12 | Plain, mild steel | 320 | 407.4 |
| 12 | Deformed, HYSD | 498.7 | 579.7 |
| 20 | Deformed, HYSD | 534.8 | 670.3 |

Table 4.17 Mixture composition details for bond strength analysis

| Run | Cement content ($kg/m^3$) | w/c ratio | CA/TA (Vol. %) | Run | Cement content ($kg/m^3$) | w/c ratio | CA/TA (Vol.%) |
|---|---|---|---|---|---|---|---|
| 1 | 350 | 0.54 | 50 | 8 | 350 | 0.54 | 50 |
| 2 | 250 | 0.76 | 35 | 9 | 450 | 0.42 | 35 |
| 3 | 350 | 0.54 | 28.8 | 10 | 491 | 0.39 | 50 |
| 4 | 250 | 0.76 | 65 | 11 | 208.6 | 0.91 | 50 |
| 5 | 350 | 0.54 | 50 | 12 | 350 | 0.54 | 50 |
| 6 | 350 | 0.54 | 71.2 | 13 | 450 | 0.42 | 65 |
| 7 | 350 | 0.54 | 50 | | | | |

The pull out test was performed in a servo-hydraulic 40 t capacity Universal Testing Machine. The specimen was suspended from the upper cross-head of the testing machine (Fig. 4.31). Loading was done at a loading rate of 1.25 mm/minute. The displacement was measured by dial gauges attached to the reinforcing bar and concrete and the relative displacement (slip) between bar and concrete was determined. The bond stress ($\tau$) was calculated using the formula: $\tau = F/(\Pi \times d \times l)$; F, the applied load ; *d,* the nominal diameter and *l*, the embedment length.

The regression equation obtained from the statistical analysis for bond stress for a slip of 0.25 mm and ultimate bond stress are summarised in Table. 4.18

Fig. 4.31 Set up for pull out test

Table 4.18 Regression equation relating mixture composition and bond stress (water content =190 kg/m$^3$)

| Bar size and type | Regression equations | $R^2$ | F-value | Prob>F |
|---|---|---|---|---|
| | *Bond stress (MPa) at 0.25 mm slip* | | | |
| mild steel, 12 mm Φ | $3.815-0.00448*c-0.0267*C_A+0.0000182*c^2$ | 0.95 | 61.82 | <0.0001 |
| HYSD, 12 mm Φ | $1.544+0.0308*c-0.0459*C_A-0.0000917*c*C_A-0.0000285*c^2+0.000575*C_A^2$ | 0.97 | 59.44 | <0.0001 |
| HYSD, 20 mm Φ | $3.081+0.0272*c-0.0982*C_A-0.000107*c*C_A-0.0000229*c^2+0.00109*C_A^2$ | 0.98 | 91.42 | <0.0001 |
| | *Ultimate bond strength (MPa)* | | | |
| mild steel, 12 mm Φ | $5.185-0.00518*c-0.0279*C_A+0.0000197*c^2$ (pull out failure) | 0.96 | 38.45 | <0.0001 |
| HYSD, 12 mm Φ | 9.97 MPa ( steel yielding in all cases) | | | |
| HYSD, 20 mm Φ | $1.960+0.0636*c-0.115*C_A-0.0000513*c^2+0.000764*C_A^2$ (concrete failure) | 0.96 | 54.98 | <0.0001 |
| c = cement content (kg/m$^3$), $C_A$ = CA/TA (vol. %) | | | | |

### 4.6.2 Influence of Mixture Composition on Bond Stress (0.25 mm slip)

Fig. 4.32 shows the response surface and contour plot of bond stress at a slip of 0.25 mm. While the bond stress of plain bars in concrete is observed to vary linearly with cold-bonded aggregate content, the bond stress of deformed bars are influenced by the interaction effect of aggregate and cement content in addition to their quadratic effects. In both cases, the bond stress increases with an increase in cement content of the mix for a given volume fraction of aggregate. For a given cement and aggregate content, as expected, the bond stress with deformed bar is higher than the corresponding plain bar. The decrease in bond strength with increase in cold-bonded aggregate content may be attributed to the reduction in frictional resistance offered by concrete due to the proportionate decrease in sand content and increase in smooth

textured cold-bonded aggregate content. Similar behaviour has been reported in laterized concrete with variation in mix composition (Osunade, 2002).

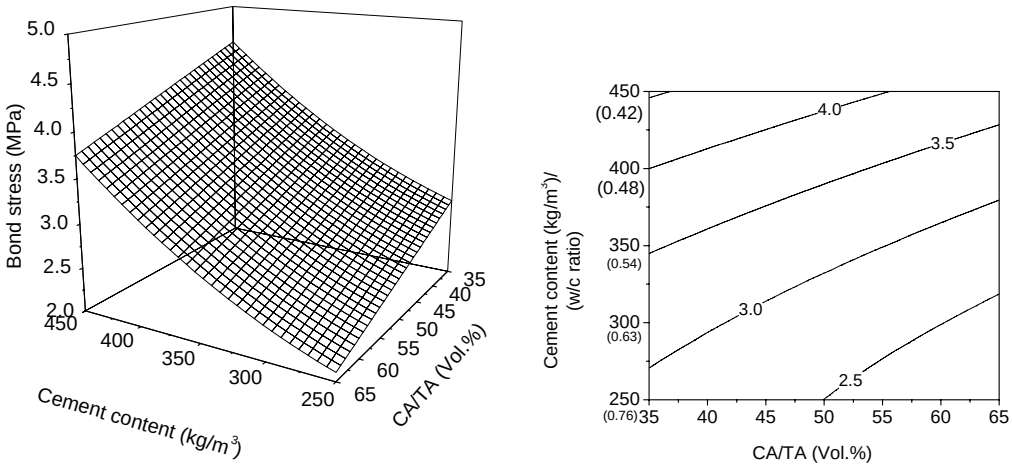


Response Surface Contour Plot

Fig 4.32 (a) Response surface and contour plot of bond stress at 0.25 mm slip (mild steel, 12 mm Φ)

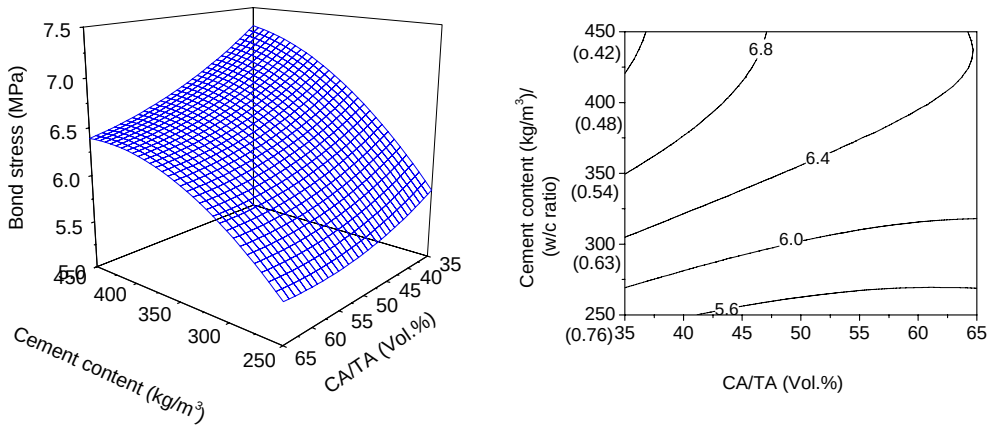


Response Surface Contour Plot

Fig 4.32 (b) Response surface and contour plot of bond stress at 0.25 mm slip (HYSD, 12 mm Φ)

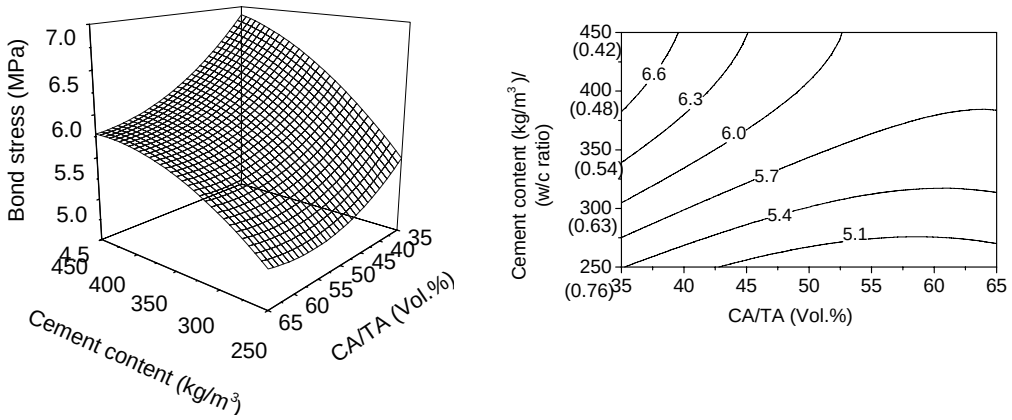


Response Surface Contour Plot

Fig 4.32 (c) Response surface and contour plot of bond stress at 0.25 mm slip (HYSD, 20 mm Φ)

### 4.6.3 Variation in Bond Stress (at 0.25 mm slip) with Compressive Strength

The variation in bond stress of cold-bonded aggregate concrete with compressive strength is presented in Fig. 4.33. The variation in compressive strength from 25 to 50 MPa results in bond strength from 2.6 to 5.2 MPa in concrete with plain bars of mild steel and 4.7 to 7.3 MPa in deformed bars. In the case of plain bars, for a given strength, effect of volume fraction of aggregate on bond strength is observed more significant only at lower strengths. This behaviour is attributed to the higher cement content and matrix strength associated with concrete of higher CA/TA ratio at higher strength level. The size effect of deformed bars on bond stress is quite marginal though higher stress is always observed in bars of smaller diameter. This conforms to the observations by earlier research on lightweight aggregate concrete (Orangun, 1967; Teo et al., 2007) and normal concrete (Ichinose, 2004). The size effect on bond strength is mainly attributable to the brittle cracking around the bars; usually reduced by confinement of concrete by spiral reinforcement (Ichinose, 2004).

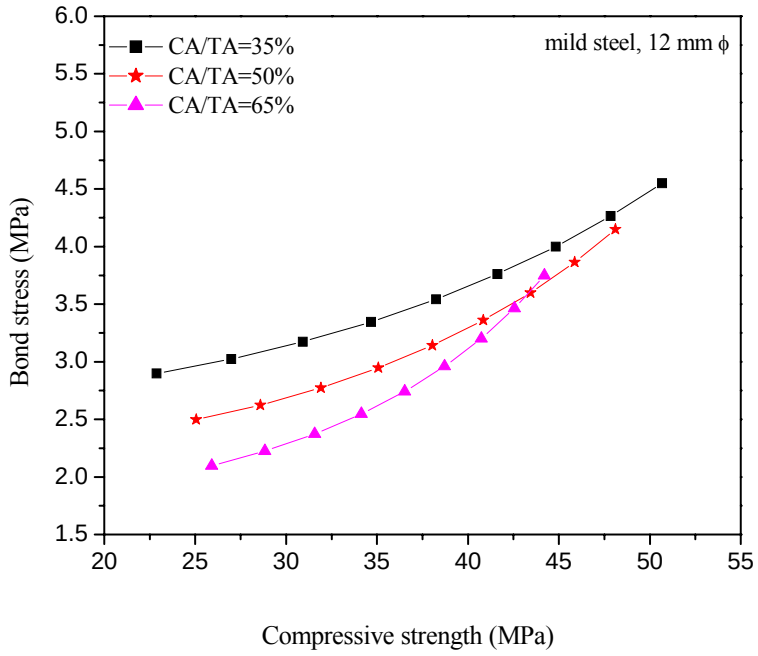


Fig.4.33 (a) Variation in bond stress (at slip of 0.25 mm) with compressive strength (mild steel, 12 mm Φ)

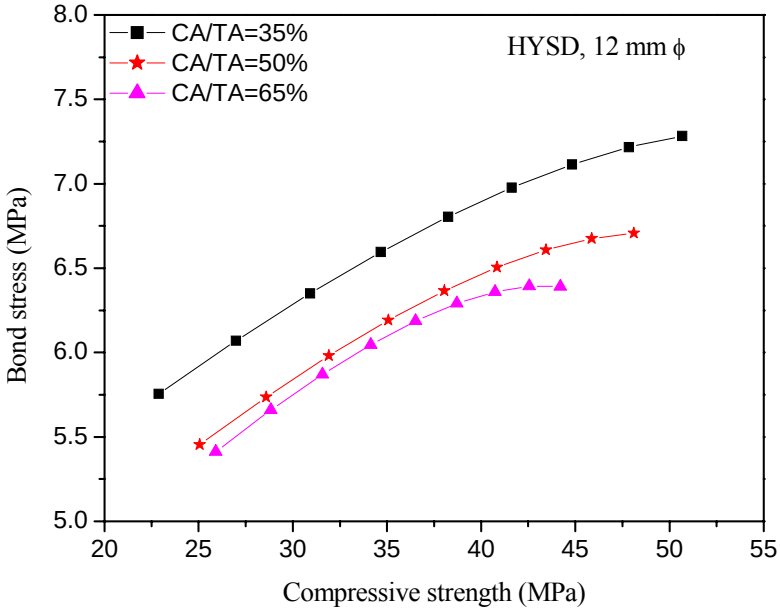


Fig. 4.33 (b) Variation in bond stress (at slip of 0.25 mm) with compressive strength (HYSD, 12 mm Φ)

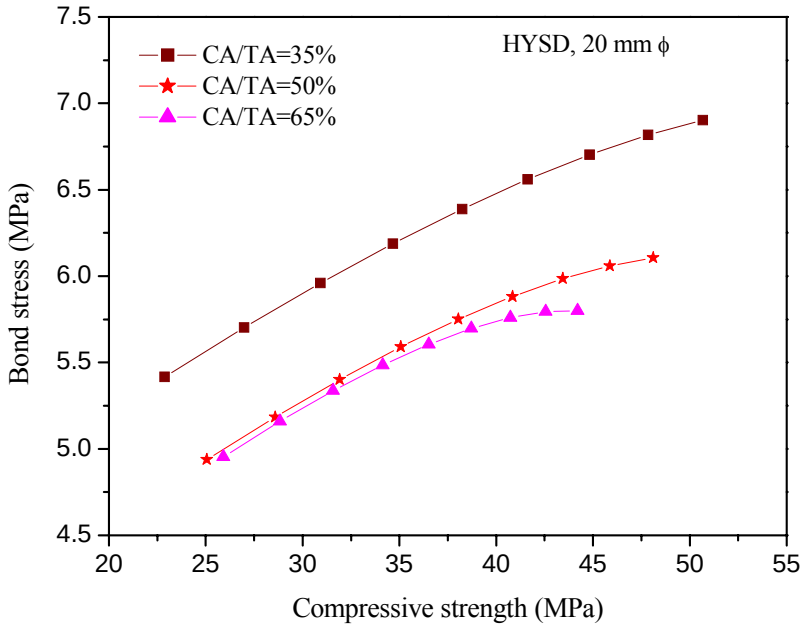


Fig.4.33 (c) Variation in bond stress (slip at 0.25 mm) with compressive strength (HYSD, 20 mm Φ)

Table 4.19 provides bond strength in cold-bonded aggregate concrete with deformed bar and relative strength for plain bar (as percentage of deformed bar). Bond strength of concrete with plain bars is 38 to 61 % of that with deformed bars; lower percentage associated with concrete containing higher volume fraction of cold-bonded aggregate.

Table 4.19 Bond strength of deformed bar and relative strength of plain bar

| Compressive strength of concrete (MPa) | Bond strength (MPa) HYSD bar | | | Mild steel bar, relative strength as percentage of HYSD bar | | |
|---|---|---|---|---|---|---|
| | CA/TA (35 %) | CA/TA (50 %) | CA/TA (65%) | CA/TA (35 %) | CA/TA (50 %) | CA/TA (65%) |
| 25 | 5.9 | 5.5 | 5.4 | 49.9 % | 45.8% | 39.0% |
| 30 | 6.3 | 5.8 | 5.7 | 49.8% | 44.5% | 37.9% |
| 35 | 6.6 | 6.2 | 6.1 | 50.8% | 45.8% | 40.7% |
| 40 | 6.8 | 6.5 | 6.3 | 52.8% | 48.8 % | 48.3% |
| 45 | 7.1 | 6.7 | 6.4 | 56.3% | 53.8% | 55.9% |
| 50 | 7.3 | - | - | 60.7% | - | - |

### 4.6.4 Influence of Mixture Composition on Ultimate Bond Strength

During loading for maximum bond strength, pull out failure was observed with plain bars irrespective of the mix, i.e., similar to the observations on normal concrete by other researchers. Steel which pulled out from concrete was almost free from any adhered concrete. Concrete was also observed with no or very little cracking of the surrounding concrete. In concrete with deformed bars of 12 mm, steel started yielding in all the mixes before bond failure. Hence ultimate bond stress was calculated based on the load at yielding. Whereas in concrete with deformed bars of 20 mm, concrete failure (before bond failure) was observed with side longitudinal cracks starting from the loaded end of the specimen.

Fig. 4.34 shows the response surface of ultimate bond strength of concrete with variation in mixture composition. Ultimate bond strength also significantly improves with an increase in cement content. For a given cement content marginal reduction in ultimate strength can be noticed with cold-bonded aggregate content as observed in bond at slip of 0.25mm.

Variation in ultimate bond strength and bond stress at slip of 0.25 mm with compressive strength in Fig. 4.35 indicate a marginal difference between the two values in the case of plain bars of mild steel due to sudden loss of bond due to slip. But in deformed bars, ultimate bond stress is more than two times as that at slip of 0.25 mm. In deformed bars, after slip of 0.25 mm, the mechanism mainly switches from adhesion to friction and rib support resulting finally in splitting failure of unconfined concrete. The ultimate bond strength of concrete is about 10 to 18% of compressive strength with plain bars of 12 mm and 32 to 46 % for concrete embedded with 20 mm bar. This is comparable to the values (19 to 42 %) reported in literature

(Orangun, 1967; Mor, 1992; Teo et al, 2007) for lightweight aggregate concrete of similar or higher strengths.

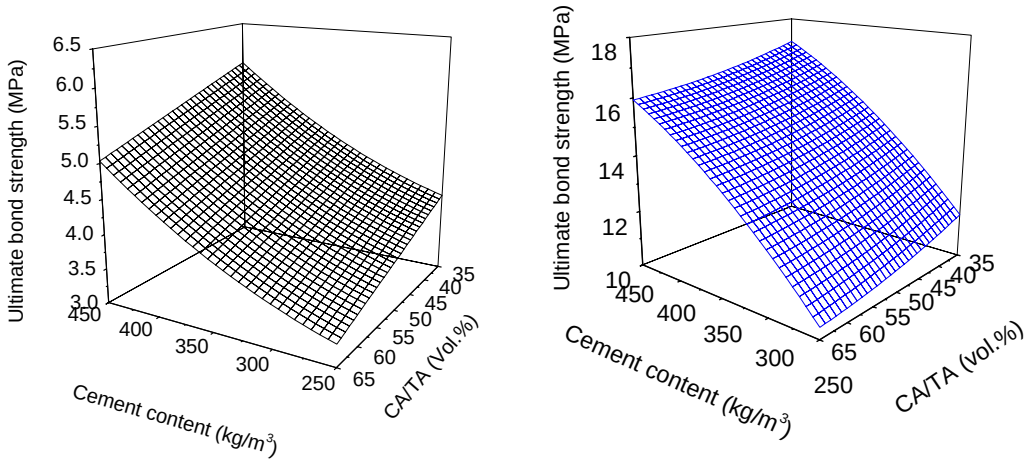


(a) Mild steel, 12 mm Φ (b) HYSD, 12 mm Φ

Fig. 4.34 Response surface of ultimate bond strength

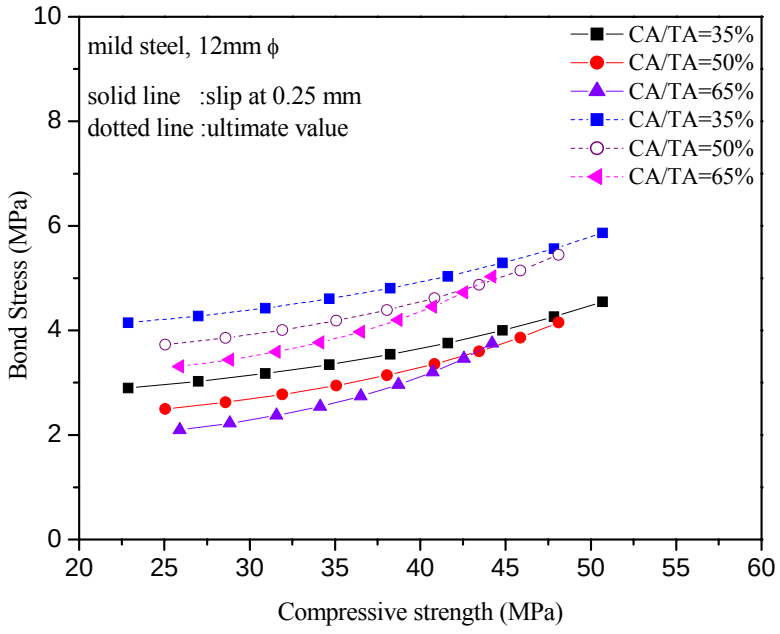


Fig. 4.35 (a) Comparison of bond stress at slip of 0.25 mm and ultimate bond strength (mild steel, 12 mm Φ)

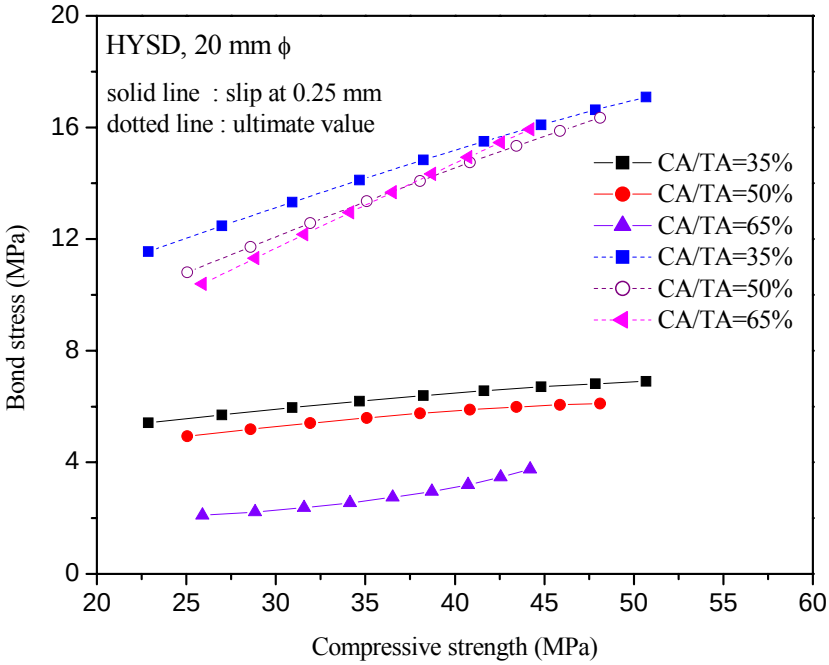


Fig. 4.35 (b) Comparison bond stress at slip of 0.25 mm and ultimate bond strength (HYSD, 20 mm Φ)

Table 4.20 provides the comparison of bond strength of cold-bonded aggregate concrete with normal weight concrete using crushed granite aggregate of similar mixture proportion with same cement content and volume fraction of coarse aggregate. Bond strength of concrete with crushed granite aggregate is higher than cold-bonded aggregate concrete both in plain (up to 33%) and deformed bars (up to 13%) attributable to the higher compressive strength of concrete with crushed granite aggregate and angular shape and rough texture of the aggregate. Orangun (1967) and Mor (1992) also reported lower bond strength in lightweight aggregate concrete which are attributed to the aggregate weakness and its texture.

Table 4.20 Comparison of bond strength of cold-bonded aggregate concrete with normal weight aggregate concrete (CA/TA=65%, water content= 190 kg/m$^3$)

| Cement content (kg/m$^3$) | Cold-bonded aggregate concrete | | | | | Normal concrete with crushed granite aggregate | | | | |
|---|---|---|---|---|---|---|---|---|---|---|
| | Comp. Strength (MPa) | Bond Stress (MPa) | | | | Comp. Strength (MPa) | Bond Stress (MPa) | | | |
| | | Mild steel bar (12 mm) | | HYSD bar (20 mm) | | | Mild steel bar (12 mm) | | HYSD bar (20 mm) | |
| | | Slip, 0.25 mm | Ultimate value | Slip, 0.25 mm | Ultimate value | | Slip, 0.25 mm | Ultimate value | Slip, 0.25 mm | Ultimate value |
| 250 | 25.8 | 2.10 | 3.31 | 4.95 | 10.39 | 25.0 | 2.65 | 4.42 | 5.09 | 11.6 |
| 350 | 36.5 | 2.71 | 3.97 | 5.63 | 13.68 | 41.0 | 3.53 | 4.95 | 6.12 | 15.1 |
| 450 | 44.0 | 3.75 | 5.03 | 5.81 | 15.93 | 52.0 | 4.60 | 5.83 | 6.57 | 17.1 |

## 4.7 SUMMARY

Having identified the factors influencing fresh and hardened properties of cold-bonded aggregate concrete, statistically designed experiments based on RSM has been adopted to understand the influence of mix composition on workability and strength behaviour of concrete for a wide range of values of the mix proportioning variables. Workability of concrete is influenced by both the water content and volume fraction of the cold-bonded aggregate along with an interaction effect between both these factors. Strength of concrete is mainly governed by the initiation of failure in matrix or matrix-aggregate bond in concretes below a cement content of 300 kg/m$^3$, (strength <30 MPa) whereas at higher cement content the predominant failure mode changes to aggregate fracture and concrete strength decreases with increase in volume fraction of cold-bonded aggregate. Using the statistical models developed a mixture design procedure for cold-bonded aggregate concrete has been proposed. Bond strength of plain and deformed bars in concrete has been evaluated and the relationship between bond strength and compressive strength of cold-bonded aggregate concrete has been brought out.

# CHAPTER 5

# PERMEATION BEHAVIOUR OF COLD-BONDED FLY ASH AGGREGATE CONCRETE

## 5.1 GENERAL

Having established the workability and strength properties of cold-bonded fly ash aggregate concrete, the next important aspect is its permeation behaviour. Knowledge of water and gas penetration and its transport characteristics on concrete are of importance as they affect the durability and manifest the deterioration of concrete. A concrete with high permeation characteristics will provide ready access for both water and harmful substances resulting in deterioration of either concrete or steel reinforcement embedded in the concrete or a combination of both. Review (section 2.4.4.1 and Table 2.3) indicated no systematic studies on gas or water penetration behaviour of cold-bonded fly ash aggregate concrete. As cold-bonded aggregate possess higher porosity, the penetrability of fluid in concrete may be different from that of normal concrete and those with rigidly bonded expanded or sintered aggregate. Zhang and Gjorv (1990b) report that lightweight aggregate with porous surface can provide improved paste-aggregate interface than aggregate with denser outer shell (sintered/expanded aggregate), leading to a reduction in the interconnected pores in the concrete. Since connectivity of pore system is a prerequisite for fluid flow, the permeation behaviour of cold-bonded aggregate concrete requires an in depth study.

In general, the pores and its distribution in concrete composite arise from its constituent materials (cement paste and aggregate) and their interactions in terms of interfacial zone and packing geometry. Hence this chapter is aimed at investigating the permeation behaviour of concrete as influenced by its mixture composition and

relating the same to the compressive strength since the fitness of concrete is often judged by its compressive strength. Here also, models are developed in terms of mix proportioning variables for analyzing their influence on permeable porosity, water absorption, sorptivity and chloride penetrability for a wide range of values of the proportioning variables.

## 5.2 MATERIALS AND MIXTURE COMPOSITION

Table 5.1 provides the factors, factor levels along with the mixture composition involved in the statistically designed experiments based on RSM to develop model equations for permeation parameters of concrete. Only pre-soaked aggregate was used in the experiments. Normal concrete using crushed granite aggregate with three cement contents (250, 350 and 450 kg/m$^3$) at a water content of 190 kg/m$^3$ and CA/TA of 65% were used in the case for a comparison with cold-bonded aggregate concrete. Cube specimens of 100 mm size were used after curing in mist room for 28 days for tests on permeable porosity, water absorption and sorptivity. Chloride ion penetrability tests used specimens of 50 mm thickness and 100 mm in diameter.

## 5.3 METHODS OF MEASUREMENT

### 5.3.1 Permeable Porosity

Apparent porosity due to volume of permeable voids in concrete relates better with the permeation characteristics of concrete. The amount of water that can penetrate into concrete, a measure of the permeable porosity, was measured on 100 mm cube using vacuum saturation method. Specimens (3 samples for each mix composition) were preconditioned in an oven at 105$\pm$5 ºC for 24 hrs prior to testing. The oven-dried samples were then subjected to vacuum for 3 hours and saturated with water for 1 hour while maintaining the vacuum and then allowed to soak for another 18$\pm$2 hrs

after removing the vacuum as per ASTM C 1202 (2005). Permeable porosity was calculated as the ratio of the difference between weights of saturated surface dry (SSD) sample after vacuum saturation and weight of oven-dried sample to the difference between weights of SSD sample and apparent weight of sample in water as discussed in section 4.2.3.1

Table 5.1 Factor levels and mix composition for statistically designed experiment on permeation

| Factors | Cement content ($kg/m^3$) | | Water content ($kg/m^3$) | | CA/TA (Vol. %) | |
|---|---|---|---|---|---|---|
| | Low level | High level | Low level | High level | Low level | High level |
| Runs | 250 | 450 | 160 | 220 | 35 | 65 |
| 1 | 350 | | 190 | | 50 | |
| 2 | 250 | | 160 | | 35 | |
| 3 | 450 | | 160 | | 65 | |
| 4 | 518.2 | | 190 | | 50 | |
| 5 | 350 | | 139.6 | | 50 | |
| 6 | 350 | | 190 | | 50 | |
| 7 | 350 | | 190 | | 50 | |
| 8 | 181.8 | | 190 | | 50 | |
| 9 | 350 | | 190 | | 50 | |
| 10 | 450 | | 220 | | 65 | |
| 11 | 350 | | 190 | | 50 | |
| 12 | 350 | | 190 | | 75.2 | |
| 13 | 350 | | 190 | | 24.8 | |
| 14 | 250 | | 220 | | 65 | |
| 15 | 350 | | 240.5 | | 50 | |
| 16 | 450 | | 160 | | 35 | |
| 17 | 450 | | 220 | | 35 | |
| 18 | 250 | | 220 | | 35 | |
| 19 | 350 | | 190 | | 50 | |
| 20 | 250 | | 160 | | 65 | |

### 5.3.2 Water Absorption

Water absorption represents the pore space, as distinct from the ease with which a fluid penetrates into the concrete under shallow waters. Absorption under normal

condition was measured on oven dried samples of 100 mm cube conditioned as mentioned above, after immersing (shallow immersion) in water at 23±2 ºC till constant mass. Absorption was expressed as the increase in mass as a percentage of oven-dried mass (ASTM C 642, 1997). Several individual pieces/portions of concrete as recommended by ASTM C 642 (1997) were not used for the test to avoid the variability caused by the water absorption of cut surface of aggregates which would likely to be exposed on the pieces of the concrete. For each run (mix) tests were carried out on three specimens and the mean value was taken for the analysis.

### 5.3.3 Sorptivity

Permeability is a measure of flow of water under pressure differential in a saturated porous medium (Hall and Yau, 1987) and for deep sea structures or water-retaining structures where the ingress of water into concrete will be governed by this mechanism under a head of water. But in other structures where concrete is rarely saturated while in use and driving force of fluids entering concrete is not the pressure differential, permeability is a wrong parameter for modeling capillary flows in concrete which are open to the ambient medium and represents an incomplete behaviour (Hall and Yau, 1987; Hall 1989). Thus, sorptivity has emerged as the most useful parameter for understanding the moisture dynamics of concrete (McCarter et al., 1992; Gopalan 1996; Martys and Ferraris, 1997; Dias 2004) which characterises the tendency of a porous material to absorb and transmit water by capillarity. The movement of water into concrete and other building materials are governed through a classical square-root time relationship (Hall, 1989). Assuming a constant water supply at the inflow surface, sorptivity ($S$) is related to the cumulative absorbed volume of water per unit area of inflow surface ($i$) and elapsed time ($t$) by the relationship, $i$

$=A+ S\sqrt{t}$ ; $A$, the constant term (intercept at t=0) represents the effect of initial water filling at the concrete surface.

As it is recognized that sorptivity is influenced by the moisture condition of concrete (McCarter et al, 1992; Hall 1989) in order to remove the saturation gradient and to realize maximum capillary suction here the tests have been conducted on 28-day cured samples (100 mm cube) conditioned in oven at 105 $\pm$ 5ºC for 24 hours and then cooled in a desiccator. The weight of the oven-dried cube was measured to the nearest 0.01 g. The surface of concrete cubes, which was parallel to the direction of casting, was placed in a tray containing water and rested on 5 mm glass rods to permit the free access of water to the inflow surface. The schematic arrangement of the test is shown in Fig. 5.1. Cut or trowelled surfaces were not exposed to direct contact of water. Any cut surface would expose the porous aggregate and would not represent the sorptivity in actual field condition. In addition, there can exist difference in the absorption characteristics between top and other molded surfaces due to casting procedures and the occurrence of bleeding and segregation (McCarter, 1993). The lower areas on the sides of the specimens adjoining the inflow face were sealed with epoxy coating to achieve unidirectional flow. The water level was maintained at 10 mm above the base of the cube. The absorption of water was measured at intervals of 4, 9, 16, 25, 36, 49, 64, 81, 100, 121, 144 and 169 minutes after the start of placing the specimen in water on wiping out the surplus water. Sorptivity $S$ of each sample was determined from the slope of the regression line represented by the experimental data $i$ against $\sqrt{t}$. For each mix sorptivity was determined for 3 samples.

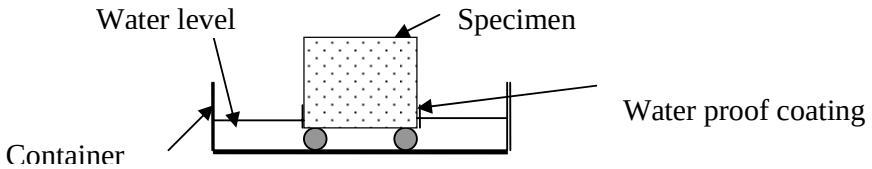


Fig. 5.1 Sorptivity test-Schematic arrangement

### 5.3.4 Chloride Penetration

The ability of concrete to resist chloride ion penetration was studied using Rapid Chloride Penetration Test (RCPT) (ASTM C1202, 2005) based on electrical conductance. This test measures the ease with which concrete allows the charge to pass through and provides an indication on the resistance of concrete to chloride-ion penetration. It is based on the principle that charged chloride ions would accelerate in an electric field towards the pole of the opposite direction. 28-day cured specimens of size 100 mm diameter and 50 mm thickness were allowed to dry at room conditions for 48 hours. The cylindrical surface of the specimens was then given two coats of epoxy. After drying off epoxy, the specimens were vacuum saturated and then fixed in the cell with one side of the cell (-) filled with 3% NaCl solution, while the other side (+) with 0.3 N NaOH solution. The test set up was connected to the power supply for a continuous period of six hours (Fig. 5.2). A potential difference of 60 V dc was maintained across the specimen throughout the test period. The voltage was recorded at 30 minutes interval. The total electrical charge passed through concrete in coulombs at the end of 6 hours was calculated. This is directly related to the chloride ion penetration through the concrete.

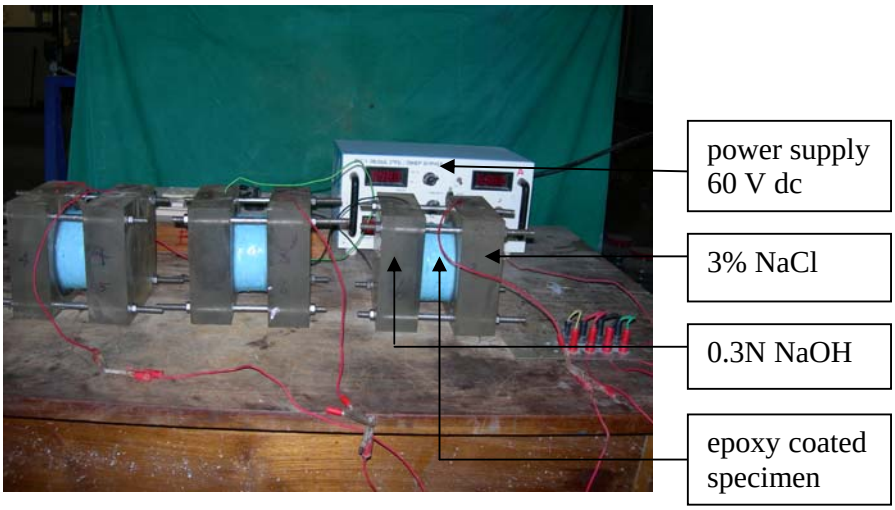


Fig. 5.2 Test set up of RCPT

### 5.3.5 Micro-structural Investigation

The permeation which is dictated by the microstructure of concrete controls the ingress of moisture, ionic and gaseous species into the concrete. A weak interfacial transition zone (ITZ) will have serious effect on durability. Therefore the microstructure of the matrix and matrix-aggregate interface of concrete was studied using a High Resolution Scanning Electron Microscope (HRSEM) equipped with Back Scattered Electron Imaging (BSEI). The interface was examined for selected mixes on both fractured and polished specimens of 25 x 25 x 10 mm size extracted from the interior of concrete at the end of 28 days. The samples were treated with acetone for preventing further hydration.

## 5.4 STATISTICAL MODEL FOR PERMEATION BEHAVIOUR

Table 5.2 presents the statistical model developed from the analysis of experimental results for permeable porosity, water absorption, sorptivity and charge passed through concrete during rapid chloride penetration test. The $R^2$-value and F statistics are observed to be within the satisfactory limits. The effect of mixture compositions on

the permeation characteristics of concrete are discussed in this section through the response surface and graphs plotted from the regression models.

Table 5.2 Statistical model for permeation characteristics

| Response | Response Model | $R^2$ | F-Value | Prob>F |
|---|---|---|---|---|
| Permeable Porosity (%) | 57.84-0.097*c-0.255*w-0.215*$C_A$+ 6.4E-04*c*$C_A$+ 5.27E-05*$c^2$+8.489E-04*$w^2$ | 0.93 | 30.8 | <0.0001 |
| Water Absorption (%) | 1.745-0.0145*c+0.049*w-0.019987*$C_A$+ 7.4E-04*c*$C_A$-3.68E-04*w* $C_A$ +8.73E-04* $C_A^2$ | 0.98 | 176.8 | <0.0001 |
| Sorptivity ($mm/min^{0.5}$) | 0.04697-8.39E-04*c+0.0017*w + 3.76E-04* $C_A$-2.58E-06*c*w +1.287E-06*$c^2$ | 0.98 | 173.2 | <0.0001 |
| Charge passed (coulombs) in RCPT | 33332.71-83.83*c-102.65*w-162.22*$C_A$+ 0.426*c*$C_A$+0.0638* $c^2$ +0.316 * $w^2$ | 0.96 | 53 | <0.0001 |
| c=cement content ($kg/m^3$); water content ($kg/m^3$); $C_A$= CA/TA (Vol.%) | | | | |

### 5.4.1 Permeable Porosity

The variation in permeable porosity of concrete with cement content and volume fraction of cold-bonded aggregate is presented through response surface and contours in Fig. 5.3 for constant water content of 190 $kg/m^3$, the centre value for this factor. In addition to the factor main effects (effect of cement content, water content and CA/TA ratio) model indicates interaction effect of cement and CA/TA ratio on the porosity of concrete. For a given volume fraction of aggregate and concrete with almost similar workability, substantial reduction in porosity (about 30 to 45 %) of concrete is achieved with an increase in cement content and subsequent reduction in w/c ratio of the mixture composition. Fig. 5.4(a) shows the SEM image at low magnification of fractured surface of cold-bonded aggregate near the aggregate shell and Fig. 5.4(b) gives the image of aggregate outer shell which has been a part of the concrete. At low magnification itself, penetration of cement paste into the aggregate surface pores can be observed.

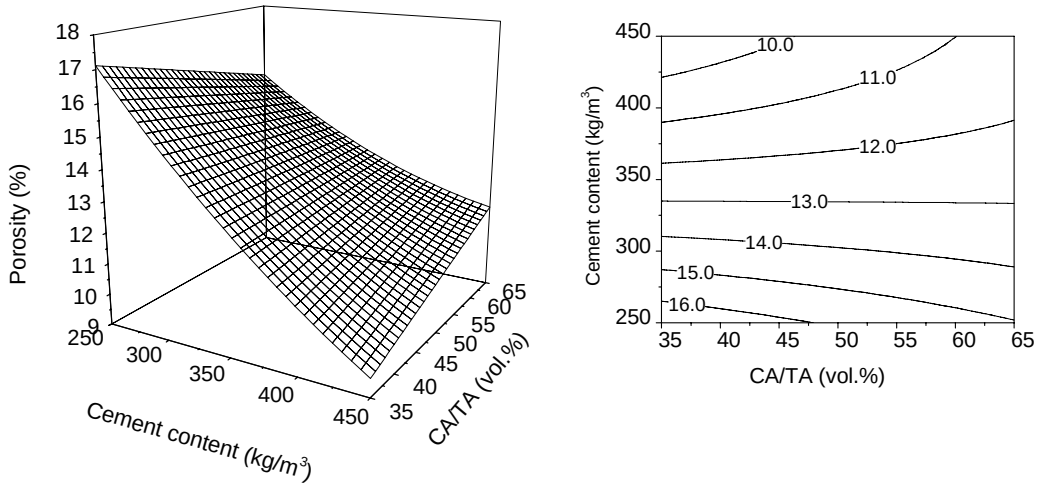


(a) Response surface (b) Contour plot

Fig. 5.3 Permeable porosity of cold-bonded aggregate concrete (water content = 190 kg/m$^3$)

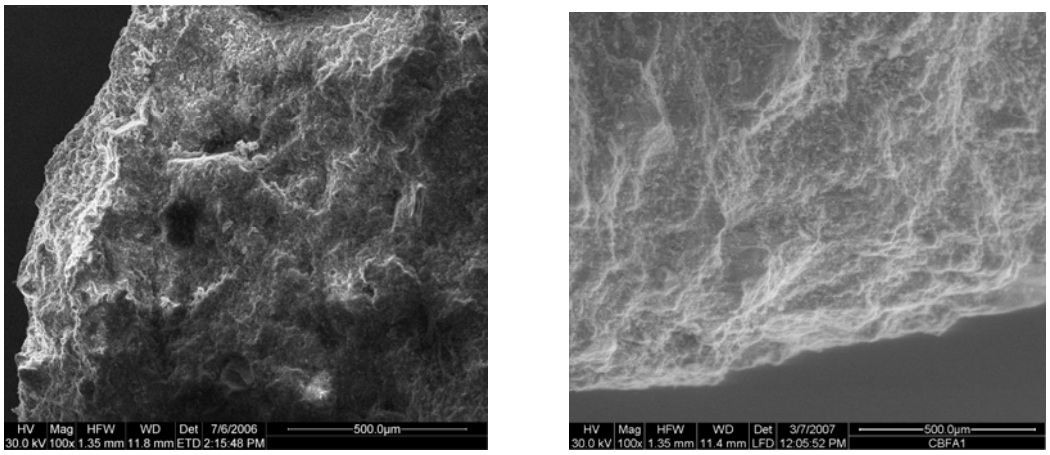


(a) Cold-bonded aggregate (b) Cold-bonded aggregate in concrete

Fig. 5.4 SEM image (100x) of cold-bonded aggregate outer shell

At cement content of 250 kg/m$^3$, BSEI (Fig. 5.5(a)) shows that the pores in matrix phase and matrix aggregate-interface are coarse (more than 10 μm) and most of which are interconnected suggesting that in addition to the matrix and matrix-aggregate porosity, the porosity of the aggregate also contributes to the concrete porosity. The similarity in microstructure of matrix phase and aggregate phase may be attributed to the hydration products (C-S-H, CH, ettringite) developed in both cement paste and Class-C fly ash.

Fig. 5.5(a-c) reveals that size of pores as well as its continuity diminishes with an increase in cement content both in matrix and matrix-aggregate interface. The matrix is somewhat dense even in concrete with 350 kg/m$^3$ cement content (Fig. 5.5(b)), suggesting that the porosity attributed by the aggregate porosity is also reduced compared to concrete with 250 kg/m$^3$ cement content. At higher cement content (Fig. 5.5(c)), effective penetration of the cement paste into the surface pores of the aggregate is observed along with formation of a higly dense matrix phase. SEM image (Fig.5.6) also shows distinct difference at the aggregate shell and the interior of aggregate. Dense region is observed to a distance more than 100 μm. The pores were finer (<10 μm) and are not inter-connected at interface while in the interior of aggregate more number of interconnected pores could be observed. The surface pores in aggregate are considered to provide interlocking sites for the cement paste to form a better interfacial transition zone (ITZ) with less micro-cracking (Zhang and Gjorv, 1992; Lo and Cui, 2004), leading to a higher reduction in porosity of concrete with an increase in cement content. As the matrix phase is dense in concrete with higher cement content, the variation in quality of ITZ appear to be the major criteria in determining the permeable porosity of concrete.

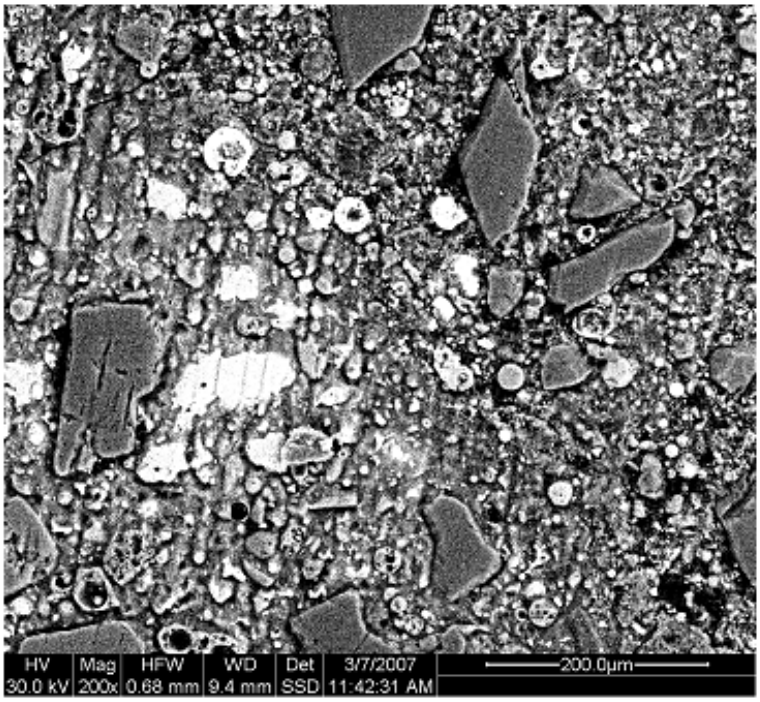


Fig. 5.5(a) BSEI (200 x) ; cement content = 250 kg/m$^3$, CA/TA = 50%

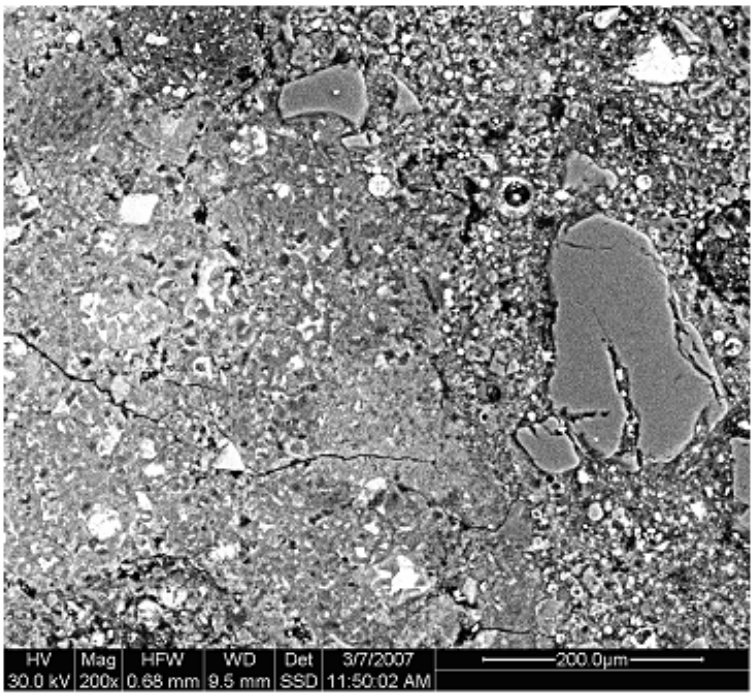


Fig. 5.5 (b) BSEI (200 x) ; cement content = 350 kg/m$^3$, CA/TA = 50%

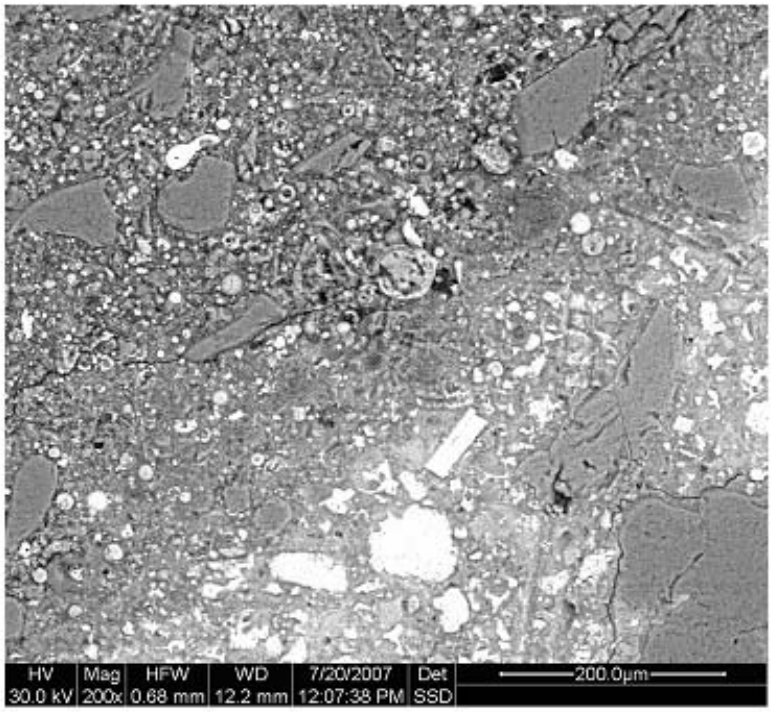


Fig. 5.5 (c) BSEI (200 x) ; cement content = 450 kg/m$^3$, CA/TA = 50%

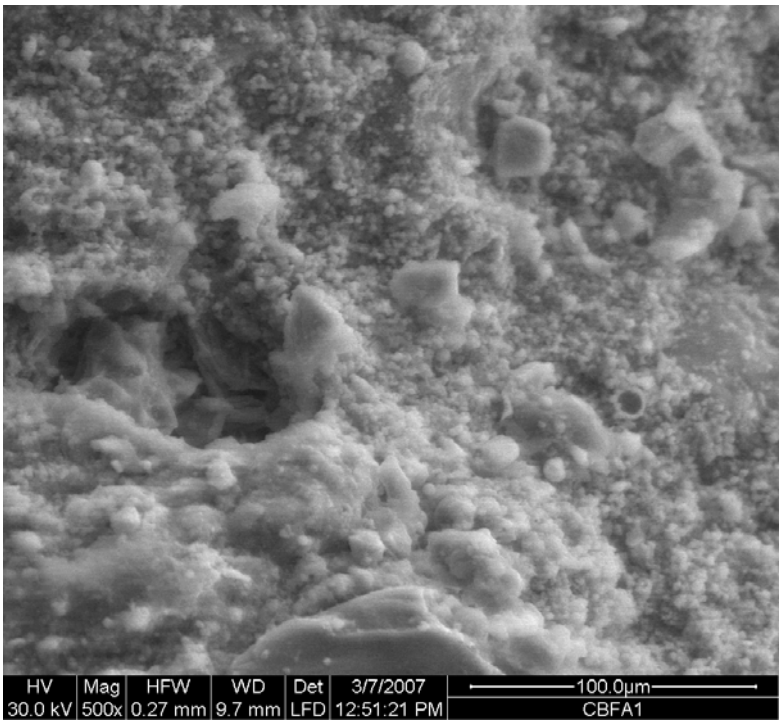


Fig. 5.6 SEM image (500x) showing penetration of cement paste into aggregate shell (cement content = 450 kg/m$^3$, CA/TA = 50%)

Further, for a given cement content (Fig. 5.7) the porosity decreases (about 20 to 33%) with a reduction in water content from 220 to 160 kg/m$^3$. For a constant water content and 250 kg/m$^3$ cement content, an increase in cold-bonded aggregate content has reduced permeable porosity of concrete. An increase in cold-bonded aggregate resuted in a reduction of fine aggregate and hence a reduction in total surface area, which in turn reduces the porosity of the matrix and also has led the available paste to bind the particles better. Such reduction in fine aggregate is also reported to result in a decrease in thickness of ITZ around sand particles (Winslow and Cohen, 1994); which constitute a source of porosity in the matrix. At the same time, porosity of matrix-aggreagte interface also changes. However, towards higher water content the variation in porosity with cold-bonded aggreagte content is very minimal.

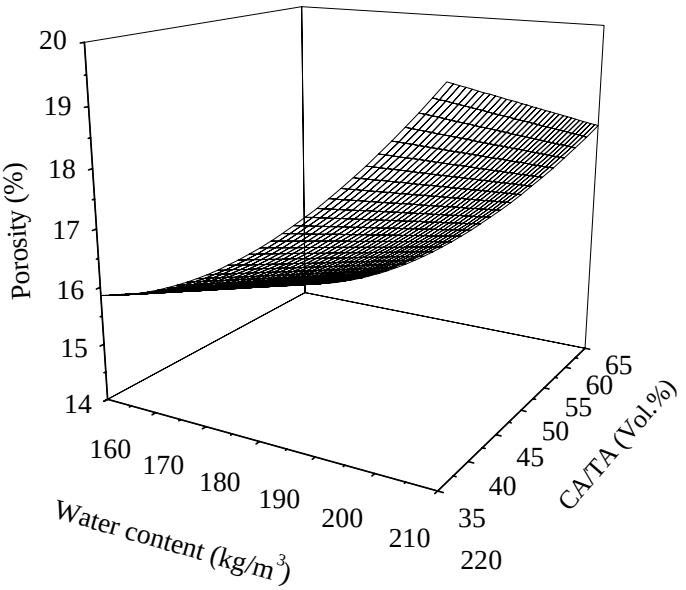


(a) cement content = 250 kg/m$^3$

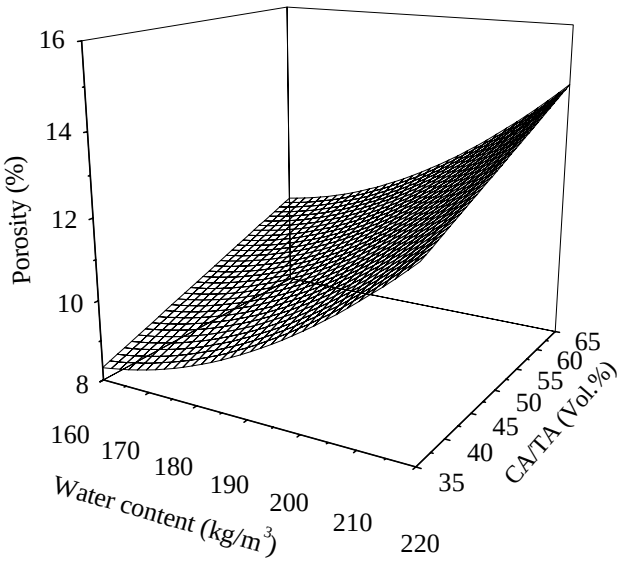


(b) cement content = 450 kg/m$^3$

Fig. 5.7 Variation in permeable porosity with water and aggregate content

As the cement content increases, to around 325 kg/m$^3$, the variation in porosity with aggreagte content is not significant (Fig. 5.3) since the changes in porosity of mortar and mortar-aggregate interface is somewhat offseted. Also, for constant water content, the porosity increases with cold-bonded aggregate content at higher cement contents (Fig. 5.7(b)). This indicates that (i) the variation in porosity of mortar phase arising from packing of materials with an increase in cold-bonded aggreagte content is minimal in concretes with higher cement content and (ii) the difference in quality of matrix-aggregate interface determines the variation in permeable porosity.

While the aggregate porosity is 38.03% (Table 4.2) the permeable porosity of cold-bonded aggregate concrete ranges between 8.5 to 19% (Fig. 5.7). Hence as compared to other factors of mixture composition, the marginal variation in porosity of concrete with an increase in aggregate content confirms that the permeable porosity of concrete depends more on the denseness of mortar phase than on the porosity of aggregate.

Similar observation has been made by Zhang and Gjorv (1991b) from a study on permeability of lightweight aggregate concrete. Table 5.3 indicates that the variation in permeable porosity of cold-bonded aggregate concrete from the corresponding crushed granite aggregate concrete is negligible at cement content of 250 kg/m$^3$. At a lower cement content the porosity attributed by the matrix-aggregate interface of the crushed granite aggregate concrete is relatively higher owing to the lower paste content for the binding of the angular aggregate, though granite aggregate is less porous. At cement content of 350 and 450 kg/m$^3$ the porosity of cold-bonded aggregate concrete is marginally higher.

Table 5.3 Permeable porosity of cold-bonded aggregate concrete and crushed granite aggregate concrete

| Cement content (kg/m$^3$) | Permeable porosity (%)of concrete with water content = 190 kg/m$^3$, CA/TA=65% and | |
|---|---|---|
| | Cold-bonded aggregate | Crushed granite aggregate |
| 250 | 15.60 | 15.13 |
| 350 | 13.07 | 11.61 |
| 450 | 11.75 | 9.92 |

**5.4.1.1 Relationship with compressive strength**

Fig. 5.8 presents the variation in permeable porosity with compressive strength of mixes with cement content ranging from 250 to 450 kg/m$^3$ and a water content of 190 kg/m$^3$ and different volume fractions of cold-bonded aggregate. For a given strength, the influence of variation of cold-bonded aggregate content in the mix, on the porosity of concrete is marginal. This is mainly due to the variation in the requirement of cement content with CA/TA ratio for achieving a particular strength (section 4.5.4) which in turn changes the porosity of mortar and or mortar-aggregate interface.

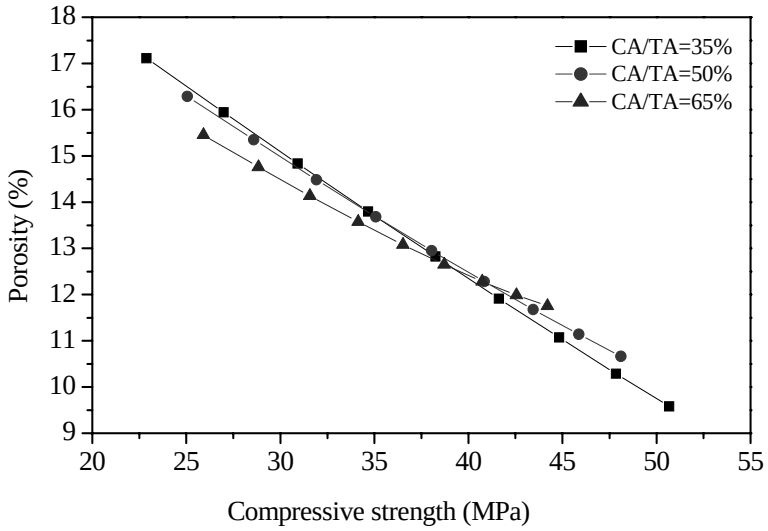


Fig. 5.8 Relationship between porosity and compressive strength

### 5.4.2 Water Absorption

The effect of mixture parameters on the water absorption of cold-bonded aggregate concrete is presented in Fig. 5.9. The cement and water contents have more pronounced influence on water absorption as compared to cold-bonded aggregate content in the mix, indicating that the absorption is mainly dependent on the pores in the mortar phase and mortar-aggregate interface than on the absorption capacity of cold-bonded aggregate as observed in the case of porosity. The variation in water absorption (Table 5.4) between similar mixes with crushed granite and cold-bonded aggregate is not significant. The water absorption of concrete is observed to be well below 10%, which is within the absorption of most good concretes (Neville, 2004). Gunduz and Ugur (2005) have reported water absorption rates of 14-22% for structural lightweight concrete with pumice aggreagte. Sahin et al. (2003) reported a reduction in water absorption with an increase in cement content in pumice aggregate concrete.

Table 5.4 Water absorption of cold-bonded aggregate concrete and crushed granite aggregate concrete

| Cement content (kg/m$^3$) | Water absorption (%) in concrete with water content = 190 kg/m$^3$, CA/TA=65% and | |
|---|---|---|
| | Cold-bonded aggregate | Crushed granite aggregate |
| 250 | 6.65 | 5.68 |
| 350 | 5.69 | 4.12 |
| 450 | 4.72 | 3.91 |

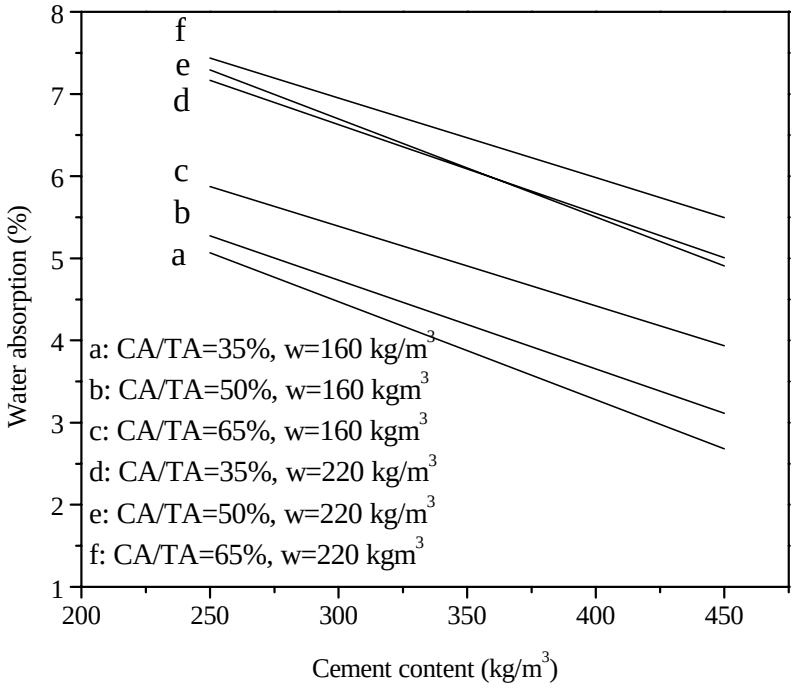


Fig. 5.9 Influence of mixture parameters on water absorption

### 5.4.2.1 Relationship with compressive strength

Fig. 5.10 presents the variation in water absorption of concrete with compressive strength. Though the water absorption is influenced by the volume fraction of aggreagte at lower strength level, where matrix is porous, the variation is quite marginal at higher strengths. The probable reason is the higher cement content and

dense matrix structure associated with higher volume fraction of aggregate for producing concrete of same strength at higher strength level where aggregate fracture is predominated.

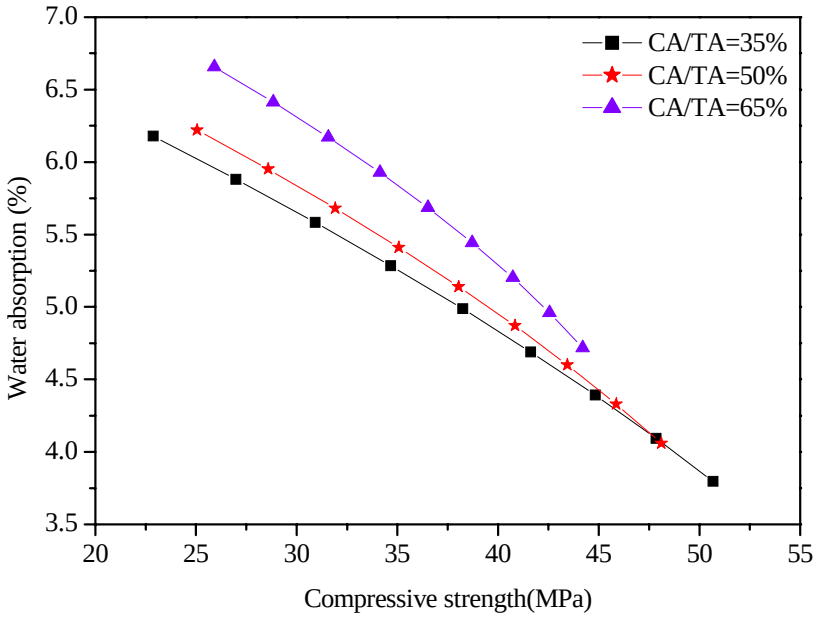


Fig. 5.10 Relation between compressive strength and water absorption

### 5.4.2.2 Relationship with permeable porosity

The relation between water absorption and porosity of concrete (with 190 kg/m$^3$ water content) presented in Fig. 5.11 exhibits almost linear variation at CA/TA of 35%, while the relation deviates from linearity as the aggregate content increases. For concrete with same porosity level, the water absorption increases with an increase in cold-bonded aggregate content. The reasons that could be attributed are (i) the reduction in density of concrete with an increase in cold-bonded aggregate content and (ii) the volume of voids which are filled with air during measurement of water absorption. In concrete with same volume of voids the reduction in density obviously would cause an increase in the water absorption as it was measured as the percentage increase in mass. However, towards low porosity the effect of cold-bonded aggregate

content does not have pronounced influence on water absorption, suggesting that apart from bulk porosity, water absorption depends on distribution of capillary pores and their continuity as highlighted by other researchers (McCarter et al., 1992; Lockington and Parlange, 2003).

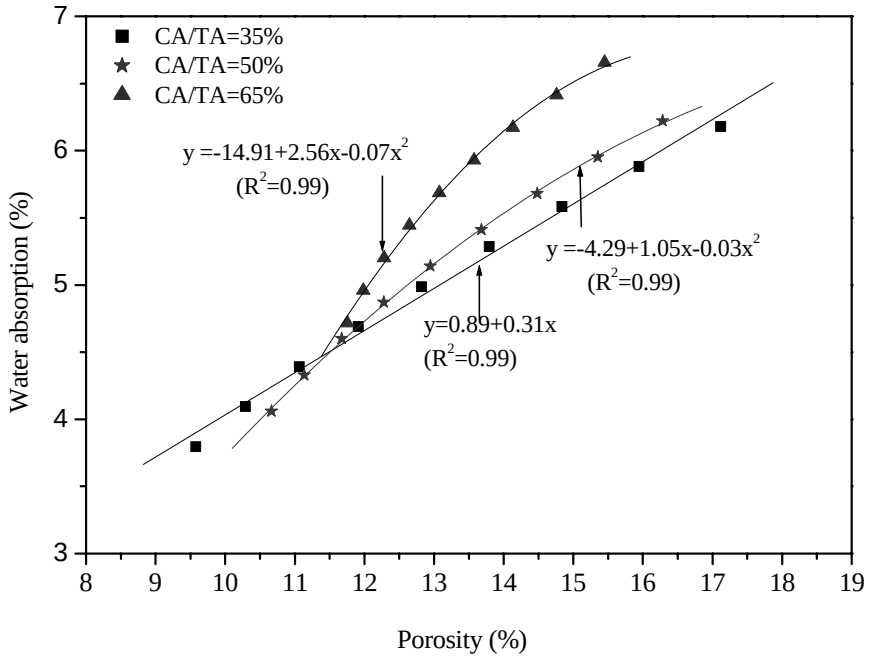


Fig. 5.11 Variation of water absorption with porosity

### 5.4.3 Sorptivity

Using the regression model, the variation in sorptivity of concrete with cement, cold-bonded aggregate content and water contents is presented in Fig. 5.12. The sorptivity is significantly influenced by the variation in cement and water contents, thereby exhibiting behaviour similar to that of water absorption. More than 300% reduction in sorptivity with an increase in cement content from 250 to 450 kg/m$^3$ indicates the presence of relatively smaller capillary pores in concretes with higher cement content. Effective diffusion of cement paste into the aggregate pores as observed in BSEI (Fig.

5.5) and the consequential formation of tortuous path can be attributed as the other reasons for this reduction in sorptivity with cement content. The reduced sorptivity reflects finer pore structure which in turn inhibits the ingress of aggressive elements into the pore system. The reduction in water content has resulted in pronounced decrease of sorptivity in mixes with lower cement where the matrix is highly porous. Fig. 5.12 also shows a marginal increase in sorptivity with cold-bonded aggregate content in the mix while the other factors of mix remaining the same. This tends to conclude that in addition to capillary pores in matrix, pores at aggregate-matrix interface of concrete increases with an increase cold-bonded aggregate content because of the reduction in paste available for making physical and chemical bond with unit quantity of aggregate. However, Table 5.5 indicates that influence of cold-bonded aggregate on reduction of resistance to water sorption is not significant as only marginal difference (0.008 to 0.018 mm/min$^{0.5}$) is observed from corresponding mixtures of concrete with crushed granite aggregate.

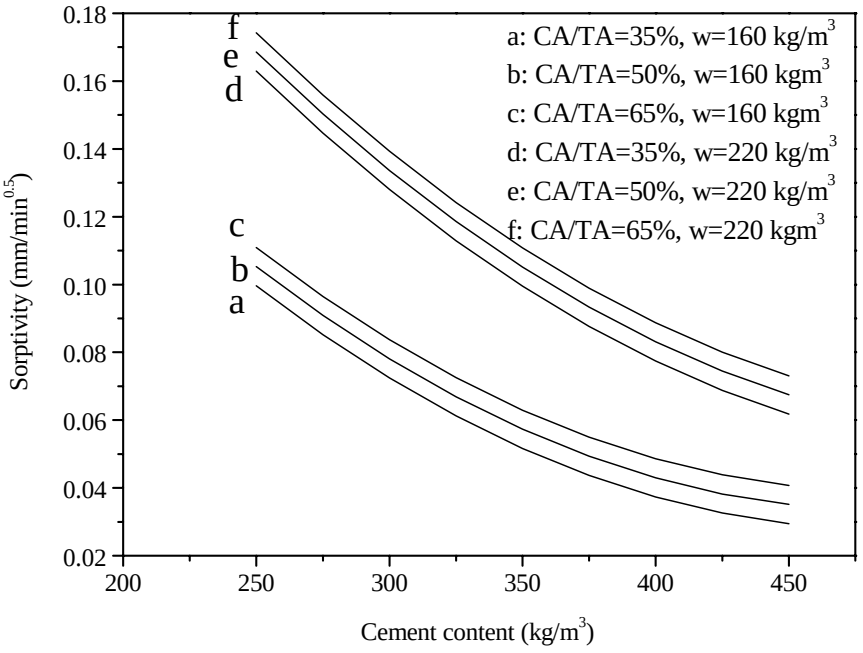


Fig. 5.12. Variation in sorptivity with mixture composition

Table 5.5 Sorptivity of cold-bonded aggregate concrete and crushed granite aggregate concrete

| Cement content (kg/m$^3$) | Sorptivity (mm/min$^{0.5}$) of concrete with water content = 190 kg/m$^3$, CA/TA=65% and | |
|---|---|---|
| | Cold-bonded aggregate | Crushed granite aggregate |
| 250 | 0.143 | 0.125 |
| 350 | 0.087 | 0.0785 |
| 450 | 0.057 | 0.049 |

#### 5.4.3.1 Relationship with compressive strength

The relationship between compressive strength and sorptivity (Fig.5.13) follows that volume fraction of aggregate influences sorptivity in low strength concretes, while beyond a strength level of 35 MPa, the sorptivity is observed to be almost independent of aggregate content. While strength is governed by the total porosity (including closed pores), the sorptivity and water absorption are mainly controlled by the continuous capillaries in concrete. At low strength level (< 30 MPa) where matrix controls concrete failure, lower cement content is associated with higher volume fraction of cold-bonded aggregate (as discussed in section 4.3.4), causing an increase in sorptivity. At higher strength level, for achieving concrete of same strength, an increase in aggregate content demands higher cement content (for compensating the aggregate weakness) which improves the micro-structural characteristics, both in matrix and matrix aggregate interface, causing no appreciable variation in sorptivity with aggregate content.

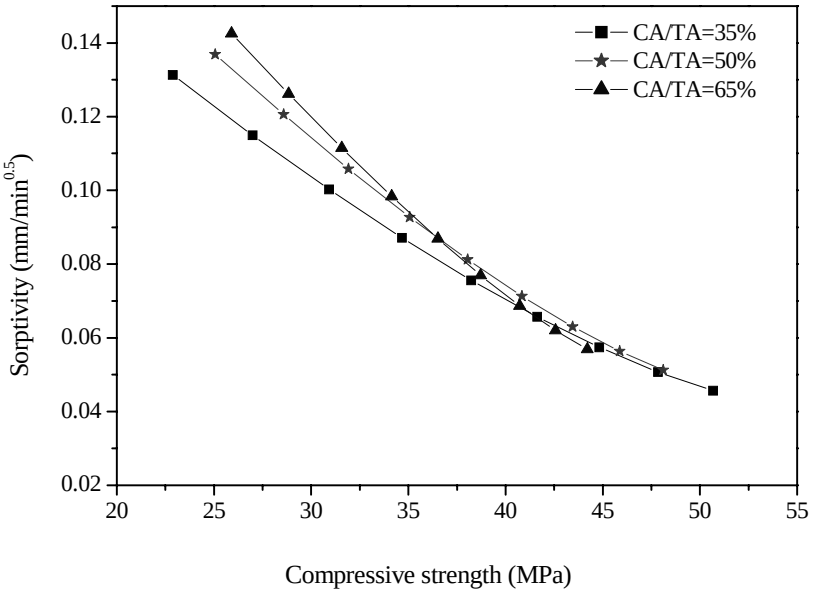


Fig. 5.13 Relationship between compressive strength and sorptivity

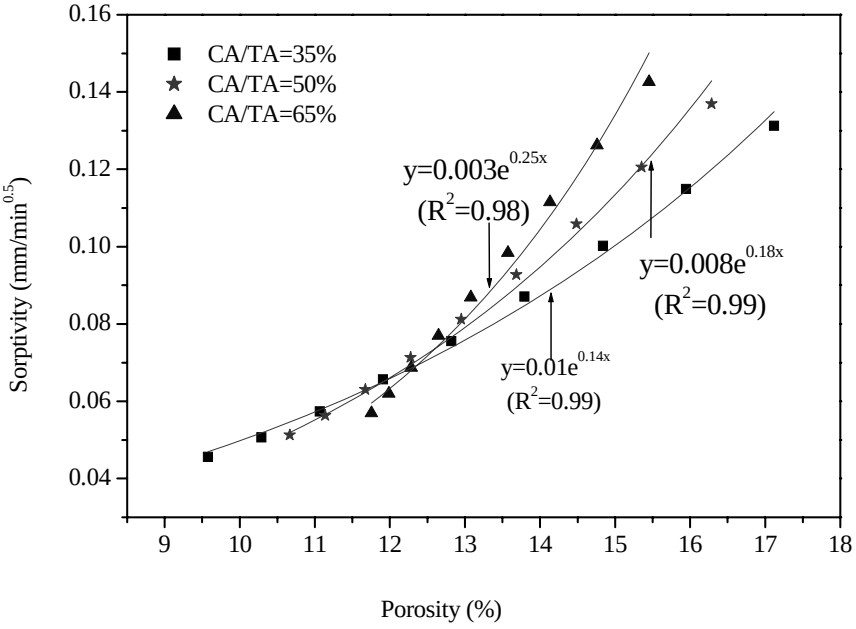


Fig. 5.14 Relationship between porosity and sorptivity

### 5.4.3.2 Relationship with permeable porosity

Fig. 5.14 indicates that in concretes of same porosity level, capillary suction increases with cold-bonded aggregate content especially in mixtures of higher porosity. The

relationship between porosity and sorptivity was observed to be exponential. Unlike permeable porosity, the sorptivity is influenced by pore parameters like fineness, its distribution and continuity as it represents the rate of absorption (Hall and Yau, 1987). It is also affected by near-surface effect of concrete, which is in direct contact with water and the tortuousity in unidirectional capillary flow.

### 5.4.4 Chloride Penetrability

The influence of variation in cement content and volume fraction of aggreagte on the charge passed through concrete during RCPT is depicted in Fig. 5.15 using response surface and contour plot. It is observed that the resistance of concrete to chloride ion penetration indicated by the charge passed through concrete is almost similar to the response of mixture composition to permeable porosity. Variation in charge passed through concrete with cement content is more predominant than variation with volume fraction of cold-bonded aggreagte. This indicates that as observed in permeable porosity and sorption, resistance to chloride penetration is also primarily depended on the porosity and pore size distribution of matrix phase and the quality of interfacial zone between LWA and mortar matrix, conforming to the observation of other researchers (Zhang and Gjorv, 1991b; Chia and Zhang 2002).

At lower cement contents (<350 kg/m$^3$) where matrix is highly porous, chloride ion penetration of concrete appears to be decreased with increase in volume fraction of aggregate (due to the reduction in mortar porosity) in concrete with constant w/c ratio. At higher cement content where the porosity in mortar phase is minimum, a marginal increase in the total charge passed through the concrete is observed with an increase in cold-bonded aggregate volume because of the reduction in quality of interface formed compared to concrete with low aggregate content as discussed in porosity and sorption characteristics. The distinct effect of water content in increasing the chloride

ion penetrability due to the reduction in denseness of both matrix and matrix-aggregate interface can also be noticed from Fig. 5.16.

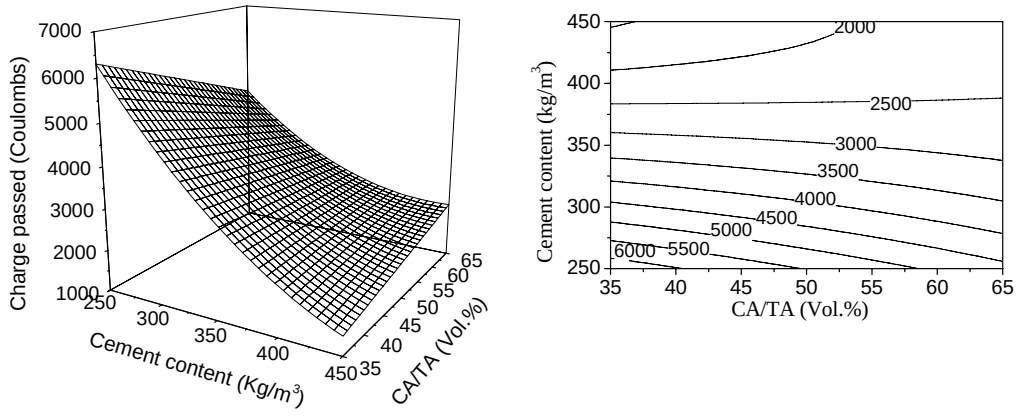


(a) Response Surface (b) Contour Plot

Fig. 5.15 Charge passed through concrete in RCPT (water content=190 kg/m$^3$ )

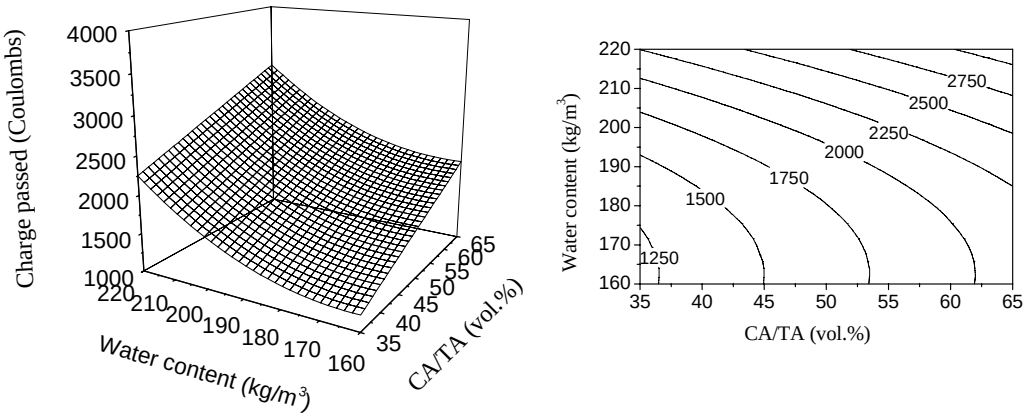


(a) Response Surface (b) Contour Plot

Fig. 5.16 Variation in charge passed with water and aggregate content in RCPT (cement content =450 kg/m$^3$)

At low cement content, eventhough the chloride penetrability indicated by the charge passed through the specimen is 'high' according to ASTM C 1202 (2005), the penetration of chloride ion is observed to be in the ' moderate ' or ' low range ' with

relatively higher cement content. The resistance of cold-bonded aggregate concrete is comparable with equivalent concrete with crushed granite aggregate (Table 5.6) and the value reported for expanded clay aggregate concrete (Table 5.7) of same cement content and w/c ratio.

Table 5.6 Charge passed through cold-bonded aggregate concrete and crushed granite aggregate concrete during RCPT

| Cement content (kg/m$^3$) | Charge passed (Coulombs) through concrete with water content = 190 kg/m$^3$ and CA/TA=65% | |
|---|---|---|
| | Cold-bonded aggregate | Crushed granite aggregate |
| 250 | 4640 | 4455 |
| 350 | 2850 | 3030 |
| 450 | 2330 | 2100 |

Table 5.7 Comparison of cold-bonded aggregate concrete and expanded clay aggregate concrete in RCPT

| Cement content (kg/m$^3$) | Charge passed in RCPT (Coulombs) w/c ratio = 0.55 | |
|---|---|---|
| | Expanded clay (Chia and Zhang, 2002) | Cold-bonded aggreagte |
| 400 | 5095 (CA/TA=60%) | 2990 to 3240 (CA/TA from 35 to 65%) |

**5.4.4.1 Relationship with compressive strength**

Fig. 5.17 presents the variation in chloride ion penetrability with compressive strength. A comparison of Figs. 5.17 and 5.13, exhibits that there exists difference between the capillary water absorption and chloride ion penetrability. It is mainly because sorptivity test evaluates the behaviour of concrete based on pores at different cross sections while RCPT provides a direct measurement of the chloride ion penetration on the bulk properties of the concrete (Lo et al., 2006). The results indicate that for a given compressive strength, higher aggregate content in the concrete would not reduce the durability of concrete due to chloride ingress because

of the higher cement content and consequent dense matrix associated with concrete of higher aggregate content at the same strength level.

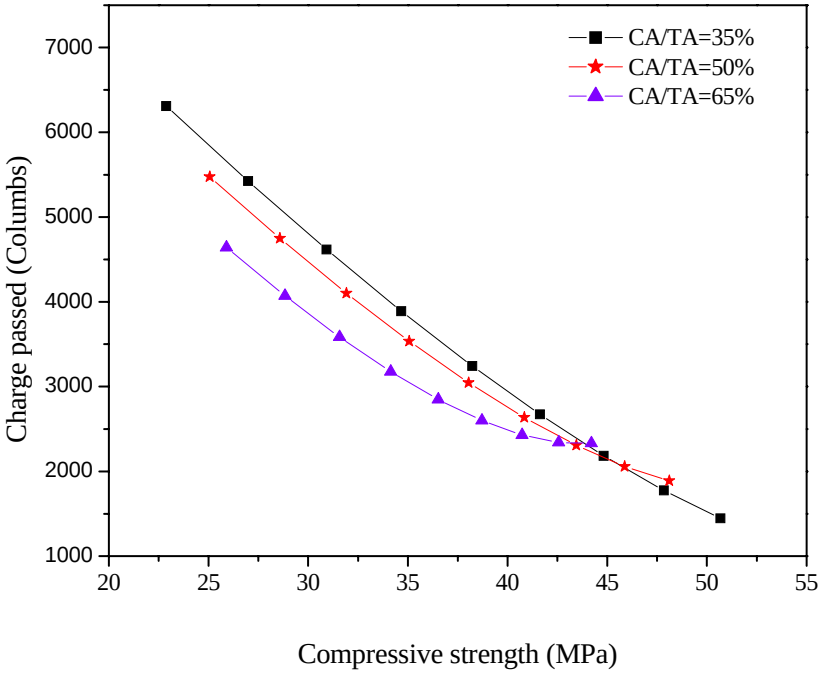


Fig. 5.17 Relationship between compressive strength and charge passed in RCPT

### 5.4.4.2 Relationship with permeable porosity

The relationship between permeable porosity and charge passed through concrete in chloride ion penetrability test is depicted in Fig. 5.18. The relationship is observed to be linear with higher $R^2$ value in concrete of different volume fractions of cold-bonded aggregate. The results indicate that for concrete with same porosity, the influence of cold-bonded aggregate content on the chloride ion penetrability of concrete is marginal. This tends to conclude that chloride ion penetration of concrete is predominantly controlled by the pore structure and permeable pores in concrete.

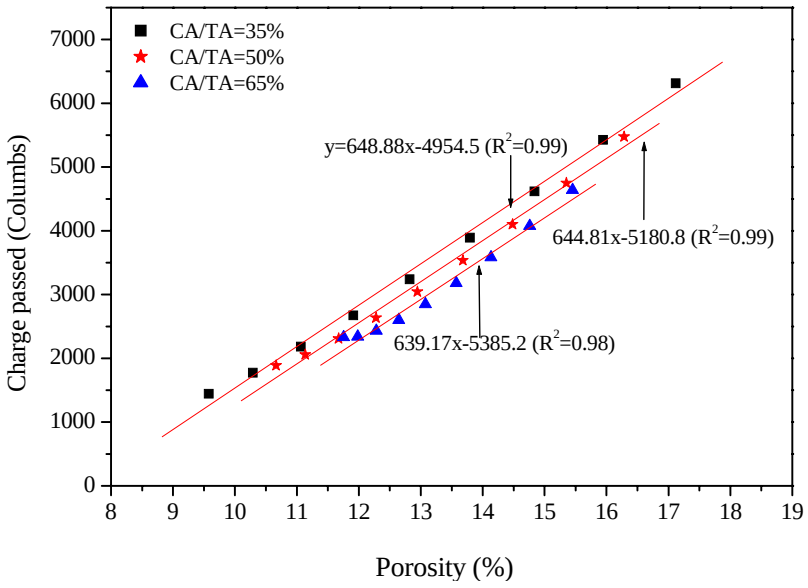


Fig. 5.18 Relationship between porosity and charge passed in RCPT

## 5.5 SUMMARY

Permeation characteristics of cold-bonded aggregate concrete with variation in mixture compositions have been studied with the help of RSM through the measurement of permeable porosity, water absorption, sorptivity and rapid chloride penetration tests. Substantial reduction observed in permeable porosity, sorption and chloride penetrability with increase in cement content and/or reduction in w/c ratio indicates that permeation behaviour of cold-bonded aggregate concrete is mainly influenced by matrix porosity and the quality of paste aggregate interface than by the porosity of aggregate. SEM image and BSEI image demonstrated penetration of cement paste into the surface pores in the aggregate with no clear distinction between bulk paste and paste aggregate interface especially in concrete with higher cement content. The relation between permeable porosity and other permeation parameters viz. water absorption, sorptivity, and chloride ion penetrability has been established. The permeation behaviour of cold-bonded aggregate concrete has been observed to be marginally higher than that of concrete with crushed granite aggregate.

# CHAPTER 6

# INFLUENCE OF CLASS-F FLY ASH ON THE BEHAVIOUR OF COLD-BONDED AGGREGATE CONCRETE

## 6.1 GENERAL

The conventional approach to high volume fly ash utilization of ash in concrete is through its use as partial replacement of cement as well as fine aggregate. Review on fly ash aggregate concrete presented in Table 6.1 indicates that most of the studies have used river sand as fine aggregate and silica fume as a part of binder. A few investigations have used sintered aggregate and fly ash as a part of fine aggregate.

Table 6.1 Review on fly ash aggregate concrete

| Author | Type of aggregate | | Binder | | Properties Studied |
|---|---|---|---|---|---|
| | Coarse Aggregate | Fine aggregate | Cement | Silica fume | |
| Swamy and Lambert (1983, 84) | Sintered fly ash | River sand | ✓ | | Strength behaviour, mixture guidelines. |
| Wegen and Bijen (1985) | Sintered fly ash | River sand | ✓ | | Strength, shrinkage, freeze-thaw behaviour |
| Zhang and Gjorv (1991a,b) | Sintered fly ash | Sintered fly ash | ✓ | ✓ | Mechanical properties, permeability |
| Chang and Shieh (1996) | Sintered fly ash Cold-bonded fly ash | River sand | ✓ | | Strength, fracture energy |
| Al-Khaiat and Haque (1998) | Sintered fly ash | Sintered fly ash | ✓ | ✓ | Strength, influence of curing |
| Kayali et al.(1999) | Sintered fly ash | 75% Sintered fly ash + 25% fly ash | ✓ | ✓ | Shrinkage of fibre reinforced concrete |
| Baykal and Doven (2000) | Cold-bonded fly ash | River sand | ✓ | | Strength, elastic modulus |
| Chi et al.(2003) | Cold-bonded fly ash | River sand | ✓ | | Strength, elastic modulus |
| Haque et al.(2004) | Sintered Fly ash | Sintered fly ash, River sand | ✓ | ✓ | Strength, durability |
| Kayali and Zhu (2005) | Sintered fly ash | 75% Sintered fly ash + 25% fly ash | ✓ | ✓ | Chloride induced corrosion |
| Gesoglu et al. (2004, 2006) | Cold-bonded fly ash | Sand | ✓ | ✓ | Strength, elastic modulus and shrinkage, effect of surface treated aggregates |

It is concluded in section 4.5.4 that cold-bonded aggregate concrete with more than 300 kg/m$^3$ cement content, the aggregate governs the strength of concrete. Hence, replacement of cement with fly ash, in high cement content mix, i.e., 450 kg/m$^3$ would be advantageous. The utilization of fly ash in cold-bonded aggregate concrete can also be increased through its use as partial replacement of fine aggregate. This chapter deals with a systematic study undertaken in cold-bonded aggregate concrete by incorporating Class-F fly ash as i) partial replacement for cement in concrete with high cement content and ii) partial replacement of sand. The compressive strength of concrete along with its permeation behaviour have been studied to understand the influences of cement content, cold-bonded aggregate content and percentage replacement of cement/sand with fly ash.

## 6.2 MATERIALS AND METHODOLOGY

### 6.2.1 Replacement of Cement with Class-F Fly Ash

Class-F fly ash, conforming to ASTM C 618 (2005) was used for the replacement of both cement and sand. The chemical composition and physical properties of fly ash used are reported in Table 6.2.

Concrete with a cement content of 450 kg/m$^3$ and water content of 175 kg/m$^3$ was chosen as the control mix. Two CA/TA ratios viz., 35%, 50 % and 65% and three cement replacement levels with fly ash viz., 10, 30 and 50% by weight of cement were adopted as summarized in Table 6.3.

### 6.2.2 Replacement of Sand with Class-F Fly Ash

Control mixes were chosen with three cement contents (250, 350 and 450 kg/m$^3$) to understand the influence of fly ash as sand replacement both in mixes with weak and

Table 6.2 Physical and chemical properties of Class-F fly ash used

| **Chemical properties** | | |
|---|---|---|
| | Fly ash | |
| | % by mass | ASTM C618 (2005) (Class-F) |
| $SiO_2$ | 63.6 | - |
| CaO | 1.57 | <10 |
| $Al_2O_3$ | 28.19 | - |
| $Fe_2O_3$ | 2.99 | - |
| MgO | 0.54 | 5 (max) |
| $Na_2O$ | 0.05 | - |
| $K_2O$ | 0.003 | - |
| $SO_3$ | 0.26 | |
| MnO | 0.03 | - |
| Loss on Ignition | 0.85 | |
| Soluble residue | - | |
| $Al_2O_3$/ $Fe_2O_3$ | - | |
| $SiO_2 + Al_2O_3+Fe_2O_3$ | 94.78 | 70 (min) |
| **Physical properties** | | |
| Fineness ($m^2$/kg) | 252 | |
| Specific gravity | 2.09 | |

Table 6.3 Mixture compositions with fly ash as cement replacement

| Cement (kg/$m^3$) Fineness (391 $m^2$/kg) | Fly ash (kg/$m^3$) Fineness (252 $m^2$/kg) | Water (kg/$m^3$) | water-binder ratio | CA/TA (Vol. %) | Sand (kg/$m^3$) | Fresh density (kg/$m^3$) | Slump (mm) | Total vol. of fly ash (Cold-bonded aggregate+ fly ash replacing cement) ($m^3$/$m^3$ of concrete) |
|---|---|---|---|---|---|---|---|---|
| 450 | 0 (0%) | 175 | 0.39 | 50 | 861 | 2127 | 55 | 0.329 |
| 405 | 45 (10%) | 175 | 0.39 | 50 | 851 | 2110 | 60 | 0.346 |
| 315 | 135 (30%) | 175 | 0.39 | 50 | 832 | 2077 | 65 | 0.382 |
| 225 | 225 (50%) | 175 | 0.39 | 50 | 813 | 2044 | 70 | 0.417 |
| 450 | 0 (0%) | 175 | 0.39 | 65 | 603 | 2060 | 85 | 0.427 |
| 405 | 45 (10%) | 175 | 0.39 | 65 | 596 | 2045 | 90 | 0.444 |
| 315 | 135 (30%) | 175 | 0.39 | 65 | 583 | 2013 | 90 | 0.477 |
| 225 | 225 (50%) | 175 | 0.39 | 65 | 569 | 1982 | 110 | 0.511 |

strong matrix. Two CA/TA ratios (50 and 65%) and two water contents (175 and 220 kg/$m^3$) were considered in this study. Due to the increase in water demand during sand replacement with fly ash (owing to the increase in specific surface) higher water

content was also selected to realize the effect of maximum replacement of sand by fly ash. The replacement of sand with fly ash was done on equal volume basis from 20% onwards. Superplasticizer was added to the mixes with fly ash for maintaining workability closer to the corresponding control mix. The details of the mix adopted are presented in Table 6.4.

### 6.2.3 Methodology

The methodology adopted for evaluating the influence of Class-F fly ash on cold-bonded aggregate concrete include studies on (i) fresh concrete properties (density and workability), (ii) compressive strength, (iii) permeation behaviour and (iv) micro-structural analysis. Workability of concrete was studied through slump test. For compressive strength and permeation behaviour, the specimens of required size and number as adopted in section 4.3.4 and 5.3 respectively were cast and cured in mist room for test at 7-day, 28-day and 90-day.

## 6.3 FRESH CONCRETE PROPERTIES

### 6.3.1 Cement Replacement with Fly ash

It is observed from Table 6.3 that the fresh density of concrete reduces with an increase in replacement level of cement with fly ash and increase in cold-bonded aggregate content. The reduction in density of mix when cement is replaced with equal weight of fly ash is due to relatively lower specific gravity of Class-F fly ash (sp. gravity-2.09) used, than the cement (sp. gravity-3.13). The workability of concrete increases with an increase in replacement of cement with fly ash, attributable to the lower specific surface of fly ash (fineness-252 $m^2$/kg) compared to cement particles (fineness- 391 $m^2$/kg) and a gradual reduction in sand content in the mix with cement replacement level (Table 6.3).

Table 6.4 Mixture compositions with fly ash as sand replacement

| Cement ($kg/m^3$) | Water ($kg/m^3$) | CA/TA (Vol.%) | Sand ($kg/m^3$), Fly ash: 0% | Slump (mm), Fly ash: 0% | Replacement of sand with fly ash | Sand ($kg/m^3$) | Fly ash ($kg/m^3$) | Superplasticizer (% by weight of cement + fly ash) | Fresh density ($kg/m^3$) | Total vol. of fly ash ($m^3/m^3$ of concrete) |
|---|---|---|---|---|---|---|---|---|---|---|
| 450 | 175 | 50 | 861 | 50 | 20% | 689 | 137 | 0.3 | 2092 | 0.395 |
| | | | | | 40% | 517 | 275 | 0.5 | 2058 | 0.461 |
| 350 | 175 | 50 | 902 | 50 | 20% | 722 | 144 | 0.25 | 2063 | 0.413 |
| | | | | | 40% | 541 | 288 | 0.4 | 2026 | 0.482 |
| | | | | | 60% | 361 | 432 | 0.6 | 1990 | 0.55 |
| 250 | 175 | 50 | 944 | 60 | 20% | 755 | 150 | 0.22 | 2032 | 0.432 |
| | | | | | 40% | 566 | 301 | 0.35 | 1994 | 0.504 |
| | | | | | 60% | 378 | 452 | 0.55 | 1957 | 0.576 |
| 450 | 175 | 65 | 603 | 85 | 20% | 482 | 96 | 0.25 | 2036 | 0.473 |
| | | | | | 40% | 362 | 192 | 0.45 | 2012 | 0.519 |
| | | | | | 60% | 241 | 288 | 0.65 | 1987 | 0.565 |
| 350 | 175 | 65 | 632 | 90 | 20% | 505 | 101 | 0.2 | 2006 | 0.496 |
| | | | | | 40% | 379 | 202 | 0.35 | 1979 | 0.544 |
| | | | | | 60% | 253 | 303 | 0.55 | 1954 | 0.592 |
| | | | | | 80% | 126 | 403 | 0.7 | 1927 | 0.641 |
| 250 | 175 | 65 | 661 | 95 | 20% | 529 | 105 | 0.15 | 1972 | 0.518 |
| | | | | | 40% | 397 | 211 | 0.25 | 1946 | 0.569 |
| | | | | | 60% | 264 | 316 | 0.4 | 1921 | 0.619 |
| | | | | | 80% | 132 | 422 | 0.65 | 1892 | 0.669 |
| 450 | 220 | 50 | 802 | 180 | 20% | 642 | 128 | 0.25 | 2037 | 0.367 |
| | | | | | 40% | 481 | 256 | 0.45 | 2004 | 0.428 |
| | | | | | 60% | 321 | 384 | 0.7 | 1972 | 0.489 |
| 350 | 220 | 50 | 844 | 190 | 20% | 675 | 135 | 0.2 | 2007 | 0.386 |
| | | | | | 40% | 506 | 270 | 0.35 | 1973 | 0.450 |
| | | | | | 60% | 337 | 404 | 0.65 | 1938 | 0.515 |
| | | | | | 80% | 169 | 538 | 1.0 | 1903 | 0.579 |
| 250 | 220 | 50 | 885 | 190 | 20% | 708 | 141 | 0.15 | 1977 | 0.406 |
| | | | | | 40% | 531 | 282 | 0.3 | 1941 | 0.473 |
| | | | | | 60% | 354 | 424 | 0.5 | 1906 | 0.541 |
| | | | | | 80% | 177 | 565 | 0.85 | 1869 | 0.608 |
| 450 | 220 | 65 | 561 | 240 | 20% | 449 | 90 | 0.2 | 1985 | 0.441 |
| | | | | | 40% | 337 | 179 | 0.4 | 1962 | 0.484 |
| | | | | | 60% | 225 | 269 | 0.6 | 1940 | 0.526 |
| | | | | | 80% | 112 | 358 | 0.8 | 1916 | 0.568 |
| 350 | 220 | 65 | 590 | 250 | 20% | 472 | 94 | 0.15 | 1952 | 0.463 |
| | | | | | 40% | 354 | 188 | 0.3 | 1928 | 0.508 |
| | | | | | 60% | 236 | 283 | 0.55 | 1905 | 0.553 |
| | | | | | 80% | 118 | 377 | 0.75 | 1881 | 0.598 |
| | | | | | 100% | - | 471 | 0.95 | 1855 | 0.643 |
| 250 | 220 | 65 | 620 | 245 | 20% | 496 | 99 | 0.1 | 1920 | 0.486 |
| | | | | | 40% | 372 | 198 | 0.25 | 1895 | 0.533 |
| | | | | | 60% | 248 | 297 | 0.4 | 1869 | 0.581 |
| | | | | | 80% | 124 | 395 | 0.65 | 1845 | 0.628 |
| | | | | | 100% | - | 494 | 0.9 | 1819 | 0.675 |

### 6.3.2 Sand Replacement with Fly Ash

Table 6.4 summarises various parameters of concrete mixes in which sand replacement with fly ash has been carried out. Unlike cement replacement with fly ash where the lowest density is 1982 kg/m$^3$, the sand replacement allows the density to fall below 1900 kg/m$^3$ when the percentage replacement increases beyond 60% in mixes of lower cement content. Hence such mixes of concrete can be qualified as lightweight aggregate concrete (ACI 211.2, 1990) at higher replacement levels. The dosage of superplasticizer required to maintain constant workability is observed to increase with an increase in sand replacement level with fly ash (Table 6.4), which is attributed to the increase in specific surface of the mix. For a particular CA/TA ratio, cement and water content, the maximum sand replacement level was restricted by the maximum recommended dosage of the admixture prescribed by the manufacturer for achieving the required workability. The concrete was observed to be cohesive at the maximum level of replacement of sand.

## 6.4 COMPRESSIVE STRENGTH OF CONCRETE

### 6.4.1 Cement Replacement with Fly Ash

The compressive strength of cold-bonded aggregate concrete with various levels of replacement of cement by Class F-fly ash is presented in Fig. 6.1 along with the density. The strength of concrete with fly ash is relatively lower than that of corresponding control mix at early ages, at all replacement levels, due to slow rate of pozzolanic reaction by fly ash. This reduction is relatively higher with an increase in fly ash content. At 90-day, it can be observed that (i) no significant variation in the compressive strength of concrete for cement replacement up to 30%, (ii) when 50% cement is replaced with fly ash, the strength varies between 79 and 87% of control

concrete, with higher percentage associated with concrete having higher volume fraction of cold-bonded aggregate.

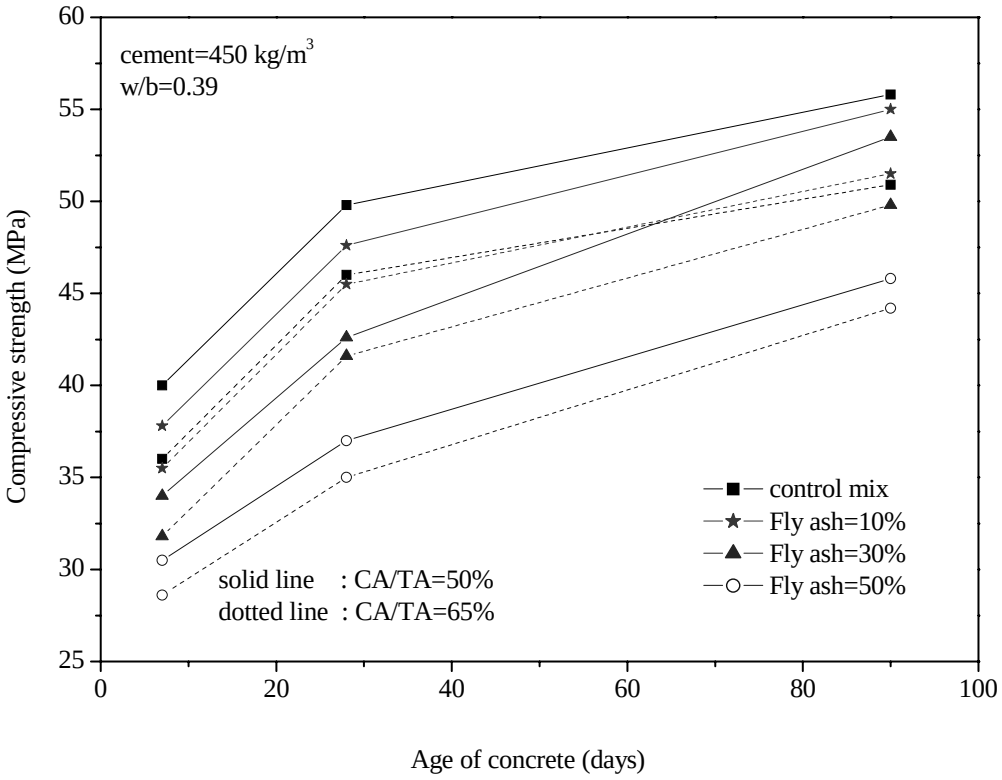


Fig. 6.1 Development of strength with age for replacement of cement with Class-F fly ash

The results in Figs. 6.1 and 6.2 suggest that the cement replacement levels can be restricted based on the target compressive strength requirement at the desired age. These observations conform to the conclusions made by Gopalan and Haque (1989) and Oner et al. (2005) with respect to normal concrete that beyond an optimum level, the strength of concrete strength reduces with an increase in replacement because of lack of adequate cement content for complete pozzolanic reaction with fly ash.

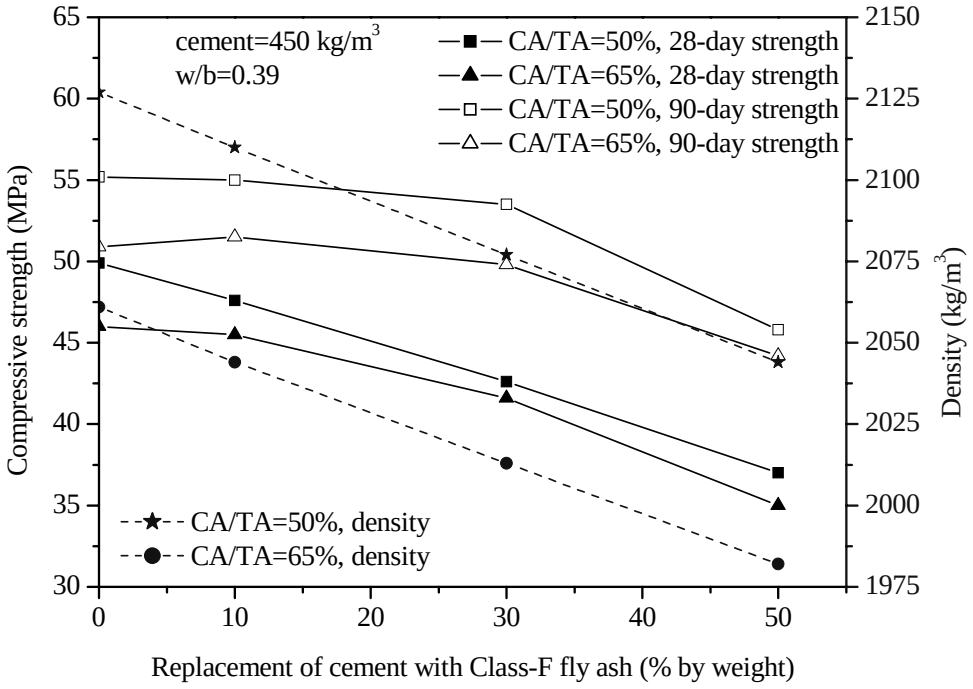


Fig. 6.2 Influence of replacement of cement with fly ash on compressive strength

### 6.4.2 Sand Replacement with Fly Ash

The variation in 28-day compressive strength of cold-bonded aggregate concrete for different replacement levels of sand with Class-F fly ash is presented in Fig. 6.3. The 28-day compressive strength of concrete with fly ash as replacement for sand is higher than the corresponding control mix, even though density of concrete decreases with replacement level, owing to the densification of matrix due to combined filler effect and pozzolanic action of fly ash. In general, the strength increases with increasing replacement level of sand up to around 60-80%. A marginal reduction in strength is observed when sand is fully replaced with fly ash, but is higher than the strength of control mix. The strength of concrete at 100% replacement level corresponds to the strength achieved at around 45 to 60% replacement level.

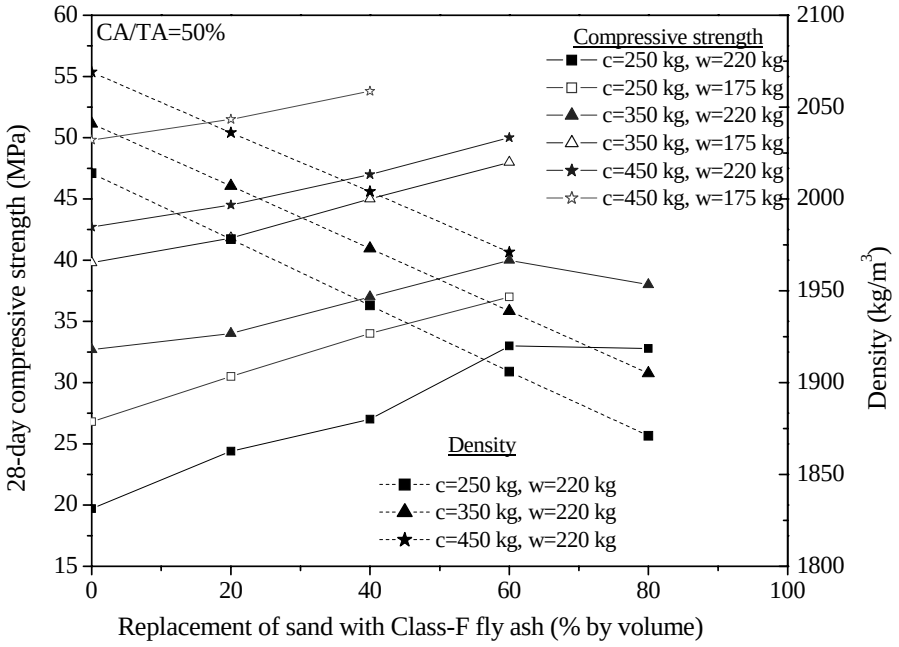


(a) CA/TA=50%

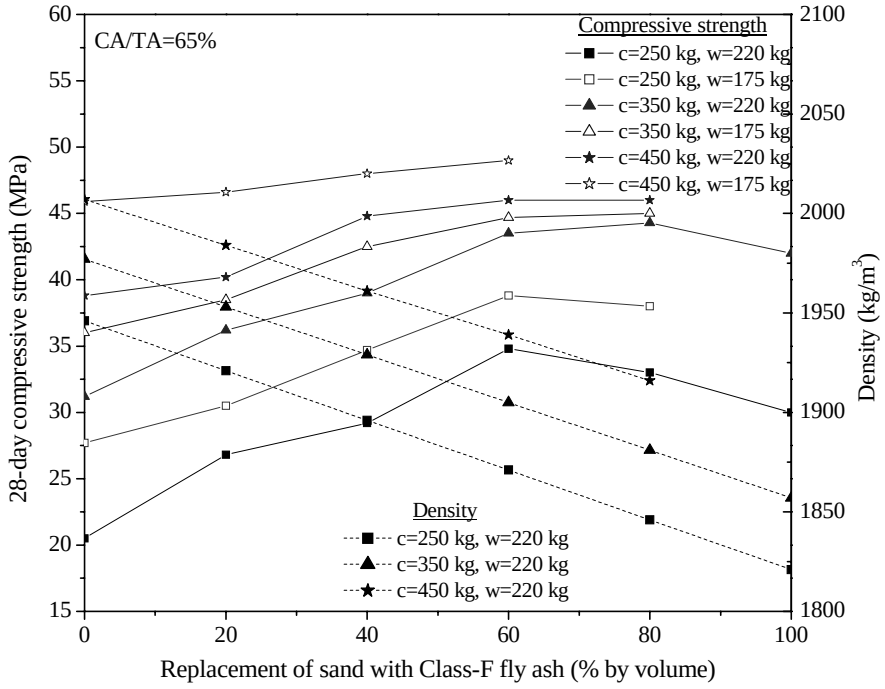


(b) CA/TA=65%

Fig. 6.3 Influence of replacement of sand with fly ash on 28-day strength

In mixes with 250 kg/m$^3$ cement content (low cement content), when 80% of sand is replaced with fly ash, the fly ash content ranges between 395 and 565 kg/m$^3$ (155 to 225% of the cement content) for CA/TA ratios of 50 and 65% respectively. As compared to the corresponding control specimen, an enhancement in strength of around 40 to 70% is achieved in mixes with cement content of 250 kg/m$^3$, while such an enhancement is only 20 to 40% and 8 to 18% respectively in mixes with cement content of 350 and 450 kg/m$^3$. Significant improvement in strength of mixtures of low cement content is mainly due to the improvement in matrix and matrix-aggregate bond which controls the concrete failure. Similar studies on 28-day strength of normal concrete with a cement content of 350 to 390 kg/m$^3$ and 50% sand replaced by fly ash report (Maslehuddin et al., 1989; Siddique, 2003) an increase of 45 to 50% as compared to control mix. At higher cement content, since the aggregate governs the failure of cold-bonded aggregate concrete, the strength enhancement is less pronounced.

The microstructure of concrete with cement content of 250 kg/m$^3$ at different replacement levels of sand with fly ash in Back Scattered Electron Imaging (BSEI) mode is presented in Fig. 6.4. The control mix (Fig. 6.4(a)) exhibits coarse pores with interconnectivity both in matrix and matrix-aggregate interface. As the fly ash content increases (Fig. 6.4 (b-d), a gradual refinement of pores and improvement in denseness of matrix and matrix-aggregate interface are observed which are consistent with improvement in compressive strength. The pores in the matrix and interface are finer (<10μm) especially in concrete with 60-80% fly ash (Fig. 6.4 (c-d)).

In concrete with 250 kg/m$^3$ cement content and fly ash replacing sand, Figs. 6.3 (a) and (b) exhibit that the strength enhancement is higher in mixes with higher CA/TA ratio as compared to the corresponding control mix. Hence it appears beneficial to use

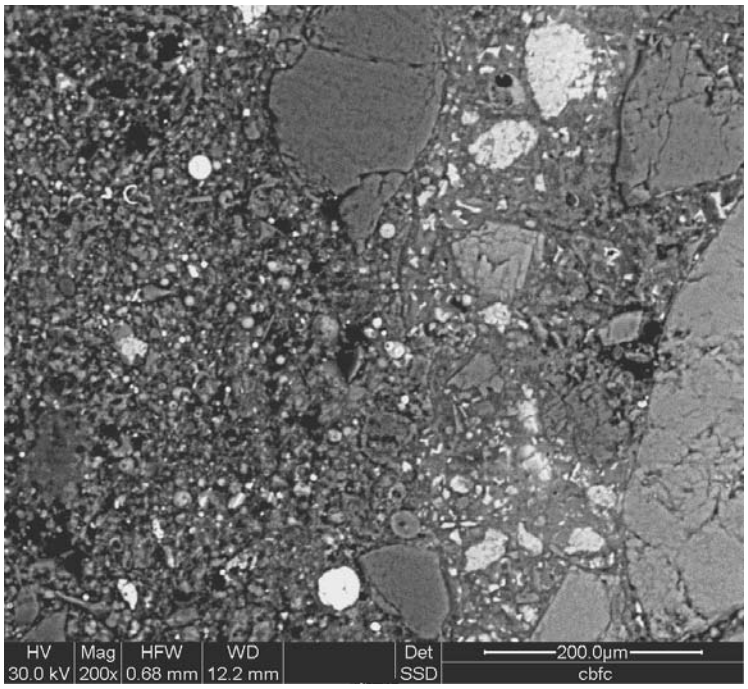


(a) fly ash = 0%

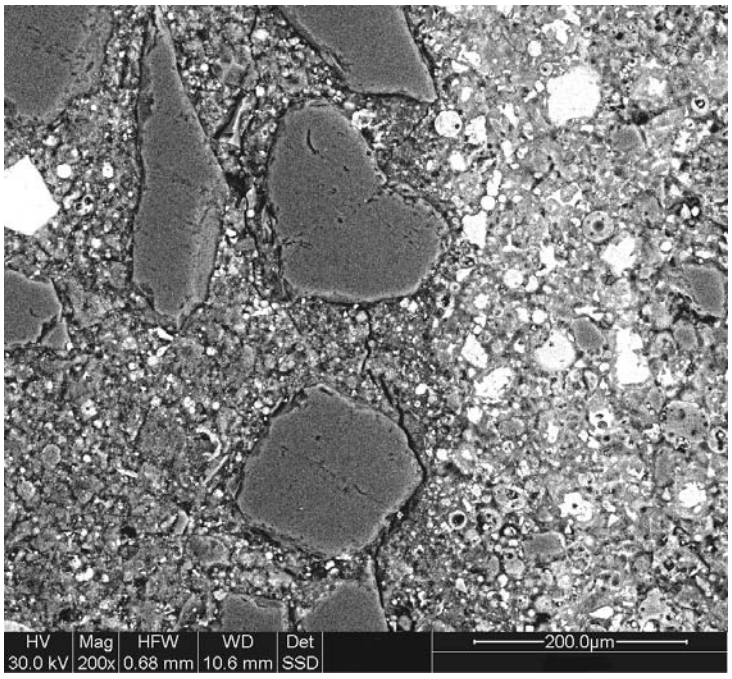


(b) fly ash = 40%

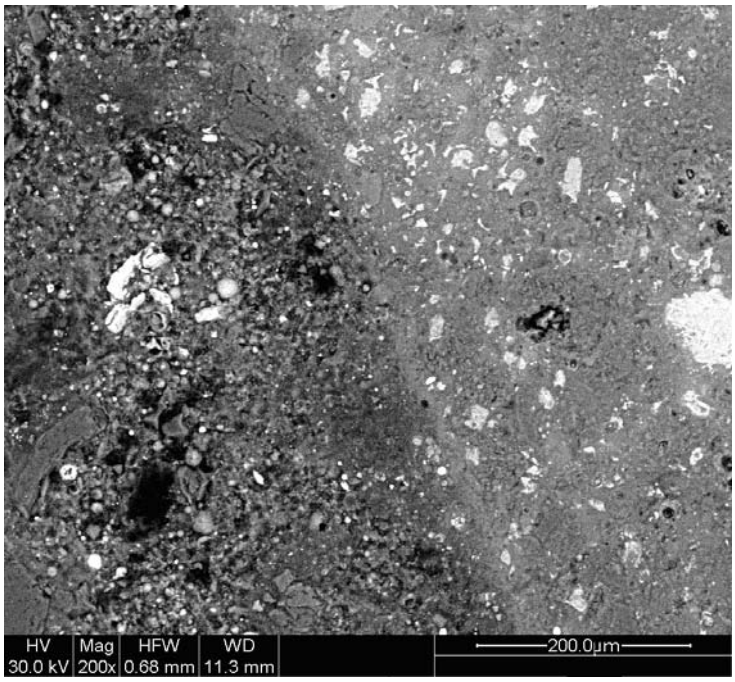


(c) fly ash = 60%

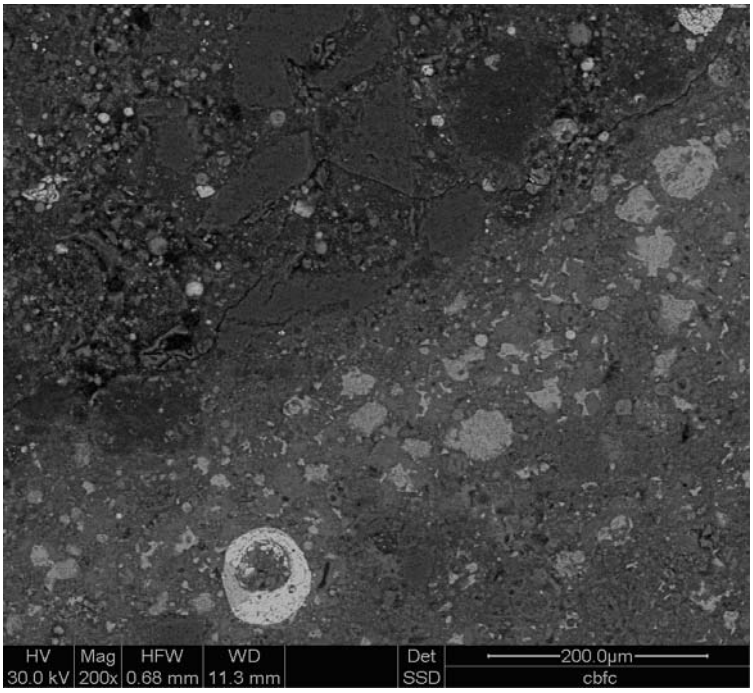


(d) fly ash = 80%

Fig. 6.4 BSEI (200x); influence of replacement of sand with fly ash (cement=250 kg/m$^3$, water=175kg/m$^3$, CA/TA-65%, 28-day)

higher CA/TA in mixes with low cement content which result in higher strength enhancement as well as use of higher total quantity of fly ash in the mix.

At the age of 7-day, the strength of cold-bonded aggregate concrete with fly ash replacing sand is marginally higher than that of the corresponding control mix (Fig. 6.5). According to Hwang et al. (2004) when sand is replaced with fly ash, higher amount of C-S-H is produced with an increase in fly ash content inhibiting large CH deposits, contributing to early strength gains, against the long period required for the strength development in cement replacement. Significant improvement in strength has been observed at 90-day especially in concrete with low cement content. The 90-day strength enhancement in control concrete is only about 40 to 54% of its 7-day strength, while this enhancement in concrete with 60% fly ash replacing sand is about 47 to 66% and 89 to 97 % respectively in mixes with cement content of 450 kg/$m^3$ (Fig. 6.5(c)) and 250 kg/$m^3$ (6.5 (a)). It is interesting to note that concrete with 250 kg/$m^3$ cement content (CA/TA 65%, water content 175 kg/$m^3$ and 60% sand replaced by fly ash) results in 90-day compressive strength of about 45 MPa, with a total inclusion of about 0.62 $m^3$ (Table 6.4) of fly ash (coarse aggregate and fine aggregate) in unit volume of concrete.

## 6.5 PERMEATION BEHAVIOUR

Permeation behaviour of concrete with variation in mix composition has already been discussed in Chapter 5. The influence of Class-F fly ash as partial replacement of (i) cement and (ii) sand on water absorption, sorptivity and chloride ion penetrability of cold-bonded aggregate concrete is dealt in this section.

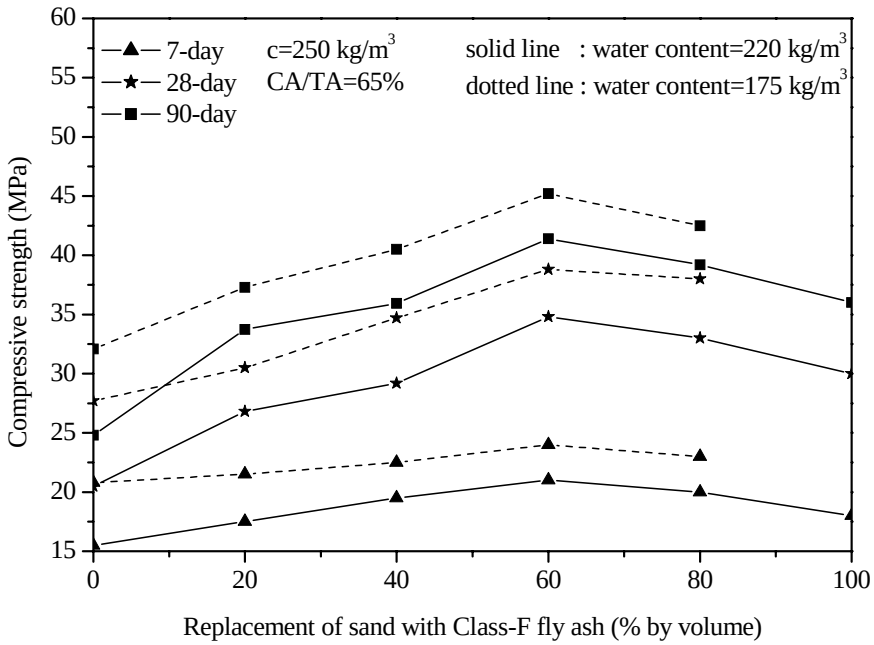


(a) cement content=250 kg/m$^3$

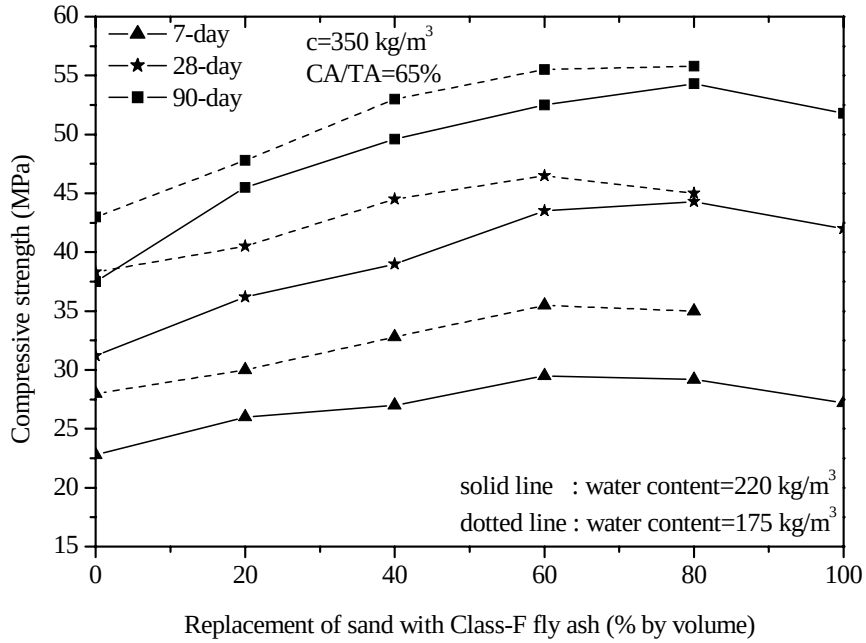


(b) cement content=350 kg/m$^3$

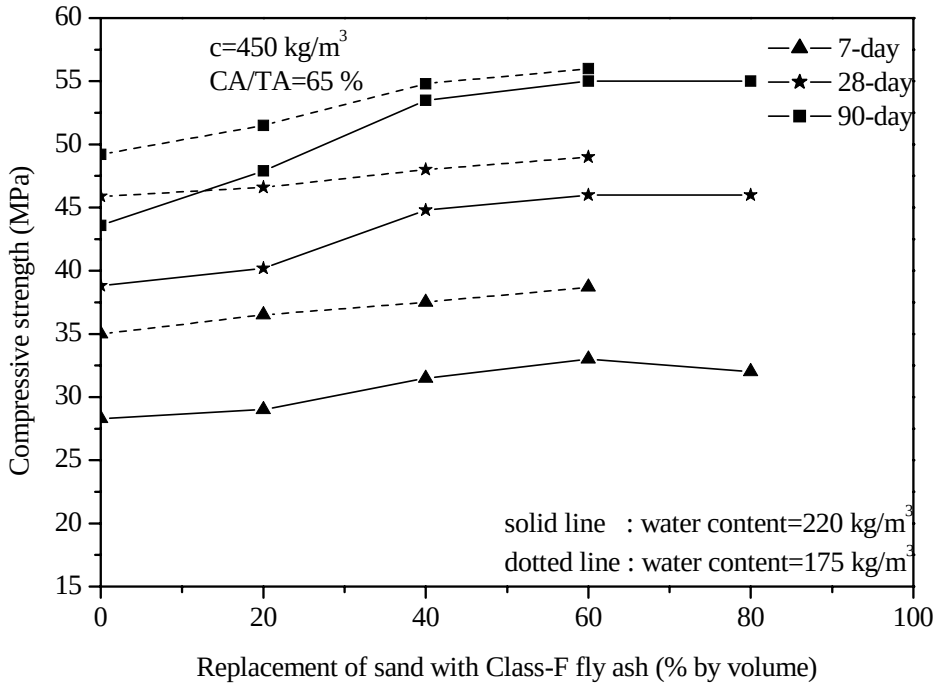


(c) cement content=450 kg/m$^3$

Fig. 6.5 Influence of replacement of sand with fly ash on development of strength

### 6.5.1 Water Absorption

#### 6.5.1.1 Cement replacement with fly ash

The variation in water absorption of cold-bonded aggregate concrete with cement partially replaced with fly ash is presented in Fig. 6.6. At 28-day, the water absorption increases with the replacement level of cement, which corroborates well with the strength development (Fig. 6.1), due to slower pozzolanic reaction of mixes with fly ash.

But at 90-day, the absorption is almost the same as that of control mix up to 30% cement replacement, which may be attributed to the matrix refinement owing to the extended pozzolanic reaction. Beyond this replacement level, the water absorption is higher than that of the control mix; comparable to the reduction in strength behaviour

observed at 50% replacement. However, about 19% increase in water absorption compared to control concrete observed at 28-day due to 50% replacement level is reduced to 10% at 90-day. At higher CA/TA ratio, due to reduction in the paste content and consequent increase in porosity, the water absorption is relatively higher. The quantity of water absorbed plotted against the dry density of concrete in Fig. 6.7 shows a marginal reduction in absorption (with reduction in density) in mixes with cement replacement up to 30%. Beyond this replacement level, though the density continues to decrease, the quantity of water absorbed increases considerably.

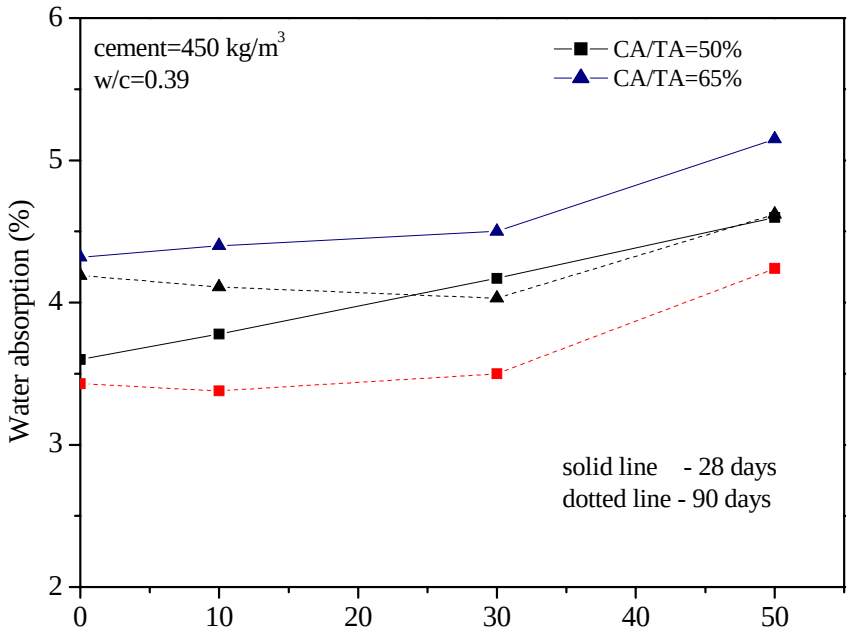


Fig. 6.6 Influence of replacement of cement by fly ash on water absorption

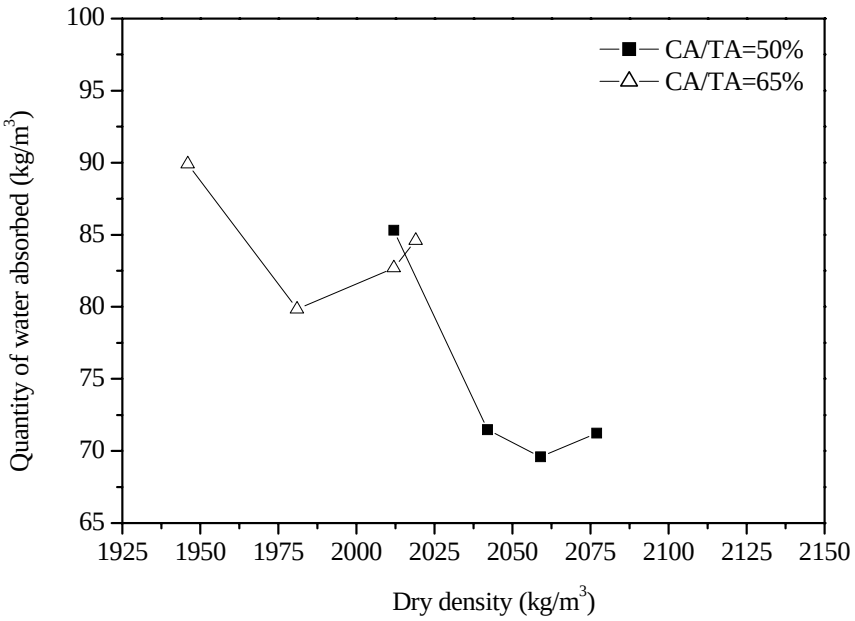


Fig. 6.7 Influence of density on water absorption
(cement replacement with fly ash, 90-day)

**6.5.1.2 Sand replacement with fly ash**

The influence of sand replacement with fly ash on water absorption of cold-bonded aggregate concrete is depicted in Fig. 6.8. For a given aggregate content, the absorption decreases continuously with an increase in replacement of sand by fly ash and reaches an optimum minimum value at about 60-80% of replacement, i.e., corresponding to a level wherein maximum improvement in strength (Fig. 6.3) has been observed. Though the water absorption increases beyond this replacement level, the absorption at 100% replacement level is considerably lower than that of the corresponding control concrete. When the sand is replaced with fly ash, an improvement in the microstructure of both matrix and matrix-aggregate interface and formation of discontinuous pores observed in BSEI (Fig. 6.4(b-d)) are attributed for this reduction in water absorption. As expected, for constant cement and aggregate contents, the effect of curing is more pronounced in mixes with fly ash than control mix due to the extended pozzolanic reaction of fly ash. Again, at a particular level of

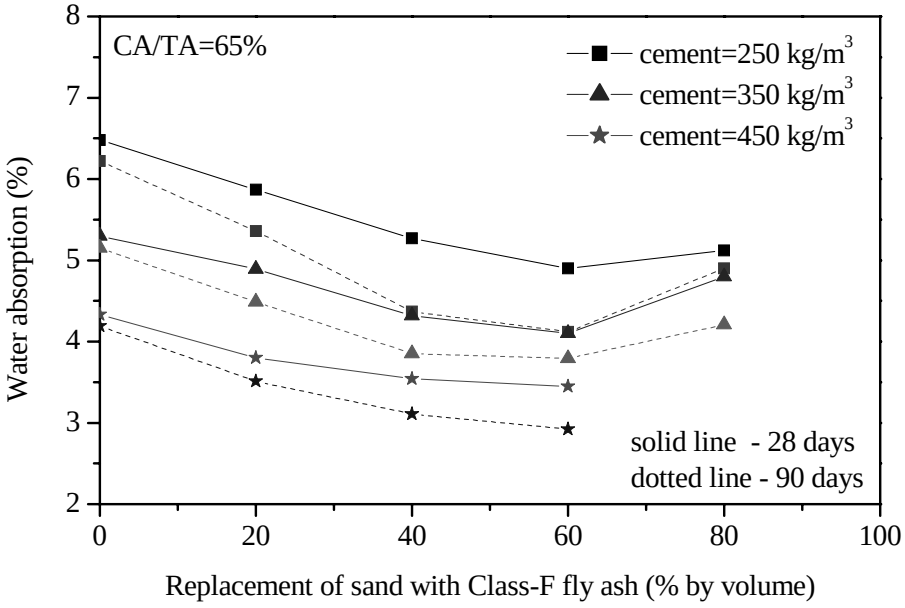


(a) water content = 175 kg/m$^3$

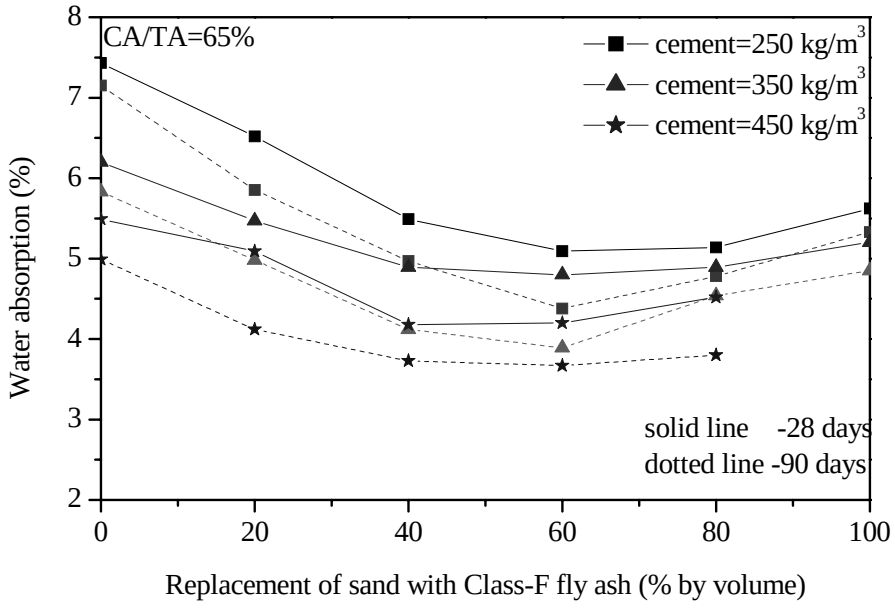


(b) water content = 220 kg/m$^3$

Fig. 6.8 Influence of sand replacement with fly ash on water absorption

replacement, results exhibit that influence of fly ash is significant in mixtures of lower cement content. The percentage reduction in water absorption at 90-day from that of control mix is about 39% in concrete with 250 kg/m$^3$ cement content while the reduction is only about 26% in concrete with cement content of 450 kg/m$^3$. Fig. 6.9 shows a steep decrease in the amount water absorbed by unit volume of concrete with a reduction in density caused by replacement of sand with fly ash but for lower levels of density which corresponds to 80 to 100% of sand replacement.

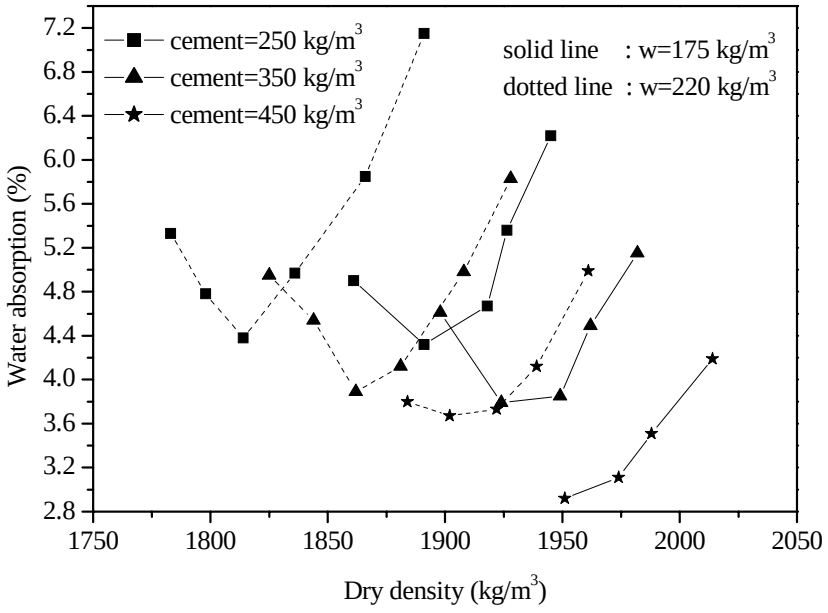


Fig. 6.9 Influence of density on water absorption
(sand replacement with fly ash, 90-day)

Fig. 6.10 presents the relation between water absorption and compressive strength of concrete in mixes with fly ash replacing sand. In general, an increase in strength of concrete is associated with a decrease in water absorption. Higher $R^2$-value in the relationship is observed in concrete with 250 kg/m$^3$ cement content as compared to mixes having higher cement content. This is mainly due to the significant improvement in strength (Fig. 6.3) and the corresponding reduction in water

absorption (Fig. 6.8) in concrete with lower cement content, while only a marginal increase in strength in mixes with higher cement content could be achieved when sand is replaced with fly ash.

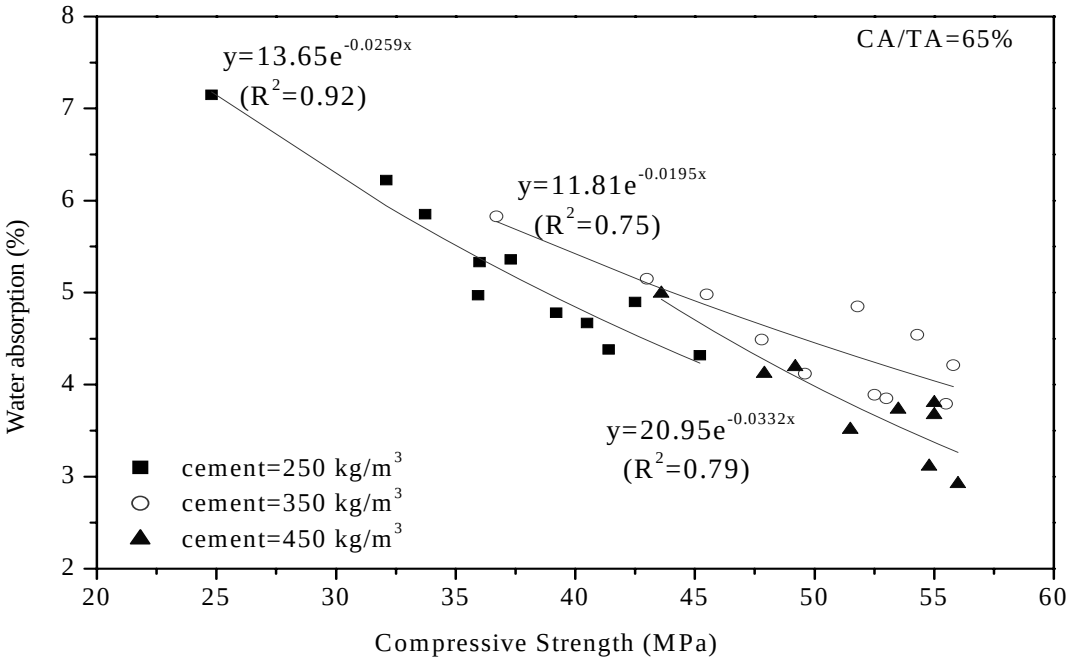


Fig. 6.10 Variation in water absorption with compressive strength
(sand replacement with fly ash, 90-day)

### 6.5.2 Sorptivity

#### 6.5.2.1 Cement replacement with fly ash

Fig. 6.11 exhibits that the sorptivity at 28-day increases with replacement level of cement with fly ash. Extended curing up to 90-day lowers the sorptivity; with the sorptivity value nearer to that of control concrete at replacement levels of 10 to 30%. This observation is comparable to the variation observed in water absorption (Fig. 6.6) while fly ash replacing cement. Similar behaviour on sorptivity has been reported for normal concrete by Bai et al. (2002) wherein after 4 months of curing, the sorptivity of concrete with 30% of fly ash was reduced to the level of control mix. For

a given binder content, sorptivity increases with an increase in cold-bonded aggregate content.

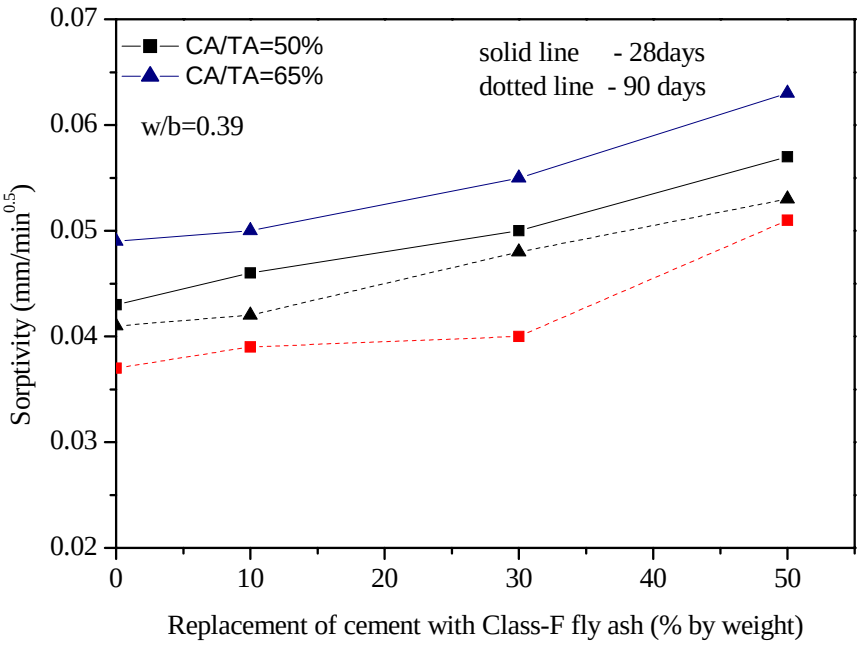


Fig. 6.11 Influence of replacement of cement with fly ash on sorptivity

### 6.5.2.2 Sand replacement with fly ash

Fig. 6.12 demonstrates the variation in sorptivity of cold-bonded aggregate concrete with fly ash as sand replacement material, wherein the beneficial effect is similar to water absorption and compressive strength. The percentage reduction in sorptivity with reference to control concrete is about 60% and 48% in mixes with lower and higher cement contents respectively. The amount of paste in the concrete increases when sand is replaced with fly ash. The consequent higher diffusion of paste into the aggregate pores resulted in formation of tortuous path apart from matrix refinement and discontinuity of pores as observed in BSEI (Fig. 6.4) causes the reduction in sorptivity with fly ash. The reduced sorptivity reflects finer pore structure, which in turn inhibits ingress of aggressive elements into the pore system.

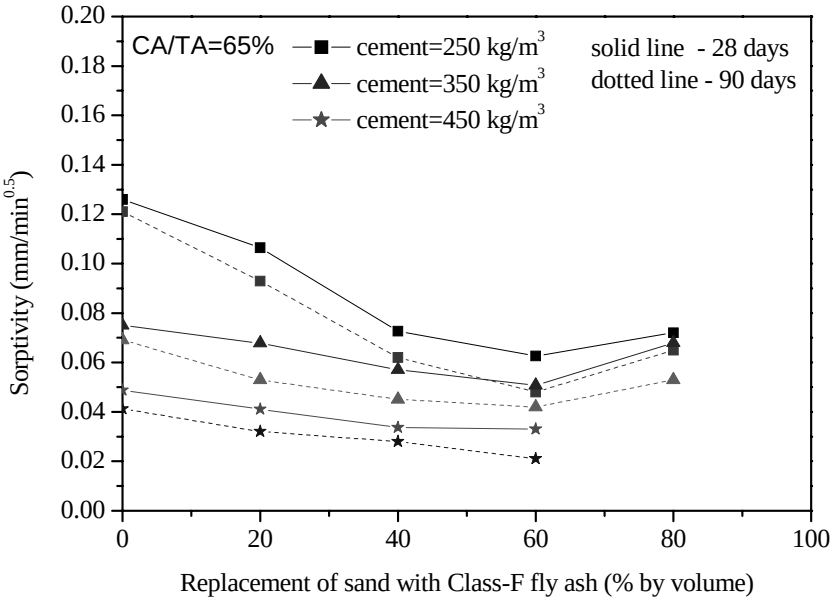


(a) water content = 175 kg/m$^3$

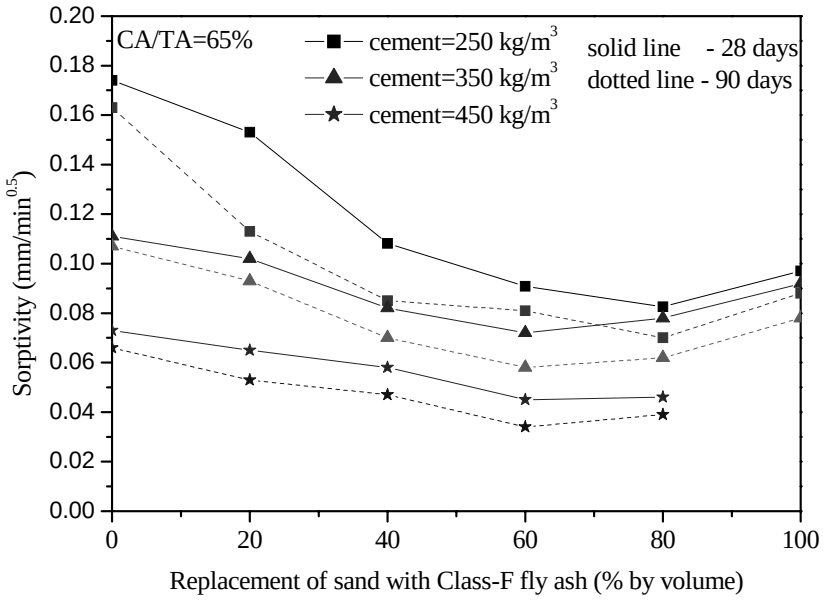


(b) water content = 220 kg/m$^3$

Fig. 6.12 Influence of replacement of sand with fly ash on sorptivity

The relation between sorptivity and density (Fig. 6.13) exhibits that sorptivity decreases with a reduction in density except beyond 80% replacement level. Fig. 6.14 shows that the strength and resistance to capillary suction (sorptivity) of fly ash concrete correlates fairly well except in mixes with higher cement content where only marginal enhancement in strength has been achieved. Similar to the influence of fly ash on compressive strength behaviour (section 6.4.2) Table 6.5 indicates the advantage of use of fly ash as partial replacement of cement and sand in reducing the sorptivity of concrete.

Table 6.5 Comparison between fly ash as part of binder and fine aggregate (CA/TA = 65%, water content = 175 kg/m$^3$, 90-day)

| Cement (kg/m$^3$) | Sand (kg/m$^3$) | Fly ash (kg/m$^3$) | Fly ash as | | Total vol. of fly ash (m$^3$/m$^3$ of concrete) | Water absorption (%) | Sorptivity (mm/min$^{0.5}$) | Charge passed (Coulombs) |
|---|---|---|---|---|---|---|---|---|
| | | | Binder (%) | Fine aggregate (%) | | | | |
| 450 | 603 | 0 | 0 | 0 | 0.427 | 4.19 | 0.041 | 1920 |
| 450 | 362 | 192 | 0 | 40 | 0.519 | 3.11 | 0.028 | 625 |
| 450 | 241 | 288 | 0 | 60 | 0.565 | 2.92 | 0.021 | 302 |
| 405 | 596 | 45 | 10 | 0 | 0.444 | 4.11 | 0.042 | 1830 |
| 350 | 632 | 0 | 0 | 0 | 0.448 | 5.15 | 0.069 | 2352 |
| 350 | 379 | 201 | 0 | 40 | 0.544 | 3.85 | 0.045 | 927 |
| 350 | 253 | 302 | 0 | 60 | 0.592 | 3.79 | 0.042 | 840 |
| 350 | 127 | 403 | 0 | 80 | 0.641 | 4.61 | 0.053 | 935 |
| 315 | 583 | 135 | 30 | 0 | 0.477 | 4.03 | 0.048 | 1960 |
| 250 | 661 | 0 | 0 | 0 | 0.468 | 6.22 | 0.121 | 4260 |
| 250 | 397 | 211 | 0 | 40 | 0.569 | 4.67 | 0.062 | 2783 |
| 250 | 264 | 316 | 0 | 60 | 0.619 | 4.32 | 0.048 | 1263 |
| 250 | 132 | 421 | 0 | 80 | 0.669 | 4.90 | 0.063 | 930 |
| 225 | 569 | 225 | 50 | 0 | 0.511 | 4.62 | 0.053 | 2105 |

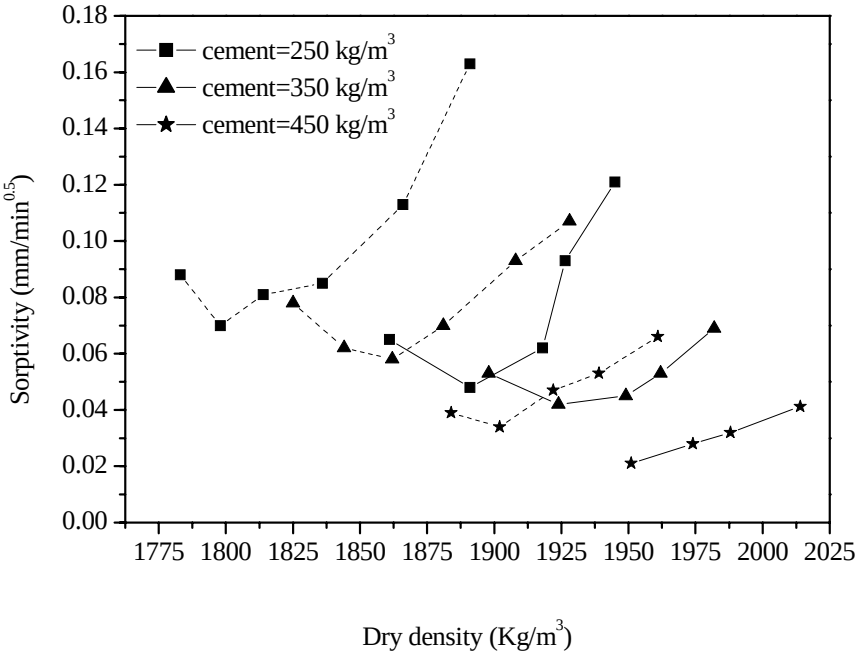


Fig. 6.13 Influence of density on sorptivity (sand replacement by fly ash, 90-day)

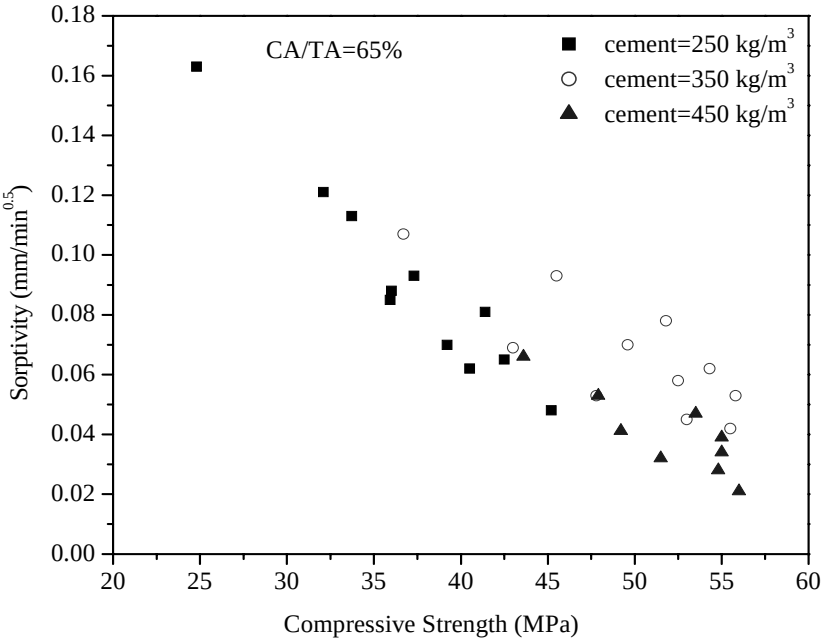


Fig. 6.14 Variation in sorptivity with compressive strength
(sand replacement by fly ash, 90-day)

### 6.5.3 Chloride Penetrability

#### 6.5.3.1 Cement replacement with fly ash

Fig. 6.15 depicts the resistance of cold-bonded aggregate concrete on the influence of replacement of cement by fly ash to rapid chloride ion penetrability. Though the charge passed through the fly ash concrete in rapid chloride penetrability test at 28-day is more than the control concrete, 90-day results suggest that about 30% cement can be replaced without much variation in chloride penetrability, i.e., if sufficient period is given for the formation of secondary hydration products before exposure to the severe chloride environment. The resistance of chloride ion penetrability behaviour of cold-bonded aggregate concrete with fly ash as partial replacement for cement is almost similar to the water absorption and sorptivity behaviour.

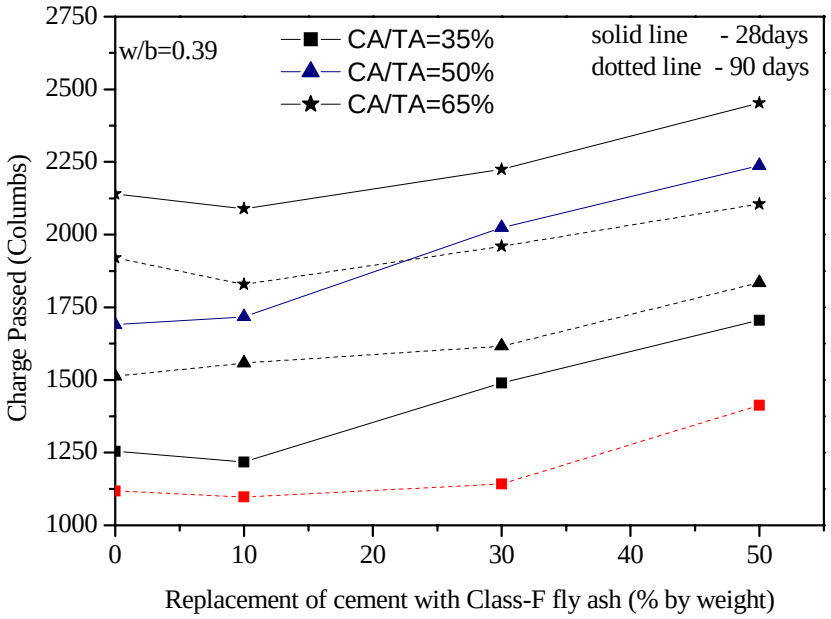


Fig. 6.15 Influence of replacement of cement with fly ash on charge passed in RCPT

### 6.5.3.2 Sand replacement with fly ash

Fig. 6.16 demonstrates a significant reduction in chloride ion penetrability with an increase in replacement of sand with fly ash which is similar to that observed in water absorption and sorptivity behaviour. Table 6.5 also presents the beneficial effect of use of fly ash as replacement of sand/cement in reducing the chloride ion penetration of cold-bonded aggregate concrete. The results of the present study corroborates well with the resistance to chloride ion penetrability of normal concrete incorporated high volume fly ash (Bilodeau et al, 1994; Langely et al., 1989) and the studies of Maslehuddin et al. (1989) wherein increased resistance to corrosion is reported when sand has been replaced by fly ash.

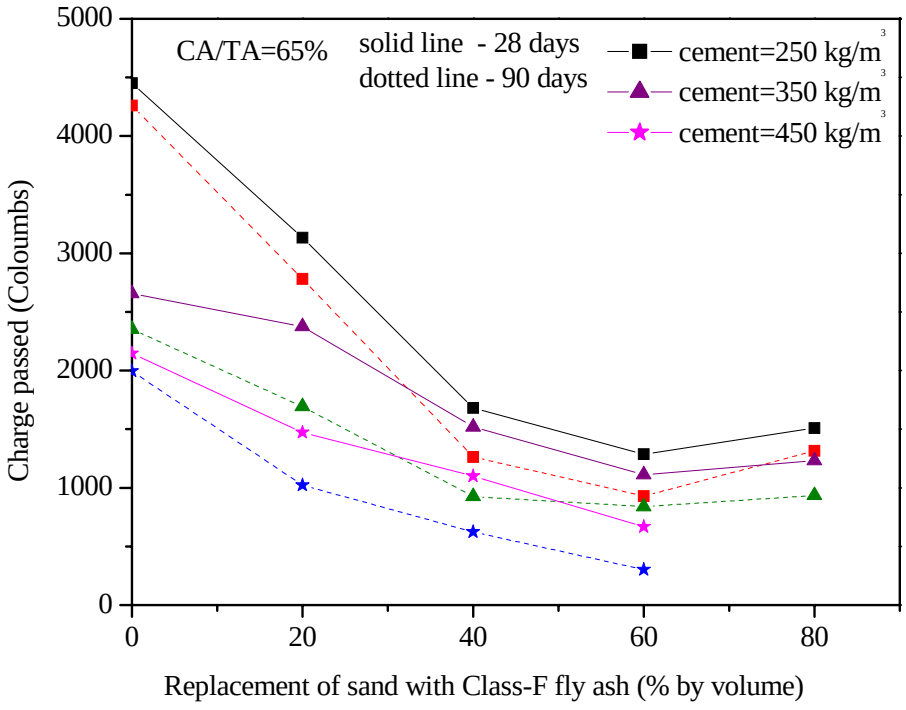


(a) water content w=175 kg/m$^3$)

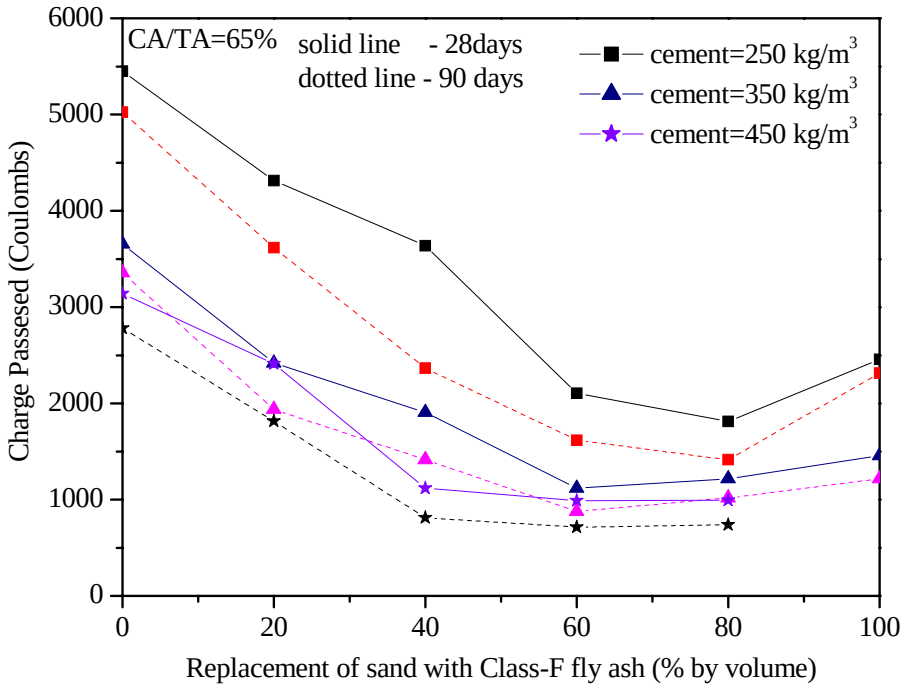


(b) water content = 220 kg/m$^3$

Fig. 6.16 Influence of replacement of sand with fly ash on charge passed in RCPT

## 6.6 SUMMARY

The influence of class-F fly ash on strength and permeation behaviour of cold-bonded aggregate concrete has been studied. Results indicated that cement replacement with fly ash must be restricted based on the target strength requirement. Fly ash as replacement for sand is higher than the corresponding control mix from the early age onwards. The strength enhancement is higher in mixes with lower cement content (250 kg/m$^3$) along with higher CA/TA ratio. The reduction in sorption and chloride ion penetrability of concrete with fly ash as replacement for sand is consistent with improvement in compressive strength. Replacement of sand with fly ash in cold-bonded aggregate concrete allows high volume utilization (up to 0.6 m$^3$/m$^3$ of concrete) of fly ash in concrete with beneficial effect on strength, causing no detrimental effect on permeation behaviour.

# CHAPTER 7

# AUTOGENOUS CURING OF COLD-BONDED FLY ASH AGGREGATE CONCRETE

## 7.1 GENERAL

It is well established that proper curing is essential for producing durable concrete. The hydration of cement is greatly reduced when the relative humidity within the capillaries drops below, about 80% (Neville, 2004). Several studies on high performance concrete have used lightweight aggregate as partial replacement for conventional coarse aggregate to facilitate internal curing and mitigate autogenous shrinkage when the relative humidity in the cement paste decreases due to hydration and drying. The saturated lightweight aggregates in concrete act as 'water reservoirs' for the unhydrated cement paste (Weber and Reinhardt, 1997). The efficiency of aggregate in facilitating internal curing is also attributed to the grain-size distribution and proximity of cement paste to the surface of aggregate (Bentz and Snyder 1999). The objectives of such studies on high strength concrete have been to identify the minimum LWA content to facilitate internal curing as its content affects the strength of concrete.

Unlike high strength concrete incorporating a small quantity of LWA, the self-curing competence of lightweight aggregate concrete containing large volume of saturated aggregate with high absorption capacity needs to be evaluated. The influence of curing conditions and the extent of curing on the strength development of concrete with sintered/expanded clay aggregates having water absorption value in the range of 12 to 13.5% have been reported. Swamy and Lambert (1983) reported a strength of not less than 90% in uncontrolled curing environment of low humidity in concrete

with sintered fly ash aggregate after 3 to 6 months. Dhir et al. (1984) studied the development of strength in air-cured concrete with expanded clay aggregate up to 365 days and concluded that the percentage gain in strength was lower than that of water-cured concrete. While the compressive strength of concrete with sintered fly ash aggregate is reported to be less sensitive to curing, Haque et al. (2004) observed that the water penetrability and depth of carbonation were affected by the extent of curing. Hence the sensitivity of high-absorptive capacity cold-bonded fly ash aggregate to curing condition is likely to be different from that of heat treated aggregate (with low surface porosity and water absorption). The mechanism of autogenous curing and autogenous deformation of lightweight aggregate concrete are reviewed first in this chapter. The effectiveness of cold-bonded aggregate on the autogenous curing behaviour of concrete is studied through an assessment of moisture migration from aggregate, degree of hydration, compressive strength, permeation behaviour and autogenous deformation at various ages by subjecting concrete to three curing regimes viz. mist curing, sealed condition and air curing.

## 7.2 AUTOGENOUS CURING OF LWAC

### 7.2.1 Mechanism of Autogenous Curing

The potentiality of water-entrainment by lightweight aggregate of high porosity for offsetting self desiccation in low water/binder ratio concrete and favouring internal curing of concrete is known for last one decade (Weber and Reinhardt, 1997; Bentz and Snyder, 1999; Bentur et al, 2001; Kovler et al., 2002). Properties of aggregate favourable for internal curing are high water absorption capacity and open pore structure. Mechanism of autogenous curing of LWAC described by Weber and Reinhardt (1997) is summarised below: The uniformly distributed porous saturated lightweight aggregates in concrete act as water reservoirs in the matrix. During

hydration a system of capillary pores are formed within the cement paste. As soon as humidity in the cement paste decreases (due to hydration and drying) a humidity gradient appears. The water required for hydration will be drawn from the relatively 'large pores' in the saturated lightweight aggregate into much smaller pores in the cement paste by capillary suction. Whereas, the outer surface of concrete which is subjected to drying, uses the water from the LWA nearer to the surface earlier than from the aggregate in the interior of the concrete. The concrete on the surface becomes more compact in a relatively short time. The more compact structure of the concrete surface will reduce the amount of water that normally would evaporate, conserving the water inside the concrete. The quantity of entrained water and the distance of water penetration into the hardening paste are the important factors in determining efficiency of internal curing (Bentz and Snyder, 1999). The internal/self curing ability of lightweight aggregate concrete is also reported to be a function of the type of LWA, its size and amount, the degree of saturation of aggregate and the amount and type of binder(s) in the mix composition.

### 7.2.2 Autogenous Shrinkage of LWAC

Autogenous shrinkage of concrete is an indication of low internal humidity in concrete. Therefore mitigation of autogenous shrinkage is essential for realising autogenous curing in concrete with low water-binder ratio. The reduction in autogenous shrinkage of concrete using lightweight aggregate mainly depends on the surface porosity and absorptive capacity of the aggregate (Kovler et al., 2004). Kohno et al. (1999) reported that concrete with lightweight aggregate of high water absorption (> 20%) could maintain autogenous expansion for several days whereas in concrete with aggregate of less absorptive capacity (< 5 %), the early age expansion was slowly changed to shrinkage. Bentur et al. (2001) has concluded that generally,

air-dried lightweight aggregate is not efficient in mitigating the autogenous shrinkage completely whereas fully saturated aggregate maintains the expansion and can develop restraining stresses of compressive nature. Therefore in concrete with a particular type of light weight aggregate, the unit quantity of aggregate in the mixture composition which in turn, the available moisture in concrete is considered as the important factor that affects the autogenous shrinkage as well the autogenous curing of concrete.

## 7.3 MATERIALS AND METHODOLOGY

### 7.3.1 Materials

Table 7.1 presents the mixes along with the curing conditions investigated. While mist curing represents the conventional laboratory curing method, sealed curing is chosen to understand the influence of cold-bonded aggregate in promoting hydration when no moisture movement is allowed both from the interior or exterior of the concrete. Air curing, typically represents the case of concrete not subjected to any specific curing condition in a region of warm humid climate.

Mixes with low water content was chosen to evaluate the effect of cold-bonded aggregate in promoting hydration by internal curing. The cement content was varied to analyze both, low strength (< 35 MPa, where matrix or matrix-aggregate bond initiates failure) and high strength mixes (wherein the failure takes place through the cold-bonded aggregate and strength decreases with volume fraction of aggregate. Required dosage of superplasticizer was added to maintain slump value of 50 $\pm$ 5 mm. From each mix, specimens for compressive strength, porosity, sorptivity, chloride ion penetrability and autogenous deformation were cast. After 2 hours of casting, all the moulds were covered with polyethylene sheets to avoid moisture loss. The specimens

were demoulded after 24 hours, weighed and stored under the respective curing conditions up to 180 days for testing of specimens at various ages.

Table 7.1 Mixture compositions and curing conditions

| Cement content ($kg/m^3$) | Type of coarse aggregate | w/c ratio | CA/TA (Vol. %) | Curing Conditions |
|---|---|---|---|---|
| 250 | Cold-bonded fly ash | 0.5 | 35 , 50, 65 | (i) Mist room curing, 23±2 ºC, 98±2% RH, 180 days<br>(ii) Sealed in aluminum foils, 23±2ºC, 180 days<br>(iii) Air curing, 23 to 37 ºC and 65 to 82% RH, 180 days |
| 350 | Cold-bonded fly ash | 0.35 | 35, 50, 65 | |
| 450 | Cold-bonded fly ash | 0.35 | 35, 50, 65 | |
| 450 | Crushed granite | 0.35 | 65 | |

### 7.3.2 Methodology/Properties Investigated

#### 7.3.2.1 Moisture movement from cold-bonded aggregate

Residual moisture content in the cold-bonded aggregate at various ages of concrete would give an indication of the moisture transfer between aggregate and concrete occurring under various curing regimes. Therefore in order to estimate the moisture transfer between aggregate and concrete, cold-bonded aggregate was extracted manually, following Holm et al. (2004), from the interior of concrete at various ages. Sufficient care was taken in extracting the aggregate and while removing the mortar layer from the aggregate surface. Approximately, 100g of aggregate was extracted in each case for the determination of residual moisture content from the 24 hour oven-dried (at 105ºC) weight. The residual moisture content is represented as the difference in mass between as-extracted aggregate and the mass after 24-hour of oven-drying expressed as a percentage of the oven-dried mass of the aggregate.

#### 7.3.2.2 Degree of hydration

The chemically bound water determining the degree of hydration of cement paste at different age was measured from the non evaporable water content of paste. For this purpose, mortar fractions were separated from concrete at different ages bearing in mind the pozzolanic property of cold-bonded aggregate. The mortar fractions were crushed and sieved through 75μm sieve to remove sand particles as suggested by Weber and Reinhardt (1997). Samples were first dried at 105 ºC for 24 hours to remove the physically bound water from the paste. The non-evaporable water content was determined as the percentage weight loss of the ignited sample corrected for the loss of ignition of the original cement sample after burning it in a muffle furnace at 1000ºC for 60 minutes (El-Dieb, 2007).

Thermal gravimetric analysis (TGA) is widely used to identify the various hydrates developed in concrete as the decomposition of which occurs at different temperatures. TGA was carried out on hydrated paste at different ages (after oven dried at 105 ºC) up to 1000 ºC at a heating rate of 10 ºC/minute under nitrogen atmosphere to verify the formation of additional hydration products with the age of concrete.

XRD analysis was undertaken at various ages to identify the polycrystalline phases of hydrated cement paste of concrete cured under different regimes through the recognition of XRD patterns that were unique for each of the crystalline phases. This technique allows the detection of $AF_t$, $AF_m$ and CH and consumption of anhydrous phases of the cement (gypsum, $C_3S$, $C_2S$, $C_3A$ and $C_4AF$), as well as the formation of C-S-H.

#### 7.3.2.3 Autogenous deformation

Concrete prisms of size 40x40x160 mm (ASTM C 157, 2004) were prepared for the autogenous deformation (shrinkage/expansion) measurements. As the maximum size

of cold-bonded aggregate is 12.5 mm, the use of such smaller test specimen is justified (Bentur et al., 2001; Zhutovsky et al., 2004). After 18 hrs of casting the specimens were sealed with aluminium tape and measurement was started. Spherical gauge plugs were attached at both ends of the specimen to facilitate length change measurement and the specimens were kept at 23 $\pm$ 2 ºC. For each combination of mix, three specimens were tested and mean value was reported. The length measurement was made up to 180 days using a length comparator with a least count of 0.002 mm. Shrinkage/expansion of the specimens with age of concrete is reported in micro strain.

#### 7.3.2.4 Compressive strength and permeation behaviour

The number of specimens and method of test for compressive strength and permeation behaviour were the same as those described in section 4.3.4 and 5.3 respectively. The specimens cured under different regimes were tested at various ages up to 180-days to understand the influence of curing condition on the strength and permeation behaviour of concrete with different mixes.

## 7.4 INFLUENCE OF CURING ON CONCRETE BEHAVIOUR

### 7.4.1 Moisture Movement in Concrete

#### 7.4.1.1 Moisture movement from cold-bonded aggregate

The variation of moisture content in the cold-bonded aggregate extracted from concretes of different curing regime up to 28-days of curing is presented in Fig. 7.1. The initial moisture content in the aggregate has been taken as 19.04%, corresponding to the moisture absorption of aggregate within 30 minutes (Table 4.2). A significant reduction in the moisture content of the aggregate is observed during early age, under all curing regimes. Considerable reduction in moisture content in the aggregate extracted from mist-cured concrete (Fig. 7.1(a)) exhibits the migration of moisture

from the aggregate as it was readily available to the paste than from the external source of mist-curing. For a particular cement content and period of curing, the residual moisture content is lower in aggregate extracted from concrete with low volume fraction of aggregate. As the quantity of aggregate in the concrete is lower, the initial entrained water in the concrete due to the aggregate is the least, causing higher moisture migration from the aggregate. For a given percentage of cold-bonded aggregate volume, the residual moisture content is lower in the aggregate extracted from concrete with higher cement content, under sealed and mist-cured regimes. This exhibits increased moisture transport to counteract the low internal humidity arising out of hydration in concrete with higher cement content.

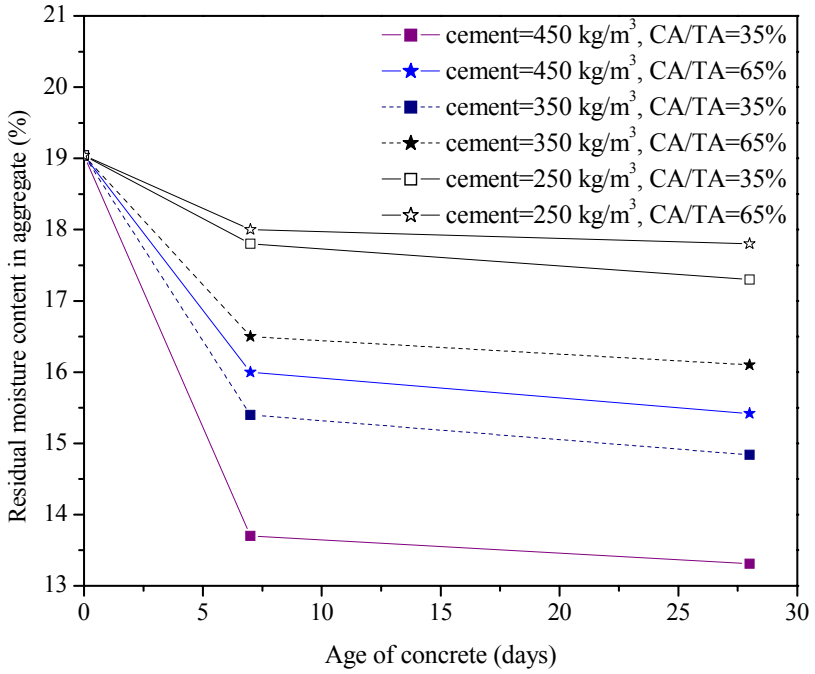


Fig. 7.1(a) Residual moisture content in aggregate extracted from mist-cured concrete

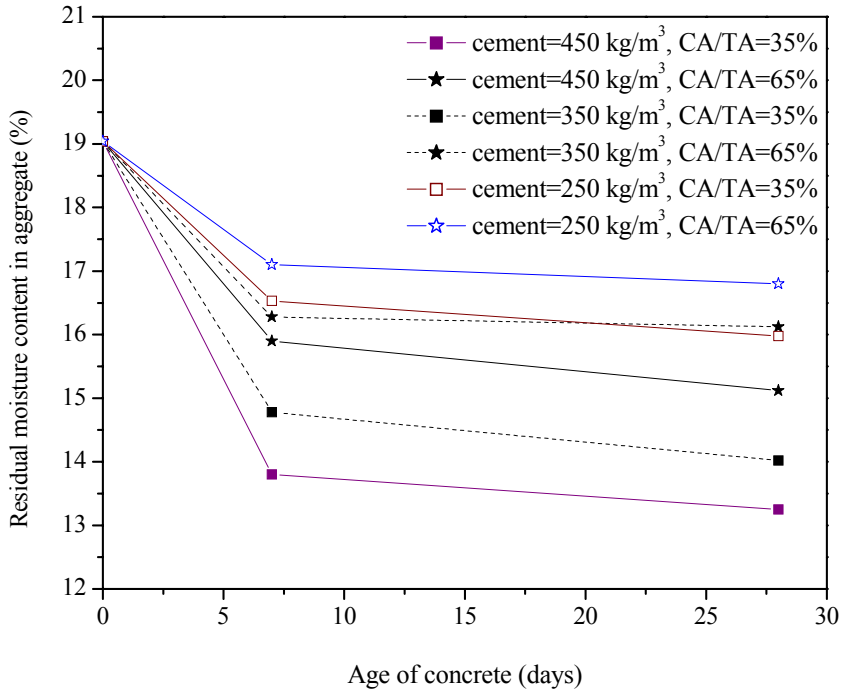


Fig. 7.1(b) Residual moisture content in aggregate extracted from sealed concrete

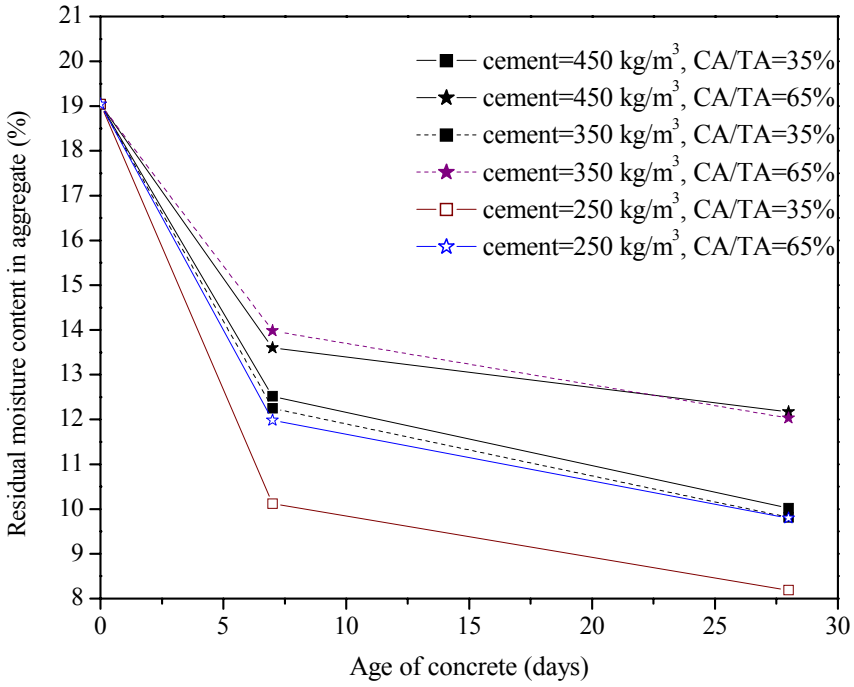


Fig. 7.1(c) Residual moisture content in aggregate extracted from air-cured concrete

The air-cured condition exhibits the least residual water content in the aggregate extracted from concrete with cement content of 250 kg/m$^3$ indicating higher moisture transfer from aggregate to the drying environment. The reason can be attributed to the less dense interfacial zone and matrix structure compared to concrete with higher cement content. Beyond 7 days, as the moisture migration from the aggregate is marginal in sealed and mist-cured condition, it can be concluded that the low internal humidity arising out of hydration is marginal beyond this period. The moisture movement continued in air-cured regime due to continuous loss of moisture through the surface of the specimen to the atmosphere.

To understand the influence of distribution of aggregate in concrete on the moisture transfer from the aggregate, paste-aggregate proximity has been determined by adopting 'protected paste volume concept' of Bentz and Snyder (1999) using the nearest surface distribution functions for poly-dispersed particles. The analytical equations proposed by Snyder, 1998 for the paste-aggregate proximity calculation has been presented in Appendix I.

Fig. 7.2 shows the volume fraction of cement paste/matrix within a given distance from the cold-bonded aggregate surface with variation in cement and aggregate content. It is observed that with an increase in volume of cold-bonded aggregate, there exists significant variation in the amount of paste fraction within 1 mm from aggregate surface. But beyond a proximity level of 3 mm the difference in paste fraction with the aggregate content is quite marginal, i.e. about 85 to 100% of paste fraction is brought within 3 mm from the aggregate surface. The least residual moisture content in the aggregate extracted from concrete with low CA/TA ratio under all curing regimes indicates the effective moisture migration from aggregate to the hydrating paste even when the paste fraction within a given distance is lower. This

suggests that the moisture in the aggregate has migrated through the hydrating paste to such a distance as to give higher internal humidity for a greater fraction of paste during the early age when the hydration is faster. In mixes with 35% cold-bonded aggregate, the results suggest that the moisture has effectively migrated from aggregate up to a distance of 4 mm within which more than 95% of paste fraction lies.

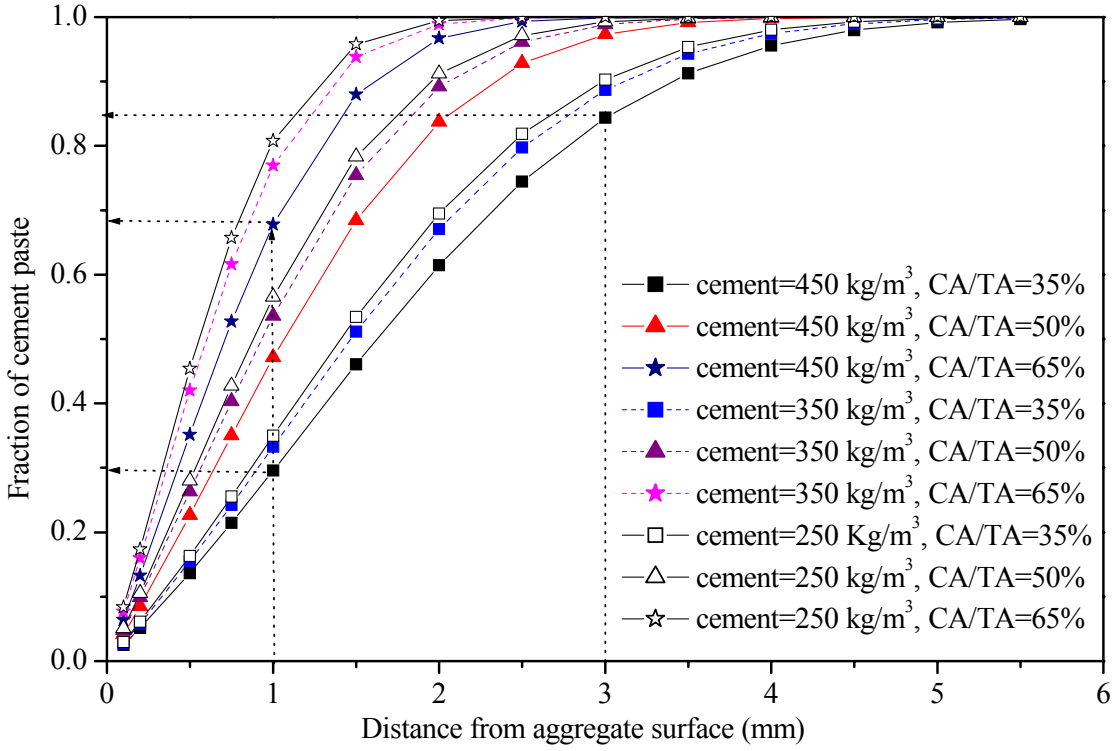


Fig. 7.2 Fraction of cement paste from cold-bonded aggregate surface

Fig. 7.3 exhibits that beyond 28 days, the change in moisture content in the aggregate under all the curing regimes is marginal, suggesting low moisture migration from aggregate irrespective of paste-aggregate proximity. This is attributed to the improvement in microstructure of the matrix and matrix-aggregate interface with the age of concrete and slower rate of hydration at later ages which in turn reduces the moisture demand. The marginal variation in residual moisture content between

aggregate extracted from sealed and mist-cured concrete shows that the influence of internal curing promoted by cold-bonded aggregate is pronounced than the external mist curing. This further highlights the effectiveness of moisture availability to the paste within a certain proximity zone as compared to those made available on the surface. For a given mix, as expected, the moisture transfer from the aggregate is the lowest in mist-cured specimen while it is the maximum in air-cured concrete. However, it is interesting to note that even at an age of 180 days the residual moisture content in the aggregate was high, i.e. 11 to 17% in the case of sealed and mist-cured specimens and 7 to 12% under air-cured condition.

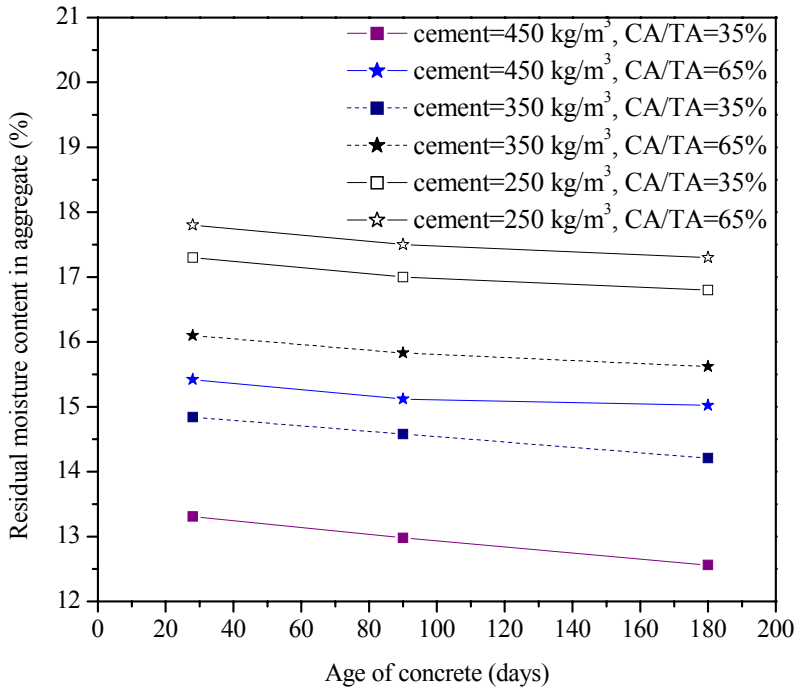


(a) mist-cured concrete

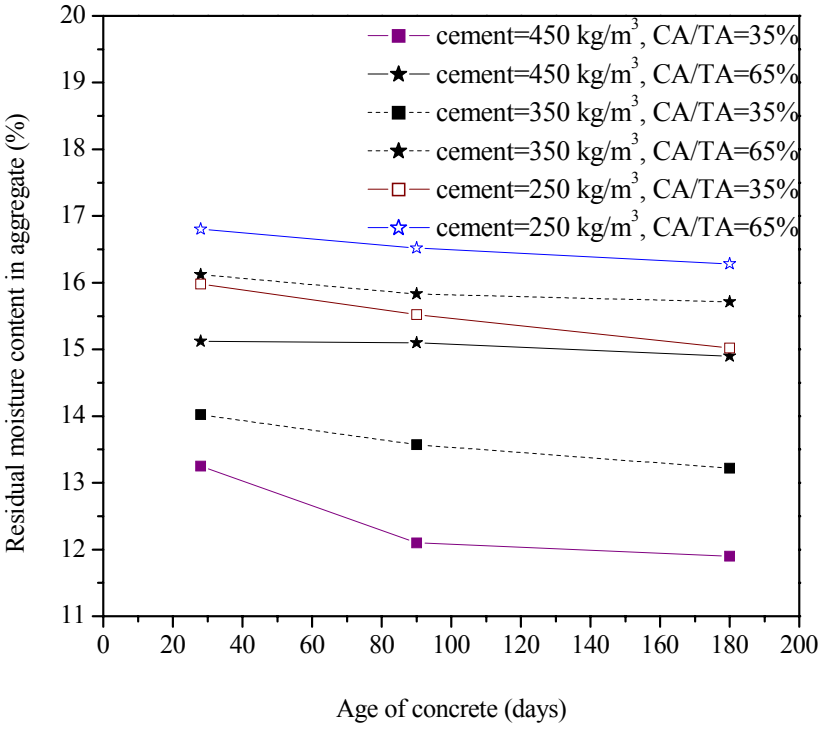


(b) sealed concrete

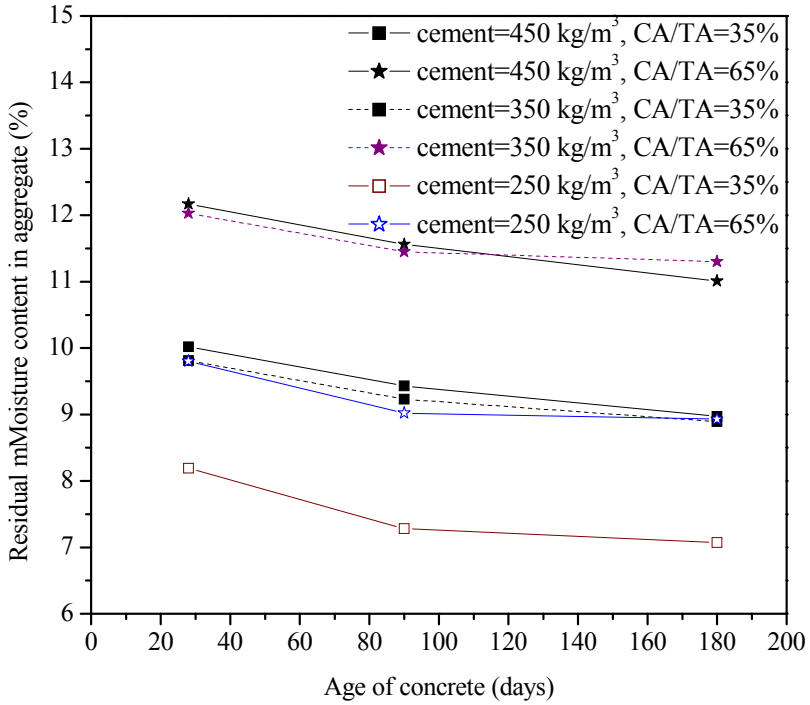


(a) air-cured concrete

Fig. 7.3 Variation in residual moisture content in aggregate with age of concrete

#### 7.4.1.2 Moisture loss from air-cured concrete

The overall moisture loss from 100 mm air-cured concrete cube specimen has been assessed as the residual moisture content in aggregate extracted from air-cured condition is the least. The moisture loss from concrete with the age of concrete is presented in Fig. 7.4. The moisture loss from the concrete is significant during early age. Inspite of significant moisture loss from the concrete with higher CA/TA ratio, the presence of residual moisture content in aggregate (Fig. 7.3(c)) indicates that the moisture is being utilized for internal curing according to the moisture gradient developed in concrete. Moreover, a significant reduction (about $30g/10^{-3}$ $m^3$) in moisture loss occurred as the cement content was increased from 250 to 450 $kg/m^3$. This is attributable to the variation in microstructure of concrete which corroborates well with the higher residual moisture observed in aggregates extracted from concrete having higher cement content (Fig. 7.3(c)). After 28 days, the moisture loss from the concrete is marginal (similar to the observations made in moisture transfer from aggregate).

#### 7.4.1.3 Minimum quantity of entrained water for internal curing

Having estimated the moisture migration from cold-bonded fly ash aggregate, as a next step a study is undertaken to verify whether the quantity of moisture migrated from aggregate is adequate for complete hydration. The requirement of entrained water ($V_{wat}$) in concrete for avoiding self-desiccation and ensuring 'complete curing' in a concrete under sealed condition has been evaluated using the relationship proposed by Bentz and Snyder (1999), which is based on the quantity of water consumed during hydration due to chemical shrinkage,

$$V_{wat}\,(m^3\ water/m^3\ concrete) = C_f.\ CS.\alpha_{max} / \rho_w.$$

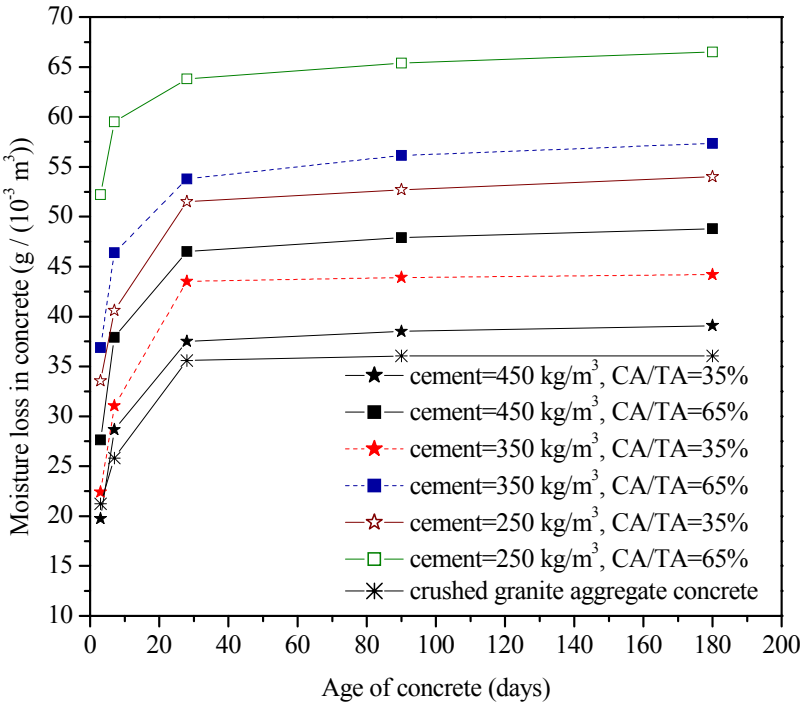


Fig. 7.4 Moisture loss in air-cured concrete

Where, $C_f$ = cement content in kg/m$^3$, CS = chemical shrinkage occurring during hydration of cement; typically 0.06 kg water per kg cement hydrated, $\alpha_{max}$ = maximum degree of achievable hydration, estimated as (w/c)/0.4; assuming complete hydration at w/c ratio of 0.4, $\rho_w$ = density of water (1000 kg/m$^3$).

The amount of water migrated from the aggregate with age of concrete is estimated as the difference between the water content in the aggregate at the time of mixing and residual water content at various age per unit volume of concrete. Fig. 7.5 compares the quantity of water migrated from aggregate under various curing regimes and the quantity needed for complete hydration. The water released from the aggregate is observed to be more than the minimum quantity required for 'complete curing' in the initial 30 days itself for all the mixes; obviously exhibiting the influence of cold-bonded aggregate in promoting internal curing. For a given cement content, the

variation in the total amount of moisture migrated from the aggregate to concrete of different CA/TA ratio is less than 5 kg/m$^3$, under mist-cured or sealed condition. Fig. 7.5(c) shows that moisture has migrated from the aggregate of concrete with 250 kg/m$^3$ cement content wherein a high w/c ratio is maintained.. The higher moisture migration/loss from the aggregate as compared to that required for 'complete curing' in sealed and mist-cured regimes may be attributed to i) utilsation of moisture by cold-bonded fly ash aggregate itself for its continuous pozzolanic reaction and ii) the capillary suction caused by the moisture gradient exists in concrete which ensures extended hydration and refinement of gel pores and capillaries.

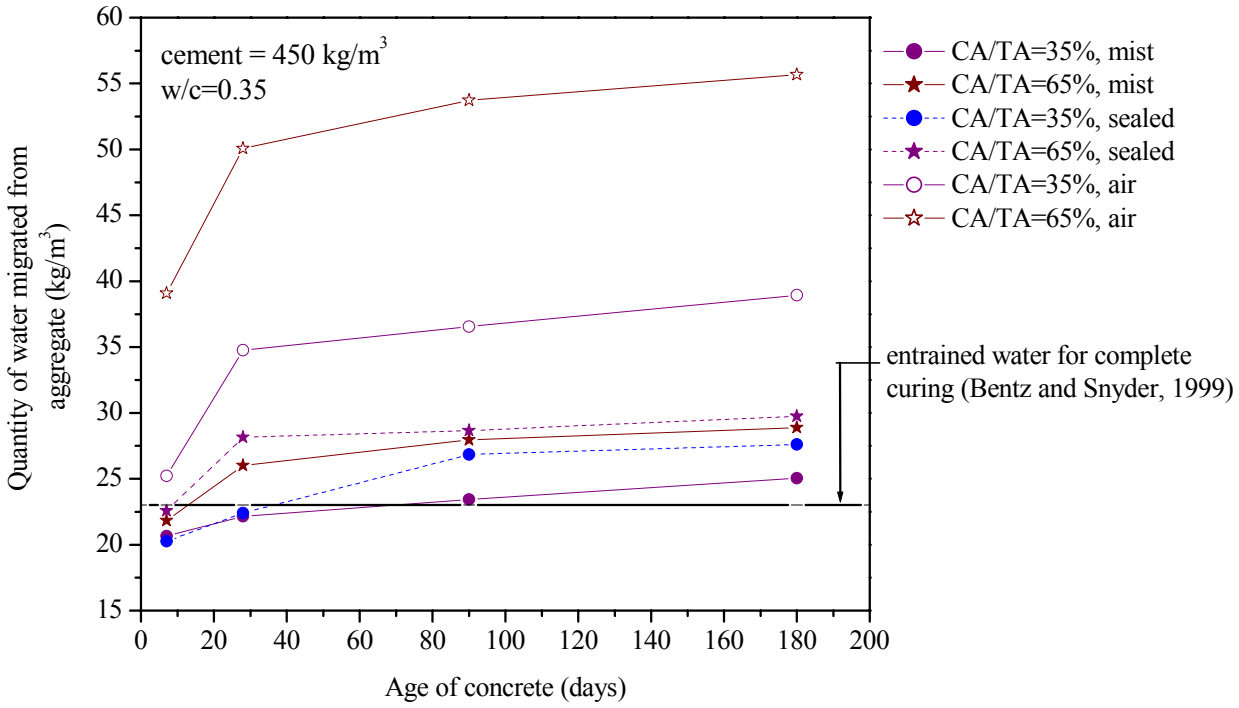


(a) cement content = 450 kg/m$^3$

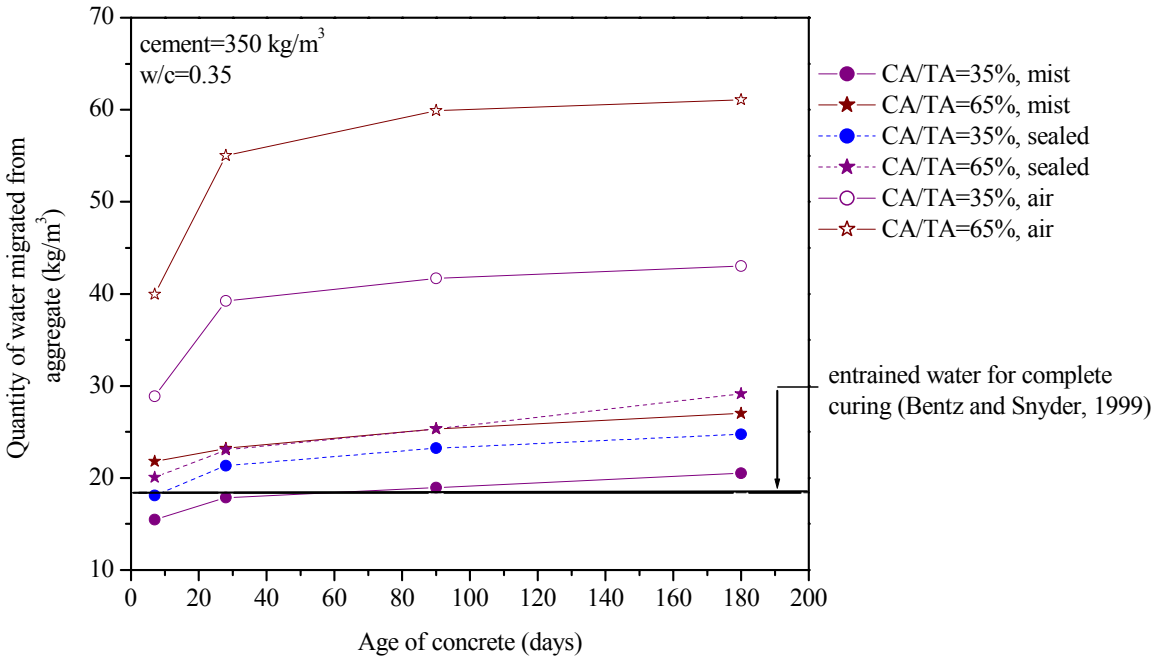


(b) cement content = 350 kg/m$^3$

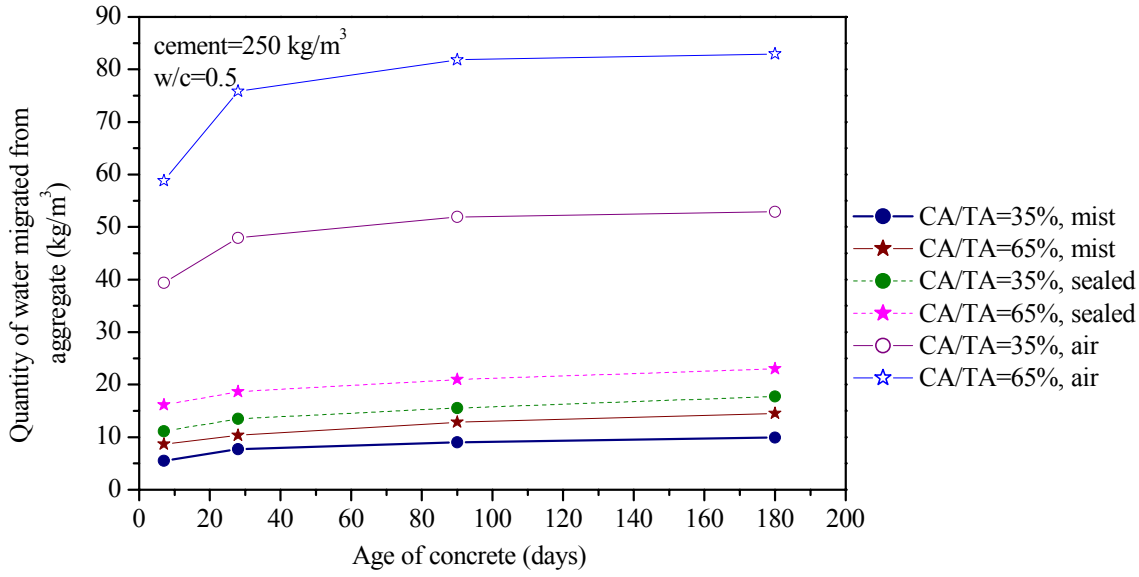


(c) cement content = 250 kg/m$^3$

Fig. 7.5 Quantity of water migrated from aggregate with age of concrete

A comparison between moisture loss from concrete (Fig. 7.4) and quantity of moisture migrated from aggregate (Fig. 7.5) from an equal volume of concrete reveals

that the moisture lost from the concrete during air curing is being compensated by the moisture migrated from aggregate, favouring conditions for autogenous curing.

### 7.4.2 Degree of hydration

#### 7.4.2.1 Non-evaporable water content

The non-evaporable water ($w_n$) in concrete with 450 kg/m$^3$ cement content subjected to different curing conditions is presented in Fig. 7.6 for a range of cold-bonded aggregate content. At a given curing period and constant aggregate content, the non-evaporable water content in concrete is almost the same under mist-cured and sealed regime, while there exists a small reduction under air-cured regime, suggesting only a marginal difference in the degree of hydration. This indicates that the variation in internal humidity between mixes under the different curing regimes is marginal, conforming to the variation in moisture transfer from aggregate (Fig.7.3). An increase in volume fraction of cold-bonded aggregate has resulted in a marginal increase in non-evaporable water content, indicating that the paste-aggregate proximity and moisture migration from 35% volume fraction of aggregate are rather adequate for compensating the reduction in internal humidity arising out of hydration and drying.

The marginal variation in the degree of hydration with cement content in Fig. 7.7 infers that the internal curing is effective even with a cement content of 450 kg/m$^3$. A comparison of non-evaporable water content with similar mix of concrete with crushed granite aggregate in Fig. 7.8 shows (i) a lower degree of hydration in all curing regimes and (ii) a higher influence of curing regimes on the degree of hydration of concrete with crushed granite aggregate than those with cold-bonded aggregate, caused by the reduction in internal humidity because of non availability of water 'reservoirs' inside the concrete.

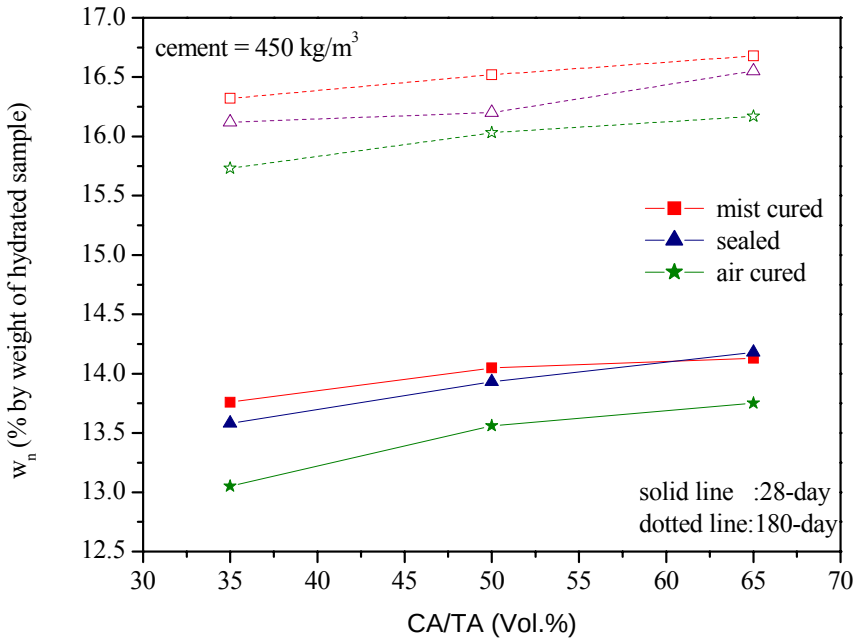


Fig. 7.6 Non-evaporable water content in concrete of different curing regimes

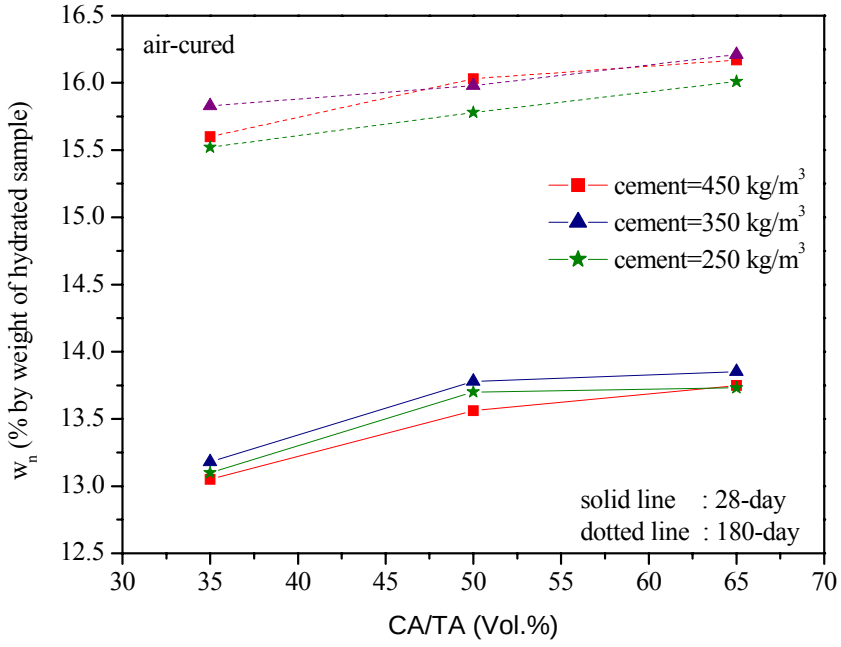


Fig. 7.7 Non-evaporable water content in concrete with different cement content

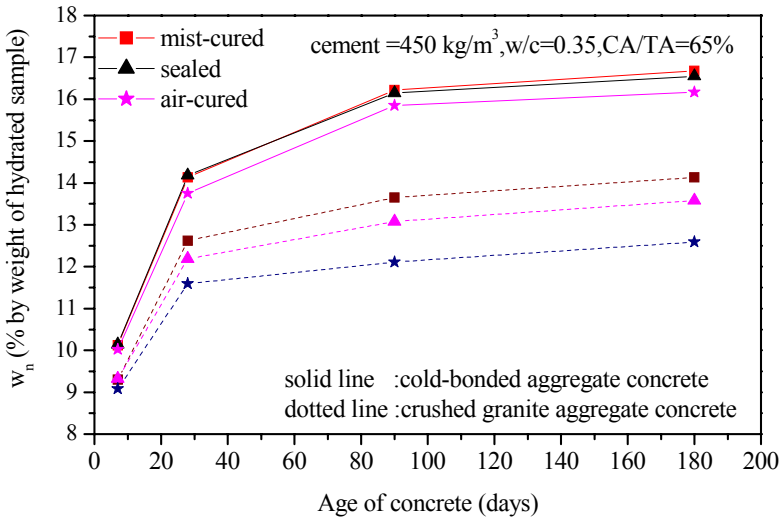


Fig. 7.8 Non-evaporable water content with age of concrete

### 7.4.2.2 Thermal gravimetric analysis

Fig. 7.9 depicts the weight loss in hydrated cement paste of air-cured samples in TGA test with an increase in temperature from 100 ºC to 1000 ºC owing to the removal of chemically bound water at various stages. The total reduction in % by weight of hydrated sample at 1000 ºC exhibits almost the same non-evaporable water content as in the furnace method (Fig. 7.6-7.8). In addition, a distinct increase in the weight loss with period of curing observed clearly indicates an increase in hydrates. Typically, the weight loss observed in TGA is divided into three parts to represent the weight loss from each of the hydration products such as C-S-H, CH, and other hydrates (Li et al., 2000; Alarcon-Ruiz et al., 2004). The weight loss between 100 ºC to 400 ºC corresponds to the loss of chemically bound water mainly from C-S-H and calcium aluminate hydrates as well as AFt and AFm. Then an abrupt weight loss near 450 ºC, associated with the dehydration of CH and the third between 700 ºC and 900 ºC, due to the decomposition of calcium carbonate and a secondary range of C-S-H dehydration. Fig. 7.9(a) shows a clear increase in weight loss due to removal of water from each of the hydration products with period of curing. For the same cement

content, a relatively higher weight loss is observed in cold-bonded aggregate concrete as compared to concrete with crushed granite aggregate. Higher weight loss in TGA indicates the formation of more hydrated products in cold-bonded aggregate concrete than in crushed granite aggregate concrete, confirming the effective utilization of moisture migrated from the aggregate for hydration. Fig. 7.9(b) demonstrates that for a given cold-bonded aggregate content, the increase in weight loss due to removal of water from each of hydrates is marginally higher in concrete with higher cement content even though the w/c ratio is less. However, the distinct increase in weight loss with period of curing represents additional hydrates and improvement in the degree of hydration, both in concrete with low and high cement contents.

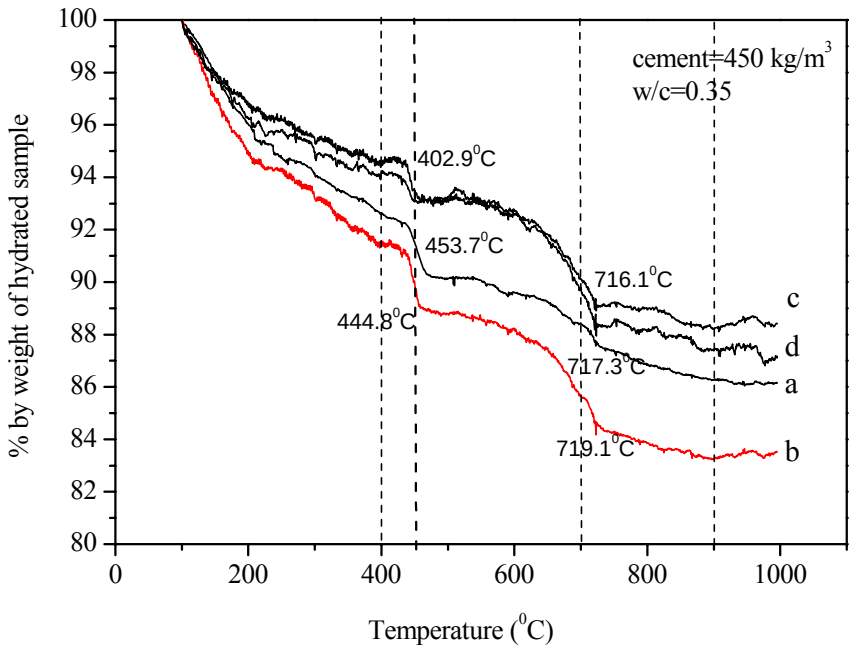


a- cold-bonded aggregate concrete (CA/TA=35%,28-day)
b- cold-bonded aggregate concrete (CA/TA=35%,180 day)
c- crushed granite aggregate concrete (28-day)
d- crushed granite aggregate concrete (180-day)

(a) Cold-bonded aggregate concrete and concrete with crushed granite aggregate

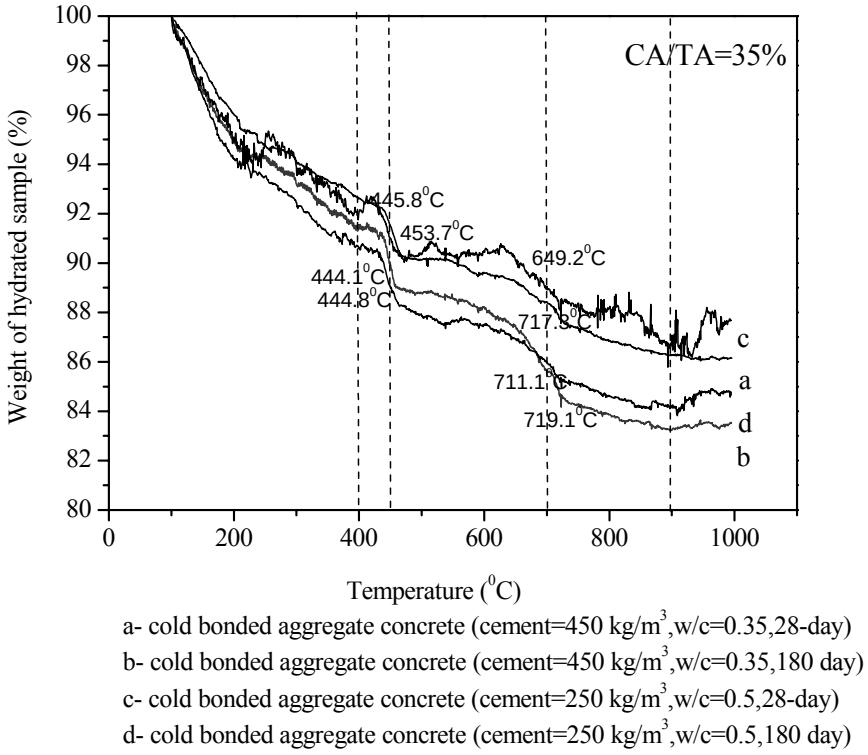


(b) Cold-bonded aggregate concrete with different cement content

Fig. 7.9 Weight loss curves of hydrated cement paste in TGA test

#### 7.4.2.3 Analysis with XRD

Crystalline phases identified in the diffractograms at each age of concrete are shown in Fig. 7.10. The relative evolution with age of the crystalline phases indicates progressive hydration for the entire period of curing. The results show qualitative difference between hydration rate of cold-bonded aggregate concrete and concrete with crushed granite aggregate. From early age onwards the peaks in the hydration products (CH and C-S-H) are highest in cold-bonded aggregate concrete (Fig. 7.10(a)) whereas relatively higher peaks can be observed in concrete with crushed granite aggregate (Fig. 7.10(c)) corresponding to $C_2S$ and $C_3S$, the unhydrated products.

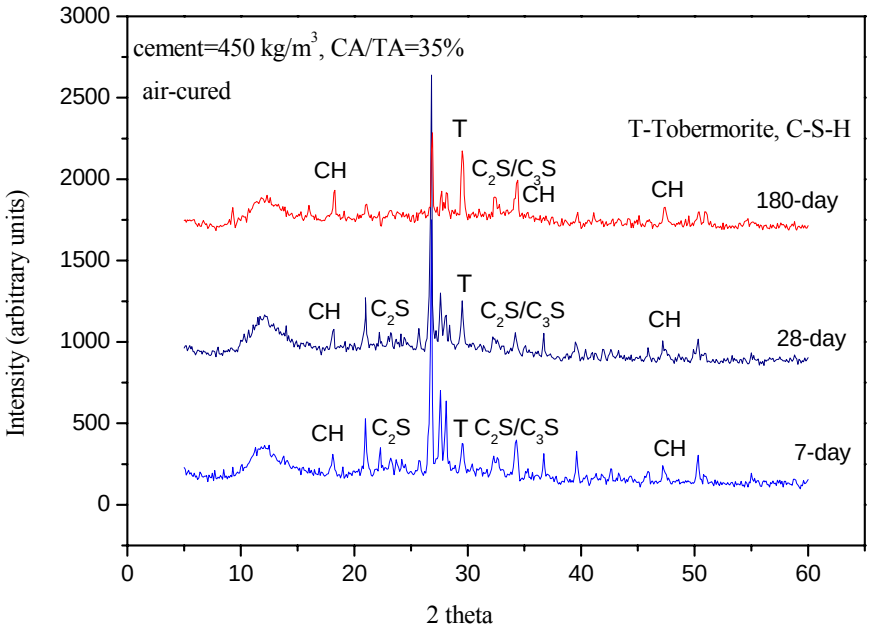


Fig. 7.10 (a) XRD pattern of cold-bonded aggregate concrete (cement = 450 kg/m$^3$)

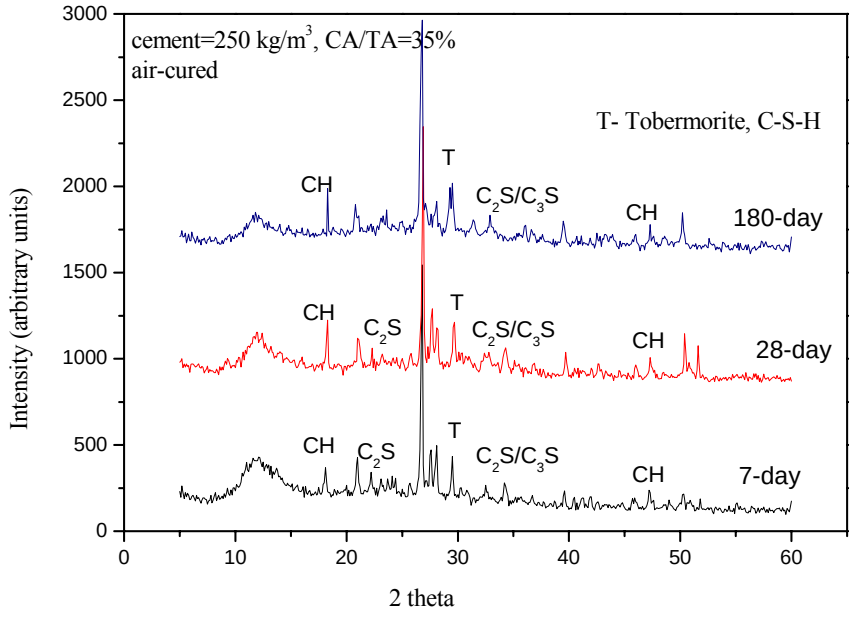


Fig. 7.10 (b) XRD pattern of cold-bonded aggregate concrete (cement = 250 kg/m$^3$)

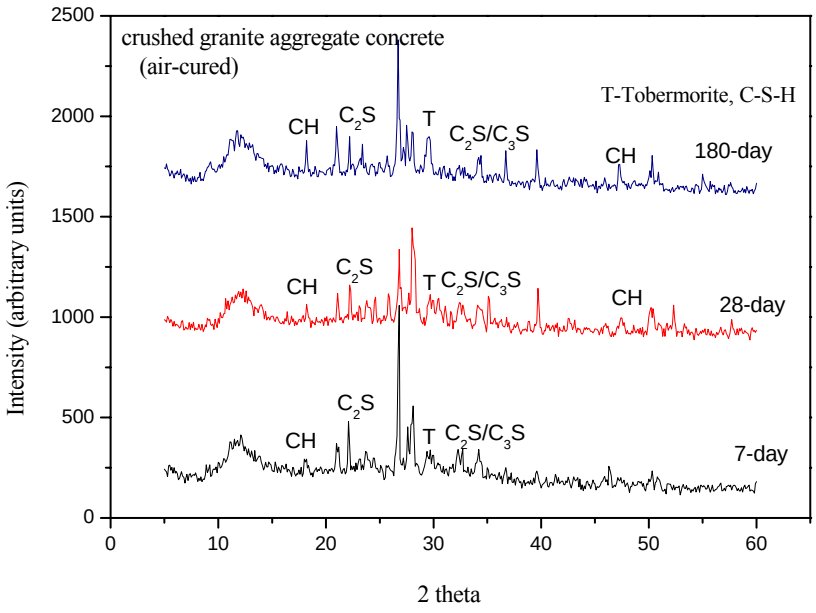


Fig. 7.10 (c) XRD pattern of concrete with crushed granite aggregate

### 7.4.3 Compressive Strength

The variation in compressive strength of cold-bonded aggregate concrete with period of curing (up to 28-days) under the three curing regimes is presented in Fig. 7.11. At 7-days, for a cement and aggregate content, the compressive strength is almost the same for concrete irrespective of the curing regimes. Also there is no appreciable reduction in strength in air-cured concrete as compared to those under other regimes, indicating that the higher moisture loss of about 60 to 75% of total loss (Fig. 7.4) in the first 7-days of exposure during air curing had not affected the compressive strength. 7-day strength varied from 71 to 82% of the 28-day strength. The higher moisture migration observed during the first 7 days (Fig. 7.1) results in a steeper strength enhancement. The 28-day strength as well shows no marked influence of curing regimes on the compressive strength. This reconfirms the observations made in 'degree of hydration' that the paste-aggregate proximity and moisture migration due to

CA/TA of 35% is adequate for the strength development of concrete under all the curing regimes.

Again, for a given curing regime, though the degree of hydration marginally increases with CA/TA ratio (Fig. 7.7), higher CA/TA leads to reduction in the strength of concrete in mixes with cement content of 350 and 450 kg/m$^3$ (Fig. 7.11(a-b)), whereas, with 250 kg/m$^3$ cement content (Fig. 7.11(c)) the strength of concrete improves with volume fraction of cold-bonded aggregate. This is due to the initiation of failure in matrix or matrix-aggregate bond in cold-bonded aggregate concrete with low cement content (<300 kg/m$^3$) and cold-bonded aggregate that governs failure in concrete with higher cement content (section 4.3.4 and 4.4.4).

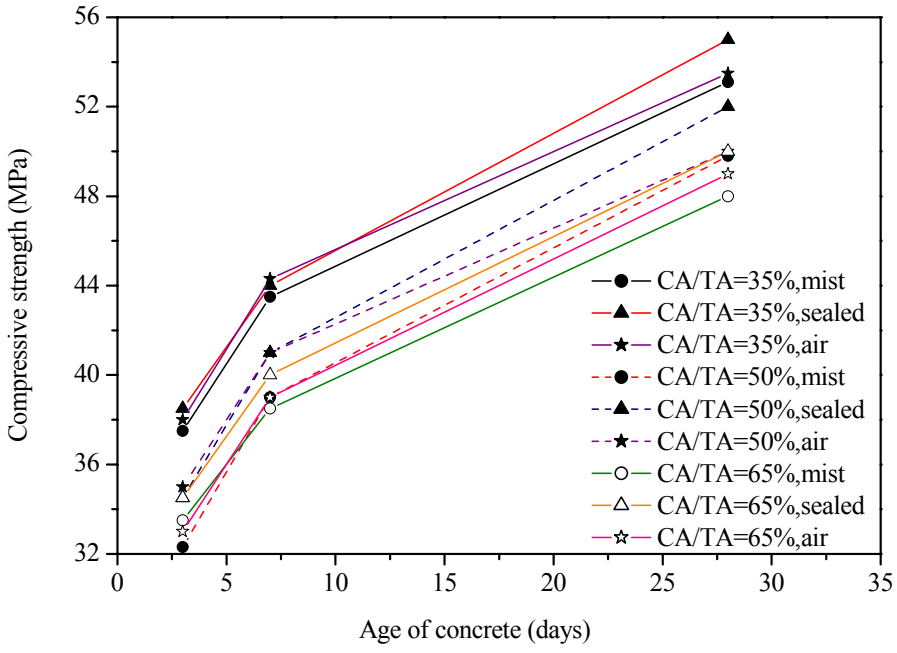


(a) cement content = 450 kg/m$^3$

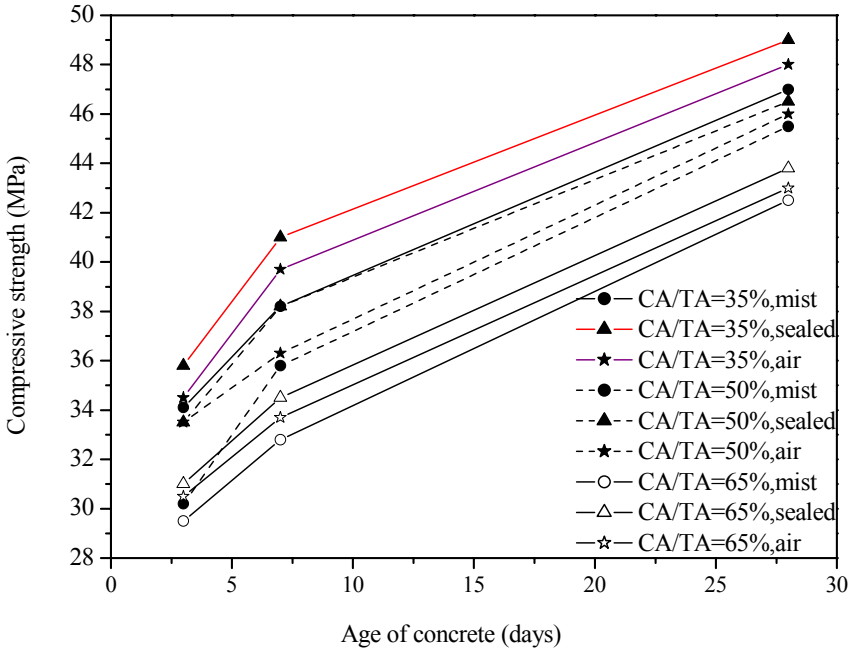


(b) cement content=350 kg/m$^3$

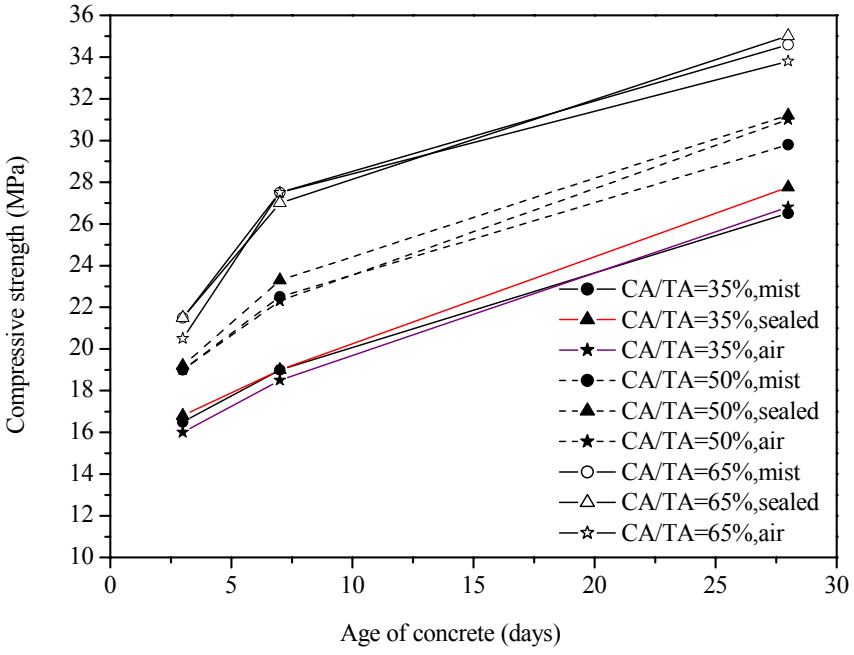


(c) cement content = 250 kg/m$^3$

Fig. 7.11 Variation in compressive strength with age (up to 28 days)

Fig. 7.12 presents 180-day strength of cold-bonded aggregate concrete cured under different curing regimes. At 180-days also, the strength of cold-bonded aggregate concrete shows no significant influence of curing regime in mixes with low and high cement content, i.e. the maximum reduction in strength of air-cured concrete is less than 5%. This is consistent with the discussion made earlier in section 7.4.2.

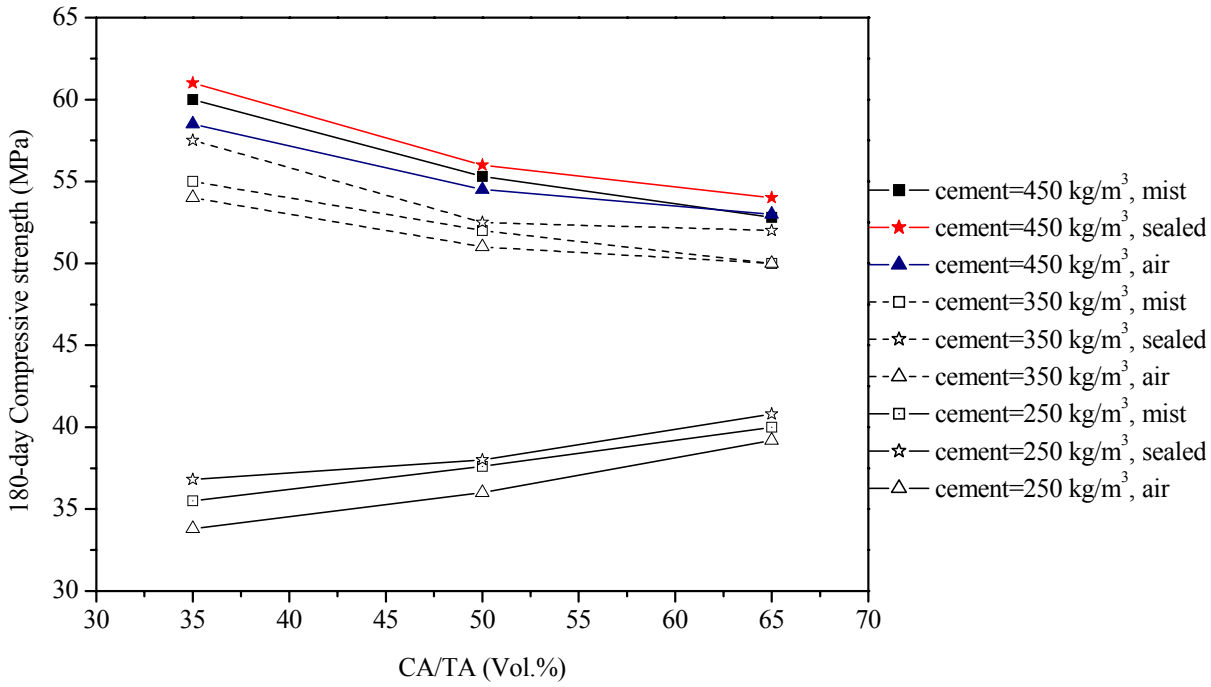


Fig. 7.12 Influence curing regimes on 180-day strength

The compressive strength of concrete with crushed granite aggregate (Fig. 7.13) exhibits a reduction in strength under both sealed and air-cured specimen as compared to mist-cured from an early age onwards and a decrease of around 10% at 180-days in air-cured concrete. The higher 180-day strength of cold-bonded aggregate concrete under sealed curing for all volume fractions of aggregate as compared to other curing regimes exhibits that the water entrained in the aggregate is sufficient for maintaining internal higher humidity for adequate curing. A marginal reduction in strength of mist-cured concrete has been attributed to the increased moisture content in concrete

at the time of testing causing a reduction in surface energy and dilation of gel particles (Bartlett and Mac Gregor, 1994).

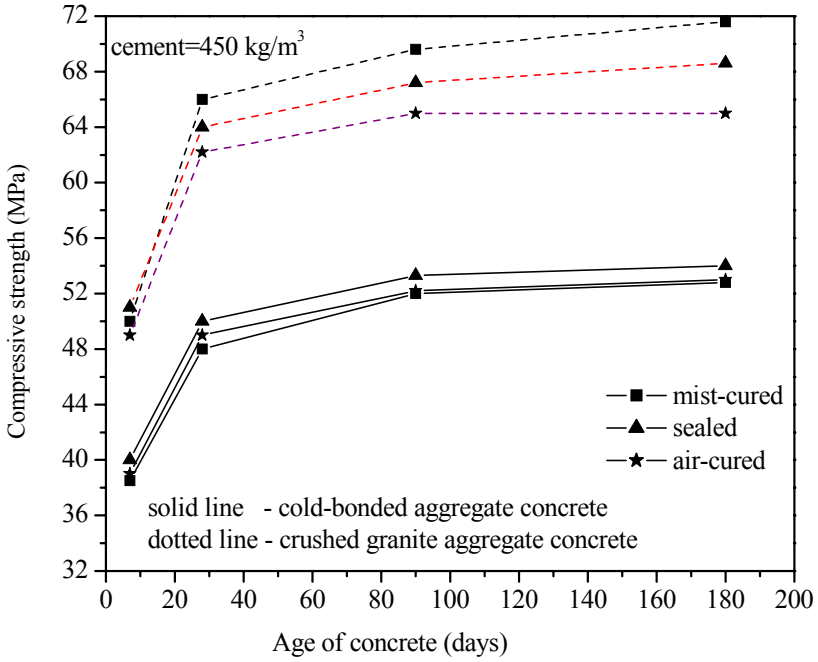


Fig. 7.13 Development of strength in concrete (up to 180-days)

### 7.4.4 Permeation Behaviour

This section presents the results of permeation behaviour studied for assessing durability of cold-bonded aggregate concrete cured under different regimes.

#### 7.4.4.1 Permeable porosity

The influence of different curing conditions on permeable porosity of concrete with a range of cement content is presented in Fig. 7.14. For a cement content and volume fraction of cold-bonded aggregate the variation in porosity between mist-cured and sealed concrete is marginal, which is similar to the behaviour observed on degree of hydration and compressive strength. However, the volume of permeable pores is

higher in air-cured concrete than under other curing regimes; this difference reduces with an increase in cement content and volume fraction of cold-bonded aggregate.

Fig. 7.14 also shows that (i) in concrete with 250 kg/m$^3$ cement content subjected to a particular curing regime, the permeable porosity decreases with an increase in CA/TA ratio and (ii) in concrete with 350 and 450 kg/m$^3$ cement contents, the permeable porosity marginally increases with an increase in CA/TA ratio (even though the paste-aggregate proximity is closer and relatively higher amount of moisture migration from aggregate to concrete with higher CA/TA ratio). The reason for such behaviour has been discussed in section 5.5.1

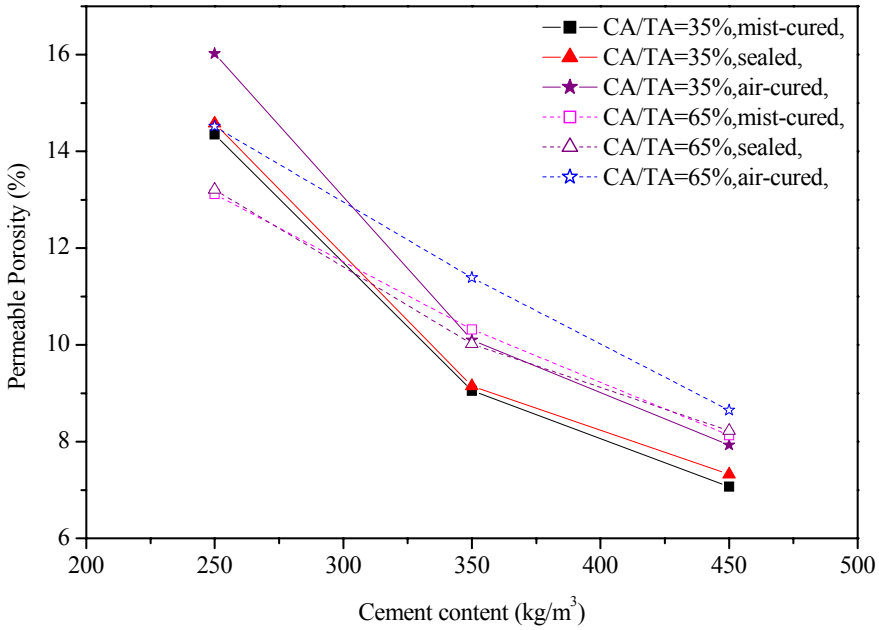


Fig. 7.14 Permeable porosity under different curing conditions (180-day)

For the same cement content, w/c ratio and CA/TA ratio, a comparison of the permeable porosities of cold-bonded aggregate concrete and concrete with crushed granite aggregate is presented in Fig. 7.15. The variation in permeable porosity due to curing conditions is more pronounced in concrete with crushed granite aggregate than in cold-bonded aggregate concrete. This variation in permeable porosity is attributed

to the variation in the degree of hydration of concrete with crushed granite aggregate exhibited under different curing regimes (Fig. 7.8).

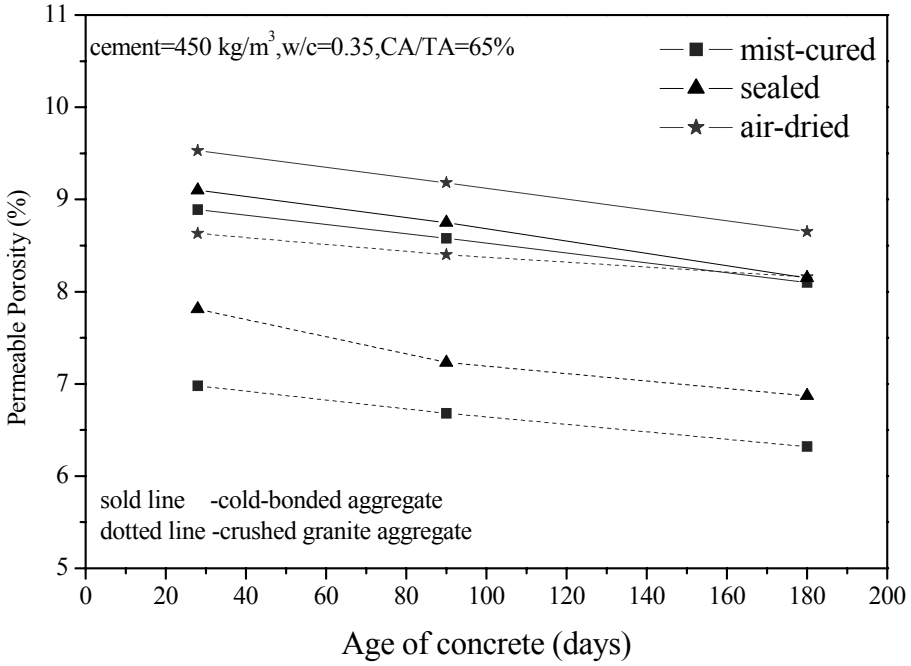


Fig. 7.15 Permeable porosity of normal concrete and cold-bonded aggregate concrete

The variation in permeable porosity of concrete with compressive strength for concretes under the three curing conditions is presented in Fig. 7.16. For the same strength level, results exhibit relatively higher permeable porosity in air-cured concrete compared to other regimes. The general observation of increased permeable porosity in air-cured concrete is possibly due to the porosity induced on the outer shell of concrete which has been continuously exposed to the atmospheric condition. The beneficial results of sealed concrete suggest that the surface porosity could be minimized by properly covering the concrete thereby avoiding loss due to evaporation.

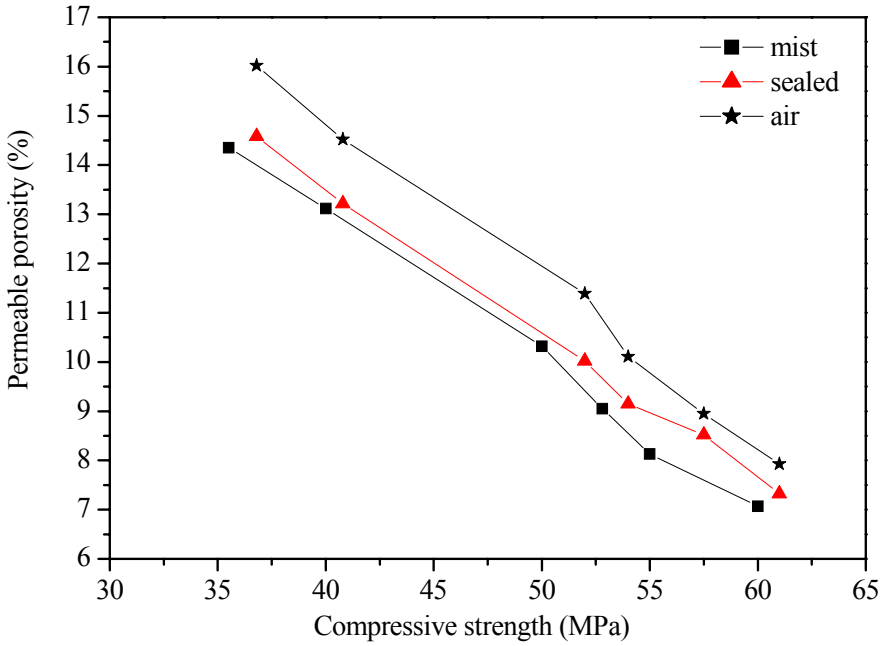


Fig. 7.16 Relation between permeable porosity and compressive strength (180-day)

### 7.4.4.2 Sorptivity

Water sorptivity of cold-bonded aggregate concrete subjected to different curing regimes is presented in Fig. 7.17 with variation in cement and cold-bonded aggregate contents. While the sorptivity of mist-cured and sealed concrete are almost the same, air-cured concrete results in higher sorptivity which corresponds well with higher permeable porosity of air-cured concrete (section 7.4.4.1). The reduced level of hydration on the surface layers of the air-cured concrete due to the rapid removal of water from the surface layers is the reason for higher sorptivity of air-cured concrete. Because of early drying off, the water released from aggregate may not be sufficient for proper curing of surface layers leading to higher porosity at the surface layers. This corroborates with Teo et al. (2007) wherein higher water permeability has been observed in laboratory air-cured lightweight concrete made with oil palm shell aggregate of 33% water absorption than that in water cured concrete.

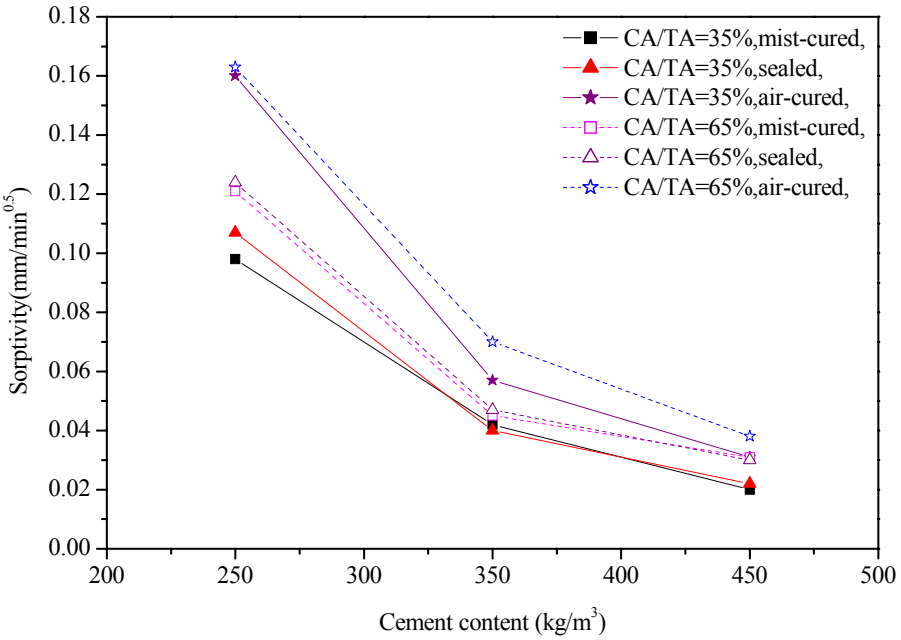


Fig. 7.17 Sorptivity of concrete under different curing conditions (180-day)

For a given aggregate content, the effect of curing on sorptivity has higher influence on concrete with 250 kg/m$^3$ cement content. This is due to the formation of continuous and interconnected capillary pores on matrix and matrix-aggregate interface due to drying and formation of less dense micro-structure in the interior of concrete as well on surface layers in concrete with lower cement content/lower strength. Dhir and Byars (1991) have also reported a substantial increase in sorptivity of air-cured normal concrete of low strength mixtures (< 30 MPa) compared to mixtures of higher design strength. However, the beneficial effect of cold-bonded aggregate can be noticed from the similar sorption behaviour of sealed concrete with that of mist-cured concrete. Companion concrete with crushed granite aggregate has shown (Fig. 7.18) 45 and 94% increase in sorptivity value from mist-cured respectively in sealed and air-cured concrete.

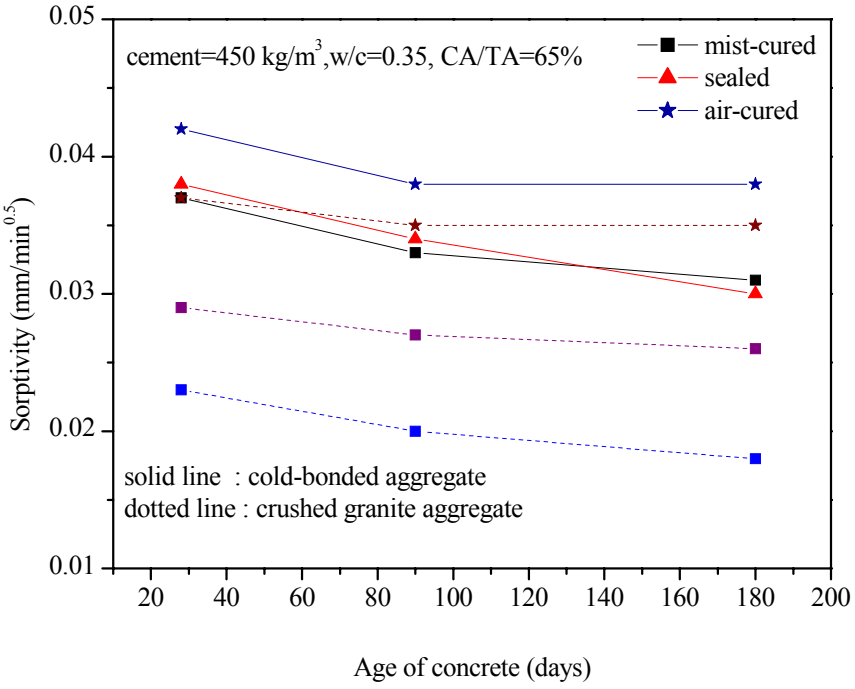


Fig. 7.18 Sorptivity of normal concrete and cold-bonded aggregate concrete

#### 7.4.4.3 Chloride penetrability

Fig. 7.19 depicts the influence of curing on resistance of concrete to chloride ion penetration. The difference between the curing methods (including air curing) is less pronounced in chloride ion penetration even though charge passed through air-cured concrete is marginally higher. Chloride penetrability of concrete in all the three curing regimes with cement content of 450 kg/m$^3$ can be categorized as 'very low' to 'low range' (ASTM C 1202, 2005). Similar to other tests, Fig. 7.20 shows relatively greater influence of curing regime on the chloride ion penetrability of concrete with crushed granite aggregate than cold-bonded aggregate caused by the variation in degree of hydration.

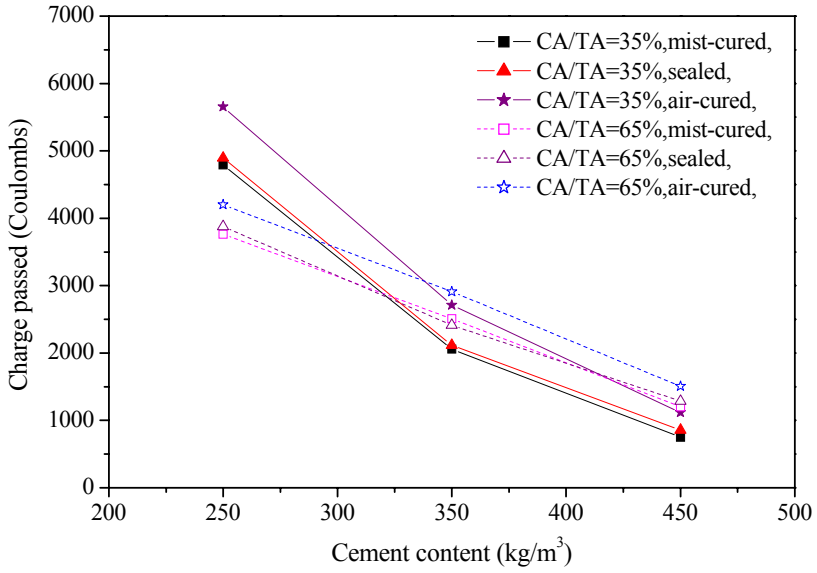


Fig. 7.19 Chloride penetrability of concrete under different curing regimes (180-day)

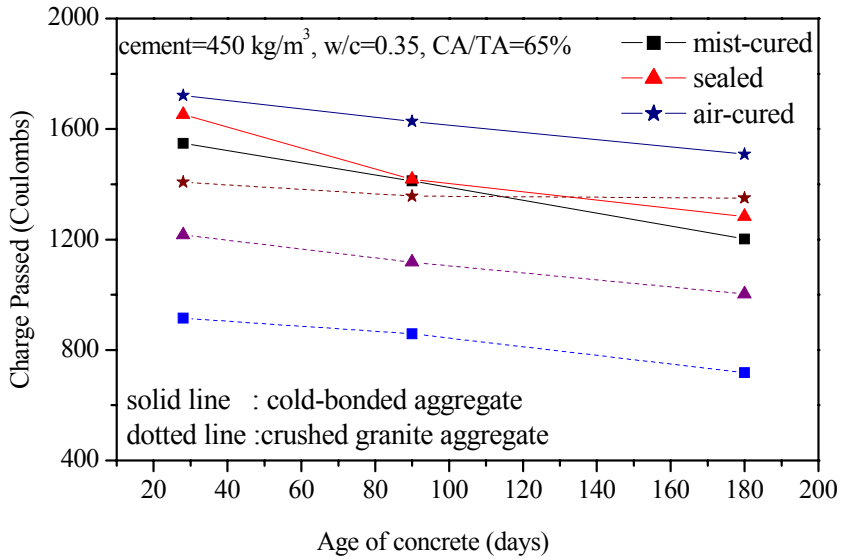


Fig. 7.20 Chloride penetrability of normal concrete and cold-bonded aggregate concrete

### 7.4.5 Autogenous Deformation

Fig. 7.21 presents the autogenous deformation in cold-bonded aggregate concrete and concrete with crushed granite aggregate. All the mixtures with cold-bonded aggregate concrete have exhibited autogenous expansion against continuous shrinkage in normal

concrete from initial stage onwards. The expansion in cold-bonded aggregate concrete is due to the expansion of cement paste, which is cured in almost saturated condition ensured by moisture migration to the matrix from cold-bonded aggregate. This behaviour is similar to the expansion of thin cement paste samples, cured under water which is reported from 1300-2200 μ strain (Neville, 2004). The amount of swelling depends on both volume fraction of aggregate and cement content in the mixture composition though the variation is less. Maximum expansion is observed in the mix with 450 kg/m$^3$ cement content and CA/TA of 65%. Closer paste-aggregate proximity and increased volume of entrained water in concrete with increase in volume fraction of aggregate are the reason for higher amount of expansion associated with higher volume fraction of aggregate.

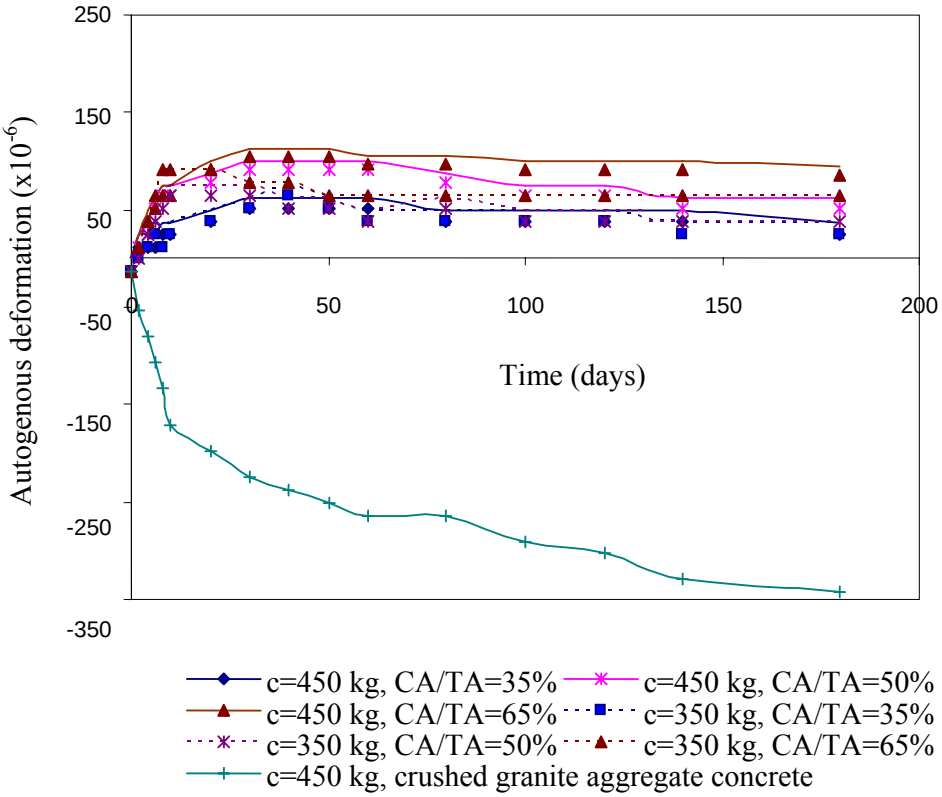


Fig. 7.21 Autogenous deformation of concrete with time

Results indicate that cold-bonded aggregate concrete is able to maintain the expansion up to 180 days though a marginal reduction is observed with time, especially in concrete with low CA/TA ratio. This indicates presence of high internal humidity in cold-bonded aggregate concrete for longer period of hydration. Similar to the observation in cold-bonded aggregate concrete, other researchers (Kohno et al., 1999; Lura et al., 2001) also reported continuous expansion (Table 7.2) for several days of measurement in concrete with lightweight aggregates having higher water absorption. Relatively low value of expansion observed in the present study as compared to the expansion (> 200 μ strain) reported by Kohno et al. (1999) with aggregate of similar water absorption can be attributed to the delay in starting the measurement in cold-bonded aggregate concrete. It has been stated that greater amount of swelling in concrete with saturated aggregate occurs within one day of casting (Kohno et al., 1999; Bentur et al., 2001; Zhutovsky et al., 2004). However from the observation in normal concrete with crushed granite aggregate, it can be concluded that cold-bonded aggregate mitigate autogeneous shrinkage of more than 300 μ strain and turns it into expansion so that self-induced tensile stress and risk of micro cracking in the concrete is fully avoided, indicating favourable condition for autogenous curing.

Table 7.2 Autogenous deformation of lightweight aggregate concrete

| Author (Year) | Binder content (kg/m3) | Water absorption of aggregate (%) | Age of concrete (days) | Autogenous deformation (μ strain) |
|---|---|---|---|---|
| Kohno et al. (1999) | 518 (w/c=0.32) | 22.3 | 100 | 200 |
| | | 4.42 | 100 | -300 |
| Bentur et al. (2001) | 493 (w/b=0.42) | 11 | 7 | 150 |
| Lura et al. (2001) | 510 (w/b=0.37) | 17 | 90 | 60 |
| Present study | 450 (w/c=0.35) | 20.46 | 180 | 37.5, 87.5, 106 |
| | 350 (w/c=0.35) | 20.46 | 180 | 37.5, 50, 87.5 |

## 7.5 SUMMARY

The influence of different curing regimes viz., mist-curing, sealed condition and air-curing on moisture migration from aggregate, degree of hydration, strength and permeation behaviour cold-bonded aggregate concrete have been studied. Significant amount of moisture transfer from aggregate in all curing regimes occurs within 28-days. Degree of hydration, compressive strength and permeation characteristics of cold-bonded aggregate concrete are observed to be less sensitive to curing condition. TGA exhibited a higher amount of hydration products in cold-bonded aggregate concrete under air-cured regime, with age as compared to air-cured concrete with crushed granite aggregate. Cold-bonded aggregate concrete has been observed to maintain autogenous expansion for longer period against continuous shrinkage in normal concrete. Beneficial results of sealed concrete suggest that efficiency of cold-bonded aggregate in supporting autogenous curing can be effectively utilized with no variation from mist-cured concrete in strength or permeation behaviour if concrete is properly covered for avoiding the evaporation loss during the initial days.

# CHAPTER 8

# CONCLUSIONS AND SCOPE FOR FURTHER WORK

## 8.1 CONCLUSIONS

The salient conclusions arising out of this research work are summarised in this section. The studies on cold-bonded aggregate concrete described here basically comes under five stages viz.; (i) influence of mix composition on workability of concrete; (ii) influence of composition on strength characteristics; (iii) permeation behaviour; (iv) influence of Class-F fly ash on the behaviour of concrete and (v) autogenous curing of concrete. The conclusions from the experimental investigations are grouped under these five sections which are applicable to the characteristics of materials used and the range of parameters investigated.

### 8.1.1 Influence of Mixture Composition on Workability

(i) Workability of concrete is influenced by both the water content and volume fraction of cold-bonded aggregate along with an interaction effect between both these factors.

(ii) For constant water content, workability of concrete improves with an increase in cold-bonded aggregate content. Hence, for a given workability, water demand can be reduced considerably by incorporating higher volume fraction of cold-bonded aggregate in the mixture proportion.

(iii) Rate of slump loss in concrete can be reduced by the use of higher volume fraction of cold-bonded aggregate in the mix.

(iv) There is no marked difference in slump or compacting factor between concrete using pre-soaked aggregate and air-dried aggregate compensated for water absorption.

### 8.1.2 Influence of Mixture Composition on Strength Characteristics

(i) Strength of concrete is mainly controlled by the initiation of failure in matrix or aggregate-matrix bond, below a cement content of 300 kg/m$^3$, whereas higher cement content predominant failure mode changes to aggregate fracture and concrete strength decreases with increase in volume fraction of aggregate.

(ii) For producing concrete of specified workability and strength up to 30 MPa, cement content in concrete can be reduced substantially by incorporating higher volume fraction of cold-bonded aggregate.

(iii) The relationship between compressive strength of concrete and its split tensile strength, flexural strength and elastic modulus are influenced by the volume fraction of cold-bonded aggregate.

(iv) There is no marked difference in compressive strength between concrete using pre-soaked aggregate and air-dried aggregate as long as water absorption is compensated by additional water during mixing.

(v) The regression models developed for workability and compressive strength can serve as typical guidelines in the design of cold-bonded aggregate concrete mixes.

(vi) Bond strength of concrete is influenced by the volume fraction of cold-bonded aggregate in the mixture proportion, both in plain and deformed bars.

### 8.1.3 Permeation Behaviour

(i) Substantial reduction in permeable porosity, water absorption, sorptivity and chloride ion penetrability of concrete with increase in cement content and/or reduction in w/c ratio suggests major influence of matrix porosity and porosity of matrix-aggregate interface on the permeation behaviour of concrete than the porosity contributed by cold-bonded aggregate**.**

(ii) The effect of cement content on microstructure of matrix and matrix-aggregate interface observed through BSEI agrees with the results of

permeation behaviour. Concrete with higher cement content is marked with a dense matrix phase and with finer and less interconnected pores at the matrix-aggregate interface, reason for significant improvement in resistance to permeation characteristics with cement content.

(iii) For a given strength, influence of cold-bonded aggregate content on permeable porosity of concrete is not significant; whereas absorption and sorptivity increases with cold- bonded aggregate content at low strength level.

(iv) Though the cold-bonded aggregates are porous, the permeation characteristic of concrete with cold-bonded aggregate concrete is only marginally higher than that of corresponding mix of normal concrete with crushed granite aggregate.

### 8.1.4 Influence of Class-F fly ash on Concrete Behaviour

(i) The workability of cold-bonded fly ash aggregate concrete increases with partial replacement of cement with fly ash, while it decreases when sand is partially replaced with fly ash.

(ii) Cement replacement levels with Class-F must to be restricted based on target strength requirement.

(iii) The 28-day strength of mixes with fly ash as replacement for sand is higher than the corresponding control mix. The strength enhancement is higher (70 %) in mixes with lower cement content (250 kg/$m^3$) and higher CA/TA ratio.

(iv) 90-day results suggest that about 30% cement can be replaced with fly ash with out much variation in its water absorption, sorptivity and chloride ion penetrability from that of the control mix. The sorption and chloride ion penetrability reduces with an increasing level of sand replacement in the mix with fly ash up to 60 to 80%. Even at 100% sand replacement level, the resistance of concrete to permeation is higher than that of the corresponding control mix.

(v) Reduction in water absorption, sorptivity and charge passed through concrete in RCPT with fly ash as replacement for sand is consistent with improvement in compressive strength. Microstructure shows improvement both in matrix and matrix-aggregate interface while replacing sand with fly ash.

(vi) Replacement of sand with fly ash in cold-bonded aggregate concrete allows high volume utilization (up to 0.6 $m^3/m^3$ of concrete) of fly ash in concrete with beneficial effect on strength, causing no detrimental effect on permeation behaviour.

### 8.1.5 Autogenous Curing

(i) Moisture migration from cold-bonded aggregate is influenced by the curing conditions, cement content and volume fraction of aggregate in the mixture composition. Significant amount of moisture transfer from aggregate in all curing regime occurs within 28-days.

(ii) Moisture migrated from aggregate is more than the minimum entrained water required for ensuring 'complete curing'.

(iii) Degree of hydration indicated by non-evaporable water content is less sensitive to curing condition and the variation in degree of hydration due to increase in cold-bonded aggregate content from 35 to 65% is marginal. TGA exhibited a higher amount of hydration products in cold-bonded aggregate concrete with age as compared to concrete with crushed granite aggregate.

(iv) Influence of curing condition on the compressive strength of cold-bonded aggregate concrete is marginal and maximum reduction in 180-day strength of air-cured cold-bonded aggregate concrete in a warm humid climate compared to mist-cured is less than 5%.

(v) While permeation behaviour of sealed and mist-cured concrete is almost same, air-cured concrete shows marginal increase in permeation parameters.

(vi) Cold-bonded aggregate concrete maintains autogenous expansion up to 180 days of measurement without self desiccation.

(vii) Efficiency of cold-bonded aggregate in supporting autogenous curing can be effectively utilised with no variation from mist-cured concrete in strength or permeation characteristics if concrete is properly covered during the initial days for avoiding the evaporation loss.

(viii) Unlike cold-bonded aggregate concrete, the curing condition has significant influence on degree of hydration, compressive strength and permeation of crushed granite aggregate concrete.

## 8.2 SCOPE FOR FURTHER WORK

This study forms an initial part in the ensuing long-term investigations on cold-bonded fly ash aggregate concrete. The areas on which continued research can be undertaken to provide better understanding of the material and thus be of more use to the construction industry are:

(i) Investigations on shrinkage and creep of cold-bonded aggregate concrete

(ii) Investigations on long term durability of cold-bonded aggregate concrete.

(iii) Studies on functional characteristics of cold-bonded aggregate concrete.

(iv) Studies on fiber reinforced cold-bonded aggregate concrete.

(v) Methods of enhancing strength of cold-bonded aggregate and its influence on the properties of concrete.

# APPENDIX I

## Paste-aggregate Proximity

Analytical equation proposed by Snyder (1998) for air entrained concrete and later on for paste-aggregate proximity (Bentz and Snyder, 1999) based on the nearest surface distribution functions for poly-dispersed particles allows the estimation of paste volume fractions with in a certain distance from the cold-bonded aggregate surface directly from the aggregate particle size distribution, the aggregate being simulated as spheres.

The paste-aggregate proximity calculation requires the following defined quantities

n : number of cold-bonded aggregates per volume

$V_a$ : volume fraction of cold-bonded aggregates in total volume of concrete

$V_m$ : paste/matrix volume fraction

A : specific surface area of aggregate

r : aggregate radii

$f$(r) : probability density function of aggregate radius

$\langle R^k \rangle$ : expected value of $R^k$ for the radius distribution

$s$ : spacing distribution parameter

For the paste-aggregate system considered here, these quantities can also be defined analytically by the following equations

$$V_a = \frac{4}{3} \prod n \langle R^3 \rangle$$

$$V_m = 1 - V_a$$

$$A = \frac{4 \prod n \langle R^2 \rangle}{\frac{4}{3} \prod n \langle R^3 \rangle}$$

$$\langle R^K \rangle = \int_0^\infty r^k f(r) dr$$

Also, the results requires the terms given below

$$\xi_k = \frac{\prod}{3} n 2^{k-1} \left\langle R^k \right\rangle$$

$$c = \frac{4\left\langle R^2 \right\rangle}{1 - V_a}$$

$$d = \frac{4\left\langle R \right\rangle}{1 - V_a} + \frac{12\xi_2}{(1-\xi_3)^2} \left\langle R^2 \right\rangle$$

$$g = \frac{4}{3(1-V_a)} + \frac{8\xi_2}{(1-V_a)^2} \left\langle R \right\rangle + \frac{16}{3} \frac{B\xi_2^{\,2}}{(1-V_a)^3} \left\langle R^3 \right\rangle$$

The value of *B* depends upon the exact way the system is constructed. For the calculations performed here, *B*=0. If $e_a(s)$ represents the probability of a random point not being with in a distance *s* of cold-bonded aggregate surface, the probability of finding the nearest aggregate surface within a distance *s* of a randomly chosen point is the compliment of the aggregate exclusion probability.

$E_a{}'(s) = 1 - e_a(s)$, where

$$e_a(s) = 1 - \frac{4\prod}{3} n \left\langle (s+r)^3 \Theta(s+r) \right\rangle \qquad \text{when } s < 0$$

$$= (1 - V_a) \exp\left[ - \prod n (cs + ds^2 + gs^3) \right] \qquad \text{when } s > 0, \qquad \text{with } s < 0$$

corresponding to a sphere with radius (-*s*) being entirely inside an aggregate.

Hence, the probability of finding the nearest aggregate surface a distance s from a random point in the paste portion is

$E_a(s) = \dfrac{E_a{}'(s>0) - V_a}{1 - V_a}$, after substituting the value for $E_a{}'$

$$= 1 - \exp[-\prod n(cs + ds^2 + gs^3)]$$

The above equation also gives the fraction of matrix/paste volume within a distance *s* of an aggregate surface, which is equivalent to the paste-aggregate proximity cumulative distribution function (CDF).

# REFERENCES


1. **ACI Committee 211.2** (1990) Standard practice for selecting proportions for structural lightweight concrete. *ACI Materials Journal*, **87**, 638-651.

2. **Aictin, P.C. and P.K. Mehta** (1990) Effect of coarse aggregate characteristics on mechanical properties of high strength concrete. *ACI Materials Journal*, **87** , 103-107

3. **Al- Khaiat, H. and M.N. Haque** (1998) Effect of initial curing on early strength and physical properties of lightweight concrete. *Cement and Concrete Research*, **28**, 859-866.

4. **Alarcon-Ruiz, L., G. Platret, E. Massieu, and A. Ehrlacher** (2005) The use of thermal analysis in assessing the effect of temperature on a cement paste. *Cement and Concrete Research*, **35**, 609-613.

5. **Arnaouti, C. and S.R. Sangakkara** (1984) Creep and Shrinkage in a lightweight aggregate concrete. *Magazine of Concrete Research*, **36**, 165-173.

6. **ASTM C 109** (2002) Standard test method for compressive strength of hydraulic cement mortars (using 2-in or [50mm] cube specimens). *American Society of Testing and Materials*, United States.

7. **ASTM C 1202** (2005) Standard test method for electrical indication of concrete's ability to resist chloride ion penetration. *American Society of Testing and Materials*, United States.

8. **ASTM C 127** (2004) Standard test method for density, relative density (specific gravity) and absorption of coarse aggregates. American Society of Testing and Materials, United States.

9. **ASTM C 157** (2004) Standard test method for length change of hardened hydraulic-cement mortar and concrete. *American Society of Testing and Materials*, United States.

10. **ASTM C 29/ 29 M** (2003) Test Method for bulk density ("unit weight") and voids in aggregate. *American Society of Testing and Materials*, United States.

11. **ASTM C 330** (2005) Standard specification for lightweight aggregates for structural concrete. *American Society of Testing and Materials*, United States.

12. **ASTM C 469** (2002) Standard test method for static modulus of elasticity and poisson's ratio of concrete in compression. *American Society of Testing and Materials*, United States.

13. **ASTM C 496/C 496M** (2004) Standard test method for splitting tensile strength of cylindrical concrete specimens. *American Society of Testing and Materials*, United States.

14. **ASTM C 567** (2005) Standard test method for determining density of structural lightweight concrete. *American Society of Testing and Materials*, United States.

15. **ASTM C 618** (2005) Standard specification for coal fly ash and raw or calcined natural pozzolan for use in concrete. *American Society of Testing and Materials*, United States.

16. **ASTM C 642** (1997) Standard test method for density, absorption, and voids in hardened concrete. *American Society of Testing and Materials*, United States.

17. **ASTM C 78** (2002) Standard test method for flexural strength of concrete (Using simple beam with third point loading). *American Society of Testing and Materials*, United States.

18. **ASTM E 122** (2000) Standard practice for calculating sample size to estimate, with a specified tolerable error, the average for characteristic of a lot or process. *American Society of Testing and Materials*, United States.

19. **Babu, K.G. and D.S. Babu** (2003) Behaviour of lightweight expanded polystyrene concrete containing silica fume. *Cement and Concrete Research* **33**, 755-762.

20. **Bai Y, R. Ibrahim and P.A.M. Basheer** (2004) Properties of lightweight concrete manufactured with fly ash, furnace bottom ash and Lytag. Proceedings of *International workshop on Sustainable Development and Concrete Technology*, China, May 20-21, 77-87.

21. **Bai, J., S. Wild and B.B. Sabir** (2002) Sorptivity and strength of air-cured and water-cured PC–PFA–MK concrete and the influence of binder composition on carbonation depth. *Cement and Concrete Research*, **32,** 1813-1821.

22. **Balendran, R.V., F.P. Zhou, A. Nadeem and A.Y.T Leung** (2002) Influence of steel fibres on strength and ductility of normal and lightweight high strength concrete. *Building and Environment*, **37**, 1361-1367.

23. **Bartlett, F.M. and J.G. MacGregor** (1994) Effect of moisture condition on concrete core strengths. *ACI Materials Journal*, **91**, 227-236.

24. **Batis, G., N. Kouloumbi and A. Katsiamboulas** (1996) Durability of Reinforced lightweight Mortars with Corrosion Inhibitors. *Cement, Concrete and Aggregates*, **18**, 118-125.

25. **Baykal, G. and A.G. Doven** (2000) Utilization of fly ash by pelletization process; theory, application areas and research results. *Resources, Conservation and Recycling*, **30**, 59-77.

26. **Bentur, A., S. Igarashi and K. Kovler** (2001) Prevention of autogenous shrinkage in high-strength concrete by internal curing using wet lightweight aggregates**.** *Cement and Concrete Research*, **31**, 1587-1591.

27. **Bentz, D.P. and K.A. Snyder** (1999) Protected paste volume in concrete: Extension to internal curing using saturated lightweight fine aggregate. *Cement and Concrete Research*, **29**, 1863-1867.

28. **Bijen, J.M.J.M.** (1986) Manufacturing processes of artificial lightweight aggregates from fly ash. *The international journal of Cement Composites and Lightweight Concrete*, **8**, 191-199.

29. **Bilodeau, A., R. Cheriver and V. M. Malhotra** (1995) Mechanical properties, durability and fire resistance of high strength lightweight concrete. Proceedings of *International Symposium on Structural Lightweight Aggregate Concrete*, Norway, 591-603.

30. **Bilodeau, A., V. Sivasundaram, K.E. Painter and V.M Malhotra** (1994) Durability of concrete incorporating high volumes of fly ash from sources in the U.S. *ACI Materials Journal*, **91**, 3-12.

31. **Bilodeau, A., V.K.R. Kodur and G.C. Hoff** (2004) Optimization of the type and amount of polypropylene fibres for preventing the spalling of lightweight concrete subjected to hydrocarbon fire. *Cement and Concrete Composites*, **24**, 163-174.

32. **Bremner, T.W. and T.A. Holm** (1986) Elastic compatibility and the behaviour of concrete. *ACI Materials Journal*, **83**, 244-250.

33. **BS 812 Part: 110** (1990) Methods of determination of aggregate crushing value. British Standard Institution, London.

34. **Campione, G., C. Cucchiara, L. La Mendola and M. Papia** (2005) Steel–concrete bond in lightweight fiber reinforced concrete under monotonic and cyclic actions. *Engineering Structures*, **27,** 881-890.

35. **Carlsson, J.E.** (2000) The influence of curing condition on the chloride diffusion in lightweight aggregate concrete. Proceedings of *International Symposium on Structural Lightweight Aggregate Concrete*, Norway, June, 866-873.

36. **Chandra, S. and L. Berntsson** *Lightweight aggregate concrete; science, technology and applications*. Standard Publishers Distributors, India, 2004.

37. **Chandra, S., L. Berntsson and Y. Anderberg** (1980) Some effects of polymer addition on the fire resistance of concrete. *Cement and Concrete Research*, **10,** 367-375.

38. **Chang, T. and M.M Shieh** (1996) Fracture Properties of lightweight concrete. *Cement and Concrete Research*, **26**, 181-188.

39. **Cheeseman, C. R., A. Makinde and S. Bethanis** (2005) Properties of lightweight aggregate produced by rapid sintering of incinerator bottom ash. *R*esources *Conservation and Recycling*, **43**, 147-162.

40. **Chen, B. and J. Liu** (2008) Experimental application of mineral admixtures in lightweight concrete with high strength and workability. *Construction and Building Materials,* **22**, 655-659.

41. **Chi, J.M., R. Huang, C.C. Yang and J.J. Chang** (2003) Effect of aggregate properties on the strength and stiffness of lightweight concrete**.** *Cement & Concrete Composites,* **25**,197-205.

42. **Chia, K.S. and M.H. Zhang** (2002), Water permeability and chloride penetrability of high strength lightweight aggregate concrete. *Cement and Concrete Research*, **32**, 639-645.

43. **Chia, K.S., C.C. Kho and M.H. Zhang** (2005) Stability of fresh lightweight aggregate under vibration. *ACI Materials Journal*, **102**, 347-354.

44. **CIB** (1999) Agenda 21 on Sustainable Construction. *International council for Research and Innovation in Building and Construction CIB Report Publication 237,* The Netherlands.

45. **Clarke, J.L.** *Structural Lightweight aggregate concrete*, Blackie Academic and professional, 1993.

46. **Curico, F., D. Galeota, A. Gallo and M.M Giammatteo** (1998) High performance lightweight concrete for the precast prestressed concrete industry. *Recent Advance in Concrete Technolog*y, SP 179-24, 389-404.

47. **Demirboga, R. and R. Gul** (2003) Thermal conductivity and compressive strength of expanded perlite aggregate concrete with mineral admixtures. *Energy and Buildings,* **35**, 1155-1159.

48. **Demirboga, R., I. Orung and R. Gul** (2001) Effects of expanded perlite aggregate and mineral admixtures on the compressive strength of low density concretes. *Cement and Concrete Research*, **31**, 1627 –1632.

49. **Demirdag, S. and L. Gunduz** (2008) Strength properties of volcanic slag aggregate lightweight concrete for high performance masonry units. *Construction and Building Materials*, **22**, 135-142.

50. **Dhir, K.R., and E.A. Byars** (1991) PFA concrete: Near Surface absorption properties. *Magazine of Concrete Research*, **43**, 219-232.

51. **Dhir, K.R., G.C. Mays and H.C. Chua** (1984) Lightweight structural concrete with algite aggregate: Mix design and properties. *The International Journal of Cement Composites and Lightweight Concrete*, **6**, 249-260.

52. **Dias, W.P.S.** (2004) Influence of drying on concrete sorptivity. *Magazine of Concrete Research,* **56,** 537-543.

53. **El-Dieb, A.S.** (2007) Self curing concrete: water retention, hydration and moisture transport. *Construction and Building materials*, **21**, 1282-1287.

54. **FIP** Manual of lightweight aggregate concrete (1983) Surrey University Press, Glasgo and London.

55. **Fly ash Mission India,** http://www.tifac.org.in (visited on 1/8/2006)

56. **Fujiki, E., K. Kokubu, T. Hosaka, T. Umehara and N. Takaha** (1998) Freezing and Thawing Resistance of Lightweight Aggregate Concrete. Proceedings of *fourth CANMET/ACI/JCI International Conference on Recent Advances in concrete technology* , Japan, SP 179- 47, 791-814.

57. **Gao, J., W. Sun and K. Morino** (1997) Mechanical properties of steel fiber-reinforced high strength lightweight concrete. *Cement and Concrete Composites*, **19**, 307- 313.

58. **Gao, X.F., Y.T. Lo and C.M. Tam** (2002) Investigation of micro-cracks and micro structure of high performance lightweight aggregate concrete. *Building and environment*, **37**, 485-489.

59. **Gesoglu, M., T. Ozturan and E. Guneyisi** (2004) Shrinkage cracking of lightweight concrete made with cold-bonded fly ash aggregates. *Cement and Concrete Research*, **34**, 1121 –1130.

60. **Gesoglu, M., T. Ozturan and E. Guneyisi** (2006) Effects of cold bonded fly ash aggregate properties on the shrinkage cracking of lightweight concretes. *Cement and Concrete Composites*, **28**, 598-605.

61. **Gesoglu, M., T. Ozturan and E. Guneyisi** (2007) Effects of fly ash properties on characteristics of cold bonded fly ash lightweight aggregates. *Construction and Building Materials*, **21**, 1869-1878.

62. **Gjorv, O.E., K. Tan and P.J.M. Monteiro** (1994) Effect of elevated curing temperature on the chloride permeability of high strength lightweight concrete. *Cement Concrete and Aggregates*, **16**, 57-62.

63. **Gopalan M.K and M.N. Haque** (1989) Mix design for optimal strength development of fly ash concrete, *Cement and Concrete Research***, 19,** 634-641**.**

64. **Gopalan M.K**. (1996) Sorptivity of fly ash concretes. *Cement and Concrete Research*, **26**, 1189-1197.

65. **Grubl** (1979) Mix design of lightweight aggregate concrete for structural purpose. *The International Journal of Lightweight concrete*, **1**, 63-69.

66. **Gunduz, L. and I. Ugur** (2005) The effects of different fine and coarse pumice aggregate/cement ratios on the structural concrete properties without using any admixtures. *Cement and Concrete Research*, **35,** 1859-1864.

67. **Hall, C.** (1989) Water sorptivity of mortars and concretes: a review. *Magazine of Concrete Research*, **41**,147, 51-61.

68. **Hall, C. and M.H.R. Yau** (1987) Water movement in porous building materials-IX. The water absorption and sorptivity of concretes. *Building and Environment*, **80**, 77-78.

69. **Haque, M.N.** (1996) Strength development and drying shrinkage of high-strength concretes. *Cement and Concrete Composites*, **18**, 333-342.

70. **Haque, M.N., H. Al-Khaiat, O. Kayali** (2004) Strength and durability of lightweight concrete. *Cement and Concrete Composites*, **26**, 307-314.

71. **Harikrishnan, K. I. and K. Ramamurthy** (2006) Influence of pelletization process on the properties of fly ash aggregates. *Waste Management*, **26**, 846-852.

72. **Harikrishnan, K.I. and K. Ramamurthy** (2004) Study of parameters influencing the properties of sintered fly ash aggregates. *Journal of Solid Waste Technology and Management*, **30**, 136-142.

73. **Holm, T.A.** (1994) Lightweight concrete and aggregates. *Standard Technical Publication 169 C, American Society for Testing Materials*, 522-531.

74. **Holm, T.A., O.S. Ooi and T.W. Bremner** (2004) Moisture dynamics in lightweight aggregate and concrete. Expanded Shale, Clay and Slate Institute, Publication # 9340.

75. **Hossain, K.M.A.** (2004) Properties of volcanic pumice based cement and lightweight concrete**.** *Cement and Concrete Research*, **34,** 283-291.

76. **Hwang**, **K., T. Noguchi and F. Tomosawa (2004)** Prediction model of compressive strength development of fly-ash concrete. *Cement and Concrete Research***, 34,** 269-276**.**

77. **Ichinose, T., Y. Kanayama, Y. Inoue and J.E. Bolander** (2004) Size effect on bond strength of deformed bars. *Construction and Building Materials*, **18**, 549-558.

78. **IS 1199** (2004) Methods of sampling and analysis of concrete. *Bureau of Indian Standards*, New Delhi, India.

79. **IS 12269** (2004) Specification for 53 grade ordinary Portland cement. *Bureau of Indian Standards*, New Delhi, India.

80. **IS 2386**: Part IV (2002) Methods of test for aggregates for concrete. *Bureau of Indian Standards*, New Delhi, India.

81. **IS 2770**: Part I (2002) Methods of testing bond in reinforced concrete Part 1 Pull-out test. *Bureau of Indian Standards*, New Delhi, India.

82. **IS 383** (2002) Specification for coarse and fine aggregates from natural sources for concrete. *Bureau of Indian Standards*, New Delhi, India.

83. **IS 456** (2000) Plain and reinforced concrete-code of practice. *Bureau of Indian Standards*, New Delhi, India.

84. **IS 516** (2004) Methods of test for strength of concrete. *Bureau of Indian Standards*, New Delhi, India.

85. **Jamal, A., A. Khalid, M.N. Haque and E. Khalid (1999)** Lightweight concrete in hot coastal areas. *Cement and Concrete Composites*, **21**, 453-458.

86. **Jaroslav, S. and Z. Ruzickova** *Pelletisation of Fines*. Elsevier Science Publishing Company, INC, New York, 1988.

87. **Jau, W-Chen and G.G. Wu** (1995) Performance of lightweight concrete panels subjected to fire. Proceedings of *CEB/FIP International symposium on Structural Lightweight aggregate concrete*, Sandefjord, Norway, 180-191.

88. **Johnston, C.D. and V.M. Malhotra** (1987) High-strength semi-lightweight concrete with up to 50% Fly ash by Weight of Cement. *Cement, Concrete and Aggregate,* **l9**, 101-112.

89. **Kayali, O and B. Zhu** (2005) Chloride induced reinforcement corrosion in lightweight aggregate high-strength fly ash concrete, *Construction and Building Materials,* **19,** 327-336.

90. **Kayali, O., M.N. Haque and B. Zhu** (1999) Drying shrinkage of fibre-reinforced lightweight aggregate concrete containing fly ash. *Cement and Concrete Research*, **29**, 1835-1840

91. **Kayali, O., M.N. Haque and B. Zhu** (2003) Some characteristics of high strength fiber reinforced lightweight aggregate concrete. *Cement and Concrete Composites*, **25**, 207-213.

92. **Khayat, K. H**. (1991) Deterioration of Lightweight Fly Ash Concrete due to Gradual Cryogenic Frost Cycles. *ACI Materials Journal,* **88**, 233-239.

93. **Kimura, S., K. Kimura, H. Kamiya and M. Horio** (2004) A novel fludized bed process to produce fine-grade artificial lightweight aggregates. *Powder Technology*, **146**, 111-120.

94. **Kohno, K., T. Okamoto, Y. Isikawa, T. Sibata and H. Mori** (1999) Effects of artifical aggregate on autogenous shrinkage of concrete. *Cement and Concrete Research*, 29, 611-614.

95. **Kovler, K., A. Bentur and S. Zhutovsky** (2002) Efficiency of lightweight aggregates for internal curing of high strength concrete to eliminate autogenous shrinkage. *Materials and Structures*, **34**, 97-101

96. **Kovler, K., A. Souslikov and A. Bentur (2004**) Pre-soaked lightweight aggregates as additives for internal curing of high-strength concretes. *Cement, Concrete and Aggregates*, **26(2)**, paper ID CCA 12295.

97. **Langley, W.S, G.G. Carette and V.M. Malhotra** (1989) Structural concrete incorporating high volumes of ASTM Class F Fly Ash. *ACI Materials Journal,* **86**, 507-514.

98. **Li, D., J. Shen, Y. Chen, L. Cheng and X. Wu** (2000) Study of properties of fly ash- slag complex cement. *Cement and Concrete Research*, **30**, 1381-1387.

99. **Lo, T.Y. and H.Z. Cui** (2004) Effect of porous lightweight aggregate on strength of concrete. *Materials Letters*, **58**, 916-919.

100. **Lo, T.Y., H.Z. Cui, A. Nadeem and Z.G. Li** (2006) The effects of air content on permeability of lightweight concrete. *Cement and Concrete Research*, **36**, 1874-1878.

101. **Lo, Y., X.F. Gao and A.P. Jeary** (1999) Microstructure of pre-wetted aggregate on lightweight concrete. *Building and Environment*, **34**, 759-764.

102. **Lo,T.Y., H.Z. Cui and Z.G. Li** (2004) Influence of aggregate pre-wetting and fly ash on mechanical properties of lightweight concrete. *Waste Management*, **24**, 333-338.

103. **Lockington, D.A. and J-Y. Parlange** (2003) Anomalous water absorption in porous materials. *Journal of Physics D: Applied Physics*, **36**, 760-767.

104. **Loudon, A.G.** (1979) The thermal properties of lightweight concretes. *The International Journal of Lightweight Concrete*, **1**, 71-85.

105. **Lura, P.** (2003) Autogenous deformation and internal curing of concrete. *Ph.D Thesis*, TUDelft, The Netherlands.

106. **Lura, P., K. Van Breugel and I. Maruyama** (2001) Autogenous and drying shrinkage of high strength lightweight aggregate concrete at early ages- the effect of specimen size. Proceedings of *RILEM International Conference on Early age cracking in cementitious systems (EAC'01)*, 337-344.

107. **Lydon, F.D.** (1987) Observations on the density and quality of concrete. *International Journal of Cement Composites and Lightweight Concrete*, **9**, 205-216.

108. **Lydon, F.D.** (1995) Effect of coarse aggregate and water/cement ratio on the intrinsic permeability of concrete subject to drying. *Cement and Concrete Research*, **25**, 1737-1746.

109. **Lydon, F.D. and R.V. Balendran** (1980) Some properties of higher strength light-weight concrete under short-term tensile stress. *International Journal of Cement Composites and Lightweight Concrete*, **2**, 125-139.

110. **Lytag**, http://www.lytag.net/projects.html (visited on 15/05/2007).

111. **Manikandan, R.** (2006) Influence of pelletization and hardening process parameters on the properties of fly ash aggregates, *Ph.D Thesis*, Indian Institute of Technology, IIT , Madras

112. **Manikandan, R. and K. Ramamurthy** (2007) Influence of fineness of fly ash on the aggregate pelletization process, *Cement and Concrete Composites*, **29**, 456-464.

113. **Mannan, M.A. and C. Ganapathy** (2002) Engineering properties of concrete with oil palm shell as coarse aggregate. *Construction and Building Materials*, **16,** 29-34.

114. **Martys, N.S. and C.F. Ferraris** (1997) Capillary transport in mortars and concrete. *Cement and Concrete Research*, **27**, 747-760.

115. **Maslehuddin, M., A.I. Al-Mana, M. Shamim, and H. Saricimen** (1989) Effect of sand replacement on the early-age strength gain and long term corrosion resisting characteristics of fly ash concrete. *ACI Materials Journal*, **86**, 58-62.

116. **Mays, C. and A. Barnes** (1991) The performance of lightweight aggregate concrete structures in service. *The Structural Engineer*, **69**, 351-361.

117. **McCarter W.J., H. Ezirim and M. Emerson** (1992) Absorption of water and chloride into concrete. *Magazine of Concrete Research*, **44**, 31-37.

118. **McCarter, W.J.** (1993) Influence of surface finish on sorptivity of concrete. Journal of Materials in Civil Engineering, *ASCE*, **5**, No. 1, 130 – 136.

119. **Mehta, P.K. and P.J.M. Monteiro** *Concrete: microstructure, properties and materials*. Indian Concrete Institute, India, 2005.

120. **Montgomery, D.S.** *Design and analysis of experiments.* John Wiley & Sons, New York, N.Y., 2001.

121. **Mor, A.** (1992) Steel-concrete bond in high strength lightweight concrete. *ACI Materials Journal*, **89**, 76-82.

122. **Neville, A. M.** *Properties of Concrete*. Pearson Education Pvt. Ltd, Singapore, 2004.

123. **Nilsen, A.U and P.C. Aitcin** (1992) Properties of high-strength concrete containing light, normal and heavy weight aggregate. *Cement, Concrete and Aggregate*, **14**, 8-12.

124. **Nilsen, A.U., J.M. Monteiro and O.E. Gjorv** (1995) Estimation of elastic modulus of lightweight aggregate. *Cement and Concrete Research*, **25,** 276-280.

125. **Oner, A., S. Akyuz and R. Yildiz** (2005) An experimental study on strength development of concrete containing fly ash and optimum usage of fly ash in concrete. *Cement and Concrete Research*, **35**, 1165-1171.

126. **Orangun, C.O.** (1967) The bond resistance between steel and lightweight-aggregate (Lytag) concrete. *Building Science*, **2,** 21-28.

127. **Osunade, J. A**. (2002) The influence of coarse aggregate and reinforcement on the anchorage bond strength of laterized concrete. *Building and Environment*, **37**, 727-732.

128. **Pfeifer, D.W.** (1967) Sand replacement in structural lightweight concrete-Tensile strength. *ACI Journal*, Title No. 64-35, 384-392.

129. **Pfeifer, D.W.** (1968) Sand replacement in structural lightweight concrete-creep and shrinkage studies. *ACI Journal*, Title No. 65-11, 131-139.

130. **Poon, C.S., Z.H. Shui, L. Lam, H. Fok and S.C. Kou** (2004) Influence of moisture states of natural and recycled aggregates on the slump and compressive strength of concrete. *Cement and Concrete Research,* **34**, 31-36.

131. **Rudnai, G**. *Lightweight Concretes*. Akademiai kiado, Budapest, 1963.

132. **Rutledge, S.E. and A.M. Neville** (1966) The influence of cement paste content on the creep of lightweight aggregate concrete. *Magazine of Concrete Research,* **18**, 69-74.

133. **Sahin, R., R. Demirboğa, H. Uysal and R. Gül** (2003) The effects of different cement dosages, slumps and pumice aggregate ratios on the compressive strength and densities of concrete. *Cement and Concrete Research,* **33**, 1245-1249.

134. **Sari, D. and A.G. Pasamehmetoglu** (2005) The effects of gradation and admixture on the pumice lightweight aggregate concrete, *Cement and Concrete Research,* **35**, 936-942.

135. **Sarkar, S.L., S. Chandra and L. Berntsson** (1992) Interdependence of microstructure and strength of structural lightweight aggregate concrete. *Cement and Concrete Composites,* **14,** 239-248

136. **Short, A. and W. Kinniburgh** *Lightweight concretes*. Asia Pubulishing House, 1963.

137. **Siddique, R** (2003) Effect of fine aggregate replacement with Class F fly ash on the mechanical properties of concrete. *Cement and Concrete Research,* **33**, 539-547

138. **Slate, O.F, A.H. Nelson and Martinez** (1986) Mechanical properties of high strength lightweight concrete. *ACI Journal,* **83**, 606-613.

139. **Smadi, M. and E. Migdady** (1991) Properties of high strength tuff lightweight aggregate concrete. *Cement and Concrete Composites*, **13**, 129-135.

140. **Snyder, K. A.** (1998) A numerical test of air void spacing equations. *Advanced Cement Based Materials*, **8**, 28-44.

141. **Swamy, R.N. and G.H. Lambert** (1981) The microstructure of Lytag aggregate. *The International Journal of Cement Composites and Lightweight Concrete*, **3**, 273-282.

142. **Swamy, R.N. and G.H. Lambert** (1983) Mix design and properties of concrete made from PFA coarse aggregates and sand. *The International Journal of Cement Composites and Lightweight Concrete*, **5**, 263-275.

143. **Swamy, R.N. and G.H. Lambert** (1984) Flexural behaviour of reinforced concrete beams made with fly ash coarse aggregates. *The International Journal of Cement Composites and Lightweight Concrete*, **6**, 189-200.

144. **Tangtermsirikul, S. and A.C. Wijeyewickrema** (2000) Strength evaluation of aggregate made from fly ash. *Science*. *Asia*, **26**, 237-241.

145. **Tasdemir, M.A., S. Akyuz and N. Uzunhasanaglu** (1988) Creep of lightweight aggregate concrete under variable stresses. *Cement, Concrete and Aggregates,* **10**, 61-67.

146. **Tay, J. H., K. Y. Show and S. Y. Hung** (2002) Concrete aggregates made from sludge-marine clay mixes. *Journal of Materials in Civil Engineering*, ASCE, **14**, 392-398.

147. **Teo, D.C.L., M.A. Mannan, V.J. Kurian and C. Ganapathy** (2007) Lightweight concrete made from oil palm shell (OPS): Structural bond and durability properties. *Building and Environment*, **42**, 2614-2621.

148. **Topcu, I.B.** (1997) Semi lightweight concretes produced by volcanic slags, *Cement and Concrete Research*, **27**, 15-21.

149. **Vaysburd, A.M**. (1996) Durability of lightweight Concrete Bridges in severe Environments. *Concrete International*, **18**, 33-38.

150. **Verma, C. L., S. K. Handa, S. K. Jain and R. K. Yadav** (1998) Techno-commercial perspective study for sintered fly ash lightweight aggregate in India. *Construction and Building Materials*, **12**, 341-346.

151. **Videla, C. and M. Lopez** (2000) Mixture Proportioning Methodology for Structural Sand Lightweight Concrete, *ACI Materials Journal*, **97**, 281-289.

152. **Wainwright, P. J. and D. J. F. Cresswell** (2001) Synthetic aggregates from combustion ashes using innovative rotary kiln. *Waste Management*, **21**, 241-246.

153. **Wang, H.Y. and K.C. Tsai** (2006) Engineering properties of lightweight aggregate concrete made from dredged silt. *Cement and Concrete Composites*, **28,** 481-485.

154. **Wasserman, R. and A. Bentur** (1997) Effect of lightweight fly ash aggregate microstructure on the strength of concretes. *Cement and Concrete composites*, **27**, 525-537.

155. **Wasserman, R. and A. Bethur** (1996) Interfacial interactions in lightweight aggregate concretes and their influence on the concrete strength. *Cement and Concrete Composites*, **18**, 67-76.

156. **Weber, S. and H.W. Reinhardt** (1997) A new generation of high performance concrete: Concrete with autogenous curing. *Advanced Cement Based Materials*, **6**, 59-68.

157. **Wegen, V. G. J. L. and J. M. J. M. Bijen** (1985) Properties of concrete made with three types of artificial PFA coarse aggregates. *Cement and Concrete Composites*, **7**, 159-167.

158. **Wilson, H.S and V.M. Malhotra** (1988) Development of high strength lightweight concrete for structural applications. *The International Journal of Cement Composites and Lightweight concrete*, **10**, 79-90.

159. **Winslow, D.N. and M.D. Cohen** (1994) Percolation and pore structure in mortars and concrete. *Cement and Concrete Research*, **24**, 25-37.

160. **Xiao, J and H. Falkner** (2007) Bond behaviour between recycled aggregate concrete and steel rebars. *Construction and Building Materials*, **21**, 395-401.

161. **Yang, C. C. and R. Huang** (1998) Approximate strength of LWA using Micromechanics method. *Advanced Cement Based Materials*, 7, 133-138.

162. **Yang, C.C.** (1997) Approximate elastic moduli of lightweight aggregate, *Cement and Concrete Research*, **27**, 1021-1030.

163. **Zhang, M.H and O.E. Gjorv** (1990a) Characteristics of lightweight aggregate for high strength concrete. *ACI Materials Journal*, **88**, 150-158.

164. **Zhang, M.H and O.E. Gjorv** (1990b) Microstructure of the interfacial zone between lightweight aggregate and cement paste. *Cement and Concrete Research*, **20**, 610-618.

165. **Zhang, M.H. and O.E. Gjorv** (1991a) Mechanical properties of high strength Lightweight concrete. *ACI Materials Journal*, **88**, 240- 247.

166. **Zhang, M.H and O.E. Gjorv** (1991b) Permeability of High strength lightweight concrete. *ACI Materials Journal*, **88**, 463-469.

167. **Zhang, M.H and O.E. Gjorv** (1990c) Pozzolanic reactivity of lightweight aggregates. *Cement and Concrete research*, **20**, 884-890.

168. **Zhang, M.H. and O.E. Gjorv** (1992) Penetration of cement paste into lightweight aggregate. *Cement and Concrete Research*, **22**, 47-55.

169. **Zhutovsky, S., K. Kovler and A. Bentur** (2004) Influence of cement paste matrix properties on the autogenous curing of high performance concrete. *Cement and Concrete Composites*, **26**, 499-507.

# LIST OF PAPERS SUBMITTED ON THE BASIS OF THIS THESIS

1. **Glory Joseph and K. Ramamurthy,** Effect of cold-bonded fly ash aggregate on workability and mechanical properties of concrete, *Journal of Institution of Engineers (India),* Vol. 89, November 2008, 33-38.

2. **Glory Joseph and K. Ramamurthy**, Workability and strength behaviour of concrete with concrete with cold-bonded fly ash aggregates, *Materials and Structures*, RILEM, 2008 (accepted for publication).

3. **Glory Joseph and K. Ramamurthy**, Influence of fly ash on strength and sorption characteristics of cold-bonded fly ash aggregate concrete, *Construction and Building Materials*, 2008 (accepted for publication).

4. **Glory Joseph and K. Ramamurthy,** Strength and permeation characteristics of cold- bonded fly ash aggregate concrete, *Proceedings of International Conference on Sustainable Concrete Construction*, India, 8-10 Feb. 2008, 125-131.

5. **Glory Joseph and K. Ramamurthy,** Autogenous curing of cold-bonded fly ash aggregate concrete, *Cement and Concrete Research* (under review).

6. **Glory Joseph and K. Ramamurthy,** Mix proportions and penetrability of cold-bonded fly ash aggregate concrete, *Journal of ASTM International* (under review).